

Dissertation zur Erlangung des Doktorgrades  
der Fakultät für Chemie und Pharmazie  
der Ludwig–Maximilians–Universität München

**Functional characterization of the  
Mediator subunit MED25**

Lisa Santolin  
aus  
S.Bonifacio, Italien  
2006

## Erklärung

Diese Dissertation wurde im Sinne von § 13 Abs. 3 bzw. 4 der Promotionsordnung vom 29. Januar 1998 von Herrn Prof. Dr. Meisterernst betreut.

## Ehrenwörtliche Versicherung

Diese Dissertation wurde selbständig, ohne unerlaubte Hilfe erarbeitet.

München, am 31.07.2006

Lisa Santolin

Dissertation eingereicht am	31.07.2006
1. Gutachter	Prof. Dr. Meisterernst
2. Gutachter	Prof. Dr. Jansen
Mündliche Prüfung am	21.11.06

## SUMMARY

In this study a structure–function analysis has been employed to analyze transcriptional regulation through the Mediator subunit MED25. A relationship could be established between predicted structural domains and functional characteristics of this protein. Most critically the region responsible for interaction of MED25 with the Mediator was identified. Immunoprecipitation experiments demonstrated that the so–called VWA domain (von–Willebrand A domain, amino acids 1–290) is both sufficient and required for this contact. Site–directed mutagenesis indicates that this binding reaction involves the non–conserved loop SR2, which is protruding from this domain. Based on the results of this analysis a model was proposed, in which the primary contact is established by ionic forces and is further stabilized by hydrophobic interactions.

The previously identified ACID domain was reported to bind to VP16. Targeted mutagenesis of four different motifs in this region impaired not only transcriptional activation through MED25 but also led to reduced binding to VP16. In particular a lysine–rich motif is also present in two domains of PTOV1, a close homolog of MED25. Noteworthy, K518 is not conserved in the PTOV1\_B domain, which in contrast to PTOV1\_A and the ACID domain of MED25 does not bind to VP16. This led to the hypothesis that K518 is critically involved in the binding of VP16 to MED25.

Furthermore it could be demonstrated that MED25 contains an intrinsic transcriptional activation capacity, which is localized in the region 290–715. This indicates additional recruitment of other factors to promoters through this region. Together with the Mediator binding VWA–domain and the VP16–interaction domain this region might facilitate transcriptional activation.

A genome–wide screen showed downregulation of c–Jun and FosB following overexpression of MED25. Interestingly, expression of GSK3 $\beta$ , a downstream target of which is cyclin D1, seems to be stimulated by MED25. Together with the finding that overexpression of MED25 leads to activation of a p21 reporter, this raises the possibility that MED25 is involved in cell cycle control.

An overlap has been discovered by comparison of MED25 target genes and genes identified previously as target for the viral activator EBNA2. The close homology between the activation domains of EBNA2 and VP16 implies a common mechanism of

transcriptional activation by these two viral proteins through MED25. The involvement of MED25 in gene activation by viral activators might indicate a role for this Mediator subunit in viral transcription.



This work was contributing to the following publications:

Mittler G., Stühler T., **Santolin L.**, Uhlmann T., Kremmer E., Lottspeich F., Berti L., and Meisterernst M.

“A novel docking site on Mediator is critical for activation by VP16 in mammalian cells”  
The EMBO Journal, 22 (24), 6494-6504, 2003.

Leal A., Huehne K., Bauer F., Sticht H., Berger P., Suter U., Morera B., Saifi M., Lupski J. R., Ekici A., Pasutto F., **Santolin L.**, Meisterernst M., Reis A., Rautenstrauss B.

“MED25 transcription activator carries an Abelson family SH3 recognition motif altered in autosomal recessive Charcot–Marie–Tooth disease 2B2” (submitted)

## TABLE OF CONTENTS

---

<b>1. INTRODUCTION.....</b>	<b>1</b>
1.1 EUKARYOTIC GENE EXPRESSION: FROM GENES TO PROTEINS.....	1
1.2 EUKARYOTIC TRANSCRIPTION.....	3
1.2.1 <i>Promoter structure</i> .....	3
1.2.2 <i>Chromatin</i> .....	6
1.2.2.1 Chromatin modification and chromatin remodelling.....	7
1.2.3 <i>RNA Polymerase II</i> .....	10
1.2.3.1 The carboxyl-terminal domain (CTD).....	11
1.2.4 <i>General transcription factors</i> .....	12
1.2.5 <i>The Mediator complex</i> .....	16
1.2.5.1 Mammalian Mediator.....	17
1.2.5.2 Mediator-activator interaction.....	20
1.2.5.3 Mediator-Pol II interaction.....	22
1.2.6 <i>Activators</i> .....	23
1.2.6.1 The viral activator VP16.....	24
1.2.6.2 The Epstein-Barr virus nuclear antigen 2 (EBNA2).....	26
1.3 PTOV1.....	28
1.4 THE CHARCOT-MARIE-TOOTH (CMT) DISEASE.....	29
1.5 ENGINEERING OF THE MOUSE.....	30
1.5.1 <i>The advent of ES cells</i> .....	30
1.5.2 <i>Traditional gene-targeting</i> .....	31
1.5.3 <i>Site-specific recombinase (SSR) technology</i> .....	31
1.6 OBJECTIVES.....	35
<b>2 MATERIALS AND METHODS.....</b>	<b>36</b>
2.1 MATERIALS.....	36
2.1.1 <i>Chemicals and biochemicals</i> .....	36
2.1.2 <i>Additional material</i> .....	38
2.1.3 <i>Instruments</i> .....	39
2.1.4 <i>General buffers</i> .....	40
2.1.5 <i>Enzymes</i> .....	43
2.1.6 <i>Antibodies</i> .....	44
2.1.7 <i>List of plasmids</i> .....	44
2.1.8 <i>List of oligonucleotides</i> .....	47
2.2 MOLECULAR BIOLOGY.....	51
2.2.1 <i>Cloning</i> .....	51
2.2.2 <i>Site directed mutagenesis</i> .....	55
2.2.3 <i>RT-PCR</i> .....	56
2.2.4 <i>Microarrays</i> .....	57
2.2.5 <i>Dot blot</i> .....	59
2.2.6 <i>Genomic DNA extraction</i> .....	61
2.2.7 <i>Southern blot</i> .....	62
2.3 CELL BIOLOGY.....	64
2.3.1 <i>Cell lines</i> .....	64
2.3.2 <i>Growth conditions</i> .....	64
2.3.3 <i>Freezing and thawing conditions</i> .....	65
2.3.4 <i>Transfection of the cells</i> .....	65

## TABLE OF CONTENTS

---

2.3.5 Luciferase assay and $\beta$ -GAL assay.....	68
2.3.6 Immunofluorescence.....	68
2.3.7 Embryonic stem cell culture .....	69
2.4 BIOCHEMISTRY .....	72
2.4.1 Isolation of nuclear extract from HEK 293T and 721B cells.....	72
2.4.2 Sodium dodecyl sulphate polyacrylamide gel electrophoresis (SDS PAGE)..	72
2.4.3 Western blot.....	73
2.4.4 Immunoprecipitation of MED25 derivatives with MED15 antibody.....	74
2.4.5 Immunoprecipitation of flag-MED25(A335V) with FLAG-M2 antibody.....	75
2.4.6 Expression and purification of GST-VP16 derivative proteins.....	75
2.4.7 GST-VP16 pull down.....	76
2.5 MOUSE KEEPING .....	76
<b>3. RESULTS .....</b>	<b>77</b>
3.1 STRUCTURE-FUNCTION ANALYSIS OF MED25.....	77
3.1.1 Mapping of a minimal Mediator-interaction domain.....	79
3.1.2 Transcription activation analysis of MED25 deletion constructs.....	80
3.1.3 Site-directed mutagenesis of MED25 ACID and VWA domain.....	82
3.1.3.1 Dissection of the Mediator-interaction domain of MED25 using VWA point mutants.....	85
3.1.3.2 Study of the transcriptional activation function of MED25 point mutants with respect to their expression levels.....	91
3.1.3.3 Dissection of the VP16-interaction domain of MED25 using ACID-domain-MED25 point mutants.....	93
3.2 MED25 MUTATION AND HUMAN PATHOGENESIS: CHARCOT-MARIE-TOOTH DISEASE ...	97
3.2.1 Study of transcriptional activation potential and Mediator-binding capacity of MED25 (A335V) mutant.....	97
3.3 IDENTIFICATION OF MED25 TARGET GENES .....	99
3.3.1 Generation of an inducible cell line expressing MED25.....	101
3.3.2 RNA expression profiling of NIH-ER-MED25 cell line and RT-PCR analysis.....	103
3.3.3 Generation of an inducible cell line expressing a dominant negative mutant of MED25.....	105
3.3.4 Genome-wide analysis of transcriptional regulation by ER-MED25-NTD ..	107
3.3.5 Activation of p21 promoter by MED25.....	109
3.4 TOWARDS THE GENERATION OF A MED25 CONDITIONAL KNOCK-OUT MOUSE .....	112
3.4.1 Organization of MED25 genomic locus.....	112
3.4.2 Targeting strategy for the generation of a conditional null allele .....	113
3.4.3 Screening strategy by Southern blot analysis .....	115
3.4.4 Selection of a genomic clone from a 129/Ola mouse library .....	116
3.4.5 Generation of a MED25 conditional null allele .....	117
3.4.6 Transfection of ES cells and determination of a homologous recombinant..	118
3.4.7 Injection of homologous recombinant ES cells in mouse blastocysts and generation of MED25 chimeras.....	119
<b>4. DISCUSSION.....</b>	<b>122</b>
4.1 IDENTIFICATION AND CHARACTERIZATION OF THE MEDIATOR-INTERACTING MODULE OF MED25.....	122

## TABLE OF CONTENTS

---

4.2 CHARACTERIZATION OF THE VP16–INTERACTING MODULE OF MED25 .....	124
4.3 MED25 IN CHARACTERIZED BY AN INTRINSIC TRANSCRIPTION ACTIVATION CAPACITY ..	127
4.4 A ROLE FOR MED25 IN CELL CYCLE CONTROL .....	129
4.5 POSSIBLE IMPLICATION OF MED25 IN EBNA2 ACTIVATION.....	132
4.6 MED25 AND CHARCOT–MARIE–TOOTH DISEASE (CMT) .....	135
4.7 AN ATTEMPT TO CREATE A MED25 CONDITIONAL KNOCK–OUT MOUSE.....	136
<b>5. REFERENCES.....</b>	<b>139</b>
<b>6. APPENDIX.....</b>	<b>159</b>
6.1 SUPPLEMENTARY FIGURES.....	159
6.2 MICROARRAY ANALYSIS .....	160
<b>ACKNOWLEDGEMENTS.....</b>	<b>166</b>
<b>CURRICULUM VITAE .....</b>	<b>167</b>

## 1. INTRODUCTION

### 1.1 Eukaryotic gene expression: from genes to proteins

The process of gene expression is a broad and complex event characterized by a number of steps in the pathway from gene sequence to active protein. The expression level of most genes is regulated by transcription factors which can be considered the starting point of the transcription process in the nucleus. Once activated, transcription factors bind to gene regulatory elements and, through interaction with other components of the transcription machinery, promote access to DNA and facilitate the recruitment of the RNA polymerase enzymes to the transcriptional start site. Three RNA polymerase enzymes function in eukaryotes: RNA polymerase I, II, III. Transcription of protein-coding genes is catalysed by RNA polymerase II. The transcription "initiation" process characterized by the generation of a nascent RNA is soon followed by the "capping" process during which the newly generated RNA is modified by the addition of a "cap" structure at its 5' end. This structure protects the new transcript from attacks by nucleases and later serves as a binding site for proteins involved in export of the mature mRNA into the cytoplasm and its translation into protein. The capping process seems also to promote the transition from initiation to "elongation", in which RNA polymerase II moves from 5' to 3' along the gene sequence and extends the transcript. Upon reaching the end of a gene, the newly synthesized RNA is cleaved and a polyadenosine tail is added to the 3' end of the transcript. These three steps are called "termination", "cleavage" and "polyadenylation" respectively. Since genes are composed of coding sequences (exons) which are interrupted by uncoding sequences (introns), the introns are removed from the transcripts in a step called pre-mRNA "splicing". In eukaryotes "transcription", the process by which information is transferred from DNA to RNA, takes place in the nucleus. By contrast "translation", the process by which the information is transferred from RNA to protein takes place in the cytoplasm. Therefore processed mRNA molecules are "packaged" by factors that bind to them in the nucleus and direct them into the cytoplasm through interactions with proteins that line the nuclear pores. Translation of mRNA into proteins takes place on large ribonucleoprotein complexes called ribosomes and is mechanistically analogous to transcription. The nascent

polypeptide chain undergoes "folding" and often "posttranslational modification" to generate the final active protein.

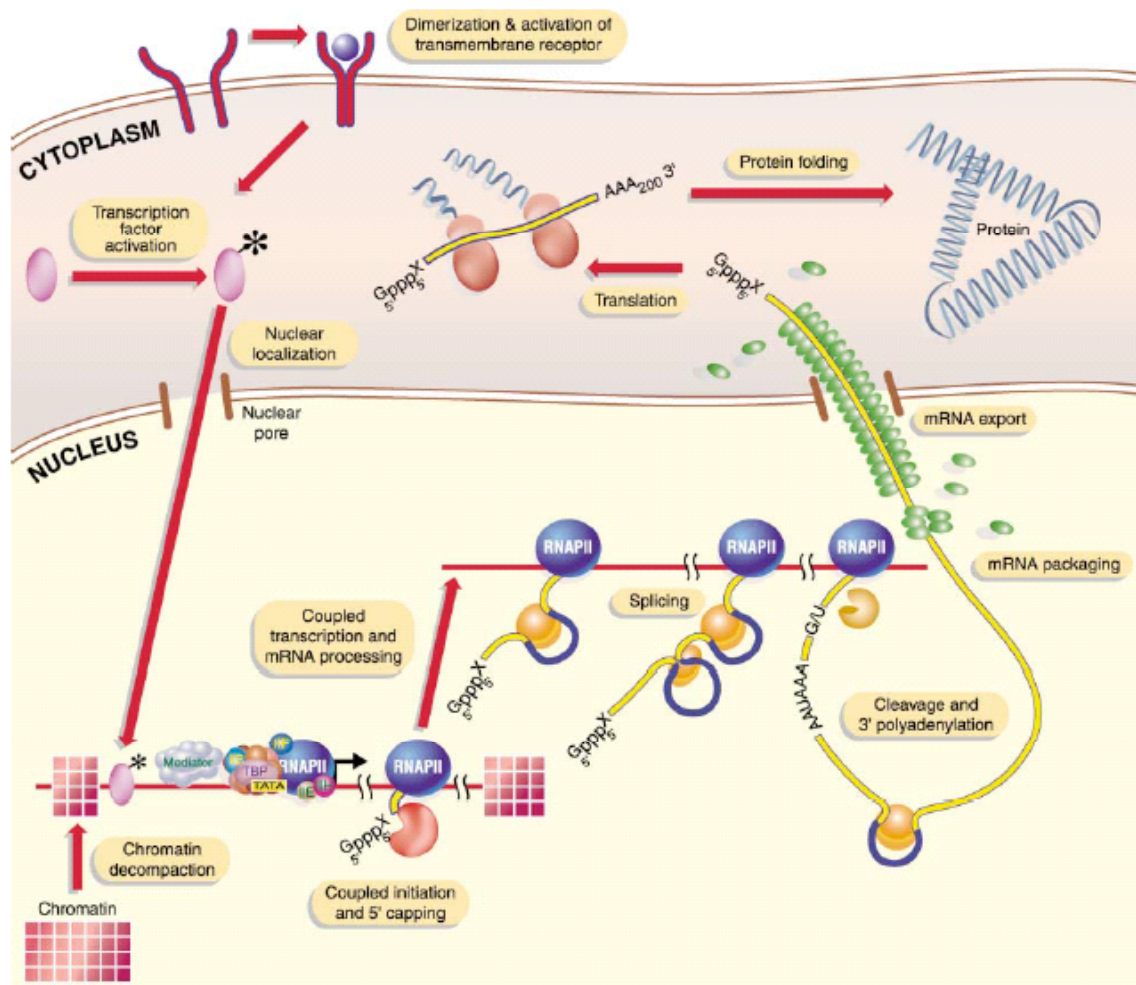


**Figure 1.** A contemporary view of gene expression (from Orphanides and Reinberg, 2002)

The complexity of each of the steps in the pathway from gene to protein has required that they be studied in isolation, mostly by the use of classical biochemistry. While this type of approach has been very useful, on the other end it shows some limitations. Each step is studied separately, forcing to look at the different processes in the pathway as if they would be unconnected events. In contrast to this traditional view of gene expression, in recent years a growing number of genetic studies have revealed functional links between the protein factors that carry out the different steps in the gene expression pathway. Similarly, conventional biochemical approaches and large-scale

mapping of protein–protein interaction networks have uncovered physical interactions between the various machineries. The picture that is emerging is one in which most steps are physically and functionally connected ensuring efficient transfer from one manipulation to the next (Orphanides and Reinberg, 2002). Figure 1 illustrates this contemporary view of gene expression.

## **1.2 Eukaryotic transcription**

While the transcription machinery of eukaryotes is much more complex than that of prokaryotes or archaea, the general principals of transcription and its regulation are conserved. Bacteria and archaea have only one polymerase, while eukaryotes utilize three nuclear enzymes to synthesize different classes of RNA:

- RNA polymerase I transcribes rRNA
- RNA polymerase II transcribes mRNA
- RNA polymerase III transcribes tRNA and other small RNAs.

The promoters for RNA polymerases I and II are mostly upstream of the start point while some promoters for the RNA polymerase III lie downstream of the start point. Each promoter contains characteristic sets of short conserved sequences that are recognized by the appropriate class of factors. Both, RNA polymerase I and III recognize a relatively restricted set of promoters, and rely upon a small number of accessory factors. In contrast, class II genes promoters which are utilized by RNA polymerase II show a higher complexity in their structure. Achieving transcription in these promoters requires the integration of several variables: cis–acting factors (DNA and chromatin), trans–acting factors (transcription activators and associated complexes), the basal transcription machinery (RNA polymerase II and general transcription factors), three dimensional structures and nuclear organization (Asturias, 2004; van Driel et al., 2003).

### **1.2.1 Promoter structure**

Eukaryotic genes transcribed by RNA polymerase II are categorized as class II genes. The promoters of these genes are composed of sequences which serve as recognition sites for the recruitment of the different regulators involved in the transcriptional process.

These sequences are conventionally divided in core elements and distal regulatory elements.

### **Core promoter elements**

Core promoter elements define the site for assembly of the transcription preinitiation complex (PIC) and include the TATA element, the initiator element (Inr), the downstream promoter element (DPE) and the TFIIB recognition element (BRE). Most promoters contain one or more of these elements, but none of these elements is absolutely essential for promoter function.

The TATA box is represented by an AT-rich sequence which is located upstream of the start site. The distance of the TATA box from the transcriptional start site varies with the species being 40 to 120 base pairs in yeast and 25 to 30 base pairs in higher eukaryes. The TATA sequence is the binding site for the TATA-binding-protein (TBP). Mutational analysis and random selection for functional TATA elements defined TATAAA as the consensus TATA sequence in yeast (Chen, 1988; Singer et al., 1990; Wobbe and Struhl, 1990). However, the tremendous flexibility of TBP to bind variants of the TATA sequence makes it difficult to identify genuine TBP-binding sites from sequence alone (Lee and Young, 2000). In contrast to the initial belief that most class II genes promoters contain a TATA element, only about 30% of mRNA genes analysed in *Drosophila* contain a recognizable TATA (Ohler et al., 2002). In *Drosophila* and human many of these non-TATA containing promoters contain some combination of Inr and DPE elements (Smale and Kadonaga, 2003).

The Inr element can be defined as the DNA sequence encompassing the transcriptional start site. Inr elements have been identified at many promoters, both TATA-containing and TATA-less, and have been implicated in transcriptional control by directing accurate initiation in a TATA-independent manner (Weis and Reinberg, 1992). Various factors can bind to Inr element and these may facilitate recruitment of the transcription apparatus (Lee and Young, 2000). Inr and DPE likely serve as binding sites for the TBP Associated Factor (TAF) subunits of the general factor TFIID. Cross link experiments have shown that TAF1 and TAF2 are normally positioned close to Inr (Oelgeschlager et al., 1996) and that TAF6 and TAF9 lie close to the DPE (Burke and Kadonaga, 1997). Proper function of a DPE containing promoter requires an Inr element, probably



because these elements cooperatively promote the correct binding of TFIID (Burke and Kadonaga, 1997).

The BRE element is a sequence contributing to high affinity binding of TFIIB and TFB to the human and archaeal TBP–DNA complex (Lagrange et al., 1998; Qureshi and Jackson, 1998). In archaeal the BRE is the primary determinant of transcription orientation (Bell et al., 1999; Littlefield et al., 1999).

### **Distal regulatory elements**

The second category of promoter elements, the distal regulatory elements, is gene-specific sequences that control the rate of transcription initiation since they are bound by transcriptional regulators. Transcription factors bound at these elements influence the initiation of transcription by contacting other factors of the basal apparatus directly or indirectly through the binding to a transcriptional co-factor which in turn contacts the basal apparatus. Distal regulatory elements include upstream activating sequences (UASs), enhancers, LCRs, upstream repressing sequences (URSs), silencers, insulators and MARs.

UAS and enhancers serve as recognition site for activators. In metazoans enhancers can be located hundreds of kilobases from their target genes and function independently from the orientation and the distance from the core promoter. In contrast to the enhancer element, the yeast UAS elements localize within few hundred base pares of the transcription start site and work only when positioned upstream of the TATA box (Blackwood and Kadonaga, 1998; Guarente and Hoar, 1984; Struhl, 1984). A locus control region (LCR) is defined as a set of elements that is sufficient to fully activate a linked gene in a tissue-specific, copy-number-dependent manner, independent from its position of integration in a transgenic mouse. While an enhancer is typically marked by one DNase I hypersensitive site (DHS) where transcription factors interact, LCR is characterized by a number of such sites that can be clustered or scattered. Activities commonly attributes to LCRs include chromatin opening activity, enhancer activity, and capability to establish domains of histone modification. Moreover LCRs elements are implicated in establishment of replication timing and DNA demethylation (Simon et al., 2001). Recent findings demonstrated that GTFs and RNA polymerase II bind to enhancers and LCRs before the activation of gene transcription in functional gene

expression domains. Founded on these observations, a new theory attributes at least to some of these regulatory domains a role as nucleation centres for PIC assembly to regulate timing of gene activation during development, differentiation and the cell cycle (Szutorisz et al., 2005).

URSs are DNA sequences bound by sequence-specific repressors. Inhibition of transcription mediated by URS-repressor complexes can take place in different fashions including interference with the activator-UAS binding, interference with the activation domain of an activator-UAS complex and finally targeting directly the core transcriptional machinery or indirectly recruiting an additional complex which targets the core transcriptional machinery blocking it (Johnson, 1995). Silencers are sequence elements that can repress promoter activity in an orientation and position-independent manner. Silencing proteins are thought to interact with histones to coat the targeted DNA sequence therefore repressing transcription in this region.

Insulators are elements that prevent the passage of activating or inactivating effects. They have been identified in two circumstances: when an insulator is placed between an enhancer and a promoter it prevents the enhancer from activating the promoter; alternatively, when an insulator is placed between an active gene and heterochromatin, it protects the gene against the inactivating effect that spreads from the heterochromatin. Usually insulators possess both properties.

Matrix attachment regions (MARs), sometimes also called scaffold attachment regions (SARs), are AT-rich sequences that act as anchor to the nuclear matrix. MARs can either form selective and transient or permanent anchors and have been proposed among other functions to facilitate transcription by positioning adjacent genes in the vicinity of the transcriptional machinery (Bode et al., 2003; Heng et al., 2004).

### **1.2.2 Chromatin**

The DNA in the cells is packaged into a highly organized and compact nucleoprotein structure known as chromatin. The basic organizational unit of chromatin is the nucleosome, which consists of 146 bp of DNA wrapped almost twice around a protein core containing two copies each of four histone proteins: H2A, H2B, H3 and H4 (Luger and Richmond, 1998). These small positively charged proteins show high conservation

among eukaryotes and are the protein building blocks of our chromosomes. In contrast to the original view which was referring to chromatin as a static organizational framework for DNA, it is becoming nowadays more and more clear that chromatin plays an essential role in regulating gene transcription by modulating access of the transcriptional apparatus to genes (Narlikar et al., 2002). Chromatin is not uniform with respect of gene distribution and transcriptional activity. It is organized into domains defined as euchromatin and heterochromatin which have different chromosomal architecture, transcriptional activity and replication timing. Heterochromatin is thought to consist of regular nucleosomal arrays, which impede access by nucleases and contain a high proportion of transcriptionally inactive repetitive sequences interrupted by relatively few genes (Elgin and Grewal, 2003; Grewal and Moazed, 2003). In contrast to heterochromatin, euchromatin is considered to be decondensed because it is characterized by irregular nucleosome spacing, is relatively gene rich and is potentially transcriptionally active (Elgin and Grewal, 2003). However, these differences are not always clear-cut as a recent analysis of the human genome showed that some pericentromeric regions (considered examples of constitutive heterochromatin) are decondensed and that some euchromatic regions are condensed (Gilbert et al., 2004). Tissue specific gene expression patterns and global gene silencing are established and maintained by so called epigenetic mechanisms which are represented by chromatin modification and chromatin remodelling. Epigenetic marks of silent chromatin in higher eukaryotes are histone hypoacetylation, di- or trimethylation of lysine 9 at histone H3 (H3K9 di- or trimethylation) as well as cytosine methylation (Fischle et al., 2003; Grewal and Moazed, 2003; Wu et al., 2005). Euchromatin is characterized by histone hyperacetylation and dimethylation of lysine 4 at histone H3 (H3K4 dimethylation) (Fischle et al., 2003).

### **1.2.2.1 Chromatin modification and chromatin remodelling**

The covalent modification of nucleosomal DNA and core histones, and ATP-dependent chromatin remodelling are important in the regulation of gene expression, DNA replication and many other biological processes. Increasing evidences indicate that the proteins involved in these processes do not act alone but interact with one another,

often forming large complexes that regulate higher order chromatin structure and the accessibility of chromatin to various factors

### **Histone modification enzymes**

Modifications of core histones at the lysine, arginine, and serine residues that lie in their amino-terminal tails include acetylation, methylation, phosphorylation and ubiquitylation. Several classes of enzymes appear to be involved in these mechanisms: histone acetyltransferases (HATs), histone deacetylases (HDACs), histone methyltransferases (HMTs) and histone kinases (Narlikar et al., 2002). Recruitment of HATs and HMTs to promoters by activators is crucial for the activation of many classes of genes (Jenuwein and Allis, 2001; Roth et al., 2001; Struhl, 1998; Turner, 2000; Zhang and Reinberg, 2001). Conversely, recruitment of HDACs by transcriptional repressors leads to deacetylation of the histone tails and is required for repression. Several transcription co-activators such as p300/CBP, Gcn5, PCAF, TAF250 and the p160 family nuclear receptor display intrinsic histone acetyltransferase (HAT) activity. Among HMTs enzymes, those that target arginine residues have been up to date associated with activation of transcription, whereas those implicated in lysine modification are context dependent. Methylation of lysine 9 of histone H3 (H3K9) by SUV39 is associated with repression (Richards and Elgin, 2002) while methylation of lysine 4 by Set 1 complex in yeast (Roguev et al., 2001) or Set 9 in human (Nishioka et al., 2002) leads to transcriptional activation. Interestingly, it appears that methylation at lysine 9 can be converted from a repressive signal to an active signal by methylation of lysines 4 or 27 on the same tails. It appears like the transcriptional consequence of any individual histone tail modification is influenced by other modification on the same tail (Strahl and Allis, 2000; Turner, 2000). Considering the number of modification that can occur at different histone tails it becomes quiet obvious how complex is the relationship between histone tail modification and gene expression. This observation has led to the proposal that the modification state of the histone tail make up a so called *histone code* read by proteins that modulate transitions between the different chromatin states (Strahl and Allis, 2000; Turner, 2000). Several examples are given that support the hypothesis that histone modifications may create specific binding sites for accessory proteins. The heterochromatin protein 1 (HP1) uses its chromodomain to recognise the histone H3

lysine 9 modification. Polycomb, a protein with similarity to HP1 belonging to the Polycomb group (PcG) proteins, recognizes and binds methylated histones and the histone methyltransferases responsible for their methylation (Craig, 2005). Many proteins involved in modulating chromatin structure use their bromodomain for the recognition of histone tails acetylated at specific lysines (Doerks et al., 2001; Jeanmougin et al., 1997). It is likely that bromodomains and chromodomains have evolved to recognize histone tails carrying specific modifications, although it is important to point out that not all proteins containing these domains possess this function.

### **ATP-dependent remodelling complexes**

ATP-dependent chromatin remodelling complexes facilitate access of DNA binding proteins to DNA by repositioning nucleosomes at the promoter or by inducing conformational changes in nucleosomes (Narlikar et al., 2002). They function using the energy of ATP hydrolysis to introduce superhelical torsions into nucleosomal DNA, which leads to the formation of nucleosomes that contain exposed DNA bulges or loops (Narlikar et al., 2002). In mammalian cells three classes of chromatin-remodelling protein complexes have been identified. SWI/SNF/Brm, ISWI and Mi-2/NuRD contain different ATPase subunits and associated proteins (Peterson, 2002).

### **DNA methylation**

Together with histone modifications, DNA methylation serves as an epigenetic mark for active or inactive chromatin. DNA methylation regulates gene expression through several distinct mechanisms. It can directly block transcription regulatory factors from binding to their target sequences or, alternatively, it can repress gene expression through several methyl-CpG-binding proteins (MECPs) that "read" DNA-methylation patterns. In mammals, the proteins identified up to date which are involved in this type of transcriptional regulation have been divided in two classes: DNA cytosine methyltransferases (Dnmt1, Dnmt2, Dnmt3a and Dnmt3b) and Methyl-CpG-binding proteins (MECP2, MBD1, MBD2, MBD3, MBD4 and Kaiso). The first group of proteins is characterized by highly conserved cytosine-methyltransferase motifs in their catalytic domain. Dnmt1 is a maintenance methyltransferase, which restores DNA-methylation patterns by methylating hemi-methylated CpG sites after DNA replication (Bestor,

1992). Dnmt3a and Dnm3b are required to initiate *de novo* methylation and establish new methylation patterns during development (Okano and Li, 2002). Both Dnmt1 and Dmmt3a have been shown to interact with histone deacetylases (HDACs) and can repress transcription (Burgers et al., 2002). The second group of proteins contain a methyl–CpG–binding domain (MBD) except for Kaiso which binds methylated CGCG through its zinc–finger domain (Prokhortchouk et al., 2001). There are several examples of complexes between Methyl–CpG–binding proteins and histone deacetylases. For instance, MECP2 forms a complex with HDACs and the co–repressor protein Sin3a to repress transcription in a methylation dependent manner (Jones et al., 1998; Nan et al., 1998). Moreover, together with the ATP–dependent remodelling complex NuRD, which contains also histone deacetylase activity, MBD2 forms a complex able to repress methylated promoters and to remodel methylated chromatin with high efficiency (Feng and Zhang, 2001; Ng et al., 1999; Wade et al., 1999; Zhang et al., 1999b). These two complexes provide a mechanistic link between DNA hypermethylation and histone deacetylation in transcriptional repression.

### 1.2.3 RNA Polymerase II

RNA Polymerase II (Pol II) lies at the centre of the transcription machinery interacting with general transcription factors in the preinitiation complex (PIC), breaking these interactions upon initiation and promoter clearance and associating with another set of factors during elongation and termination. The high resolution structures of bacterial polymerase and of yeast Pol II have given the first detailed insight about the molecular mechanism used by the transcriptional machinery (Cramer et al., 2000; Cramer et al., 2001; Gnatt et al., 2001; Zhang et al., 1999a). Yeast Pol II is composed of 12 subunits encoded by RPB1 to RPB12 genes. Based on structural similarities found in between Pol II and either the other two polymerases or the bacterial polymerase, Pol II subunits can be classified into three categories: subunits of the core domain having homologous counterparts in bacterial polymerase (Rpb1, 2, 3, and 11); subunits shared between all three nuclear polymerases (Rpb5, 6, 8, 10, and 12); subunits specific to Pol II but not essential for transcription elongation (Rpb4, 7, and 9) (Hahn, 2004). Pol II subunits organize in four mobile elements termed Core, Clamp, Shelf and Jaw Lobe that move

relative to each other. There is extensive structural conservation among the subunits of eukaryotic RNA polymerase II. Indeed six subunits of human Pol II can functionally replace their homologs in yeast ref (McKune et al., 1995). The two largest Pol II subunits, Rpb1 (about 200 kDa) and Rpb2 (about 150kDa) are the most highly conserved subunits and they are also homologous to the  $\beta'$  and  $\beta$  subunits, respectively, of bacterial RNA polymerase. Mutations at the genes encoding for these two subunits, RPB1 and RPB2, have revealed their involvement in specific functions of Pol II, namely the selection of the start site during transcription initiation (Arndt et al., 1989; Berroteran et al., 1994; Hekmatpanah and Young, 1991) and the overcoming of transcriptional arrest during transcription elongation (Archambault et al., 1992; Powell and Reines, 1996). As for Rpb1 and Rpb2, mutations at the level of RPB9 gene affect the accuracy of initiation probably explainable with the interaction between Rpb9 subunit and TFIIB (Sun et al., 1996). The Rpb4 and Rpb7 are functionally related. These two subunits can be dissociated from Pol II. *In vitro* studies performed using an Rpb4 null mutant of Pol II, which lacks Rpb7 as well, have demonstrated the role played by these two subunits in transcription initiation but not elongation. Moreover, it seems like these two subunits can shuttle between RNA polymerase II molecules (Edwards et al., 1991).

#### **1.2.3.1 The carboxyl-terminal domain (CTD)**

The largest subunit of Pol II contains a carboxyl-terminal domain (CTD) characterized by a tandem repeat of the consensus sequence Tyr-Ser-Pro-Thr-Ser-Pro-Ser. Ser2 and Ser5 are both sites of phosphorylation. Despite the high conservation of CTD among eukaryotes, the length of the repeats varies from 26 in yeast to 52 in human, suggesting that length increases with increasing genome complexity (Hampsey, 1998). In mammals CTD appears to be unstructured in crystallographic studies (Cramer et al., 2001). The CTD acts as a platform for assembly of factors that regulate the different phases of transcription, initiation, elongation, termination and mRNA processing (Hirose and Manley, 2000; Proudfoot et al., 2002; Shatkin and Manley, 2000). This special function of CTD might require the existence of a mechanism by which the CTD can "signal" to the machinery the phase of transcription it is engaged in and, therefore, the status of its transcript. Two observation provided support for the existence of such a

mechanism. First, the phosphorylation pattern of the CTD changes during transcription. After recruitment of a hypophosphorylated Pol II to promoters during PIC formation, phosphorylation of serine 5 in the CTD motif occurs between transcription initiation and disruption of the interactions between Pol II and the promoter (promoter clearance). Differently, modification of serine 2 is found only when the polymerase is associated with the coding region (Komarnitsky et al., 2000). Second, different processing factors recognize distinct regions of the CTD (Fondell et al., 1996). Therefore a "CTD code" may exist by which changes in CTD phosphorylation triggered upon completion of each stage of transcription or mRNA processing reaction may create docking sites for enzymes that catalyse the next processing step (Orphanides and Reinberg, 2002). Two cyclin dependent kinases target the CTD for phosphorylation: the CDK7 subunit of the general transcription factor TFIID and the CDK8 component of the Mediator complex (Lee and Young, 2000). Even though positive regulation of transcription was originally attributed only to CDK7, new findings have proven that both kinases can promote transcription and that both kinases are required for maximal inhibition of transcription (Liu et al., 2004). Phosphorylation of the CTD by these kinases also destabilizes the PIC leading to formation of the so-called Scaffold complex, composed of GTFs and cofactors remaining at the promoter after Pol II departure. After initiation, another factor such as the positive transcription elongation factor b (P-TEFb), which contains the Cdk/cyclin pair CDK9 and cyclinT, promotes phosphorylation of Ser2 resulting in recruitment of the RNA processing and polyadenylation/termination factors to elongating Pol II (Ahn et al., 2004; Bentley, 2002). A phosphatase activity responsible for dephosphorylation of CTD has been associated to the protein Fcp1. (Chambers and Dahmus, 1994). CTD phosphatase activity is regulated by TFIIB and TFIIIF. The RAP74 subunit of TFIIIF stimulates CTD phosphatase activity whereas TFIIB inhibits the stimulatory activity of TFIIIF. Since the dephosphorylated form of Pol II preferentially enters the PIC, Pol II CTD might regulate Pol II recycling (Hampsey, 1998).

#### **1.2.4 General transcription factors**

Unlike the prokaryotic enzymes, eukaryotic RNA polymerases cannot recognize the promoters of their target genes. Therefore they rely on a series of accessory factors



known as the general transcription factors (GTFs) (Orphanides et al., 1996; Roeder, 1996). GTFs include TFIIA, TFIIB, TFIID, TFIIIE, TFIIF, TFIIH. Pol II and GTFs position at core promoters in a state termed the preinitiation complex PIC. Pol II and GTFs were originally identified as independent, chromatographically distinct factors. Later on, however, the purification of preassembled complexes from yeast and human cells generated the idea that GTFs, Pol II and other regulatory factors are recruited at promoters as a preformed complex, in the form of a holoenzyme. Recently, this model has been questioned by reports demonstrating that certain holoenzyme components are recruited to some promoters independently of Pol II, (Bhoite et al., 2001; Cosma et al., 2001). These observations rather support a view where the transcriptional machinery assembles in a step-wise manner at promoters. Once assembled, the transcription apparatus is still in an inactive state. A dramatic conformational change occurs in which 11–15 bp surrounding the transcription start site are melted and form a single strand bubble (open complex formation) (Wang et al., 1992). Initiation of transcription begins with synthesis of the first phosphodiester bond of RNA. Pol II goes repeatedly through this process generating multiple short RNAs (abortive initiation) before it productively initiates synthesis of full length RNAs (promoter clearance). After pausing 25–30 bp from the start site Pol II is thought to release its contacts to the core promoter and the rest of the transcription machinery (promoter escape) and enters the stage of transcription elongation. *In vitro*, after initiation of transcription by Pol II many of the transcription factors remain behind at the promoter in the scaffold complex, which can then rapidly recruit the remaining general factors to promote transcription reinitiation.

### **TFIID: TBP and TAFs.**

TFIID is a complex composed of TBP (TATA binding protein) and about 14 TAFs (TBP associated factors). TBP is a universal transcription factor required for initiation by all three eukaryotic RNA polymerases (Hernandez, 1993). TBP recognizes the TATA box element therefore helping the transcription machinery to correctly position at core promoters. Resolution of the crystal structure revealed that TBP resembles a symmetrical saddle which sits on the DNA inducing a sharp DNA bend accompanied by a partial unwinding of base pairs that may be instrumental in the process of initiation (Lee and Young, 2000). TBP has shown to play an important role in transcriptional

activation via direct interaction with the activation domain of many gene-specific activators (Nikolov and Burley, 1994). TAFs function in promoter recognition as well as in positive and negative regulation of transcription. TAFs have been shown to be functional targets of transcriptional activators *in vitro*. Some TAFs are also subunits of complexes lacking TBP involved in covalent chromatin modification and transcriptional coactivation such as yeast SAGA and SLIK/SALSA (Spt-Ada-Gcn5-Acetylase and SAGA-like complex) and the human complexes pCAF and STAGA (p300/CBP and Spt-TAF-Gcn5-Acetylase). Although most genes are dependent on at least some TAFs for normal regulation, an important class of promoters seems independent of any TAF. In yeast, these completely TAF-independent promoters recruit TBP but not the TAFs upon gene activation. It is possible that at these genes TFIID is replaced by another TAF-containing complex such as SAGA (Hahn, 2004).

### **TFIIA**

One of the major functions of TFIIA is stabilizing the TBP-DNA interaction while binding to TBP. TFIIA interacts with numerous activators and it might be critical for transcriptional activation and to antagonize transcriptional repressors. In fact, it has been shown that TFIIA displaces blocks of several negative transcriptional regulators from the TFIID complex (Lee and Young, 2000).

### **TFIIB**

TFIIB is involved in the selection of transcription start sites, as demonstrated by the observation that mutations in TFIIB cause a shift in the transcription start site ref 40, 452. TFIIB enters the PIC after TBP and as a prerequisite for recruitment of Pol II. Not only TFIIB interacts directly with TBP and Pol II but also with other GTFs including the RAP30 and RAP74 subunits of TFIIF and the TAF<sub>II</sub>40 subunit of TFIID. TFIIB has also been implicated as the direct target of many gene-specific transcriptional activators, leading to the proposal that certain activators stimulate transcription by TFIIB recruitment (Hampsey, 1998).

**TFIIF**

TFIIF is composed of two subunits, RAP30 and RAP74. TFIIF has several characteristics reminiscent of bacterial sigma factor. These include tight binding to Pol II, suppression of non-specific DNA binding and stabilization of the preinitiation complex. TFIIF is critical for tight wrapping of DNA, possibly inducing torsional strain in the DNA, thereby facilitating promoter melting. TFIIF can also stimulate polymerase elongation rates by suppressing transient pauses during transcription. As mentioned above, RAP74 stimulates CTD phosphatase activity. Even though RAP30 and RAP74 were originally thought to function exclusively in initiation and in elongation, respectively, both subunits are now known to function in both processes (Hampsey, 1998; Lee and Young, 2000).

**TFIIE**

TFIIE interacts directly with the unphosphorylated form of Pol II, with both subunits of TFIIF and with TFIIH. TFIIE is also a direct target of certain transcriptional activators. Biochemical analyses revealed that human TFIIE is composed of two subunits (TFIIE $\alpha$  and TFIIE $\beta$ ) that form a  $\alpha_2\beta_2$  heterodimer. Functions attributed to TFIIE include recruitment of TFIIH to the PIC, stimulation of TFIIH-dependent phosphorylation of the Pol II CTD and stimulation of TFIIH-dependent ATP hydrolysis. TFIIE is likely to play a role in melting of promoter DNA. It contains a zinc ribbon motif that is implicated in DNA binding and TFIIE can bind regions of single stranded DNA, suggestive of a role in opening or maintaining an open promoter complex. The requirement of TFIIE seems to be promoter-specific (Hampsey, 1998; Lee and Young, 2000).

**TFIIH**

TFIIH shows at least three enzymatic activities: DNA-dependent ATPase, ATP-dependent helicase and CTD kinase. These activities are distributed in two domains, a core domain containing two DNA helicase activities (XPB and XPD) and a kinase domain containing a kinase/cyclin pair (CDK7/cyclin C). The helicase activity found in XPB is essential for promoter opening (open complex formation), and also for transition from abortive to productive elongation. In general, helicases act by destabilizing double stranded nucleic acid through the ATP hydrolysis-dependent motion of two separate domains that interact with single and double stranded nucleic acids. Using this

mechanism, the XPB helicase binding to promoter DNA as a subunit of TFIIH, likely initiates unwinding by introducing torsional strain in the DNA near the transcription start site. However the exact mechanism of XPB helicase action is still not completely clarified (Hahn, 2004). While XPB appears to be the primary helicase involved in transcription, XPD is required for nucleotide excision repair. Mutations in the XPB and XPD helicases are responsible for several genetic diseases in humans including xeroderma pigmentosum, Cockayne's syndrome, and trichothiodystrophy. The TFIIH kinase CDK7 phosphorylates serines at the CTD of Pol II. In mammalian systems but not in yeast the TFIIH kinase also functions as Cdk activating kinase (CAK) and regulates cell cycle transitions (Lee and Young, 2000).

### **1.2.5 The Mediator complex**

The initiation of eukaryotic messenger RNA synthesis is an elaborate process catalysed by RNA polymerase II and the general transcription factors (GTFs). This process, however, is further complicated by the requirement of a very large multisubunit "adaptor" that bridges RNA polymerase II and its myriad DNA binding regulatory proteins and transduces both positive and negative signals that turn on and off messenger RNA synthesis in response to the ever changing microenvironment of the cell. This adaptor which is ubiquitously expressed and evolutionarily conserved from yeast to man has been named Mediator for its role in mediating transcription signals from DNA binding transcription factors bound at upstream promoter elements and enhancers to RNA polymerase II and the general initiation factors bound at the core promoter surrounding the transcriptional start site.

Early studies of activator functions in systems reconstituted with DNA templates and purified RNA polymerase II and corresponding GTFs revealed that additional "coactivator" or "mediator" activities were required for activator function but not for basal (activator-independent) transcription (Flanagan et al., 1991; Meisterernst et al., 1991). In human cell, the USA (Upstream Stimulatory Activity) coactivator activity was resolved into a number of negative cofactors and positive cofactors that act jointly both to selectively repress basal transcription and to facilitate activator-dependent transcription (Meisterernst et al., 1991). The Mediator complex was identified and first purified from S.

cervisiae by Kornberg and co-workers, by virtue of its ability to promote activator-dependent transcription by purified RNA polymerase II and the GTFs *in vitro* (Kim et al., 1994a). This study brought to light for the first time the complexity of the complex which in yeast is composed of about twenty subunits. In addition to defining the subunit composition of the yeast Mediator complex, Kornberg and co-workers' characterization of the biochemical properties of their purified Mediator preparations led to the initial identification of the known Mediator associated activities. They and others provided direct evidence that Mediator binds tightly not only to the transcriptional activation domains of DNA binding transcription factors (Hengartner et al., 1995; Koh et al., 1998) but also to RNA polymerase II to form the so called "holoenzyme" (Kim et al., 1994b; Koleske and Young, 1994). Moreover, the binding of Mediator to Polymearse II was found to stimulate phosphorylation of the CTD heptad repeats by TFIIH-associated CTD kinase and, in the same work, yeast Mediator was shown to stimulate transcription initiation in an activator-independent fashion (Kim et al., 1994a). Very recently *in vitro* experiments have shown that Mediator enhances basal transcription facilitating the recruitment of TFIIIB during PIC assembly (Baek et al., 2006).

#### **1.2.5.1 Mammalian Mediator**

Since its original description in yeast cells as the reversibly associating coactivator component of the Polymerase II holoenzyme, multiprotein Mediator-like complexes have been isolated from mammalian cells using diverse approaches and include the thyroid hormone receptor-associated proteins/SRB-Med containing cofactor (TRAP/SMCC) (Fondell et al., 1999; Gu et al., 1999; Ito et al., 1999; Malik et al., 2000), activator-recruited factor-large (ARC-L) (Naar et al., 1999; Taatjes et al., 2002), vitamin D receptor-interacting proteins (DRIP) (Rachez et al., 1999), positive cofactor 2 (PC2) (Malik et al., 2000), cofactor required for Sp1 activation (CRSP) (Ryu et al., 1999; Taatjes et al., 2002), mouse Med (Jiang et al., 1998) and rat Med (Brower et al., 2002; Sato et al., 2003a; Sato et al., 2003b; Tomomori-Sato et al., 2004) complexes. Despite significant similarities in the subunit compositions of mammalian Mediator complexes isolated in different laboratories, apparent differences were notable. Although the reason for these differences is not known, recent proteomic analyses suggests that most of the

Mediator-associated proteins identified in different laboratories are bona fide subunits of the complex (Sato et al., 2004).

Up to date the mammalian Mediator contains 28–30 subunits (Sato et al., 2004) the nomenclature of which has recently been revised (Table 1) (Bourbon et al., 2004).

**Table1.** Mediator subunit nomenclature according to Bourbon et al., 2004

<b>New name</b>	<b>S. cerevisiae</b>	<b>H. sapiens</b>	<b>Location</b>
MED1	Med1	TRAP220	middle
MED2	Med2	–	tail
MED3	Pgd1/Hrs1/Med3	–	tail
MED4	Med4	TRAP36/DRIP36	middle
MED5	Nut1	–	middle/tail
MED6	Med6	hMED6/Drip33	head
MED7	Med7	hMed7/Drip34	middle
MED8	Med8	Arc32	head
MED9	Cse/Med9	Med25	middle
MED10	Nut/Med10	hNut2/hMed10	middle
MED11	Med11	HSPC296	head
MED12	Srb8	TRAP230/DRIP240	kinase
MED13	Srb9	TRAP240/DRIP250	kinase
MED14	Rgr1	TRAP170/DRIP150/CRSP150	tail
MED15	Gal11	ARC105	tail
MED16	Sin4	TRAP95/DRIP92	tail
MED17	Srb4	TRAP80/DRIP77/CRSP77	head
MED18	Srb5	P28B	head
MED19	Rox3	LCMR1	head
MED20	Srb2	hTRFP/p28a	head
MED21	Srb7	hSrb7/p21	middle
MED22	Srb6	Med24/Surf5	head
MED23	–	TRAP150 $\beta$ /DRIP130/CRSP130/hSur2	?
MED24	–	TRAP100/DRIP100/CRSP100	?
MED25	–	ARC92/ACID1	?
MED26	–	ARC70/CRSP70	?
MED27	–	TRAP37/CRSP347	?
MED28	–	Fksg20	?
MED29	–	Hintersex	?
MED30	–	TRAP25	?
MED31	Soh1	hSoh1	middle
CDK8	Srb10/Ssn3/Ume5	hSrb10/CDK8	kinase
Cyclin C	Srb11/Ssn8/Ume3	hSrb11/CycC	kinase

In yeast, genetic (Lee et al., 2000), biochemical (Myers and Kornberg, 2000), and structural (Dotson et al., 2000) studies have provided evidences that the subunits of the Mediator complex organize into sub-modules. A number of observations seem to point to an analogous structural organization within the mammalian Mediator complex as well. Twenty of these subunits, which are invariably found in PC2, are conserved in all eukaryotes, seem to be tightly associated and probably form the central core of the

complex. Among the subunits which show weaker association to the complex, MED16, MED23 and MED24 form apparently a module as suggested by knock out experiments that show interdependent loss of these factors (Ito et al., 2000; Stevens et al., 2002). Also MED13, MED12, CDK8 and Cyclin C are poorly represented in PC2, which is consistent with the ability of these four subunits to form a genetic, functional and physically separable module within the yeast complex (Borggreffe et al., 2002), to which a negative regulation of transcription has been attributed (Gu et al., 1999; Sun et al., 1998). Finally, MED26 and MED25 are found in association with subpopulations of Mediators and therefore define additional human Mediator variants termed CRSP and A-MED respectively (Mittler et al., 2003; Taatjes et al., 2002; Taatjes et al., 2004). At present, MED21-MED7 subunits of the core module represent the only part of Mediator for which the X-ray structure was resolved at high level (Baumli et al., 2005). Nevertheless a raw draft has been developed through the mapping of protein-protein interactions as well as biochemical and EM analysis (Asturias et al., 1999; Dotson et al., 2000; Guglielmi et al., 2004; Sato et al., 2003a; Sato et al., 2003b). On the basis of the close similarity in the overall 3D structure, deduced from cryo-electron microscopy (cryo-EM) studies of the mammalian and yeast Mediator complexes, it is possible to discern defined parts which are called "head", "middle" and "tail". A schematic view of the mammalian Mediator complex is given in figure 2.

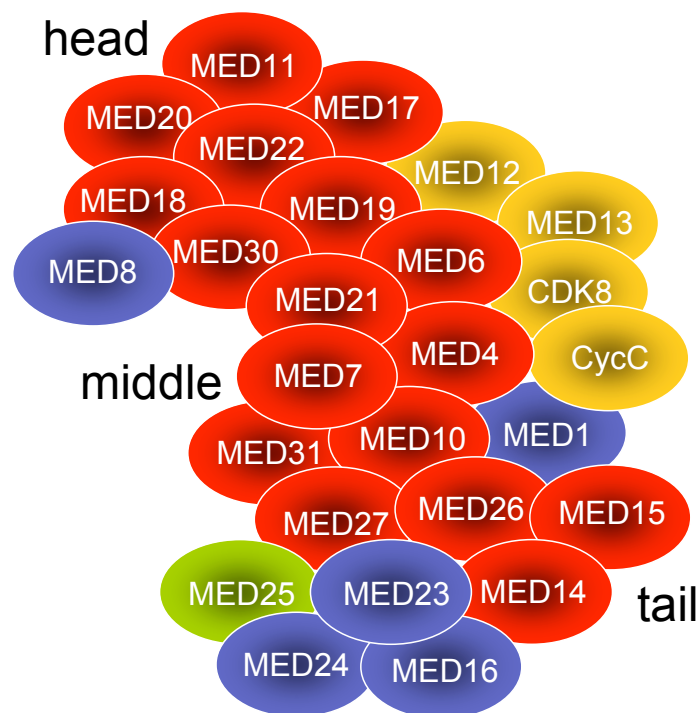


**Figure 2.** The Mediator complex. Core complex subunits found in most PC2 are indicated in red. Subunits loosely associated to the core are depicted in blue. The Kinase module subunits are in yellow. In green is shown MED25, the subunit studied in this work (adapted from Malik, 2005)

### 1.2.5.2 Mediator–activator interaction

Although Mediator functions as a general coactivator complex required for most Pol II driven transcription in eukaryotes, different parts of Mediator seem to regulate distinct sets of genes via the activator–specific function of individual Mediator proteins. Even though the genetic analysis of Mediator function in higher eukaryotes is limited compared with the extensive studies in yeast, investigations in *C. elegans* (Kwon et al., 1999; Moghal and Sternberg, 2003; Singh and Han, 1995; Wang et al., 2004; Zhang and Emmons, 2000) *Drosophila* (Boube et al., 2000; Gim et al., 2001; Janody et al., 2003; Kim et al., 2004; Park et al., 2001a; Park et al., 2003; Park et al., 2001b; Treisman, 2001) and mouse (Ge et al., 2002; Ito et al., 2000; Lau et al., 2003; Stevens et al., 2002) demonstrate that specific activator–gene functions of individual Mediator subunits are required to regulate particular developmental processes (Table 2).



**Table 2.** Mediator–interacting activators. Adapted from (Blazek et al., 2005)

<b>Activator</b>	<b>Mediator subunit</b>
ER $\alpha$ and ER $\beta$	MED1
AR	MED1
GR	MED1, MED14
TR $\alpha$	MED1, MED21
TR $\beta$	MED1
VDR	MED1
RAR $\alpha$	MED1
RXR $\alpha$	MED1
PPAR $\alpha$	MED1
PPAR $\gamma$	MED1
HNF–4	MED1, MED14
FXR	MED1
ROR $\alpha$	MED1
STAT2	MED14, MED17
Elk–1	MED23
Esx/Elf–3	MED23
C/EBP $\beta$	MED23
SMAD2/SMAD3/SMAD4	MED15
DSX <sup>F</sup>	MED29
SOX9	MED12
Dif	MED17, MED16, MED23, MED25
E1A–13S	MED23
RTA	MED12
VP16	MED25, MED17
Myc	Cdk8
p53	MED1, MED17
BRCA1	MED1
HSF	MED17, MED23, MED25
Aryl HC receptor	MED1
SREBP–1a	MED14

The best understood mechanism of Mediator recruitment by activators is given by the nuclear receptors. The activation function 2 (AF2) contained in the activation domain of nuclear receptors binds one or both of the so-called nuclear receptor boxes (LXXLL) of the MED1 subunit to recruit the entire Mediator complex. To date several nuclear receptors have been shown to bind the MED1 subunit in this fashion (Table 2). Gene targeting of MED23 revealed an essential role in MAP kinase signalling through Elk–1, as well as for activation by the adenoviral E1A protein (Stevens et al., 2002). Studies in *Xenopus* embryos have revealed that the MED15 subunit is required for the function of SMAD2–SMAD4 and SMAD3–SMAD4 complexes. Another well studied example of activator–Mediator interaction is provided by Herpes simplex VP16, which interacts with MED17 (Ito et al., 1999), and MED25 (Mittler et al., 2003). Moreover, a recent study carried out by Kim et al. in *Drosophila* using the siRNA approach, has revealed that

particular sets of Mediator proteins are required for expression of specific genes whereas others are required generally (Kim et al., 2004). Screening for activator-binding Mediator subunits, Kim et al have also demonstrated that a group of *Drosophila* Mediator subunits MED16, MED17, MED23 and MED25 bind HSF and Dif activators, acting as an activator-interacting module as previously shown in yeast (Lee et al., 1999).

Taking all together these data it is tempting to speculate that in addition to the recruitment of Mediator at promoters mediated by the interaction with activators, multiple activators targeting distinct Mediator subunits could lead to synergistic effects (Malik and Roeder, 2000). Alternatively, subtle changes in Mediator conformation resulting from interactions with distinct activators could confer activator-specific properties (Taatjes et al., 2002).

### **1.2.5.3 Mediator-Pol II interaction**

Because of the original isolation of the yeast Mediator complex as a component of the Pol II holoenzyme, it has been assumed that the predominant role of Mediator is to nucleate PIC assembly via interaction with Pol II. In fact, it has been proved that mammalian Mediator can interact and be isolated with Pol II (Malik et al., 2005; Sato et al., 2004; Wang and Berk, 2002). Moreover it has been demonstrated that CRSP interacts with the CTD of the largest subunit Rpb1 of Pol II (Naar et al., 2002). In addition to these findings, evidence is mounting that there might be other domains of Pol II that play an important role in Mediator's function. The high resolution structural analysis of Pol II (Cramer et al., 2001) and the electron microscopy analysis of Mediator (Davis et al., 2002), both conducted in yeast, have provided new information regarding the orientation of these two molecules respect to each other and within the preinitiation complex. The tail Mediator domain extends away from Pol II while middle and head Mediator modules show multiple contacts with Pol II. In the Pol II complex these interactions are centred on Rpb3, Rpb11 subunits but additionally involve portion of Rpb1, Rpb2, Rpb6 and Rpb12 subunits. Although the contacts between Pol II and Mediator are extensive, a large fraction of Pol II surface remains available for interaction with other components of the PIC (Chadick and Asturias, 2005). Dramatic

conformational changes are observed when yeast Mediator interacts with Pol II, compared to those observed when human Mediator binds activators. The fact that Mediator undergoes different type of conformational changes depending on the interaction–partner could be interpreted as a possible mechanism of signal integration carried out by Mediator in transcription regulation. Despite the existence of a holoenzyme form where Mediator is found in a pre–complex with Pol II, several observations reported a temporal disjunction in the order of recruitment of the two molecules at target genes (Park et al., 2001b; Shang et al., 2000; Sharma and Fondell, 2002). Therefore, Mediator and Pol II might exist in equilibrium between associated and free forms, which could enable step–wise assembly of a PIC.

### 1.2.6 Activators

Activation of transcription is achieved by the contribution of transcriptional regulator proteins that bind to short sequence motifs found in the promoter and enhancer regions of genes. The regulatory sequences of most eukaryotic genes contain binding sites for multiple transcription factors, allowing each gene to respond to multiple signalling pathways and facilitating the fine tuning of transcript levels (Lefstin and Yamamoto, 1998; McKenna and O'Malley, 2002). As a minimum, activator and other transcription factors that bind specific consensus sequences in DNA are characterized by two different domains: a DNA binding domain that recognizes and binds a specific DNA sequence and an activation domain capable of interacting with coactivators in the transcriptional initiation complex in a manner that increases the rate of transcription.

Common identified motifs of DNA binding domain include:

- **helix–turn–helix (HTH):** this motif is characterized by one alpha helix which lies in the wide groove of DNA and a second one which lies at an angle across DNA.
- **zinc finger:** contains a cluster of histidine and/or cysteine residues that form a coordination complex with zinc ion to fold the protein into a short finger–like loop.
- **leucine zipper:** consists of a stretch of amino acids with a leucine residue in every seventh position. Through this motif two proteins are bound to form a dimer. The

stretch of positively charged residues adjacent to each zipper is involved in DNA binding.

Among identified activation domains very well defined are the glutamine-rich domain (Sp1, CREB), the acidic activation domain (VP16, p53, E1A, GAI4, NFkB), the proline-rich domain (SMAD4, AP-2) and the serine-/threonine-rich domain (Sox-2, Sox-4).

The activity of transcription factors can be regulated in different fashions. One of them is the transport of the protein between the nuclear and cytoplasmic compartments. This transport occurs through nuclear pores which, in the proteins, recognize specific sequences called nuclear export signal (NES) and nuclear localization signal (NLS). Simply masking a NLS or NES by covalent modification or through binding of a transport inhibitor prevents the recognition of these signals by the transport machinery. Another important way of regulating transcription factors is represented by ubiquitination. Recently, many reports have linked the ubiquitination protease activity to both activation and degradation of transcription factors. In yeast, ubiquitination potentiates the activity of the activation domain of VP16 and also targets it for destruction (Salghetti et al., 2001). In addition to protein ubiquitination, a number of other posttranslational modifications play important roles in regulating transcription factors activity. These include protein phosphorylation, acetylation of lysine residues and methylation of arginine and lysine residues (Zhang and Reinberg, 2001).

#### **1.2.6.1 The viral activator VP16**

The acidic activator of the herpes simplex virus (VP16) is one of the most widely used model for activators. The virion protein VP16 does not contain a domain which binds directly the DNA. However, a specific consensus sequence is recognized by a complex where VP16 interacts directly with the DNA binding protein Oct-1 and the accessory protein HCF-1 (Gerster and Roeder, 1988; Katan et al., 1990; Kristie et al., 1989; O'Hare and Goding, 1988; Xiao and Capone, 1990). The transcriptional activation domain (TAD) of VP16 resides within the carboxyl terminal residues 411–490 (Greaves and O'Hare, 1989; Triezenberg et al., 1988a; Triezenberg et al., 1988b; Werstuck and Capone, 1989). Within the same domain are two subregions, spanning amino acids

411–456 (VP16H1) and amino acids 450–490 (VP16H2), either of which can function to activate expression of target genes (Regier et al., 1993; Tal-Singer et al., 1999; Walker et al., 1993). Both subdomains have been studied by mutational analysis, indicating key roles for specific hydrophobic and acidic residues (Cress and Triezenberg, 1991; Regier et al., 1993; Sullivan et al., 1998; Walker et al., 1993). Of special importance are several aromatic residues, the mutation of which revealed to be critical for activation of transcription. These amino acid residues include Phe 442 (mutated to Pro) located in the H1 subregion and Phe 473/475/479 (mutated to Ala) located in the H2 region (figure 3).

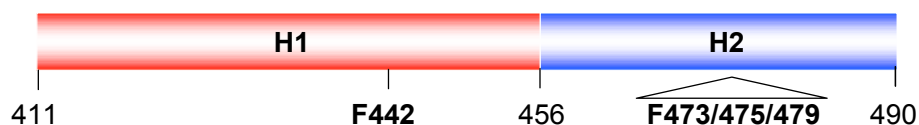


**Figure 3.** Schematic view of the VP16 transactivation domain (TAD). The two subdomains, H1 and H2, are indicated in different colours and can function independently from each other. The amino acid residues critical for activation of transcription are indicated in bold.

The mechanism of transcription activation by VP16 TAD has been extensively investigated. It promotes the enhancement of transcription rates and increases the number of functional active promoters (Ghosh et al., 1996; Ranish et al., 1999). It facilitates open complex formation (Jiang et al., 1994) and increases the processivity of RNA polymerase II (Yankulov et al., 1994). Moreover it promotes the assembly of the pre-initiation complex through interaction with TFIID (TAF9 and TBP) and/or TFIIB (Chi et al., 1995; Choy and Green, 1993; Ingles et al., 1991; Lin and Green, 1991; Stringer et al., 1990). The TAD of VP16 has been shown to interact with other basal transcription factors including TFIIA, TFIIF and TFIIH (Triezenberg, 1995; Zhu et al., 1994). VP16 activation domain binds also the positive cofactor PC4 (Ge and Roeder, 1994; Kretzschmar et al., 1994). In yeast, two mechanisms of chromatin modification have been attributed to VP16 TAD. In the first one, it relieves nucleosome-mediated repression by recruitment of the histone acetyltransferase (HAT) complexes SAGA and NuA4 (Ikeda et al., 1999; Utley et al., 1998). In the second one, it targets the Swi/Snf complex facilitating chromatin remodelling (Memedula and Belmont, 2003; Neely et al., 1999). Evidences for interaction with p300 have also been reported (Herrera and Triezenberg, 2004; Ikeda et al., 2002; Kraus et al., 1999). Importantly, among the other

target of the transcriptional machinery, VP16 TAD has been found to specifically interact with the Mediator complex through two subunits, MED17 (Ito et al., 1999) and MED25, (Mittler et al., 2003). In particular, the critical role of MED25 in VP16 activated transcription has been demonstrated by the dominant negative effect exerted by its functional domain ACID (Mittler et al., 2003).

### 1.2.6.2 The Epstein–Barr virus nuclear antigen 2 (EBNA2)

The DNA tumour virus Epstein–Barr virus (EBV) was the first virus to be isolated from a tumour biopsy sample and to be implicated in the development of human cancer. EBV is able to infect and immortalize resting B cell transforming them in a lymphoblastoid cell line (LCL). Among the about 80 genes encoded by this virus, only nine are translated and are acting in concert to induce and maintain B cell proliferation. These nine genes include six EBV nuclear antigens (EBNA1, –2, –3A, –3B, –3C, –LP) and three latent membrane proteins (LMP1, –2A, –2B) localized in the plasma membrane of the infected B cells. (Zimber-Strobl and Strobl, 2001). In immortalized B cells all the viral genes are expressed under the control of the viral transcription factor EBNA2. EBNA2 has been identified in two variants, EBNA2A and EBNA2B which share about 50% sequence homology.

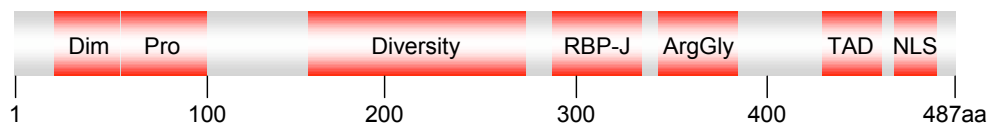


**Figure 4.** Structural organization of EBNA2 in functional domains. The protein contains a negatively charged region which likely plays a role in homodimerization (Dim), a polyne stretch (Pro), a diversity region (Diversity), a RBP–J interaction domain (RBP–J), an arginine–glycine rich stretch (ArgGly), a transactivation domain (TAD) and a nuclear localization signal (NLS). (After Zimber–Strobl and Strobl, 2001)

EBNA2 is structured in characteristic domains: a negatively charged region at the amino–terminus which likely plays a role in dimerization (Dim); a polyproline stretch (Pro); a diversity region where the homology between the two variants is very low; a RBP–J binding domain (RBP–J); a 18 amino acid arginine– glycine rich stretch (ArgGly); a negatively charged transactivating domain (TAD); a nuclear localization signal at the

carboxyterminus (NLS) (figure 4) (Bornkamm and Hammerschmidt, 2001; Zimmer-Strobl and Strobl, 2001).

EBNA2 lacks the capability to directly bind DNA. To transactivate cellular and viral genes, EBNA2 needs to bind RPB-J, a protein also known as CBF-1 (Cp-binding factor 1) (Grossman et al., 1994; Henkel et al., 1994; Waltzer et al., 1994; Zimmer-Strobl et al., 1994). RPB-J is a DNA binding protein ubiquitously expressed and highly conserved in evolution. It is also the downstream target of the cell-surface receptor Notch (Artavanis-Tsakonas et al., 1999). In the absence of EBNA2 and the intracellular part of Notch, (Notch-IC), RPB-J acts as a transcriptional repressor by recruiting a histone deacetylase (HDAC) coreceptor complex to the promoter (Hsieh et al., 1999; Kao et al., 1998). In addition, RPB-J has been shown to interact with two factors of the basal transcription machinery, TFIIA and TFIID, leading to the destabilization of the TFIIA-TFIID interaction which is required for initiation of transcription (Olave et al., 1998). Both, EBNA2 and Notch-IC bind to the transcriptional repression domain of RPB-J thereby relieving repression by replacing the HDAC corepressor complex by their transactivation domain (Hsieh and Hayward, 1995; Hsieh et al., 1999; Kao et al., 1998). The interaction of RPB-J with EBNA2 is necessary but not sufficient to induce gene expression. Other factors involved in promoter activation have not yet been identified. Only in the LMP1 promoter, the binding of the factor PU.1 (and Spi-B) which is supposed to interact with EBNA2, is absolutely necessary for EBNA2 mediated transactivation (Johannsen et al., 1995; Laux et al., 1994; Sjoblom et al., 1995). Interestingly, functional and structural homologies have been reported in between the viral proteins EBNA2 and VP16. In fact, the chimeric virus where the acidic activation domain of EBNA2 is replaced by the acidic activation domain of VP16 can still efficiently transform B cells and transactivate expression of EBV and B-cell genes (Cohen, 1992; Cohen and Kieff, 1991). Like VP16 and many other transcriptional activator proteins, EBNA2 is able to interact with components of the basal transcription machinery, including TFIIB, TAF40, TFIIF as well as with coactivator complexes like hSNF5, p300, CBP and PCAF (Tong et al., 1995a; Tong et al., 1995b; Wang et al., 2000; Wu et al., 1996). In a new study it has been reported that EBNA2 stimulates RNA polymerase II recruitment and CDK9-mediated phosphorylation of Ser5 of the CTD (Bark-Jones et al., 2006). The antiapoptotic effect provoked by EBNA2-induced LMP1 in B cells is mediated by the induction of the

antiapoptotic proteins Bcl-2, Mcl-1 and A20 (Gregory et al., 1991; Henderson et al., 1991; Laherty et al., 1992). Moreover, recent results obtained using a genome wide array approach provided new insights about EBNA2 target genes (Zhao et al., 2006).

### 1.3 PTOV1

PTOV1 (Prostate Tumour Overexpressed Protein 1) was identified as a novel gene and protein during a differential display screening for gene expression in prostate cancer (Benedict et al., 2001). PTOV1 is overexpressed in 71% of prostate carcinoma and barely detectable in normal prostate epithelium (Santamaria et al., 2003). PTOV1 gene is located in the 19q13.3 chromosome and encodes for a protein that consists of two highly related sequence blocks arranged in tandem that are conserved from Drosophila to humans. Each of the two domains of PTOV1 shows a very high homology sequence to the ACID domain of the Mediator subunit MED25 (figure 5 and supplementary figure 1), the gene of which is also located in the 19q13.3 chromosome.

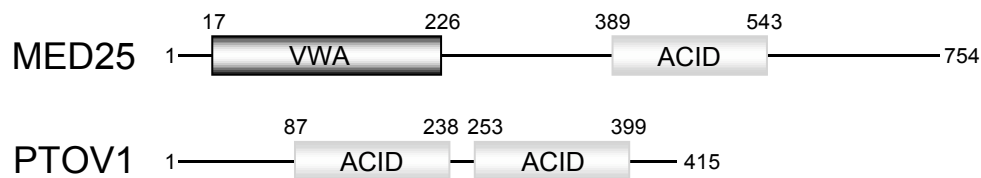


**Figure 5.** Schematic view of the functional domains of MED25 and PTOV1. PTOV1 contains two domains which show a very high homology with each other and with the ACID domain of the Mediator subunit MED25.

However, while the ACID domain of MED25 interacts physically with the activation domain of the viral activator VP16 (Mittler et al., 2003), it has been demonstrated that this is not the case for the tandem repeat of PTOV1 (Yang F. 2003). In a recent study, a yeast two-hybrid screen analysis has yielded to the identification of a PTOV1 specific partner, the lipid-raft associated protein flotillin-1 (Santamaria et al., 2005). In the same study, PTOV1 and flotillin-1 are shown to be strong inducers of cell proliferation and both required for normal cell proliferation. Moreover they have been shown to act in a mutual interdependence in order to achieve their mitogenic effect, which is strictly related to their nuclear localization. PTOV1 physically interacts with flotillin-1 and



depletion of PTOV1 by RNA interference prevents the nuclear localization of flotillin–1 (Santamaria et al., 2005). While PTOV1 contains two putative consensus bipartite nuclear localization signals (Benedit et al., 2001), flotillin–1 lacks any putative NLS. Therefore it is possible that PTOV1 provides the signal for nuclear import of flotillin–1 (Santamaria et al., 2005). To date there are no evidences that link PTOV1 function to MED25. It is however tempting to speculate that the double repeat of ACID domains in the PTOV1 protein could serve as an interaction site to titrate out the recruitment of proteins that act through the binding with MED25, thereby modulating their function.

#### **1.4 The Charcot–Marie–Tooth (CMT) disease**

Charcot–Marie–Tooth (CMT) disease or hereditary motor and sensory neuropathy (HMSN) represents a group of frequent genetically and clinically heterogeneous peripheral neuropathies (Mostacciuolo et al., 1991; Shy et al., 2005; Skre, 1974). CMT has historically been divided into predominantly demyelinating and predominantly axonal forms, CMT1 and CMT2, respectively (Vance, 2000). Mutation in the gene encoding for the transcription factor Krox 20 (EGR2), which is absolutely necessary for the transition from promyelinating to myelinating stage of Schwann cell development, has been shown to cause CMT1. Two other forms of CMT1 disease, CMT1A and CMT1B have been related to point mutations in the genes encoding the myelin proteins PMP22 and P0, respectively (Kamholz et al., 1999). Autosomal recessive demyelinating and autosomal recessive axonal forms of CMT have been described. For the latter form, ARCMT2, mutations on the *LMNA* and *GDAP1* (ganglioside–induced differentiation–associated protein 1) genes have been identified (Cuesta et al., 2002; De Sandre-Giovannoli et al., 2002).

Recently, a new autosomal recessive CMT variant has been identified in an extended Costa Rican family (CR–P) with Spanish and Amerindian ancestors (Berghoff et al., 2004; Leal et al., 2001). The neuropathy maps to the 19q13.3 chromosome and has been related to a mutation in the Mediator subunit MED25. The MED25 mutation A335V, which is located within a predicted SH3–recognition motif, seems to be the major responsible for the CMT2B2 form of CMT disease (Leal. et al., submitted).

## 1.5 Engineering of the mouse

One powerful method to understand the role of human genes is to investigate the function of homologous genes in model organisms. In addition to the fact that almost every human gene has a counterpart in the mouse genome, the mouse is unique in its applicability to human horganogenesis, immunology, neurobiology, reproduction, behaviour and epigenetics. The use of the mouse model to explore gene function depends on the methodologies available to manipulate the genome.

### 1.5.1 The advent of ES cells

A major technical breakthrough in manipulating the mouse genome was the advent of embryonic stem (ES) cells. These cells were first isolated from the inner cell mass of mouse blastocysts to generate permanent cell lines in 1981 (Evans and Kaufman, 1981; Martin, 1981). The contribution of ES cells to both, somatic and germ line tissues, was shown after their reintroduction into a blastocyst (Bradley et al., 1984). A significant step was represented by the development of gene–targeting, a strategy based on the introduction of DNA sequences into a chromosome by homologous recombination (Capecchi, 1989; Smithies et al., 1985). The genetic background of ES cells mostly used is the inbred strain 129/Sv (Hooper et al., 1987), however ES cells derived from other strains were also generated (i.e. C57BL/6 and Balb/c). ES cells derived from different strains show a different capability to undergo homologous recombination and germ line transmission. In order to maintain ES cells lines in a uncommitted state they have to be cultured in the presence of differentiation inhibiting factors. These factors are provided by mitotically inactivated feeder cells, which serve as a matrix for ES cells and by the addition of Leukaemia Inhibitory Factor (LIF) to the culture medium (Hilton, 1992). A routinely used method for generation of chimeric mice is the injection of ES cells derived from 129/Sv mouse strain (white colour coated) and carrying the desired alteration into the blastocoel of blastocysts isolated from female C57BL/6 donors (black colour coated) (Bradley et al., 1984). To test male ES cell chimeras for germ line contribution they are bred to wild– type C57BL/6 females. If the targeted ES cells contributed to the germ line, the offspring will exhibit an agouti coat colour. Other strain combinations of ES cells

versus blastocysts are possible. It is, however, important to choose the right combination in order to allow immediate and efficient recognition of ES derived mice from the coat colour.

### 1.5.2 Traditional gene-targeting

To generate a knock-out (KO) mouse, the traditional gene-targeting strategy is to replace the target gene, or at least an essential part of it (up to about 20 kilobases (Zou et al., 1994)) with a positive selection marker, usually the neomycin phosphotransferase gene (neo), permitting isolation of recombinant ES cells in culture. A standard replacement vector contains the positive selection marker flanked by genomic DNA homologous to the target. A negative selection gene, usually the herpes simplex virus thymidine kinase (HSV-tk) or the diphtheria toxin A subunit (DTA) gene, is placed on one end of the vector. The negative selection marker enriches for the desired homologous recombination event over random integrations by killing cells that have retained the negative selection gene. The traditional method of gene-targeting presents two potential pitfalls. The first one is that many genes serve an essential function, and therefore the elimination of their activity throughout the entire animal can result either in early embryonic lethality, precluding the analysis of gene function at later stages, or, alternatively, a masking of the full mutant phenotype due to genetic compensatory mechanisms. The second pitfall is the maintenance of the positive selection cassette within the targeting gene. Its presence can cause a number of problems, such as the disruption of neighbouring gene expression due to strong transcriptional regulatory elements frequently present in selection cassette (Lerner et al., 1993; Ohno et al., 1994).

### 1.5.3 Site-specific recombinase (SSR) technology

The problems related to the traditional gene-targeting method have been overcome by the advent of the site-specific recombinase (SSR) technology. The revolutionary approach is based on the use of the so-called  $\lambda$  integrases Cre (causes recombination of the bacteriophage P1) and Flp (named for its ability to invert or "flip" a DNA segment

in *S. cerevisiae*). Both Cre and Flp are able to recombine with high fidelity specific sequences of DNA, called *loxP* and *FRT* respectively. (Dymecki, 1996; Stark et al., 1992). Cre and Flp share a common mechanism of DNA recombination that involves strand cleavage, exchange, and ligation (Sadowski, 1995). Although distinct at the nucleotide level, *loxP* and *FRT* sites share an overall structure which includes two 13 base pair palindromic sequences, or inverted repeats, separated by an 8 base pair asymmetric core, or spacer, sequence (Branda and Dymecki, 2004). With the use of site-specific recombinases a new concept of mouse engineering was introduced. The main feature of conditional knock-out mice is that the deletion of a special gene of interest can be controlled in a spatial or temporal manner. To achieve this type of control, a target gene is engineered which contains *loxP* or *FRT* sequences flanking the gene segment of interest. A strain bearing a conditional allele of a single gene can be crossed to several lines with differing recombinase expression patterns allowing to study the role of a gene in different tissues, while the target gene will remain intact in other cells of the mouse where the recombinase is not expressed (figure 6).

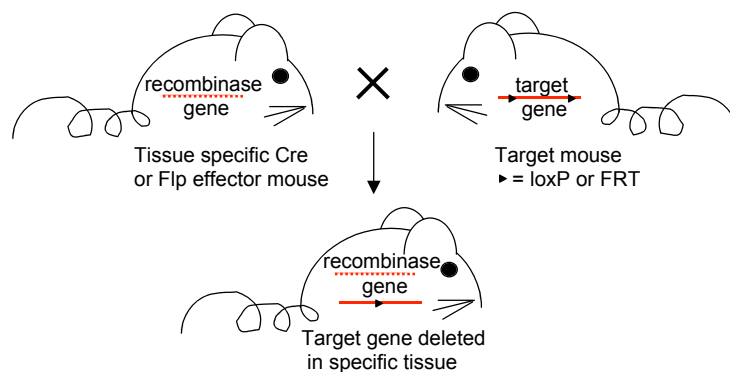


**Figure 6.** Scheme for recombinase-based gene modifications. A mouse expressing the recombinase in selected tissues or lineages (effector mouse) is crossed to a mouse carrying a gene segment flanked by recognition target sites (target mouse) to generate a mouse where the target gene is deleted in the cells expressing the recombinase.

Therefore, conditional gene modification provides the potential for careful analysis of gene inactivation in specific cell lineages. In many cases, however, gene inactivation is not complete due to a failure of the recombinase to modify the target gene in all cells expressing the recombinase. Such a phenomenon, called mosaicism, precludes an analysis of a null phenotype in the target lineage, due to the existence of wild-type cells

that may mask a potential defect. To easily detect in which cells recombination has taken place it is possible to include a reporter construct (such as one that encodes *LacZ*) downstream of the floxed region, so that recombination both inactivates the target gene and activates the reporter (Moon and Capecchi, 2000). The positive selection marker is also flanked by either of *loxP* or *FRT* sequences. Two main strategies are applied while creating a conditional allele where the positive selection marker can be removed (figure 7). In the dual-recombinase strategy the targeting vector carries two different site-specific recombinase systems, one flanking the gene segment of interest and the other one flanking the positive selection marker. This strategy offers the advantage to remove the positive selection cassette without influencing the removal of the gene segment of interest. Alternatively, in the tri-*lox* approach both, the selection cassette and the gene segment, are flanked by *loxP* sites (Gu et al., 1993). With this alternative approach, however it is difficult to obtain a partially deleted allele in which the gene segment remains floxed but the positive selection cassette has been removed (Kaartinen and Nagy, 2001). Recently, the problem has partially been solved with the identification of a new Cre recombinase, MeuCre40 (Leneuve et al., 2003).

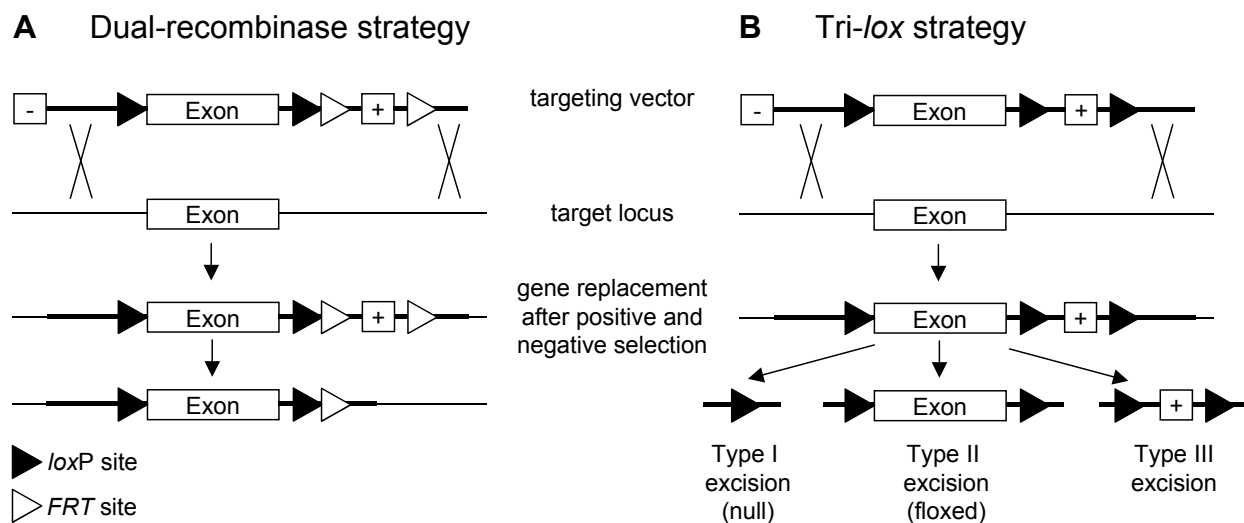


**Figure 7.** Strategies for removing the selection cassette from a conditional allele by the use of SSR. The dual-recombinase strategy offers the advantage that the cassette can be excised leaving the exon in place (see text).

The removal of the selection cassette can be achieved either *in vivo* or *in vitro*. A benefit of removing the positive selection marker in ES cells is that the second allele can be subsequently modified with the same targeting vector to create homozygous for the desired alteration. On the other hand, retaining the selection cassette leaves the opportunity to create a so called "hypomorphic allele" characterized by the presence of the neo<sup>r</sup> cassette which can partially disrupt gene expression. In this case, if the dual-recombinase strategy was applied to create the targeting vector, three mouse lines can be generated: the original lines expressing the hypomorphic allele (if the neo interferes with gene expression); one line expressing only the floxed allele, generated by mating the original line to a FLP-expressing mouse; one line carrying a null allele, generated by breeding the original line to a cre-expressing mouse (Lewandoski, 2001).

Recently, a number of groups have launched large-scale, random mutagenesis screens using either gene-trap vectors in ES cells (Hansen et al., 2003; Stryke et al., 2003) or the chemical agent N-ethyl-N-nitrosourea (ENU) *in vivo* (Coghill et al., 2002; Herron et al., 2002; Hrabe de Angelis et al., 2000; Nolan et al., 2000). The two strategies differ in the types of mutations produced. A standard gene-trap vector contains a promoterless reporter gene flanked by an upstream splice acceptor and a downstream polyadenylation (polyA) signal sequence (Gossler et al., 1989). When inserted into an intron, transcriptional activation of the "trapped" gene will result in a fusion transcript composed of upstream coding sequences and the reporter (usually a  $\beta$ -gal-Neo fusion cassette). This gene-trap design generally produces a null allele while simultaneously revealing the expression of the endogenous gene. Variations in the design of gene-trap have increased the efficiency and selectivity of gene trapping in ES cells (Stanford et al., 2001). Currently, BayGenomics (<http://bygenomics.ucsf.edu>) and the German Gene Trap Consortium (<http://genetrap.de>) are the largest libraries of gene-trap ES cells lines available to the public. Combined, these resources contain insertions in about 14% of genes currently annotated in Ensembl (Branda and Dymecki, 2004).

## 1.6 Objectives

The aim of this work was to dissect functional and structural aspects of the MED25 Mediator subunit. MED25 was purified in association to the Mediator complex and to the viral activator VP16. Since MED25 has been identified in Meisterernst and Naar laboratories rather recently, many questions about its function are still open. To address those questions three main lines of investigation were chosen in this work. First of all, a structure–function analysis of the protein was carried out based on the existence of the two functional domains VWA and ACID. With the generation of MED25 deletion constructs and MED25 point mutants we aimed to the identification of MED25 critical domains and possibly MED25 critical amino acids involved in Mediator and VP16 interactions.

In order to clarify whether MED25 has a specific function in relation to other Mediator subunits, a second approach was chosen to identify MED25 cellular targets. To follow this line of investigation inducible cell lines expressing MED25 derivatives were generated and used for microarray analysis.

Finally, to explore MED25 *in vivo* function, the generation of a MED25 conditional knock–out mouse has been chosen as a third approach for the characterization of MED25.

## 2 MATERIALS AND METHODS

### 2.1 Materials

#### 2.1.1 Chemicals and biochemicals

Acetic Acid	Roth
Acrylamide solution 30% (Rotiphorese Gel A)	Roth
Agarose	Gibco
Ammonium persulfate (APS)	Merck, Roth
Ammonium sulphate	Merck
Ampicillin (Ap)	Roth
Aprotinin	Sigma
Bacto Agar	Difco
Bacto Trypton	Difco
Bacto Yeast Extract	Difco
Benzamidin	Sigma
BES (N,N-bis[2-hydroxyethyl]-2-aminoethanesulfonic acid)	Sigma
Bisacrylamide solution 2%	Roth
Boric Acid	Roth
Bradford reagent	BioRad
Bromophenol Blue	Sigma
BSA (10 mg/ml) (bovine serum albumin)	NEB
Coomassie brilliant blue R-250	Sigma
Dimethylsulfoxide	Sigma
Dithiothreitol (DTT)	Roth
DMEM medium	Gibco
dNTPs	MBI, Roche
Ethanol (EtOH)	Merk
Ethidium bromide	Sigma
Ethylendiamintetraacetate disodium salt (EDTA)	Merck



EGTA	Merck
Fetal calf serum (FCS)	Gibco
Gancyclovir	Sigma
Gelatine	LGC Promochem
Geneticin G– 418 sulphate	Gibco
Glucose	Merck
Glycerol	Roth
Glycine	Roth
Hepes	Biomol
Histogel mounting medium	Linaris
4– hydroxytamoxifen (OHT)	Sigma
Hygromycin	PAA
Isopropanol	Merck
Leupeptin	Roche
LIF, ESGRO	Chemicon International
Light oil	Sigma
Magnesiumchloride	Merck
$\beta$ –Mercaptoethanol	Sigma
Methanol	Merck, Roth
Milk powder	Heirler Cenovis, Roth
NP40 (IGEPAL CA630)	Sigma
ONPG	Sigma
Penicillin–Streptomycin	Invitrogen
Phenol Chlorophorm Isoamil 25/24/1	Roth
Phenylmethylsulfonfuoride (PMSF)	Biomol, Roth
Ponceau S	Sigma
Protein G–Sepharose	Amersham
Potassium clorid	Sigma
Potassium hidroxyd	Roth
RPMI 1640–Medium	Gibco
Sodium azide	Sigma
Sodium carbonate	Merck

Sodium chloride	Merck, Roth
Sodium Citrate	Merck
Sodiumdodecylsulphate (SDS)	Merck, Roth
Sodium hydroxid	Merck
Tetramethylethylendiamin (TEMED)	Sigma, Roth
Top agar	Sigma
Trishydroxidmethyl–aminomethan (Tris)	Sigma
Triton X–100	Sigma
Trypsin–EDTA solution	Gibco
Xylene cyanole	Fluka

### 2.1.2 Additional material

Disposable plastic material	Greiner, Nunc, Falcon
DNA maxi and midi preps kit	Qiagen, NucleoBond
ECL detection system	Perkin Elmer
Film X–OMAT, BioMax	Kodak
GFX Gel Band Purification Kit	Amersham
Luciferase Assay System Kit	Promega
Megaprime DNA labelling system Kit	Amersham
Membrane Hybond–N+	Amersham
MicroSpin columns G25	Amersham
Miniprep Kit	Amersham
Nitrocellulose membrane	BioRad
Nucleobond AX Plasmid DNA Kit	Macherey & Nagel
Qiagen RNeasy Kit	Qiagen
Siliconized Plastic tubes	Sorenson
SYBR Green PCR Kit	Applied Biosystem
Steril filter (0.22/0.45 µm)	Roth
ThermoScript™ RT–PCR system Kit	Invitrogen
TNT Coupled Retyculocyte Lysate System Kit	Promega
Whatman 3MM Paper	Whatman

### 2.1.3 Instruments

Acrylamide gel electrophoresis	Amersham/Hoefler/BioRad
Agarose gel electrophoresis	BioRad
Autoradiography cassette	Amersham/Kodak
Centrifuges	Avanti, Beckman Multifuge 3 L–R, Heraeus Zentrifuge 5417, 5415R, Eppendorf
Confocal light microscope	TCS SP2, Leica
Developing machine	Curix60, Agfa
Electroblot, semi–dry	BioRad
Electroporator	Gene Pulser II, BioRad
Gaiger counter	LB122, Berthold
Gel drier	GD2000, Hoefer
Heating block	Eppendorf
Homogenizer	Douncer, Wheaton
Incubator	WJ311, Forma Scientific Unequip, Unitherm B6200, Heraeus
Instant Imager	Packard
Light microscope	Axiovert 25, Zeiss
PCR–Thermocycler	GeneAmp 5700, Applied Biosystem
pH–Meter	Calimatic 760, Knick
Photometer	GeneQuant Pro, Amersham
Rotors	JA10, JA25–50, SW41, SW28, Beckman
UV–Illuminator	Bachofer (254 nm, 366 nm)

### 2.1.4 General buffers

#### 2x BBS:

For 100ml use 1.07g BES (N,N-bis[2-hydroxyethyl]-2-aminoethanesulfonic acid), 1.6g NaCl, 0.027g Na<sub>2</sub>HPO<sub>4</sub>. Adjust to pH 6.96 with NaOH before adding H<sub>2</sub>O to 100ml. Sterilize with 0.22µm filter and store aliquots at -20°C.

#### BCx buffer:

20mM Tris-HCl pH 7.3, 0.2mM EDTA, 20% Glycerol, mM KCl. Before use add freshly 0.2mM PMSF, 0.2mM DTT, 2µg/µl Aprotinine, 0.1% NP40, 0.1mM Benzamidine.

#### β-GAL substrate solution:

1.1mM MgCl<sub>2</sub>, 1mg/ml ONPG, 82mM Na<sub>2</sub>HPO<sub>4</sub>, 18mM NaH<sub>2</sub>PO<sub>4</sub>, 50mM β-Mercaptoethanol.

#### BL21 lysis buffer:

20 mM Hepes pH 7.5, 100 mM KCl, 1 mM EDTA, 10% Glycerol, 0.1% NP-40, 5mM β-Mercaptoethanol. Add protease inhibitors before use.

#### CaCl<sub>2</sub> 0.25M:

For 20ml use 1.1g CaCl<sub>2</sub>•6H<sub>2</sub>O. Sterilize with 0.22µm filter and store aliquots at -20°C.

#### Coomassie Staining solution:

For 1L use 500ml H<sub>2</sub>O, 400 ml MeOH, 100ml Glacial acetic acid, 0.25g Coomassie R-250. For destaining prepare the same solution without Coomassie R-250.

#### 6x DNA loading buffer:

30% glycerol, 0.25% Bromphenol Blue, 0.25% Xylene Cyanole in TAE buffer.

#### Dot blot hybridisation solution:

6X SSC, 0.5%SDS, 5x Denhardt's solution, 100µg/ml tRNA.

**0.5M EDTA (pH 8.0):**

For 1L use 186.1g EDTA 2 H<sub>2</sub>O. Adjust to pH 8.0 with about 20g NaOH before adding H<sub>2</sub>O to 1L.

**ES cells lysis buffer:**

10mM NaCl, 10mM Tris–Cl pH 7.5, 10mM EDTA, 0.5% Sarcosyl, 0.4mg/ml proteinase K freshly added.

**GST fusion protein elution buffer:**

25mM Tris–HCl pH 8.2 RT, 100mM KCl, 10% Glycerol, 0.1% NP–40, 30mM reduced Glutathione. Add protease inhibitors before use.

**HEGN 100:**

25mM Hepes–KOH pH 7.6, 0.2mM EDTA pH 8.0, 100mM KCl, 10% glycerol, 0.1% NP40.

**LB medium:**

For 1L use 10g Trypton, 5g Yeast extract, 5g NaCl. To prepare LB–agar plates add 15g Top agar to 1L LB. Autoclave.

**6x SDS loading buffer:**

0.35M Tris–HCl pH 6.8, 0.12mg/ml Bromphenolblue, 10% (w/v) SDS, 30% (v/v) glycerol, 50mM DTT.

**NEX A:**

10mM HEPES pH 7.9, 10mM KCl, 0.1mM EDTA pH 8.0, 0.1mM EGTA pH 8.0. Immediately before use add 1.0mM DTT, 0.5mM PMSF, 2µg/µl Aprotinin, 2µg/µl Leupeptin.

**NEX B:**

20mM HEPES pH 7.9, 0.4M NaCl, 1mM EDTA pH 8.0, 1mM EGTA pH 8.0, 10% Glycerin. Immediately before use add 1mM DTT, 1mM PMSF, 2µg/µl Aprotinin, 2µg/µl Leupeptin.

**PBS 20x:**

For 1L solution use 160g NaCl, 4g KCl, 28.8g Na<sub>2</sub>HPO<sub>4</sub>, 4.8g KH<sub>2</sub>PO<sub>4</sub> in H<sub>2</sub>O.

**Southern blot transfer buffer:**

0.4M NaOH, 0.6M NaCl.

**20x SSC:**

For 2L use 350g NaCl, 176g Sodium Citrate. Adjust to pH 7.0 with NaOH.

**50x TAE:**

For 1L use 242g Tris, 57.1ml glacial acetic acid, 100ml 0.5M EDTA pH 8.0.

**Tail lysis buffer:**

100mM Tris pH 8.5, 5mM EDTA, 0.2% SDS, 200mM NaCl, 100µg/ml proteinase K freshly added.

**10x TBE:**

For 5L use 275g Boric Acid, 46.5g EDTA and 540g TRIS.

**10x TBS:**

For 1L use 24.2g Tris, 80g NaCl, 2g KCl. Adjust pH to 7.6 with HCl concentrate before adding H<sub>2</sub>O to 1L.

**TBS-BG:**

For 1L use 20ml 1M Tris-HCl pH 7.6, 28ml NaCl 5M, 1ml KCl 3M, 1.5ml MgCl<sub>2</sub> 1M, 5g glycine, 5g BSA, 0.5ml TWEEN20, 0.5g Na-Azid.

**1x TBS-T:**

For 1L use 100ml 10x TBS, 2ml 10% TWEEN20

**1x TE:**

10mM Tris-HCl pH7.5 and 1mM EDTA pH 8.0.

**10x TGS:**

For 1L use 30.2g Tris, 148g glycine, 10g SDS.

**5x Western blot transfer buffer:**

For 1L use 72g glycine, 15g Tris.

**1x Western blot transfer buffer:**

For 1L use 200ml 5x buffer, 200ml MeOH, 600ml H<sub>2</sub>O.

**2.1.5 Enzymes**

Calf intestine alkaline phosphatase	Fermentas
DNase	Invitrogen, Qiagen
Klenow Fragment	Fermentas
Lysozim	Sigma
Pfu Polymerase	Fermentas
Pfu Turbo	Stratagene
Polynucleotide Kinase (PNK)	MBI
Proteinase K	Roche
Restriction enzymes	NEB or Fermentas
RNase A	Roche
T4 DNA ligase	Fermentas
Taq polymerase	Fermentas
Vent polymerase	NEB

### 2.1.6 Antibodies

**Table 3.** Primary antibodies used in this work

PRIMARY ANTIBODY	ORIGIN	PROVIDER	DILUTION WB	DILUTION IF
MED7 (3E12–4)	rat	E. Kremmer	1:5	
MED15 (6C9)	rat	E. Kremmer	1:5	
MED25 (9C2)	rat	E. Kremmer	1:5	
Flag M2 (F 3165)	mouse	Sigma	1:2000	
ER (sc–543)	rabbit	Santa Cruz	1:500	1:50
ER (sc–8002)	mouse	Santa Cruz	1:500	
GAL 4 (sc–577)	rabbit	Santa Cruz	1:1000	
Myc (9E10)	mouse	E. Kremmer	1:20	

**Table 4.** Secondary antibodies used in this work

SECONDARY ANTIBODY	PROVIDER	DILUTION WB	DILUTION IF
Anti Rabbit	Promega	1:5000	
Anti Mouse	Promega	1:5000	
Anti Rat	Jackson ImmunoResearch	1:3000	
Anti Rabbit FITC	Promega		1:25

### 2.1.7 List of plasmids

**Table 5.** Plasmid used in this work.

PLASMID ID	PARENTAL PLASMID	DESCRIPTION	CLONED BY
pLS1	pBAC	MED25 genomic DNA fom 129/Ola mouse strain	BAC library
pLS2	pBAC	MED25 genomic DNA fom 129/Ola mouse strain	BAC library
pLS3	pBAC	MED25 genomic DNA fom 129/Ola mouse strain	BAC library
pLS4	pBAC	MED25 genomic DNA fom 129/Ola mouse strain	BAC library
pLS5	pBAC	MED25 genomic DNA fom 129/Ola mouse strain	BAC library
pLS6	pBAC	MED25 genomic DNA fom 129/Ola mouse strain	BAC library
pLS7	pBAC	MED25 genomic DNA fom 129/Ola mouse strain	BAC library
pLS8	pBAC	MED25 genomic DNA fom 129/Ola mouse strain	BAC library
pLS9	pNeohAP	contains a <i>FRT/NEO/FRT/LoxP</i> cassette	Capecchi
pLS10	pK <sup>o</sup> Neo6TK	contains a Timidine Kinase cassette	Gertraud Stelzer
pLS11	pK <sup>o</sup> Neo6TK/pNeohAP	pK <sup>o</sup> Neo6TK (–Neo) + <i>FRT/Neo/FRT/LoxP</i> (pNeohAP)	LS
pLS12	pK <sup>o</sup> Neo6TK/pNeohAP	pLS11 (– <i>AscI/Spel</i> fragment)	LS
pLS13	pCI (pLB27A)	mouse MED25 genomic DNA (exon 3–exon 10)	LS



pLS14	pK°Neo6TK/pNeohAP	pLS12 (+ SmaI fragment HRR3')	LS
pLS17	pK°Neo6TK/pNeohAP	pLS14 (+ BglII/BamHI fragment Intron 10)	LS
pLS18	pK°Neo6TK/pNeohAP	pLS17 (+ BglII fragment from pLS13)	LS
pLS20	pK°Neo6TK/pNeohAP	pLS18 (+ EcorV/LoxP sequence in SpeI)	LS
pLS23	pWWWP-luc	p21(-2325/+8)_Luc	Kardassis
pLS24	pGL2basic	p21(-215/+8)_Luc	Kardassis
pLS25	pGL2basic	p21(-143/+8)_Luc	Kardassis
pLS26	pGL2basic	p21(-2325/+8delta-122/-60)_Luc	Kardassis
pLS29	pEP7/EBV vector	ER-MED25	LS
pLS35	pCI_Neo_vector	GAL/Myc-MED25(290-754)	LS
pLS36	pCI_Neo_vector	GAL/Myc-MED25(290-730)	LS
pLS37	pCI_Neo_vector	GAL/Myc-MED25(290-685)	LS
pLS38	pCI_Neo_vector	GAL/Myc-MED25(1-685)	LS
pLS39	pCI_Neo_vector	Flag-MED25(290-754)	LS
pLS40	pCI_Neo_vector	Flag-MED25(290-730)	LS
pLS41	pCI_Neo_vector	Flag-MED25(290-685)	LS
pLS42	pCI_Neo_vector	Flag-MED25(1-730)	LS
pLS43	pCI_Neo_vector	Flag-MED25(1-685)	LS
pLS45	pEP7/EBV vector	ER-MED25-NTD	LS
pLS47	pCI_Neo_vector	GAL/Myc-MED25(1-393)A335V mut	LS
pLS48	pCI_Neo_vector	Flag-NLS-MED25(1-754)A335V mut	LS
pLS49	pCI_Neo_vector	Flag-NLS-MED25(1-393)A335V mut	LS
pLS50	pCI_Neo_vector	Flag-MED25(1-754)A335V mut w/o NLS	LS
pLS51	pCI_Neo_vector	Flag-MED25(1-393)A335V mut w/o NLS	LS
pLS52	pCI_Neo_vector	GAL/Myc-MED25(1-754)A335V mut	LS
pLS53	pEP7/EBV vector	ER	LS
pLS56	pCI_Neo_vector	GAL/Myc-p78	LS
pLS57	pCI_Neo_vector	GAL/Myc-MED25-mut5_FHF473AAA	LS
pLS58	pCI_Neo_vector	GAL/Myc-MED25-mut14_WPQK444APQA	LS
pLS59	pCI_Neo_vector	GAL/Myc-MED25-mut15_W408A	LS
pLS60	pCI_Neo_vector	GAL/Myc-MED25-mut18_KKIF518AAIA	LS
pLS61	pCI_Neo_vector	GAL/Myc-MED25-mut9_LRSL646ARSAA	LS
pLS62	pCI_Neo_vector	GAL/Myc-MED25-mut7_HMVL219AMAA	LS
pLS63	pCI_Neo_vector	GAL/Myc-MED25-mut19_YR487AA	LS
pLS64	pCI_Neo_vector	GAL/Myc-MED25-mut1_Y152A	LS
pLS65	pCI_Neo_vector	GAL/Myc-MED25-mut2_Y161A	LS
pLS66	pCI_Neo_vector	GAL/Myc-MED25-mut3_F47A	LS
pLS67	pCI_Neo_vector	GAL/Myc-MED25-mut4_Y66A	LS
pLS68	pCI_Neo_vector	GAL/Myc-MED25-mut10_FR465AA	LS
pLS69	pCI_Neo_vector	GAL/Myc-MED25-mut11_Y39A	LS
pLS70	pCI_Neo_vector	GAL/Myc-MED25-mut16_RK186AA	LS

pLS71	pCI_Neo_vector	GAL/Myc-MED25-mut6_F125A	LS
pLS72	pCI_Neo_vector	GAL/Myc-MED25-mut8_KT443AA	LS
pLS73	pCI_Neo_vector	GAL/Myc-MED25-mut13_T138A	LS
pLS74	pCI_Neo_vector	GAL/Myc-MED25-mut17_VVFFV17LVFL	LS
pLS75	pET21b	hHis-MED25(394-543) K411/413A D418A mut	Sonja Baumli
pLS76	pET21b	hHis-MED25(394-543) E437/442A K440A mut	Sonja Baumli
pLS77	pET21b	hHis-MED25(394-543) K478A mut	Sonja Baumli
pLS78	pET21b	hHis-MED25(394-543) K518/519/520A mut	Sonja Baumli
pLS79	pCI_Neo_vector	GAL/Myc-MED25-mut20_Q137A	LS
pLS80	pCI_Neo_vector	GAL/Myc-MED25-mut21_T138D	LS
pLS81	pCI_Neo_vector	GAL/Myc-MED25-mut22_NS147/148AA	LS
pLS82	pCI_Neo_vector	GAL/Myc-MED25-mut23_Y151F	LS
pLS83	pCI_Neo_vector	GAL/Myc-MED25-mut24_E157R	LS
pLS84	pCI_Neo_vector	GAL/Myc-MED25-mut25_Y161F	LS
pLS85	pCI_Neo_vector	GAL/Myc-MED25-mut26_E167A	LS
pLS86	pCI_Neo_vector	GAL/Myc-MED25-mut27_ER175/176AA	LS
GAL-MED25(1-754)	pCI_Neo_vector	Gal/Myc-MED25(1-754)	TH
pTH24	pCI_Neo_vector	Gal/Myc-PTOV1_A	TH
pTH25	pCI_Neo_vector	Gal/Myc-PTOV1_B	TH
SB93	pET24b	dHis-MED25(514-656)	Sonja Baumli
SB94	pET24b	dHis-MED25(514-663)	Sonja Baumli
SB105	pET21b	hHis-MED25(394-543)	Sonja Baumli
pLB52	pBACe 3.6	mouse genomic DNA Acc. N. AC069498	LB
pLB58		human cDNA MED25 Acc. N. AL136746	LB
pLB60	pCI_Neo_vector	Flag-MED25(1-715) w/o NLS	LB
pLB67	pCI_Neo_vector	Gal/Myc-MED25(1-183)	LB
pLB68	pCI_Neo_vector	Gal/Myc-MED25(389-543)	LB
pLB77	pCI_Neo_vector	Gal/Myc-MED25(1-290)	LB
pLB78	pCI_Neo_vector	Gal/Myc-MED25(1-393)	LB
pLB79	pCI_Neo_vector	Gal/Myc-MED25(1-543)	LB
pLB80	pCI_Neo_vector	Gal/Myc-MED25(183-393)	LB
pLB85	pCI_Neo_vector	Gal/Myc-MED25(1-226)	LB
pLB86	pCI_Neo_vector	Gal/Myc-MED25(1-200)	LB
pLB90	pCI_Neo_vector	Gal/Myc-MED25(393-754)	LB
pLB92	pCI_Neo_vector	Flag-MED25(1-754) w/ NLS	LB
pLB105	pCI_Neo_vector	Gal/Myc-MED25(1-715)	LB
pLB113	pCI_Neo_vector	Gal/Myc-MED25(1-570)	LB
pLB114	pCI_Neo_vector	Gal/Myc-MED25(1-613)	LB
pLB115	pCI_Neo_vector	Gal/Myc-MED25(1-667)	LB
pLB116	pCI_Neo_vector	Gal/Myc-MED25(543-715)	LB
pLB117	pCI_Neo_vector	Gal/Myc-MED25(393-715)	LB

pTS1		Flag-MED25(144-715)	TS
pTS2		Flag-MED25(290-715)	TS
pTS3		Flag-MED25(541-715)	TS
pGEX-VP16H1	pGEX	GST-VP16-H1	TS
pGEX-VP16H1mut	pGEX	GST-VP16H1mut	TS

## 2.1.8 List of oligonucleotides

**Table 6.** Oligonucleotides used in this work

OLIGO ID	SEQUENCE 5'→ 3'	GENERAL USE
PC6exon1up	ATGGTCCCCGGATCCGAAGGCC	screening mouse MED25 BACs library for targeting vector generation
PC6exon1down	ACTCTATGGCAGGCAGCAGGTA	screening mouse MED25 BACs library for targeting vector generation. ProbeA for southern blot on the 5' side
PC6exon9up	TTCACCCATCAACCCTCTCCA	screening mouse MED25 BACs library for targeting vector generation
PC6exon9down	CCAGAGACGGCGCCCCAGGCTG	screening mouse MED25 BACs library for targeting vector generation
PC6PreExon1	ACTGCTTCGCTTCCAAGTCCCG	screening mouse MED25 BACs library for targeting vector generation
PC6Exon3up	TATGGTGAACCCAGTACAGCC	screening mouse MED25 BACs library for targeting vector generation
PC6postExon3	CTTCATCTCCTCGTTGACAGGT	screening mouse MED25 BACs library for targeting vector generation
PC6Exon14down	CCCGCGCTGTTGCTCCAGCTTC	screening mouse MED25 BACs library for targeting vector generation
PC6prepreExon1	AACGGAGCCAAGCGCTTCAGCG	screening mouse MED25 BACs library for targeting vector generation. ProbeA for southern blot on the 5' side
pLS12TKup	GGCGTCTGTGGCTGCCAAACAC	sequencing of pLS12
PC6HRR3'down	CCCGGGGCCCTCACCAAGTTGG	Homology recomb region 3' for targeting vector
PC6HRR3'up	CCCGGGCTATACAGAGAAACTC	Homology recomb region 3' for targeting vector

PC6probe3'down	CCCTCAGACTCTCAGGGGACTG	probeB for ES southern blot on the 3' side w/ oligo PC6probeBup
pLS16/ <i>loxP</i> seqdown	CGCCTGACACGCCACGCTGAAG	sequencing of pLS16( <i>loxP</i> site orientation)
PC6/ <i>loxP</i> downEcoRV	CTAGTGATATCATAACTTCGTATAGCATAATTATACGAAGTTATA	/ <i>loxP</i> site of targeting vector
PC6/ <i>loxP</i> PupEcoRV	CTAGTATAACTTCGTATAATGTATGCTATACGAAGTTATGATATCA	/ <i>loxP</i> site of targeting vector
PC6intron10down	CGAGATCTGATGCCCCACTTCTGGA	reconstitution of the missing part of intron 10 in the targeting vector
PC6intron10up	CGGGATCCCTGTCCTGGAACCTCACTTTGTAGACC	reconstitution of the missing part of intron 10 in the targeting vector
B-actinFw	TGCGTTGTTACAGGAAGTCCC	human RT-PCR
B-actinRev	CTATCACCTCCCCTGTGTGGA	human RT-PCR
p21-FW	CATGTGTCTGGTTCCCGTT	human RT-PCR
p21-Rev	TCAGCATTGTGGGAGGAGC	human RT-PCR
PC6probeBup	CCCAGGCAGAGTACTGTTGGTC	probeB for ES southern blot on the 3' side w/ oligo PC6probe3'down
pLS19intron10seqdown	GCACCCGACTGCTCTTCCGAAG	sequencing of pLS19 (intron 10)
PC6/ <i>loxP</i> EcoRVup	TGGGGCCCTAAAATGGCCAGGA	genotyping clone 5A of MED25 inducible KO by PCR w/oligo pLS16/ <i>loxP</i> seqdown
PC6NeoFRTup	CGTGCTTTACGGTATCGCCGCT	genotyping clone 5A of MED25 inducible KO by PCR w/oligo PC6HRR3'down
PC6intron8up	CTGTGGGAGAAACCAGCGTGAG	genotyping clone 5A of MED25 inducible KO by PCR w/oligo PC6/ <i>loxP</i> downEcoRV
PC6intron8down	TGGGCCCACGCTGTGAGTTCTA	genotyping clone 5A of MED25 inducible KO by PCR w/oligo Neo down
Neo down	GCGATAGAAGGCGATGCGCTGC	genotyping clone 5A of MED25 inducible KO by PCR w/oligo PC6intron8down
PC6NeoFRT/ <i>loxP</i> down	GTGAGGTTGTTACAGACTACAATCTG	sequencing of PCR products from clone 5A of MED25 inducible KO
ER-Acid1up	CGCGGCTAGCTTAAAAGGAACTTTATTGGGTGT	cloning of pLS29
ER-Acid1down	ATAGTCGACGATGGTCCCCGGGTCCGAG	cloning of pLS29,pLS45
hVacid2190stop-Xbal	CGTCTAGATCAGCAGGCCCGGCTGGGGGAA	cloning of pLS36,pLS40,pLS42 and pLS44
hVacid2055stop-Xbal	CGTCTAGATCACTGGCAGTCCAGCCCGAGGGG	cloning of pLS37, pLS38,pLS41 and pS43
ER-hAcid1NTDup-stop	TACTGCTAGCTCACTCCACTGCATTCTGCGC	cloning of pLS45
hAcid1A335Vup	CAGGTGGTGGCTTGGGGACGCCAGGGGGTCTGG	cloning of

		pLS47,pLS48,pLS49
hAcid1A335Vdown	CCAGGACCCCCTGGCGTCCCCAAGCCACCACCTG	cloning of pLS47,pLS48,pLS49
JunRev	GACCCTCTCCCCTTGCAAC	mouse RT-PCR (c-Jun)
JunFW	ATACTCTCTCCCCGGCAAC	mouse RT-PCR (c-Jun)
FosBrev	AATGTTCCATGCAGCACGG	mouse RT-PCR (FosB)
FosBfw	CTCCAGCTTTCACCTCGTGAG	mouse RT-PCR (FosB)
hAcid1Y39Adown	GGGCTCCGCAAGCACGCCCTGCTCCCGGCCATC	cloning of pLS69
hAcid1Y39Aup	GATGGCCGGGAGCAGGGCGTGCTTGC GGAGCCC	cloning of pLS69
hAcid1Y66Adown	CTATGGGGGGACCCAGGCCAGCCTCGTGGTGTTCT	cloning of pLS67
hAcid1Y66Aup	GAACACCACGAGGCTGGCCTGGGTCCCCCATAG	cloning of pLS67
hAcid1Y152Adown	CTGCAACTACCCCCAGCCTTGTTCCTGCTGTTG	cloning of pLS64
hAcid1Y152Aup	CAACAGCAGGCAACAAGGCTGGGGGTGAGTTGCAG	cloning of pLS64
hAcid1Y161Adown	GTTGAGAGCACCCACGGCCTCTGGATGCACAACCTG	cloning of pLB65
hAcid1Y161Aup	CAGTTGTGCATCCAGAGGCCGTGGTGTCTCAAC	cloning of pLB65
hAcid1F47Adown	CCGGCCATCGAGTATGCTAATGGTGGTCCTCCTG	cloning of pLB66
hAcid1F47Aup	CAGGAGGACCACCATTAGCATACTCGATGGCCGG	cloning of pLB66
hAcid1F125Adownnew	CACAGCCTTGCAGCTGGCTGATGACTTCAAGAAG	cloning of pLS71
hAcid1F125Aup	CTTCTGAAGTCATCAGCCAGCTGCAAGGCTGTG	cloning of pLS71
hAcid1HMVL219AMAAdown	GAGCCAGGACCCGAGGGCCATGGCGGCGTTTCGGGGACTCGTG	cloning of pLS62
hAcid1HMVL219AMAAup	CACGAGTCCCCGAACCGCCGCATGGCCCTCGGGTCTGGCTC	cloning of pLS62
hAcid1VVFV17LVFLdown	GAGCGTGGTGGCCGACCTGGTGTCTTCTGATTGAGGGTACGGCC	cloning of pLS74
hAcid1VVFV17LVFLup	GGCCGTACCCTCAATCAGAAACACCAGGTGCGCCACCACGCTC	cloning of pLS74
hAcid1RK186AAdown	CTCCATTGTGTCTCCCGCGGCGCTGCCTGCGCTTCGG	cloning of pLS70
hAcid1RK186AAup	CCGAAGCGCAGGCAGCGCCGCGGGAGACACAATGGAG	cloning of pLS70
hAcid1T138Adown	GAGCAGATTGGCCAGGCGCACCGGTCTGCCTC	cloning of pLS73
hAcid1T138Aup	GAGGCAGACCCGGTGCCTGGCCAATCTGCTC	cloning of pLS73
hAcid1W408Adown	GAGCGGGGTCTGGAGGCGCAAGAGAAACCCAAAC	cloning of pLS59
hAcid1W408Aup	GTTTGGGTTTCTCTTGCCTCCAGGACCCCGCTC	cloning of pLS59
hAcid1WPQK444APQAdown	CTGAAGACGGAGCAGGCGCCCCAGGCGCTGATCATGCAGCTC	cloning of pLS58
hAcid1WPQK444APQAup	GAGCTGCATGATCAGCGCCTGGGGCGCCTGCTCCGTCTTCAG	cloning of pLS58
hAcid1KKIF518AAlAdown	CTGTACTCGTCCAAGGCGGCGATCGCCATGGGCTCATCCCC	cloning of pLS60
hAcid1KKIF518AAlAup	GGGGATGAGGCCCATGGCGATCGCCGCTTGGACGAGTACAG	cloning of pLS60
hAcid1YR487AAAdown	GTCTCTCAAAGGCTCGCCGCATCATGGGCAACGGC	cloning of pLS63
hAcid1YR487AAup	GCCGTTGCCCATGATGGCGGCGAGGCCTTTGAGAGAC	cloning of pLS63
hAcid1FHF473AAAAdown	CTCAAGGATGGTCCAGGCGCTGCCACCAACAAGGACCTG	cloning of pLS57
hAcid1FHF473AAAup	CAGGTCCTTGTGGTGGCAGCGGCTGGACCATCCTTGAG	cloning of pLS57
hAcid1KT443AAAdown	CATGGCGAGAACCCTGGCGGCGGAGCAGTGGCCCCAG	cloning of pLS72
hAcid1KT443AAup	CTGGGGCCACTGCTCCGCCGCCAGGTTCTCGCCATG	cloning of pLS72
hAcid1FR465AAAdown	CACCCTGGGCCCTTTGGCCGCGAACTCAAGGATGGTC	cloning of pLS68

hAcid1FR465AAup	GACCATCCTTGAGTTCGCGGCCAAAGGGCCAGGGTG	cloning of pLS68
hAcid1LRSL646ARSAAdown	GGGGCCAACCCTCAGGCGCGAAGCGCCGCCCTCAACCCACCACCG	cloning of pLS61
hAcid1LRSL646ARSAUp	CGGTGGTGGGTTGAGGGCGGCGCTTCGCGCCTGAGGGTTGGCCCC	cloning of pLS61
newhcJunFW	GAGAGGAAGCGCATGAGGA	human RTPCR(cJun)
hcJunrev210705	CCACCTGTTCCCTGAGCAT	human RTPCR(fosB)
newFosB last 2 exons FW	TCACCCCAGAGGAAGAGGAGA	human RTPCR
hfosbrev210705	TCCGACTCCAGCTCTGCTTT	human RTPCR
Med25Q137Afw	CGCGAGCAGATTGGCGCGACGCACCGGGTCTGC	cloning of pLS79
Med25Q137Arev	GCAGACCCGGTGCCTCGCGCCAATCTGCTCGCG	cloning of pLS79
Med25T138Dfw	GAGCAGATTGGCCAGGACCACCGGGTCTGCCTC	cloning of pLS80
Med25T138Drev	GAGGCAGACCCGGTGGTCTCGCCAATCTGCTC	cloning of pLS80
Med25NS147/148AAfw	GCCTCCTCATCTGCGCCGCACCCCCATACTTGTTG	cloning of pLS81
Med25NS147/148AArev	CAACAAGTATGGGGGTGCGGCGCAGATGAGGAGGC	cloning of pLS81
Med25Y151Ffw	GCAACTCACCCCATCTTGTTCCTGCTGT	cloning of pLS82
Med25Y151Frev	ACAGCAGGCAACAAGAATGGGGGTGAGTTGC	cloning of pLS82
Med25E157Rfw	CTTGTTGCCTGCTGTTCCGAGCACCACGTA CTCTG	cloning of pLS83
Med25E157Rrev	CAGAGTACGTGGTGTCCGAACAGCAGGCAACAAG	cloning of pLS83
Med25Y161Ffw	GTTGAGAGCACCACGTTCTCTGGATGCACA ACTG	cloning of pLS84
Med25Y161Frev	CAGTTGTGCATCCAGAGAACGTGGTGTCTCAAC	cloning of pLS84
Med25E167Afw	ACTCTGGATGCACA ACTGCGAATCTTGTGCAGCAG	cloning of pLS85
Med25E167Arev	CTGCTGCACAAGATTCGAGTTGTGCATCCAGAGT	cloning of pLS85
Med25ER175/176AAfw	GTGCAGCAGATTGGGGCGGCGGGGATCCACTTCTCC	cloning of pLS86
Med25ER175/176AArev	GGAGAAGTGGATCCCCGCCGCCCAATCTGCTGCAC	cloning of pLS86
BCL2_RT_fw	TCGCCCTGTGGATGACTG	human RTPCR (BCL2)
BCL2_RT_rev	GGCAGGCATGTTGACTTCAC	human RTPCR (BCL2)
hVacidEcorI	GGAATTCGAGGCTGCCAAGAACCAGAAG	cloning of pLS35, pLS36, pLS37
hVacid ende XbaI	CGTCTAGATTA AAAAGGAACTTTATTGGG	cloning of pLS35, pLS39
hPC6-ATG-EcorI	GGAATTCATGGTCCCCGGGTCCGA	cloning of pLS38
hVacid NLS XhoI	CCGCTCGAGCCCAAGAAGAAGCGGAAGGTGGAGGCTGCCAAGAACCAGAAG	cloning of pLS39, pLS40, pLS41
hPC6ATGNLSXhoI	TCGAGCCCAAGAAGAAGCGGAAGGTGATGGTCCCCGGGTCCGAGGGC	cloning of pLS42, pLS43

## 2.2 Molecular biology

### 2.2.1 Cloning

For each cloning step described, standard protocols were employed for restriction digestion, dephosphorylation, ligation and transformation of bacteria. In general, DNA digestions were carried out from a minimum of 2 hours to overnight at 37°C using 2 units of enzyme (Fermentas MBI or New England Biolab) per µg of DNA. In the case of vectors, phosphate groups were removed by adding Calf Intestine Alkaline Phosphatase (CIAP, Fermentas MBI) to the digest solution for an additional hour. Before ligation DNA vectors or fragments were purified with PCI (Phenol Chloroform Isoamil 25/24/1, Roth) and precipitated with EtOH 100% or purified over an agarose gel and recovered using the Gel Band Purification Kit (Amersham, Cat. N. 27–9602–01). Vector backbone and insert were ligated overnight at 16°C usually in a 1:3 ratio in a total volume of 30µl using 2 µl of T4 DNA ligase (Fermentas MBI, Cat. N. EL0015). Transformation of competent cells was performed mixing 15µl of ligation solution with 50µl of bacteria (usually DH5α) and leaving them in ice for 10–15 minutes. After heat shock, which was taking place at 42°C for 45 seconds followed by 1–2 minutes in ice, cells were diluted in 1 ml LB medium and shaken at 37°C for 1 hour. Bacteria were finally centrifuged at full speed for 30 seconds at RT, resuspended in 100µl of left over LB and plated in LB–agar plates containing 100µg/ml Ampicillin (or any other suitable antibiotic) where they were growing overnight at 37°C. Single colonies were used to inoculate 3ml of LB medium and left overnight at 37°C shaking. The following day DNA was extracted from the bacteria cultures via mini preps, performed using the miniprep kit (Amersham) according to the manufacturer's instructions. Positive clones were verified by restriction digest and re-transformed to be able to inoculate bigger amounts of culture (100–200ml) which were processed for DNA extraction using midi or maxiprep kits (NucleoBond or Qiagen).

**MED25 conditional knock-out targeting vector (pLS20):** the back-bone of the targeting construct (pLS11, 7666bp) was made by fusing two plasmids, pLS9 (kindly provided by Capecchi and described by (Moon and Capecchi, 2000)) and pLS10. A SpeI/ClaI fragment containing a Neomycin cassette was removed from pLS10 and replaced with a 3421bp SpeI/ClaI fragment cut from pLS9 and containing a *FRT*-flanked

Neomycin cassette followed by a *loxP* site. Methylation of *Clal* site in DH5 alpha bacterial strain makes the restriction of this DNA sequence not possible. Therefore, in order to be able to perform this cloning step, both plasmids were expressed in a Dam negative bacterial strain called GM2163. Beside this step, the rest of the cloning was carried out using DH5 $\alpha$  bacteria. A 300bp *Ascl*/*SpeI* fragment was removed from pLS11, blunt ends generated by feeling in the overhanging sequences with Klenoow, and finally the plasmid re-ligated to create the vector pLS12 (7300bp). An 8000bp *BglIII* fragment containing the genomic sequence of MED25 from exon 1 to exon 10 was cut from pLS2 (BAC clone selected from a 129/Ola mouse cosmid library via Dot blot analysis) and inserted in a pCI vector (pLB27A) generating pLS13. In the mean time, the homologous recombinant region 3' was synthesized by PCR using PC6HRR3'down and PC6HRR3'up primers and pLS2 as template. The fragment was cut with *SmaI* and inserted through the same restriction site in pLS12, generating pLS14. A missing DNA sequence of 200bp belonging to the intron 10 was also synthesized by PCR, using PC6intron10down and PC6intron10up primers on pLS2 DNA template and cut with *BamHI* and *BglIII* in order to clone it into pLS14 through the *BglIII* site. Ligation (creating pLS17) was possible due to the fact that *BamHI* and *BglIII* are isoschizomer. At this point the 8000bp *BglIII* genomic fragment coming from pLS13 was inserted in pLS17 with the generation of pLS18. The targeting vector pLS20 was resulting from last step of cloning where the annealed oligos PC6/*loxP*downEcoRV and PC6/*loxP*upEcoRV were cloned in the *SpeI* site of pLS17, therefore introducing a second *loxP* site, and an additional EcoRV restriction site necessary to discriminate in between homologous recombinant and wild type during the southern Blot analysis of the selected ES clones.

**pLS29, pLS45 and pLS53:** A *Sall*/*NheI* DNA fragment was removed from pEP7 (gb233, expressing ER–Notch) and replaced with PCR fragments coding either for MED25 full length (pLS29) or for NTD (pLS45). Alternatively the plasmid was re-ligated to generate pLS53 expressing only for the ER–LBD. PCRs were performed using pLB58 (human MED25 cDNA, clone DKFZp434K0512Q2, Gene Bank Acc. N. AL136746) as template and the following primer pairs for the synthesis of pLS29 and pLS45 respectively:



ER–Acid1down (5' ATAGTCGACGATGGTCCCCGGGTCCGAG 3')

ER–Acid1up (5' CGCGGCTAGCTTAAAAAGGAACTTTATTGGGTGT 3')

ER–Acid1down (5' ATAGTCGACGATGGTCCCCGGGTCCGAG 3')

ER–hAcid1NTDup–stop (5' TACTGCTAGCTCACTCCACTGCATTCTGCGC 3')

The following amounts of each component were used in the PCR reaction:

DNA template (100ng/μl)	1μl
dNTPs(25mM)	0.6μl
10x Buffer Pfu (–MgSO <sub>4</sub> , MBI)	5μl
MgSO <sub>4</sub>	4μl
Pfu (MBI)	0.5μl
Primer 1 (100pmol/μl)	0.25μl
Primer 2 (100pmol/μl)	0.25μl
DMSO 50%	5μl
H <sub>2</sub> O	33.4μl

PCR program:

1.	95°C	3 minutes	
2.	95°C	1 minute	
3.	60°C	1 minute	
4.	72°C	3 minutes	2x4
5.	95°C	1 minute	
6.	66°C	1 minute	
7.	72°C	3 minutes	5x21
8.	72°C	5 minutes	
9.	4°C	∞	

**pLS35, pLS36, pLS37, pLS38:** DNA fragments coding for MED25<sub>290–754</sub>, MED25<sub>290–730</sub>, MED25<sub>290–685</sub>, MED25<sub>1–685</sub>, respectively, were synthesized by PCR using pLB58 as

template (human MED25 cDNA, clone DKFZp434K0512Q2, Gene Bank Acc. N. AL136746) and the following primer pairs:

pLS35: hVacidEcoRI  
hVacidendeXbal  
pLS36: hVacidEcoRI  
hVacid2190stopXbal  
pLS37: hVacidEcoRI  
hVacid2055stopXbal  
pLS38: hPC6ATGEcoRI  
hVacid2055stopXbal

The following amounts of each component were used in the PCR reaction:

DNA template (100ng/μl)	1μl
dNTPs(25mM)	0.6μl
10x Termobuffer (NEB)	5μl
Vent Polymerase (NEB)	0.2μl
Taq Polymerase (MBI)	0.4μl
Primer 1 (100pmol/μl)	0.25μl
Primer 2 (100pmol/μl)	0.25μl
DMSO 50%	5μl
H <sub>2</sub> O	37.3μl

The employed PCR program was the same as the one previously described for pLS29 and pLS45, except for the annealing temperatures which were 45°C at step number 3 and 60°C at step 6 respectively. Each PCR fragment was cut with EcorI/Xbal and inserted in a plasmid named pLS65, in frame with its GAL/Myc-tag on the 5' site.

### 2.2.2 Site directed mutagenesis

Med25 point mutants were generated following the principle of QuickChange Site-Directed Mutagenesis Kit (Stratagene). GAL4-MED25 expressing vector was used as a template for all MED25 mutants. Oligonucleotide primers containing the desired mutation and complementary to opposite strands of the vector were designed according to the manufacturers instructions. The primers used for the synthesis of each MED25 mutant are listed in table 6. Extension of the primers was performed during temperature cycling by Pfu Turbo DNA polymerase (Stratagene). Incorporation of the oligonucleotide primers generated a mutated plasmid containing staggered nicks. Amounts of each component in the PCR reaction were used as follows:

DNA template (1ng/μl)	10μl
dNTPs(25mM)	1μl
10x Buffer	5μl
Pfu Turbo (2.5U/μl)	1μl
Primer mix (1pmol/μl)	20μl
H <sub>2</sub> O	13μl

PCR program:

1.	95°C	30 seconds
2.	95°C	30 seconds
3.	55°C	1 minutes
4.	68°C	16 minutes 2x16
5.	68°C	10 minutes
6.	4°C	∞

The product of PCR reaction was treated for a minimum of 2 hours with 1μl of DpnI endonuclease (NEB) which, being specific for methylated and hemymethylated DNA, is used to digest the parental DNA template and to select for mutation-containing synthesized DNA. The selected mutated plasmid was then transformed into XL2-Blue

supercompetent cells (Stratagene), or into high efficiency GC5 competent cells (Ampliqon IIII) following the manufacturers instructions.

### 2.2.3 RT-PCR

RNA was extracted from NIH-ER and NIH-ER-MED25 cell lines using the Qiagen RNeasy Mini, Midi or Maxi kit (Qiagen) according to the manufacture's instructions and depending on the cell's number. To eliminate residual amounts of genomic DNA, samples were treated with DNase either on the columns during the RNA extraction process using RNase-Free DNase Set (Qiagen, Cat. N. 79254), or using DNase I (Invitrogen, Cat N. 18068-015) after extraction and determination of RNA concentration. In this second case 5µg of isolated RNA were mixed with 1µl of DNase, 1µl of 10x buffer in a total volume of 10µl and incubated for 15 minutes at RT. Reaction was stopped by adding 1µl of 25mM EDTA and by heat inactivation at 65°C for 10 minutes. All the reagents were upscaled when the amount of RNA to be treated was higher. At this point about 1-2µg of DNase treated RNA were subjected to reverse transcription according to the protocol reported by the ThermoScript™ RT-PCR System (Invitrogen, Cat. N. 11146-024). The oligo dT provided by the kit was used to synthesize the first strand. The reaction was carried out at 50°C for 1 hour followed by a denaturation step at 85°C for 5 minutes. cDNA was stored at -20°C or immediately used for quantitative Real-Time PCR to reveal differences in the amount of transcripts coming from OHT stimulated samples. For this purpose the SYBR Green PCR reagents (Applied Biosystems, Cat. N. 4306736) and gene specific primers were employed as follows:

SYBR Green buffer	2.5µl
MgCl <sub>2</sub> (25mM)	2.5µl
dNTP mix	2.0µl
AmpliTaq Gold DNA polymerase (5U/µl)	0.2µl
AmpErase UNG (1U/µl)	0.2µl
H <sub>2</sub> O	13.6µl
cDNA	2.0µl
primer mix (5pmol/µl each)	2.0µl

Primers were designed with a melting temperature ( $T_m$ ) of 58°C.  $\beta$ -Actin primers were always included as a reference control. Samples obtained from reverse transcription reactions carried out without reverse transcriptase were used as negative control. PCR reactions were performed in a Applied Biosystem GeneAmp 5700 instrument setting the program to 40–45 cycles.

#### 2.2.4 Microarrays

**NIH-ER-MED25 Microarrays:** About  $2 \times 10^7$  cells/sample were collected 3 hours and 10 hours after stimulation with 1mM OHT. Since the time course experiment was performed in two different moments, a sample of nonstimulated cells (NS) was collected for each time point, with a total amount of 4 samples (NS<sub>3 hours</sub>, 3 hours, NS<sub>10 hours</sub>, 10 hours). RNA was extracted from the cells using the Qiagen RNeasy Midikit (Qiagen) according to the manufacturer's instructions. RNA, without DNase treatment, was sent to the lab of dr. Johannes Beckers (IEG, GSF, Neuberger) where a microarray analysis was carried out as follows.

##### Chip design

A glass-surface DNA-chip containing  $\approx 21000$  probes was used. About 20200 of these probes are from the commercial Lion mouse array-TAG clone set, which is mostly derived from 3'UTRs. All Lion probes have been sequenced. The remaining probes were isolated in a subtractive screen for differentially expressed genes in the mesoderm of Delta/Notch pathway deficient mouse embryos. Mouse array-TAG clones have the general ID MG-VW-XYZ and the Delta/Notch specific probes are named rda-X.

##### DNA microarrays

PCR products with 5'-aminogroup were amplified from the mouse array TAG library from Lion Bioscience comprising approximately 20200 clones (Heidelberg, Germany). PCR products were dissolved in 3-fold SSC buffer and spotted on aldehyde-coated slides (Telechem, USA) using a Microgrid TAS II spotter (Biorobotics) with 48 Stealth<sup>TM</sup> SMP3 pins (Telechem). Spotted slides were rehydrated overnight in a humid chamber containing 50–70% aqueous solution of glycerol. Rehydrated slides were immersed in blocking solution (0,1M sodium borohydride in 0,75 fold PBS with 25% ethanol) for 5 minutes, boiled in water for 2 minutes, briefly immersed in 100% ethanol

and air-dried. Slides were pre-hybridised for 1 hour in pre-hybridisation buffer (6-fold SSC, 1%BSA, 0,5%SDS) rinsed in water, dried and hybridised the same day.

#### Reverse Transcription and Fluorescent Labelling

For labelling 20µg of total RNA were used for reverse transcription and indirectly labelled with Cy3 or Cy5 fluorescent dye according the TIGR protocol ([http://pga.tigr.org/sop/M004\\_1a.pdf](http://pga.tigr.org/sop/M004_1a.pdf)). Labelled cDNA was dissolved in 30µl hybridisation buffer (6x SSC, 0,5% SDS, 5 fold Denhardt's solution and 50% formamide) and mixed with 30µl of reference cDNA solution labelled with the second dye. This hybridisation mixture was placed on a pre-hybridised microarray, under a cover slip, placed into a hybridisation chamber (Genetix) and immersed in a thermostatic bath at 42°C for at least 16 hours. After hybridisation slides were washed in 40ml of 3x SSC, 40ml of 1x SSC and 40ml of 0.25x SSC at room temperature. For drying slides were placed in an empty 50ml Falcon tube (Becton Dickinson, USA) and centrifuged at 4000 m/s<sup>2</sup>. Dried slides were scanned with a GenePix 4000A microarray scanner and the images were analysed using the GenePix Pro3.0 image processing software (Axon Instruments, USA). All data were normalised by adjusting the median of log-ratios of Cy5 to Cy3 intensities to 0. For data analysis in-house produced LabView based software was used.

**721-ER-MED25-NTD Affymetrix arrays:** About  $1 \times 10^7$  cells/sample were collected 1 hour, 10 hours and 24 hours after stimulation with 1mM OHT. One sample of nonstimulated cells (NS) was also included as a reference sample. RNA was extracted from 4 samples (NS, 1 hour, 10 hours, 24 hours) using the Qiagen RNeasy Minikit (Qiagen) according to the manufacturer's instructions. During the extraction process, RNA was treated with the RNase-Free DNase Set (Qiagen, Cat. N. 79254). RNA concentration was determined using a spectrophotometer and about 1µg/sample was sent to the company KFB, Regensburg, where affimetrix arrays were performed. For this analysis an Affymetrix Human Genome U133 Plus 2.0 Array GeneChip was employed. This chip is characterized by a complete coverage of the human genome and it is suitable for an analysis of over 47000 transcripts. It includes a total number of 54675 probe sets the sequences of which are derived from GenBank®, dbEST and RefSeq. The company in charged for the analysis sent to us a list of genes up and down-

regulated at each time point which was obtained comparing each experimental sample (derived from cells stimulated with OHT) to the baseline sample (derived from non stimulated cells). In order to reduce the number of false positives and consider only statistically relevant genes the mentioned list was additionally sorted following the instructions suggested by the GeneChip® Expression Analysis manual.

To determine robust increases:

- Probe sets in the experimental sample called "Absent" were eliminated
- Probe sets called "Increase" were selected
- 

To determine robust decreases:

- Probe sets in the baseline sample called "Absent" were eliminated
- Probe sets called "Decrease" were selected

Additionally, the genes indicated with MI (marginal increase) and MD (marginal decrease) were eliminated.

### **2.2.5 Dot blot**

Before starting to generate the MED25 conditional knock-out targeting vector an analysis of the eight pBAC clones (from library N. 121, 129/Ola mouse cosmid) received from the rzpd screening service was made to identify which of them was containing a large portion of MED25 genomic locus. These clones were selected from the center using a probe that was synthesized by PCR using the primers PC6PreExon1 and PC6exon1down on a DNA template named pLB52 (GeneBank Acc. N. AC069498, mus Musculus chromosome 7 in pBACe 3.6 vector). DNA was prepared from each clone via minipreps and from the first three clones also via maxipreps. 3µl of each sample were mixed with 0.3µl EDTA 200mM, 0.8µl of NaOH 1M and heated at 100°C for 10 minutes. After cooling down in ice for 5 minutes, samples were briefly span down before use. 22 squares were drown on a membrane which was pre-equilibrated in water, quickly dried and spotted with the DNA in duplets as described in the following table:

**Table 7.** Distribution of the cosmid clones on the filter

<b>SQUARE'S NUMBER</b>	<b>CLONE'S NAME</b>
1–2	pLS1
3–4	pLS2
5–6	pLS3
7–8	pLS4
9–10	pLS5
11–12	pLS6
13–14	pLS7
15–16	pLS8
17–18	pLS1 (maxi prep)
19–20	pLS2 (maxi prep)
21–22	pLS3 (maxi prep)

Membrane was incubated in a rotating cylinder with 10ml of dot– blot pre– hybridisation solution for 3–4 hours at a temperature equal to the  $T_m$  of the used oligoprobe subtracted of 20 degrees (i.e.  $54^\circ\text{C}$  for  $T_m=74^\circ\text{C}$ ). The oligos used as probes for this analysis are listed below:

PC6prepreExon1

PC6exon1up

PC6Exon3up

PC6exon9up

PC6Exon14down

Oligoprobes were synthesized mixing together the following components and incubating them for 20 minutes at  $37^\circ\text{C}$ :

5 pmol	oligo
1x	PNK buffer (MBI)
50 $\mu\text{Ci}$	[ $\gamma$ <sup>32</sup> P] ATP
1.5 $\mu\text{l}$	PNK (MBI)
to 20 $\mu\text{l}$	H <sub>2</sub> O

An additional amount of 0.5 $\mu\text{l}$  of PNK was added to the mixture and incubated for another 20 minutes. Finally the radio–labelled probe was added to the pre–hybridization solution and incubated overnight. The following day, the membrane was washed at RT in 6x SSC solution for 15 minutes. After an inspection of the counts with a Geiger–



counter, an additional wash was performed at 40°C for 15 minutes. Once the counts were reaching about 200cpm, the filter was sealed in a plastic bag and exposed to X-ray film (Kodak BioMax MS) at -80°C for 2 days.

### 2.2.6 Genomic DNA extraction

**From 96 well plates:** Genomic DNA was extracted from 96 well plates where TBV2 ES cells were let overgrow. Once removed from the incubator cells were washed twice with 100µl PBS and left in 50µl ES cells lysis buffer overnight at 56°C, after sealing the plates with parafilm and placing them in a humid chamber. The following day plates were removed from the incubator and left at RT for about one hour. 100µl of EtOH 100% were added to each well for another hour to provoke DNA precipitation. After precipitation to the bottom of the wells, DNA was washed 3 times with EtOH 70% turning gently the plate up side down. To get ready for the Southern blot analysis DNA was finally resuspended in 34µl of the following solution:

1mM	Spermidine
1mM	DTT
100µg/ml	BSA (NEB)
50µg/ml	RNase
1X	Buffer (NEB)
20U	BglII (50U/µl, NEB) or EcoRV (100U/µl)

Digestion was carried out overnight at 37°C. The following day 7µl of 6X DNA loading buffer were added to each well and the plate sealed with parafilm and stored at -20°C.

**From expanded clone 5A cells:** Genomic DNA was extracted from expanded MED25 homologous recombinant ES cells to confirm the genotype of the positive clone 5A. Cells were let grow onto gelatin in 1 well of a 6 well plate until confluent and then trypsinized, pelleted, washed with PBS, resuspended in 500µl of ES cells lysis buffer and incubated overnight at 56°C. To eliminate the protein content, lysate was divided in two aliquots of 250µl, and each aliquot mixed with 800µl Phenol/Clorophorm/Isoamil

(PCI, Roth). After centrifugation at full speed, the water fraction was collected and DNA precipitated by adding 40µl of a 3M Sodium Acetate solution and 800µl of EtOH 100%. DNA was then pelleted, washed with EtOH 70% and resuspended in TE buffer.

**From mouse tails:** Genomic DNA was extracted from mouse tails collected from the offspring of MED25 conditional knockout chimeras. 5–10mm of tail were cut and placed in an Eppendorf tube and left overnight at 56°C in 500µl of tail lysis buffer moderately shaking. Hair and cell debris were pelleted centrifuging the samples at full speed for 5 minutes. The supernatant was transferred into a new Eppendorf tube and mixed with 500µl of isopropanol to allow DNA precipitation. After full speed centrifugation for 15 minutes, supernatant was discarded and the pelleted DNA was washed twice with 250µl of EtOH 75%, and let dry at RT. Genomic DNA was finally resuspended in 100µl TE buffer and gently shaken for 1–2 hours at 37°C. From this preparation 15µl were used for Southern blot analysis.

### 2.2.7 Southern blot

The identification of the homologous recombinant ES cell clone for MED25 conditional knock-out was accomplished analysing genomic DNA extracted from double selected ES cell clones via Southern blot the surviving the double selection. 0.8% agarose gels were made in big chambers containing 75 pockets, and loaded with 40µl/well of genomic DNA collected in the 96 well plates (see paragraph 2.2.6). Gels were running in TAE buffer overnight at RT and at 27 Volts. After about 16 hours gels were photographed under UV light. To favour the transfer of fragments which are bigger than 10kb, depurination was promoted leaving gels in 0.25N HCl solution for 15–20 minutes on a shaker at a very low speed. Gels were then briefly washed with water and equilibrated for 45 minutes in alkaline transfer solution. The transferring of the DNA fragments onto a charged nylon membrane (Hybond-N+, Amersham, Cat.N. RPN 203B) was carried out for a minimum of 3 hours downward as follows. A 3–4 cm layer of paper towel was used as a base on top of which from bottom to top were placed as listed:

- 4 sheets of dry Watman paper
- 1 sheet of Watman paper soaked in transfer buffer
- 1 gel sized nylon membrane pre-equilibrated with buffer
- the agarose gel
- 4 sheets of Watman paper soaked in transfer buffer

The last sheet of Watman paper was reaching a box containing transfer buffer, placed at a higher level to direct the buffer floss and the transfer of the DNA from top to bottom. On top of everything were placed a plate of glass and a thick book. After blotting, the membrane was rinsed and neutralized with 2x SSC buffer, sandwiched in between 2 sheets of Watman paper and baked for 30–60 minutes at 80°C to fix the DNA. Prehybridization was carried out at 65°C for a minimum of 15 minutes placing the membrane into a rotating cylinder with 15 ml of Rapid Hyb Buffer (Amersham, Cat. N. RPN 1635). Once synthesized, 38µl of the <sup>32</sup>P radio labeled probe were added to the prehybridization solution and incubated again for a minimum of 2 hours. For the synthesis of the probes 25ng of DNA were radioactively labelled with 50 µCi of [ $\alpha^{32}$ P]dATP using the Megaprime DNA labelling system Kit (Amersham, protocol 1606) according to the manufacturer's instructions. Unincorporated radiolabelled nucleotides were removed with MicroSpin columns G25 (Amersham) to reduce background during hybridization. The probe was denatured at 95°C for 5 min, before it was added to the hybridisation solution. Probe Neo was a 383bp fragment obtained by PstI/NcoI restriction of a Neomycin cDNA contained in a pBluescript vector provided by Nathalie Uyttersprot. The following primers were used for the synthesis of the probes A and B' by PCR on the genomic DNA template pLS2:

probe A (660bp)	PC6PreExon1 (5' ACTGCTTCGCTTCCAAGTCCCG 3')
	PC6exon1down (5' ACTCTATGGCAGGCAGCAGGTA 3')
probe B' (540bp)	PC6probeBup (5' CCCAGGCAGAGTACTGTTGGTC 3')
	PC6probe3'down (5' CCCTCAGACTCTCAGGGGACTG 3')

After hybridisation, the membrane was washed at 65°C for 20 minutes with 2x SSC/0.1% SDS solution, for 15 minutes with 1x SSC/0.1% SDS solution and for 15

minutes with 0.1x SSC/0.1% SDS solution. Finally the filter was monitored with a Geiger counter and the washes were stopped when specific signals reached 30 to 60 cps. Then, the filter was sealed in a plastic bag and exposed to X-ray film (Kodak BioMAX MS) at  $-80^{\circ}\text{C}$  for a minimum of 16 hours.

## 2.3 Cell biology

### 2.3.1 Cell lines

Jurkat	Human T lymphoblastoid cell line, grow in suspension
HEK293T	Human embryonic kidney cell line, adherent
HeLa	Human epithelial cell line, cervical carcinoma, adherent
721B	Human B lymphoblastoid cell line, grow in suspension
HepG2	Human hepatoma cell line, adherent
NIH3T3	Murine fibroblast cell line, adherent

### 2.3.2 Growth conditions

Adherent cells were grown in Dulbecco's modified Eagle medium (DMEM plus 4500 mg/ml glucose, L-Glutamine, without pyruvate. Gibco Invitrogen, Cat. No. 11971-025) supplemented with 10% fetal bovine serum (FCS; Gibco Invitrogen, Cat. No. 10270-106) and 1% Penicillin-Streptomycin (Gibco Invitrogen, Cat. No. 15140-122) in culture dishes ranging from 15 and 10 cm down to 6 and 12 well plates (Nunc, Cat. No. 157150, 150350, 140675, 150628) in a tissue culture incubator under 5% CO<sub>2</sub> and at 37°C. Confluent cells were detached from the plates using 0.25% trypsin and 0.2% EDTA (Gibco Invitrogen, Cat. No. 25050-014) diluted 1:4 and seeded to a new plate. Suspension cells were grown in RPMI 1640 medium, L-Glutamine (Gibco Invitrogen, Cat. No. 21875-034), supplemented with 10% FCS and 1% Penicillin-Streptomycin. The suspension cells were grown in 25 to 175 cm<sup>2</sup> cell culture flasks. When the cells reached a density of 0.8–1x10<sup>6</sup> cells/ml, they were diluted to a new concentration of 0.2–0.4 x10<sup>6</sup> cells/ml. Cell lines transfected with EBV vectors expressing ER-tagged constructs were initially selected with 200µg/ml Hygromycin containing medium which

was replaced every 3 days for about 2 weeks. Once stable the cell line was cultured in maintenance conditions with 100µg/ml Hygromycin containing medium. To induce translocation of ER-tagged proteins into the nucleus, cells were feed at a given time with 4-hydroxytamoxifen (OHT) at a final concentration of 1µM.

### 2.3.3 Freezing and thawing conditions

Trypsinized adherent cells grown to a 90% confluence in 10 or 15 cm dishes or  $1 \times 10^7$  suspension cells, were pelleted and resuspended in 0.5–1ml of a cold solution containing 90% serum and 10% dimethyl-sulfoxide (DMSO, Sigma), aliquoted in cryovials (Nunc) and left for 24 hours at  $-80^{\circ}\text{C}$  before been stored in liquid nitrogen. For thawing, frozen aliquots were quickly hand wormed, resuspended in 10ml of their own medium, pelleted to remove residual amount of DMSO and resuspended in fresh growing medium. Adherent cells were then seeded in a dish the same size of the one they were frozen from, and suspension cells resuspended in 10ml medium and placed in a  $25\text{cm}^2$  flask at least for 24 hours and then diluted with fresh medium.

### 2.3.4 Transfection of the cells

**Calcium phosphate transfection:** HEK293T, NIH3T3 and HepG2 cells were transfected following a so called alternative protocol developed by Okayama and colleagues and described by (Sambrook, 1989), which is a modification of the classical calcium phosphate transfection method. In brief, the day before transfection cells were seeded in a 10cm plate, in 10ml growth medium, at 20% confluence in order reach 30–50% confluence at the moment of transfection. 16 to 24 hours later, a total amount of 20µg DNA at a concentration of 1µg/µl in 0.1xTE was mixed with 0.5ml of a 0.25M  $\text{CaCl}_2$  solution followed by addition of 0.5ml 2xBES-buffered-saline (BBS) solution, mixed and incubated for 10–20 minutes at room temperature. Before using them, the two solutions were also pre-equilibrated to a temperature of 20–25°C. The DNA- $\text{CaCl}_2$ -BBS mixture was then added drop wise to the dish of cells which was gently swirled to favorite distribution of the transfecting solution. After placing the cells in a humidified incubator in an atmosphere of 3.4%  $\text{CO}_2$  for 18–24 hours at 37°C, the old medium was substituted

with fresh one and normal growing conditions of 5% CO<sub>2</sub> re-established for another 24 hours. After about 48 hours cells were rinsed with PBS and harvested after leaving them for a minimum of 30 minutes in 3ml of cold PBS/EDTA 0.5mM solution. When using dishes or plates of a different size, cell density, DNA amount and reagent volumes were scaled accordingly.

In the specific case of HEK293T cells transfected with titrated amounts of MED25 mutants to analyze proteins expression in relation to the transcription activity, cells were plated in 6 well plates and transfected with 600ng of pGLMRG5, 60ng of β-Gal plasmid and 3 different concentrations (60, 300, 600ng) of MED25 derivative expression vectors (GAL-MED25<sub>1-754</sub>, pLS64, pLS70). pLB28 was used to complement the total amount of DNA to 1.2μg, 100μl of each transfecting solution was added to the DNA and distributed to the cells according to the protocol. After 48 hours cells were harvested with 3ml PBS/EDTA 0.5mM per well, of which 2 ml were processed to prepare nuclear extract and 1ml pelleted and resuspended in 100μl of reporter lysis buffer. 40μl of this cell lysate were used to perform the luciferase assay while 20μl were used for the β-GAL assay.

**PolyFect transfection:** HeLa cells were transfected using PolyFect reagent (Qiagen, Cat. N. 301105) according to the manufacturers protocol. In short, the day before transfection  $2 \times 10^5$  cells were seeded in a 6cm dish in 5ml of appropriate medium. The day of transfection cells were washed once with PBS and leaved in 3ml of fresh growth medium while 3μg DNA were diluted in 150 μl of DMEM without FCS or other additives and added to 25μl of PolyFect reagent. The Polyfect-DNA complexes were diluted with 1ml of complete medium and distributed to the cells. Because of the toxicity of the PolyFect reagent, cells were harvested after 24 hours using cold PBS/EDTA 0.5mM. When using dishes or plates of a different size, cell density, DNA amount and reagent volumes were scaled accordingly.

**Electroporation:** Jurkat cells were employed to test the transcription activity of GAL-fused MED25 deletion constructs or point mutants on a promoter carrying 5 GAL4 binding sites and fused to a luciferase reporter (pGLRGM5). Once reached a confluence of about  $0.5 \times 10^6$  cells/ml cells were pelleted and washed once with PBS. Cells were resuspended in growth medium without serum in a dilution of  $0.8-1.2 \times 10^7$  cells per

400µl medium per sample. The cell suspension was then distributed in electroporation cuvettes (Gene Pulser Cuvette, BioRad Cat. N. 165–2088) where it was mixed together with a total amount of 20µg DNA and left at RT for about 10–20 minutes. Beside the GAL4–fused luciferase reporter (pGLRMG5) and a GAL– MED25 derivative expression vector, an empty plasmid (pLB28) and a β–GAL plasmid were included to reach a total amount of 20µg DNA and to monitor the transfection efficiency, respectively. Per sample, the following amount of each plasmid was used:

pGLMRG5	10µg
β–GAL	1µg
MED25 derivative	5µg
pLB28	5µg

For the electroporation each cuvette was connected to a Gene Pulser electroporator (BioRad) and the conditions set to a capacitance of 975µF and a voltage of 250V. After the electric shock, cells were resuspended in 10ml medium per sample, transferred in 25cm<sup>2</sup> flasks and incubated at 37°C and 5% CO<sub>2</sub>. 36–48 hours later, cells were harvested for Luciferase or β–Gal assay.

**Stable transfection:** NIH3T3 cells were stably transfected with pLS29 expressing ER–MED25 or pLS53 expressing ER(LBD) randomly integrated in their genome. After failing to select NIH3T3 transfected with circular plasmid, 35µg of pLS29 or 24µg of pLS53 were linearized with NheI and with Sall respectively and 2x10<sup>6</sup> cells per each construct were transfected under 1000µF and 230V electroporating conditions. A mock control of cells electroporated without DNA was included in the experiment as a negative control. Transfected cells were resuspended in fresh growth medium and seeded in 6cm or 10cm plates. Selection with 200µg/ml Hygromycine was started after 24hours and was lasting for about two weeks. Only one surviving clone was selected from the cell line transfected with pLS29 while 5 clones were selected, expanded and frozen from cells carrying pLS53. The expression of ER(LBD) protein was checked by Western blot on the nuclear extract of each clone after induction by OHT. A single clone showing the expressed protein was used for further experiments. 721 B cells were stably transfected

with pLS45 episomally maintained and expressing ER–MED25–NTD. 15µg of circular pLS45 were mixed together with 5µg of pGFP plasmid (pML4) to control the transfection efficiency and with a cell suspension of  $5 \times 10^6$  cells in 400µl of medium without serum. Several conditions of electroporation were tested: 950µF/250V, 950µF/230V, 1000µF/250V, 1000µF/230V. Cells transfected at 230V were showing a higher transfection efficiency and were growing faster than the others. After about two weeks of selection in 200µg/ml Hygromycine the batch of cells transfected at 1000µF/230V were frozen in aliquots.

### **2.3.5 Luciferase assay and β–GAL assay**

Jurkat cells were harvested 36–48 hours after transfection, pelleted, washed once with PBS and resuspended in 200µl of 1x Reporter Lysis Buffer (Promega, Passive Lysis Buffer 5x, Cat. No. E194A). The lysate was collected in a Eppendorf tube and centrifuged at full speed for 10 minutes to clear the lysate. 40 µl were used for the luciferase assay (Promega, Luciferase Assay System, Cat. No. E1501). In the β–GAL assay, 40µl of the cell lysate were incubated together with 200µl of β–GAL substrate solution overnight at 37°C. After incubation time, the absorption at 420nm was measured in a 96 well plate reader (BIO–TEK INSTRUMENTS INC., EL800 Universal Microplate Reader) and the values used to normalize the luciferase counts to the transfection efficiency.

### **2.3.6 Immunofluorescence**

NIH–ER–MED25 or NIH3T3 cells were seeded at 20% confluence in 15cm plates on top of 4 microscope–slides previously bathed in EtOH 100% and dried. The following day OHT at a final concentration of 1µM was added to the medium. 4 hours later the medium was removed from the plates, and the cells washed with PBS and fixed on the slides for 5 minutes by addition of MeOH (–20°C) for 5 minutes to fix them on the slides. The slides were dried for about 30 minutes. At this point slides were either stored at –20°C or permeabilized with 1% Triton X–100/PBS for 10 minutes and soaked in sufficient volume of TBS–BG solution for a minimum of 15 minutes. Cells were removed



from the TBS–GB solution and the primary antibody ( $\alpha$ -ER sc543, Santa Cruz) diluted 1:50 in PBS was placed on top of them and leaved for about 1–2 hours in a humid chamber. Slides were washed 3 times for 5 minutes and then incubated for at least 30 minutes with a secondary antibody conjugated to the fluorescent dye and diluted 1:25 in a solution containing 0,5 $\mu$ g/ml DAPI (SIGMA Cat. No.–D9564) which stains the DNA and therefore makes the nucleus visible. This second incubation was carried out in a darkened humid chamber to prevent the dye from bleaching. After repeating the washing procedure described above, the slides were quickly dried and a drop of HistoGel mounting medium (Linaris) covered by a coverslip was placed right onto the cells. Before the microscope analysis slides were left at 4°C in the darkness overnight. The analysis of the samples was done with a Leica TCS SP2 confocal microscope.

### 2.3.7 Embryonic stem cell culture

TBV2 ES cells, the embryonic stem (ES) cells used in this work, are 129/Ola strain derived cells, created in the IEG department of GSF, Neuerberg. To maintain their pluripotency, ES cells were cultured in medium containing leukaemia inhibiting factor, (LIF, ESGRO, Chemicon International, Cat. N. ESG1107) on a layer of mitotically inactivated embryonic feeder cells (EMFI). The ES cell medium (DMEM, high glucose, sodium pyruvate, 15 % FCS, 2mM L–glutamine, 1000U/ml LIF, 0.1mM 2– $\beta$ –mercaptoethanol) contained FCS, which had been previously tested to promote ES cell growth and to prevent *in vitro* differentiation (PAA laboratories, Cat. N. A15041). ES and EF cells were grown in tissue culture dishes (Falcon) and kept at 37°C under humid atmosphere with 10% CO<sub>2</sub>. In normal conditions ES cell medium was changed in daily bases and cells diluted 1:4 every second day. EF cells were cultured in DMEM, high glucose, sodium pyruvate supplemented with 10% FCS, 2mM L–glutamine, 1x non essential amino acids and were never passaged more than three times. EF cells were mitotically inactivated by mitomycin–C treatment (10 $\mu$ g/ml for 2 h) before being cultured with ES cells. ES cell colony growth was stopped before they became confluent. Colonies were washed once with PBS and then treated shortly with trypsin (0.05 % trypsin, 0.02 % EDTA in PBS; Gibco) at 37°C, until the cells were detached from the dish. The cell suspension was then used for passaging, transfection, or freezing. ES

cells were frozen in 90% FCS, 10 % DMSO at  $-80^{\circ}\text{C}$  and later transferred into liquid nitrogen for long-term storage. For the transfection of the MED25 targeting construct, an aliquot of TBV2 ES cells at the 10<sup>th</sup> passage was thawed and plated on a 6cm plate. Cells were passaged in total 2 times before collecting enough cells for the electroporation. Two days before transfecting  $3 \times 10^6$  cells were distributed equally in 3 plates. 50 $\mu\text{g}$  of two preparations of the same MED25 targeting construct were linearized with NotI and resuspended in 50 $\mu\text{l}$  of PBS. The cells grown in the 3 plates were trypsinized, pooled together, and counted. Among them, 2 aliquots of  $10^7$  cells each were pelleted and resuspended in 750 $\mu\text{l}$  of transfection buffer (RPMI w/o phenol red, Gibco) and mixed together with 50 $\mu\text{l}$  of each preparation of linearized DNA. Cell were transfected under electroporating conditions of 500 $\mu\text{F}$  and 230V using a Gene Pulser II (BioRad) electroporator and left at RT for 10 minutes. Transfected cells were resuspended in 10ml of which 9ml were equally distributed onto embryonic feeder layer in 3 plates of 10cm. The remaining 1ml containing  $10^6$  cells was resuspended in 20ml and divided in 2 plates of 10cm and used as control plates.  $5 \times 10^5$  cells of non transfected cells plated in one 10cm were also used as control. 48 hours later (at day three after transfection) cells were placed under G418 (Geneticin G- 418 sulphate, 200  $\mu\text{g}/\text{ml}$ , 71% active, Gibco, Cat. N. 11811-023). Selection against HSV-*tk* containing random integrants started at day six after transfection by supplementing the medium with 2 $\mu\text{M}$  ganciclovir (Sigma, Cat. N. G2536). One of the control plates containing transfected cells was also treated as just described, while the other two (one with transfected cells and one with non transfected cells) were exclusively G418 selected. The comparison of these last two control plates allows monitoring of selection specificity, and helps to understand when it is time to start to pick colonies. The ratio of double selected colonies versus G418 selected colonies is defined as Ganciclovir enrichment, i.e. the theoretical enrichment of homologous recombinant versus random integrants while using Ganciclovir. In this experiment the number of colonies survived after G418 selection were 60 while the double resistant colonies were 20. This means that Ganciclovir killed 30% of the colonies that would have undergone G418 selection. Between day 9 and day 11 after transfection, about 500 double resistant colonies were picked, trypsinized in 5 round-bottom 96 well plates and split into 15 EMFI-containing 96-well tissue culture plates for expansion. In this way each clone was present in 3

different plates, one of which was kept in culture for longer time and finally divided in two 96 well plates treated with 0.1% gelatine (LGC Promochem, Cat. N. 440454B). Cells were kept in culture until overgrown, processed for DNA extraction and enzymatic restriction with BgIII and EcoRV and analysed by Southern blot. The other two plates were frozen at day 5 and day 7, respectively, after picking. To freeze the cells in the 96 well plates, cells were washed twice with 100µl/well PBS and left for 10 minutes in 50µl/well of trypsin containing 2% Chicken Serum. 50µl of 2x freezing medium (20% DMSO, 80%FCS) were added to each well, mixed and covered by 100µl of light oil (Sigma, Cat. N. M8410). Quickly, plates were closed and sealed with parafilm, embedded in several layers of cellulose paper sheets and stored at  $-80^{\circ}\text{C}$  until the end of the Southern blot analysis. A schematic view of the steps followed from the electroporation of MED25 targeting construct to the end of the selection process is given in figure 8).

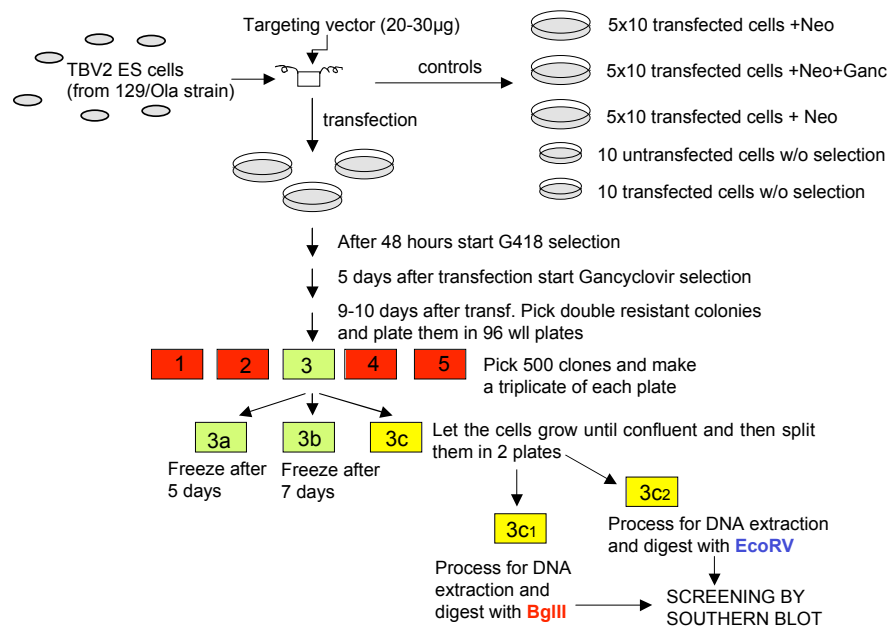


**Figure 8.** Schematic view of the steps followed to generate ES cell line containing a MED25 conditional allele.

Once finished the Southern blot analysis, the random integrant ES cell clone 5A identified was thawed from the plate which was frozen 5 days after picking. Therefore, the plate was partially immersed in few milliliters of water at  $40^{\circ}\text{C}$ , and the 100µl of

suspension cells removed from the well (avoiding to aspirate the mineral oil as well) and transferred in a 24 well plate. The cells were divided 1:2 every second day for four times and then partially processed for DNA extraction for confirmation of the genotype and partially frozen for stock storage (4 aliquots from 6cm plate each). For blastocyst injection one of these vials was thawed and plated in a 6cm dish containing feeders and 2 days later splitted 1:3 in gelatine plates, in order to be injected the following day. The injection process was carried out in the IEG department of GSF, Neuerberg.

## **2.4 Biochemistry**

### **2.4.1 Isolation of nuclear extract from HEK 293T and 721B cells**

48 hours after transfection (in the case of HEK 293T cells) or at a given time after OHT induction (in the case of 721-ER-MED25-NTD cell line), cells were harvested and washed with cold 1X PBS. Pelleted cells were then resuspended in cold NEX A buffer and left in ice for 10 minutes and permeabilized with a 0,2% final concentration of NP40 for 5 minutes. Nuclear membranes were broken mechanically using a douncer and cytoplasm was removed after centrifugation of the homogenized cells at about 200–1000g. Pellet was resuspended in NEX B buffer to a final salt concentration of 0.27M and rocked at 4°C for a minimum time of 30 minutes. Finally, samples were centrifuged at 16000g and protein concentration of supernatants was determined using Bradford reagent (BioRad).

### **2.4.2 Sodium dodecyl sulphate polyacrylamide gel electrophoresis (SDS PAGE)**

Protein were separated on an SDS-PAGE using either a maxi-gel system from Hoefer or the mini-gel system from Bio-Rad. Depending of the size of the protein, either 12–15% 170:1 acrylamide/bisacrylamide gels or 17% 85:1 acrylamide/bisacrylamide gels were used. For electrophoresis, proteins were mixed 1:6 with 6x loading buffer, heat denatured at 95°C and loaded onto the gel. Proteins were separated applying a current of 25mA for the mini-gels and 35mA for the maxi-gels. In both cases the running buffer was 1x TGS. The maxi-gels were connected to a cooling

system. For molecular weight determination, unstained marker was run in parallel (Bio–Rad, SDS–PAGE standards Low Range, Cat. No. 161–0304; Bio–Rad, SDS–PAGE standards High Range, Cat. No. 161–0303). Following electrophoresis, proteins were stained with Coomassie Brilliant blue G250 or subjected to Western blotting.

**Table 8.** Components for different percentages of SDS PAGE

	12%	15%	17%	stacking gel
<b>GelA (Roth, Cat.N.3037.1)</b>	4ml	5ml	5.7ml	1.7ml
<b>GelB (Roth, Cat.N.3039.1)</b>	0.35ml	0.44ml	1ml	0.7ml
<b>1.5M Tris–HCl (pH 8.8 RT)</b>	2.5ml	2.5ml	2.5ml	
<b>1M Tris–HCl (pH 6.8 RT)</b>				1.25ml
<b>H<sub>2</sub>O</b>	3ml	2ml	0.8ml	6.2ml
<b>10% SDS</b>	0.1ml	0.1ml	0.430	0.1ml
<b>30% APS</b>	23µl	23µl	23µl	35µl
<b>TEMED</b>	6µl	6µl	6µl	16µl

### 2.4.3 Western blot

Protein extracts were separated on a polyacrylamide gel (12–15%; Laemmli, 1970) and, by the use of a Semi–Dry Transfer Cell (Bio–Rad, Trans–Blot SD), transferred for 1 hour at 15 Volts to a nitrocellulose membrane (Bio–Rad, Cat. No. 162–0115) which was then stained with red ponceau solution to confirm the transferring of the proteins to the membrane and to evidence the bands of the protein marker (High range or Low range, Bio–Rad). The membrane was blocked with 6% milk/TBS for a minimum of 90 minutes and probed using MED7 or MED25 rat monoclonal or ER rabbit polyclonal primary antibodies in 1% milk/TBS–T (Tween 0.02%) for a minimum of 1 hour. The membrane was then washed 3 times for 10 minutes with TBS–T buffer and incubated for 30 minutes with anti–rat or anti–rabbit IgG–horseradish peroxidase (HRP) conjugates (Promega) as secondary antibodies. After washing the membrane with TBS–T as mentioned above, the membrane was quickly rinsed with TBS and with water. To detect protein bands the membrane was treated with an enhanced chemiluminescence detection system (Perkin Elmer, Western Lightning Cat. No. NEL105) according to the manufacturer's instructions and exposed to a BioMax MR film (Kodak, Cat. No. 873 6936).

#### 2.4.4 Immunoprecipitation of MED25 derivatives with MED15 antibody

MED25 deletion constructs or mutants were *in vitro* expressed and labelled with [ $S^{35}$ ]-Methionine (10 or 15mCi/ml, Amersham) using the TNT Coupled Reticulocyte Lysate System kit (Promega, Cat. No. L4611), according to the manufacturer's instructions. 3–5 $\mu$ l of each synthesized construct were resolved in a SDS PAGE gel where the protein were fixed by Coomassie staining for a minimum of 1 hour followed by destaining. To get dried, gels were alternatively framed in between cellophane films at RT overnight or further incubated in water containing 10% glycerol, placed on top of a wheat piece of thick Whatman paper and dried on a gel drier for 90 minutes at 80°C. Expression of the radioactive proteins was checked by phosphoimaging or autoradiography. For the preparation of the chromatography column MED15 rat monoclonal antibody was immobilized on protein G–Sepharose (Amersham, Protein G Sepharose Fast Flow, Cat. No. 17–0618–03) at a concentration of about 1 $\mu$ g/ $\mu$ l as follows. In a 50ml falcon tube 300 $\mu$ l of protein G were washed two times with water and two times with PBS. 50ml of the hybridoma supernatant were added to the beads and left on the roller at room temperature from a minimum of 4 hours to overnight. After removing the antibody, the beads were again washed with PBS for 3 times and left in PBS containing 0.01% Sodium Azide for storage at 4°C. For the IP, beads were pre-washed with PBS and then equilibrated with BC buffer 150. 10 $\mu$ l of MED15 coupled beads were then incubated overnight at 4°C with normalized amount of each deletion construct or with 5 $\mu$ l of each mutant together with 100 $\mu$ l of HeLa nuclear extracts (about 800 $\mu$ g), at 0.15M salt, with addition of phosphatase inhibitors. Full-length wild type MED25 construct incubated with an Isotype antibody was used as control to show the specificity of the method, and HeLa nuclear extract alone was used as positive control for the presence of Mediator. Beads were then precipitated, washed four times at 0.45M salt (with BC buffer 450) and once at 0.15M salt (with BC buffer 150). Proteins were then eluted with 20 $\mu$ l of 2x SDS sample buffer, resolved by SDS PAGE and finally transferred into a nitrocellulose membrane which was then analysed either by western blot or by autoradiography while exposing it to a BioMax film for about 3 days at –80°C. For ER–MED25 and ER–MED25–NTD coimmunoprecipitation, 500 $\mu$ g of 0.15M nuclear extract isolated from transiently transfected HEK293T cells and 721–ER–MED25–NTD cells respectively

were incubated overnight at 4°C with 10µl of MED15 antibody coupled beads. After five washes with BC buffer 150, beads were boiled in 20µl of 2x SDS sample buffer and the samples loaded into a gel and analysed by western blot.

#### **2.4.5 Immunoprecipitation of flag–MED25(A335V) with FLAG–M2 antibody**

Flag M2 mouse monoclonal antibody (SIGMA) was immobilized on protein G–Sepharose at a concentration of 2µg/µl, as described in the paragraph 2.4.4 for MED15 antibody. 500µg of nuclear extract prepared from transiently transfected HEK293T overexpressing flag–MED25 (A335V) mutant were diluted to 150mM salt and incubated overnight at 4°C with 10µl of Flag antibody coupled beads also previously equilibrated with BC buffer 150. Nontransfected cells derived nuclear extract and naked beads were used as negative controls. After washing the beads five times with BC buffer 150, proteins were eluted with 20µl of 2x SDS sample buffer, resolved by SDS PAGE and analysed by Western blot.

#### **2.4.6 Expression and purification of GST–VP16 derivative proteins**

Recombinant GST–VP16H1 and GST–VP16H1mut were expressed in BL21 *E.coli* expression strain using expression plasmids encoding the desired protein. An overnight starter culture was diluted to an OD600 of 0.1 into 200 ml LB medium and grown at 37°C. At an OD600 corresponding to 0.6–0.8 the expression of the protein was induced by addition of 0.5mM IPTG. To prevent the formation of inclusion bodies the *E.coli* culture was shifted to 30°C for 2–6 hours. Cells were harvested by centrifugation for 15 minutes at 3.500 rpm (4°C). All the following purification steps were carried out at 4°C. Cells were resuspended in 10ml of lysis buffer and lysed by incubation with 10mg of Lysozyme for 10 minutes. Samples were then placed in an ice–water bath and sonified using the microtip and an output amplitude of 30% for a total time of 2 minutes with a repetitive cycle of 10 seconds On–time and 50 seconds Off–time. The lysate was cleared by centrifugation for 10 minutes at 10.000 g (4°C). In the mean time, 200µl of Glutathione–Sepharose 4B (Amersham, Cat. No. 17–0756–01) were washed and equilibrated in Lysis–buffer. The lysate was incubated together with the beads for 90

minutes at 4°C on a rotating wheel to allow binding of the fusion protein to the matrix. The supernatant was removed and the remaining beads were subsequently washed with 100 volumes of BC2000 and BC150 buffer. The immobilized fusion proteins were eluted upon incubation with 500µl of elution buffer for 10 minutes at 4°C. For quality control, an aliquot was analyzed in a Coomassie stained SDS–PAGE gel.

#### **2.4.7 GST–VP16 pull down**

As previously described (2.4.4) MED25 mutants were S<sup>35</sup> labelled and expressed *in vitro* using the TNT Coupled Reticulocyte Lysate System kit. After having controlled the protein expression via autoradiography on a dried SDS PAGE gel, 5µl of each mutant were diluted in 210µl of HEGN 100 buffer with the addition of 1mM DTT and 0,2mM PMSF and incubated overnight at 4°C together with 10µl of GST–VP16H1 or GST–VP16H1mut (as a negative control) beads, previously equilibrated with HEGN 100 buffer. Beads were then precipitated, washed five times with the same incubation buffer, boiled in 20µl of 2x SDS sample buffer and analysed by SDS PAGE. Gels were then Coomassie stained, destained and incubated with a 10% glycerol solution for 30 minutes, placed on top of a wheat piece of thick Whatman paper and dried on a gel drier for 90 minutes at 80°C. Protein bands were revealed by exposing the gels to BioMax films for about 3 days at –80°C.

#### **2.5 Mouse keeping**

Mice were kept in the mouse facilities of GSF, Neuberberg. Chimeras generated after blastocyst injection of MED25 homologous recombinant ES cells were mated with C57BL/6 wild type mice in order to produce germ line transmitted offspring.



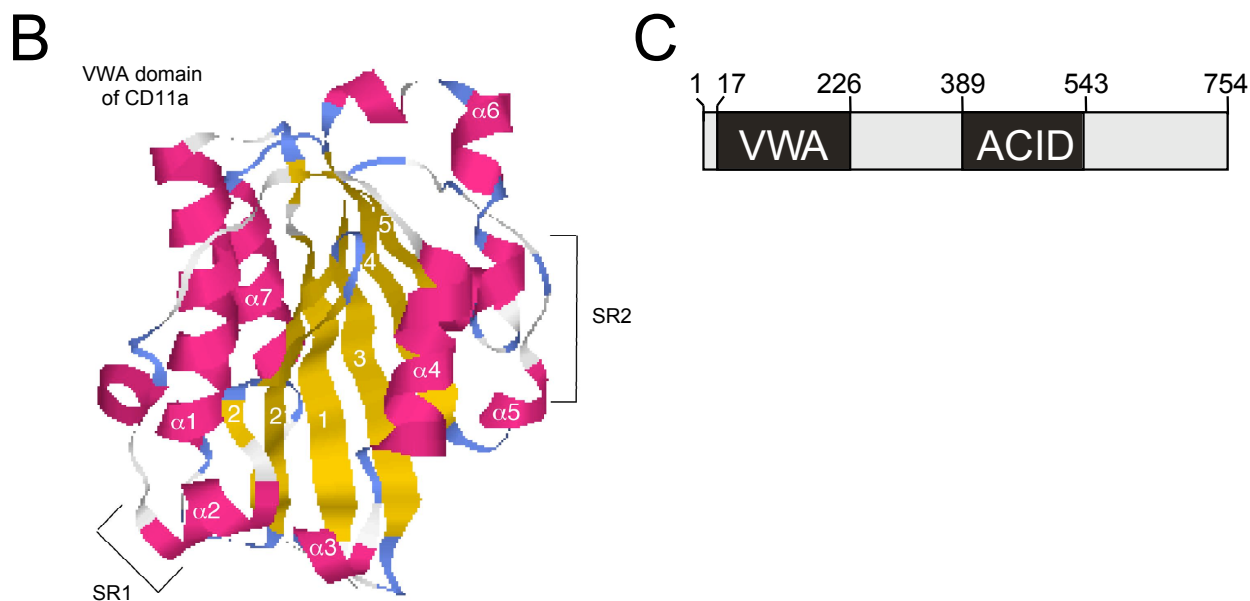
### 3. RESULTS

#### 3.1 Structure–function analysis of MED25

MED25 is a 103kD protein composed of 754 amino acids. It was originally identified as a cofactor activity necessary for transcriptional activation by the prototypic acidic herpes simplex activator VP16 in a purified RNA polymerase II transcription system. Using the activation domain of VP16 immobilized on a column the protein was purified to homogeneity by affinity chromatography and sequenced by N–terminal Edman degradation (Mittler et al., 2003). The analysis of the primary sequence of MED25 revealed the existence of two evolutionary conserved domains (figure 9A).

The VWA domain, resembles the "A" domain of the Willebrand factor. The predicted secondary structure of the MED25 VWA domain (indicated in figure 9A with stretches of "h" and "e") is related to the corresponding fold of the VWA domain of integrin CD11a; its X–ray structure is shown in figure 9B. The second conserved domain, the so–called ACID (activator interaction domain), shows sequence homology to a functional domain of the gene product of the prostate cancer overexpressed gene (PTOV–1), which contains two copies of the ACID domain. (Mittler et al., 2003). Figure 9C represents a schematic view of the domain organization of MED25. The VWA domain is localized in the N–terminal part of the protein, from amino acid 17 up to amino acid 226. The amino acids 389–543 encode the ACID domain of MED25.





### 3.1.1 Mapping of a minimal Mediator–interaction domain

After the identification of ACID as the VP16–interaction domain (Mittler et al., 2003), the structural study of MED25 was continued in an effort to find the minimal portion of MED25 capable of binding Mediator. Therefore, [<sup>35</sup>S]–methionine–labelled MED25 deletion constructs were expressed in reticulocytes, complemented with HeLa nuclear extracts as a source for the limiting human Mediator and immunoprecipitated with an anti–MED15 monoclonal antibody (6C9), which recognizes the Mediator subunit MED15 with high specificity. Incorporation of MED25 derivatives into Mediator was monitored by autoradiography. As shown in figure 10, MED25<sub>1–226</sub> coprecipitated efficiently with Mediator (lane 4). Using C–terminally extended MED25 deletion constructs, MED25<sub>1–290</sub>, MED25<sub>1–393</sub>, MED25<sub>1–543</sub> and MED25<sub>1–715</sub>, a similar result was obtained (lanes 5–7 and 12). In contrast, MED25 derivatives missing partially (lanes 2, 3, 8, 11) or completely (1, 9, 10) the VWA domain did not coprecipitate with Mediator. These data suggest that an intact VWA domain is required and sufficient for interaction of MED25 with Mediator.

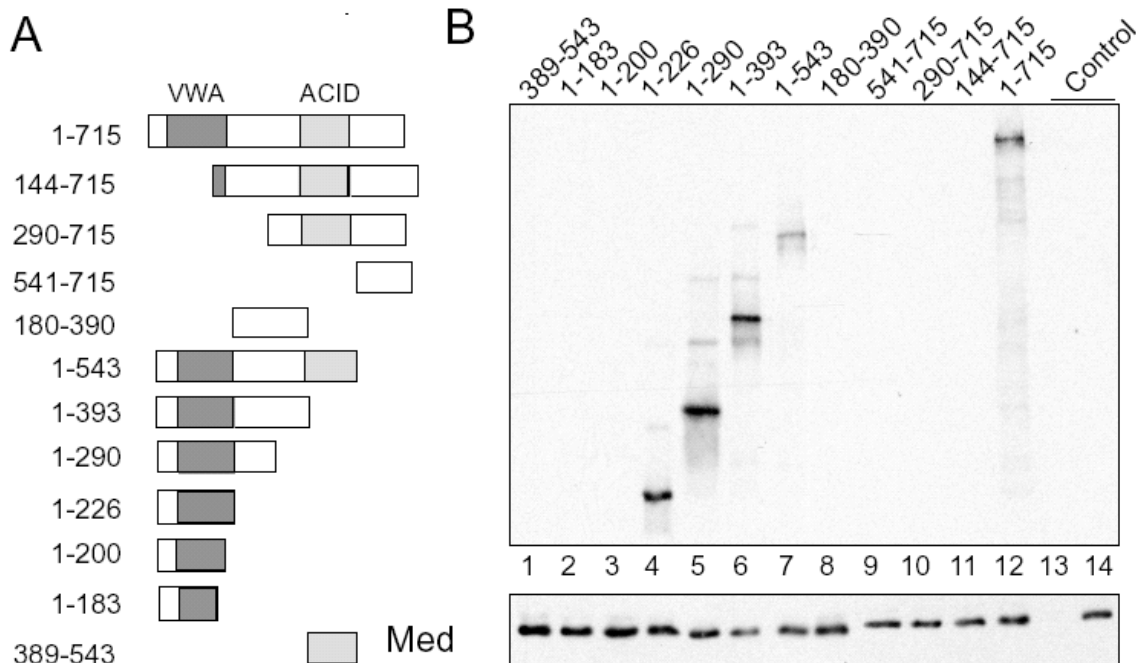


**Figure 10.** The MED25 VWA domain is the minimal domain required for Mediator–interaction. (A) MED25 deletion constructs used in this experiment. (B) Upper panel, autoradiography of the immunoprecipitation assay. MED25 deletion constructs were translated in reticulocytes, radiolabelled with  $^{35}\text{S}$ , incubated with HeLa nuclear extract and immunoprecipitated with MED15 antibody. HeLa nuclear extract alone and an isotype antibody were used as control (lanes 13 and 14). As a positive control MED25 (1–715) was used (lane 12). Only the constructs carrying an intact VWA domain were coprecipitated (lanes 4–7). Bottom panel, western blot analysis of the same membrane, probed against the Mediator core subunit MED7 to monitor levels of coprecipitated Mediator.

### 3.1.2 Transcription activation analysis of MED25 deletion constructs

Since MED25 was shown to physically interact with both Mediator and VP16, which are involved in transcriptional activation, the question was addressed whether MED25 harbours an intrinsic transcription activation domain. Towards this end, MED25 deletion mutants fused to a GAL4 DNA binding domain were cloned and their expression was confirmed by Western blot analysis of nuclear extracts isolated from transiently transfected 293T cells (data not shown). The same constructs were then expressed in Jurkat cells by transient transfection including the luciferase reporter pGLRMG5 which carries five GAL4 binding sites (figure 11B). 48 hours post–transfection cells were harvested and cell lysates were subjected to a luciferase assay. The measured relative luciferase units of the reporter alone control was used as a reference to calculate fold activation rate of the MED25 mutants.

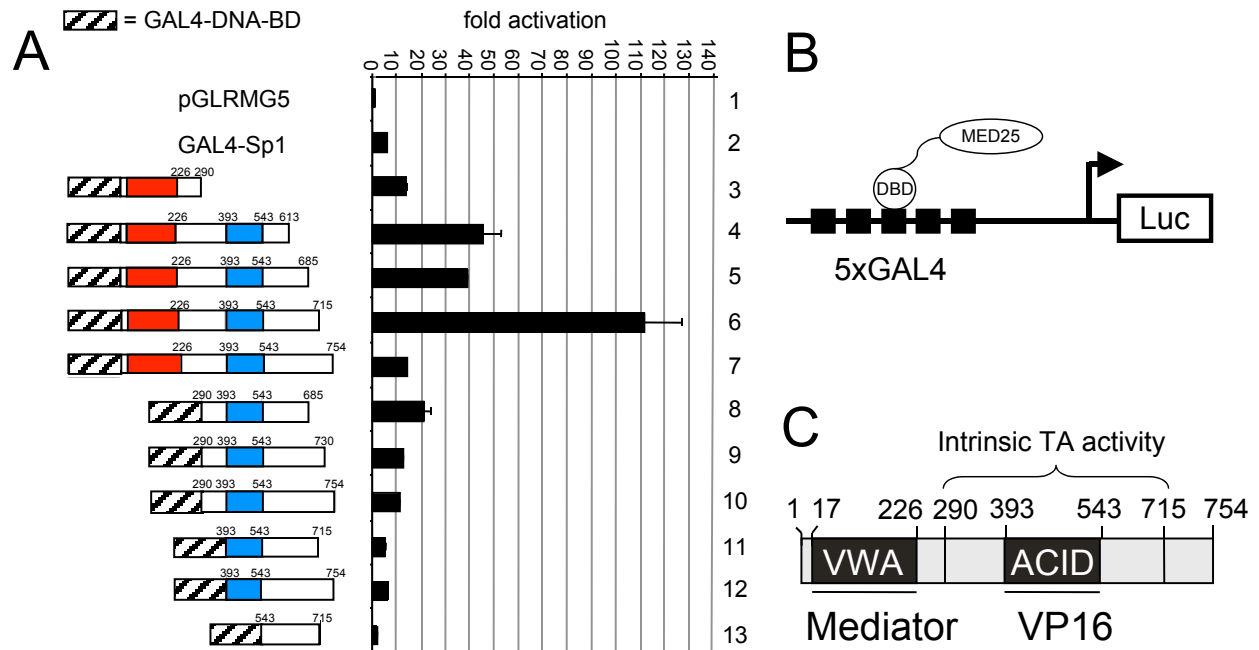


**Figure 11.** MED25 contains an activation domain. (A) Functional assay to investigate MED25 intrinsic transcription activation capability. MED25 deletion constructs fused to a GAL4–DNA–binding domain (GAL4–DNA–BD) were transfected in Jurkat cells together with a luciferase reporter fused to a promoter carrying 5 GAL4 binding sites. On the left site, the MED25 deletion construct used in this assay are depicted. On the right site, the fold activation of each construct was calculated normalizing luciferase levels to the  $\beta$ -gal activity, and setting the reporter alone control (pGLRMG5) to 1. (B) Schematic view of the pGLRMG5 reporter used in this assay. (C) Schematic view of MED25 and the identified functional domains, the VWA domain interacting with Mediator, the ACID domain interacting with VP16 and a presumptive intrinsic transcription activation (TA) activity included in between amino acids 290 and 715.

As depicted in figure 11A, the construct MED<sub>1–290</sub> (lane 3), carrying only the Mediator interaction domain, activates transcription very likely through the binding and recruitment of Mediator to the promoter. The fold activation levels induced by the other VWA–containing constructs show that the potential for transcriptional activation of MED25 is partially dependent on the C–terminal amino acids 290–715 since the gradual extension of the MED25 C–terminus results in a modest but robust increase in reporter activity (lanes 4–6). Surprisingly, transcriptional activation was still present even after removal of the Mediator binding domain (lanes 8–12) pointing towards a possibly alternative Mediator–independent transcription activation mechanism. In these constructs deletion of amino acids 290–393 of MED25 results in a decrease of transcriptional activation (lanes 11–12) and the additional removal of the ACID domain leaves only a residual transcriptional activation capacity to the MED<sub>543–715</sub> construct (lane 13). Rather unexpected was the observation that the transactivation capacity of the MED<sub>1–715</sub>

construct is significantly stronger than the one of the full-length construct MED<sub>1-754</sub> (lanes 6–7). A possible explanation for this phenomenon is that the last 39 amino acids are subject to a modification which negatively regulates the protein.

In conclusion the data presented here provide evidence for an intrinsic capacity of MED25 to activate transcription. The region responsible for this activity is located in between amino acids 290 and 715. Whether this region is additionally organized in sub domains (amino acids 290–393, ACID domain, amino acids 543–715) that act independently from each other or cooperate with each other to activate transcription is still not yet clear and needs to be further investigated.

### 3.1.3 Site-directed mutagenesis of MED25 ACID and VWA domain

To identify critical residues involved in the interaction of MED25 with its binding partners, a series of 19 different GAL4-fused MED25 variants containing point mutations were generated. Ten of them are localized within the VWA domain, eight in the ACID domain and one at the C-terminus of the protein (figure 12A). In figure 12B the relative position of the point mutations within the primary sequence of MED25 is indicated.

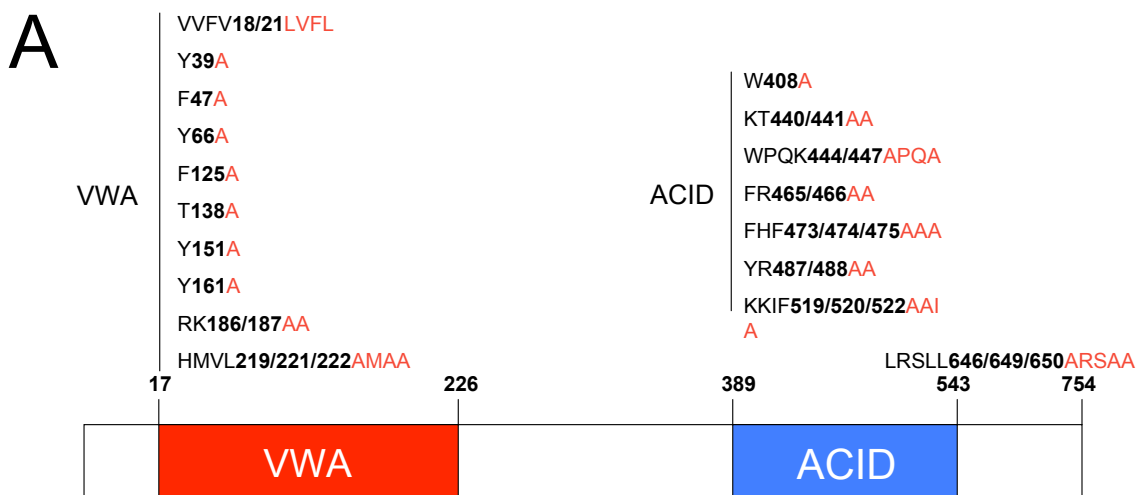
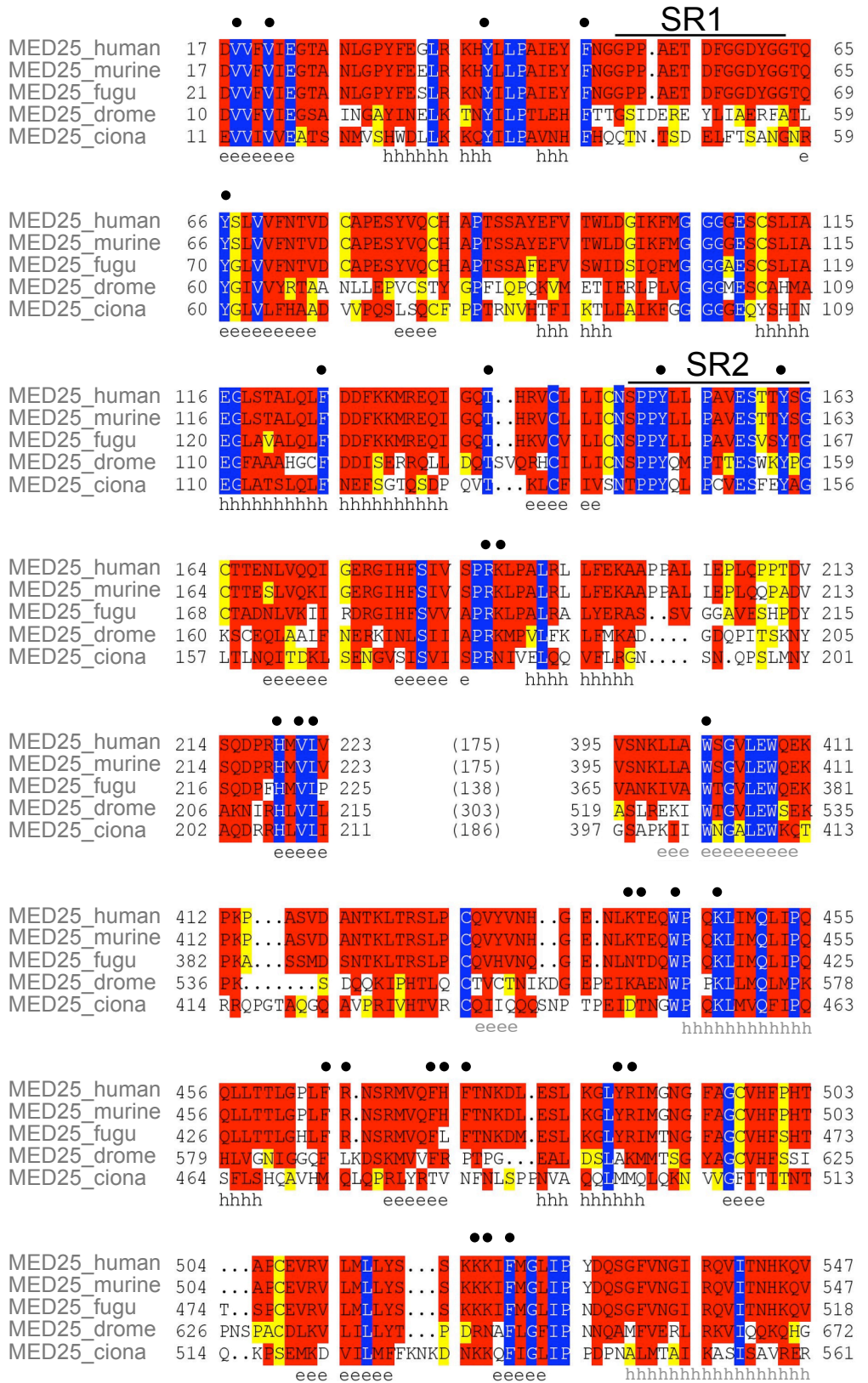


**Figure 12.** Site-directed mutagenesis of two MED25 functional domains VWA and ACID. (A) The introduced point mutations are listed on top of the domain in which they are located. (B, p.83) Distribution of the mutations relative to the primary sequence and and its conservation through evolution. Black dots indicate the amino acids targeted for point mutations.



B



VWA

ACID

In general, regarding the VWA domain, amino acids that were conserved throughout evolution and therefore possibly relevant for the function of the protein were targeted. Of particular interest are the amino acids localized in the corresponding specific region 2 (SR2) of the VWA domain represented in the X-Ray structure of CD11a (figure 9B). This region is characterized by a loop, which was shown to share little homology within the group of other VWA proteins but which is highly conserved through evolution. This indicates a possible involvement of the SR2 region in a critical function of MED25, which could be the interaction with Mediator or an unknown function (Mittler et al., 2003).

In order to study the interaction of the ACID domain with VP16 the following facts were considered for the selection of the amino acids to be mutated. First, the ACID domain binds to a highly acidic viral activator probably through positively charged residues. Second, it has been reported that aromatic residues within the activation domain of VP16 are critical for activation of transcription and for binding to its targets. Based on this knowledge particular attention was paid to amino acids that are positively charged or aromatic. More detailed information regarding mutagenesis design is found in table 9.

**Table 9.** Amino acid residues mutated in the VWA domain and in the ACID domain of the human MED25 protein.

NAME	CRITERIA FOR MUTATION	DOMAIN
VVFFV18/21LVFL	changed to the corresponding CD11a sequence	VWA
Y39A	conserved through evolution	VWA
F47A	conserved through evolution	VWA
Y66A	conserved through evolution	VWA
F125A	conserved through evolution	VWA
T138A	conserved through evolution	VWA
Y151A	conserved through evolution, located in the SR2 region, predicted phosphorylation site	VWA
Y161A	conserved through evolution and located in the SR2 region	VWA
RK186/187AA	conserved through evolution	VWA
HMVL219/221/222AMAA	conserved through evolution	VWA
W408A	conserved through evolution and aromatic	ACID
KT440/441AA	positively charged and hydrophilic/neutral	ACID
WPQK444/447APQA	aromatic and positively charged	ACID
FR465/466AA	aromatic and positively charged	ACID
FHF473/474/475AAA	aromatic and positively charged	ACID
YR487/488AA	aromatic and positively charged	ACID
KKIF519/520/522AAIA	positively charged and aromatic	ACID
LRSLL646/649/650ARSAA	nuclear-receptor box motif (LXXLL) confers binding to nuclear receptors	C-terminal region



### 3.1.3.1 Dissection of the Mediator–interaction domain of MED25 using VWA point mutants

In order to identify critical amino acid residues involved in Mediator–binding, MED25 derivatives carrying mutations in the VWA domain were tested for their potential to physically interact with Mediator. For this purpose an immunoprecipitation assay was performed. These data were combined with a functional study in an effort to understand if and how changes of the physical interaction between MED25 and Mediator would influence the transcription activation potential of MED25.

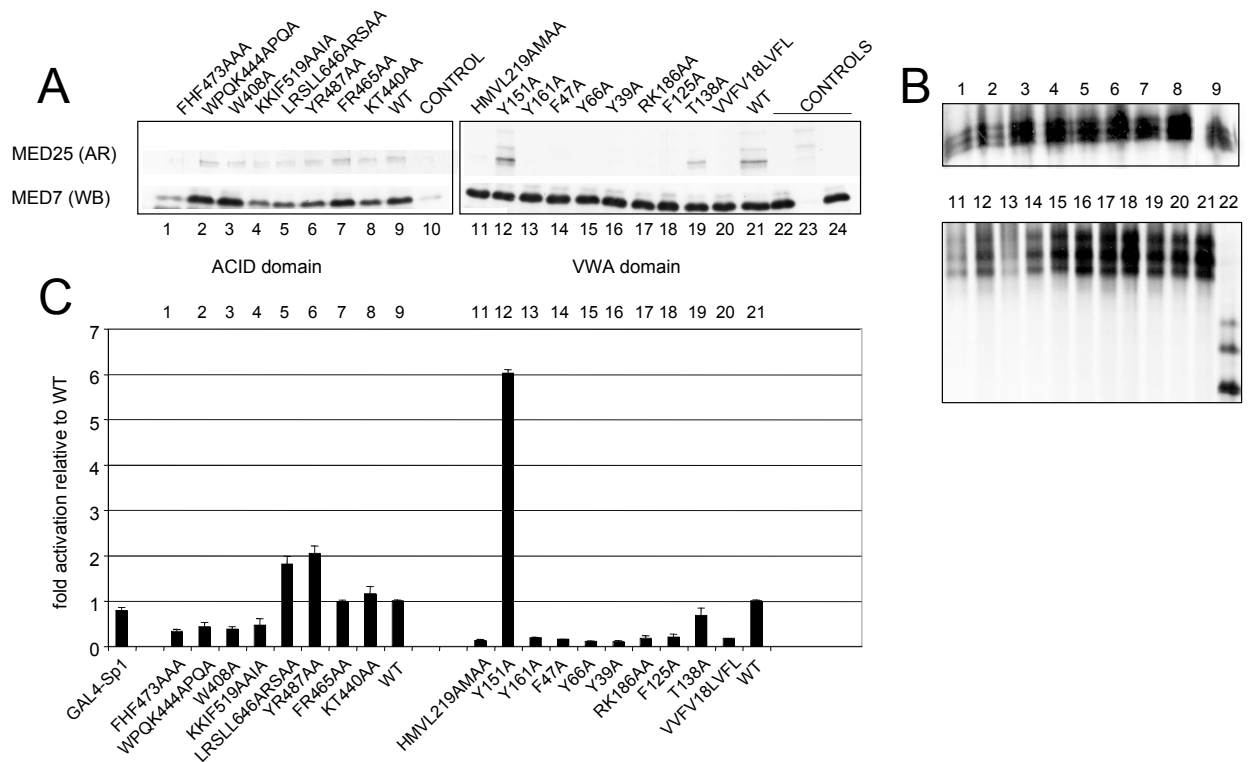


**Figure 13.** Investigation of MED25 residues critical for the Mediator–interaction. (A) Autoradiography (AR) and Western blot analysis (WB) of the immunoprecipitation assay. MED25 point mutants were translated in reticulocytes, radiolabelled with  $^{35}\text{S}$ , incubated with HeLa nuclear extract and immunoprecipitated with MED15 antibody. HeLa nuclear extract alone (lane 22), an isotype antibody (lanes 10 and 23) and MED25<sub>290–754</sub> construct (lane 24) were used as controls. As a positive control MED25 wild–type was used (lanes 9 and 21). To monitor levels of coprecipitated Mediator the membrane was probed with an antibody, which recognizes the Mediator core subunit MED7. (B) Input of the MED25 point mutants used in the immunoprecipitation assay. (C) Transcription activation analysis to test whether the mutations interfere with MED25 intrinsic transcription activation capability. MED25 point mutants were fused to a GAL4–DNA–binding domain (GAL4–DNA–BD) and transfected in Jurkat cells together with pGLRMG5 luciferase reporter. The fold activation rate of each mutant was calculated normalizing luciferase levels to the  $\beta$ -gal activity, and using the wild–type control as a reference.

### Physical interaction analysis

In analogy to the initial MED25–deletion analysis (see 3.1.1), VWA–domain–MED25 point mutants were *in vitro* translated in reticulocyte lysates, radiolabelled with  $^{35}\text{S}$ , incubated with HeLa nuclear extract and tested for binding to Mediator via immunoprecipitation using the anti–MED15 monoclonal antibody 6C9. In this assay the ACID–domain–MED25 point mutants designed for the VP16–interaction study (see 3.1.3.3) were employed as a positive control. In fact, since the ACID domain is not involved in the binding of MED25 with Mediator (figure 10) these mutants should efficiently coprecipitate with Mediator. After immunoprecipitation, proteins were resolved in a SDS gel and transferred into a nitrocellulose membrane. To confirm that Mediator was successfully immunoprecipitated the lower part of the membrane was probed against an antibody, which specifically recognizes another subunit of Mediator, MED7. The rest of the membrane was analysed by autoradiography. In figure 13A the upper bands (MED25 AR) correspond to MED25 mutants which were coprecipitated with Mediator and are therefore detected by autoradiography. Underneath, the bands of MED7 visualized by western blot (MED7 WB) monitor levels of coprecipitated Mediator. Among the mutations made in the VWA domain only two, Y151A and T138A, seem not to affect Mediator interaction (lanes 12 and 19). Moreover, the mutant Y151A rather shows a stronger incorporation in Mediator as compared to the WT construct (lane 12 versus 21). As expected, the mutations in the ACID domain were not influencing Mediator interaction (lanes 1–9). As a negative control the construct 290–754 lacking the VWA domain (lane 22) and an isotype antibody (lanes 10 and 23) were used. In figure 13B the input signals of the MED25 derivatives used in this experiment are shown.

### Transcription activation analysis

To be able to correlate structural and functional aspects of the VWA domain, the MED25 mutants used in the chromatography assay described above were also employed in a transcriptional activation assay. Therefore, MED25 point mutants fused to a GAL4 DNA binding domain were transiently transfected in Jurkat cells and tested on a luciferase reporter carrying five GAL4 binding sites as previously described (paragraph 3.1.2). Nuclear extract was isolated from part of the transfected cells and analyzed by Western

blot to confirm the expression of the MED25 mutants (data not shown). Figure 13C shows the fold activation rate of each point mutant calculated relatively to the MED25 wild type construct. Except for the mutants Y151A and T138A the fold activation rate of all the other VWA-domain point mutants was reduced to basal levels (lanes 11, 13–18, 20). While the fold activation of T138A was only slightly reduced (lane 19) the mutant Y151A showed a striking increase of activity (lane 12). Since Y151 is a predicted phosphorylation site, the assumption was made that phosphorylation of the tyrosine may negatively regulate the interaction of MED25 with Mediator. Alternatively, the substitution of a bulky residue (tyrosine) with a smaller one (alanine) may simply favor binding. Replacement of the same tyrosine with a phenylalanine could help to clarify this unresolved issue.

The ACID-domain mutants previously employed in the binding assay were used in this transcription activation study as well. Among them, YR487AA, FR465AA and KT440AA were performing similar to wild-type (lanes 6–8), while the mutants FHF473AAA, WPQK444APQA, W408A and KKIF519AAIA showed impaired capability to activate transcription with fold activation rates 40 to 50% reduced as compared to the wild type construct (lanes 1–4).

For most of the VWA-domain point mutants the data collected so far showed that impaired Mediator-interaction was associated with dramatic loss of transcription activation potential. The results of our previous functional study using MED25 deletion constructs, however, indicate that a residual intrinsic activation capacity is retained even after complete loss of Mediator interaction (figure 11, lanes 8–12). Very likely in several instances these effects result from a collapsed structure. This is suggested by the location of some of the targeted residues in predicted structured regions (figure 12B). Assuming that the structure of the VWA domain collapses upon changes of its conserved residues could help to explain the unexpected effects observed for the VWA-domain mutants in our functional assay. One hypothesis would be that the unstructured VWA domain becomes highly flexible therefore affecting the capability of the intrinsic transcriptional activation domain (290–715) to interact with other factors. However this hypothesis still needs to be validated.

Hence, additional amino acid residues located in the non-structured SR2 region and in the surrounding area were targeted. Altogether, seven additional VWA-domain-MED25 point mutants were designed that are located in this region. Depicted in figure 14 is a detail of the primary sequence of the VWA domain which includes the specific region 2 (SR2). Black dots indicate the amino acid residues targeted for the generation of a second series of VWA-domain-MED25 point mutants.

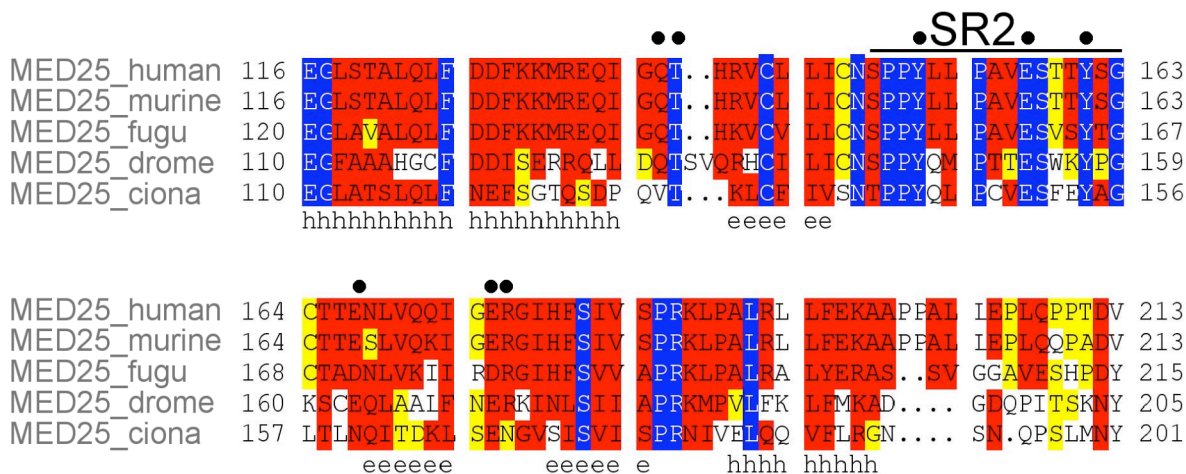


**Figure 14.** Generation of a second series of VWA-domain-MED25 point mutants. For the identification of amino acids critical in the Mediator-interaction new mutants were designed that are located in the SR2 region or in its proximity.

E157, E167 and E175 were chosen because glutamate is commonly found on the protein surface and involved in protein-protein interaction. Q137 is highly conserved throughout evolution in MED25 homologs but not at all among different VWA proteins (supplementary figure 1). Therefore it may represent an amino acid which has a MED25-specific function rather than a function associated to VWA-domain-containing proteins. T138, Y151 and Y161 mutated to alanine in a first approach (see above), this time were replaced by aspartate and phenylalanine respectively, which are characterized by similar sterical properties as compared to the wild-type amino acids. In particular, the substitution of the hydroxylated aromatic ring of Y151 with a phenylalanine was meant to elucidate whether phosphorylation or alternatively the sterical characteristics of the amino acid may affect the binding of MED25 with Mediator. In analogy with the study done with the first series of point mutants, the same assays were employed for the analysis of the new MED25 derivatives.

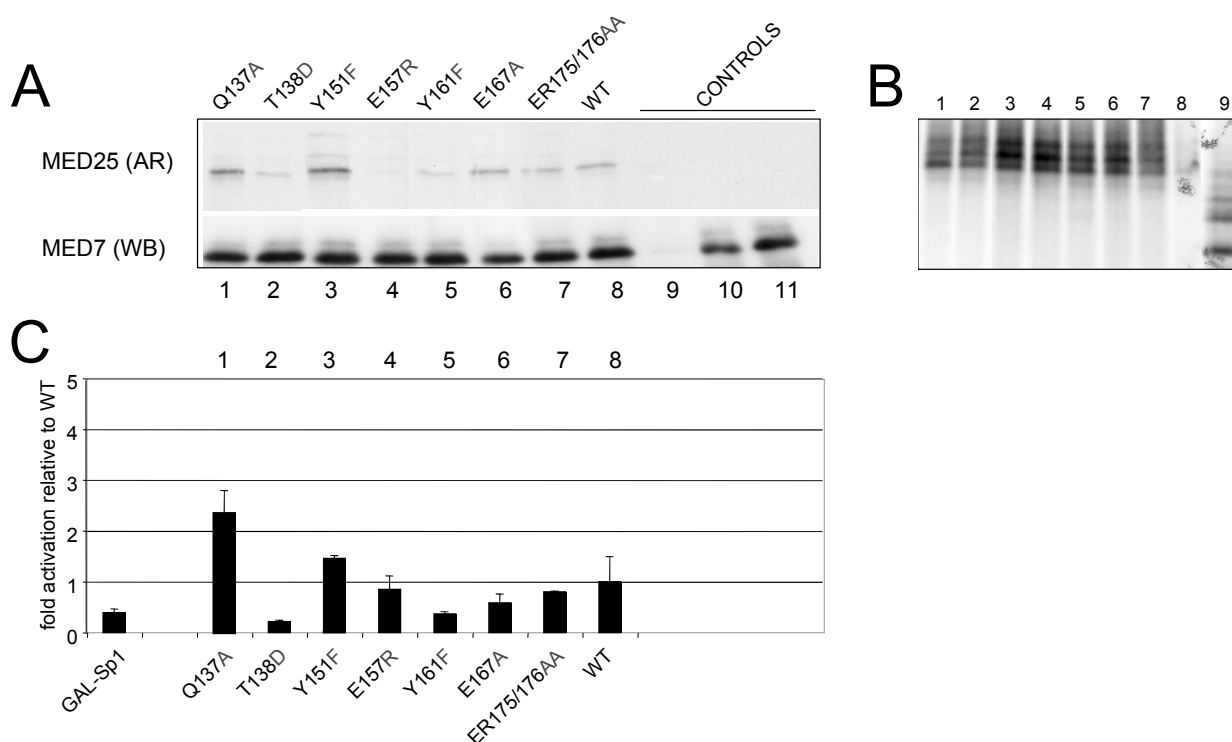


**Figure 15.** Investigation of MED25 residues critical in the Mediator–interaction using MED25 derivatives mutated in the SR2 region of VWA domain. (A) Autoradiography (AR) and Western blot analysis (WB) of the immunoprecipitation assay. MED25 point mutants were translated in reticulocytes, radiolabelled with  $^{35}\text{S}$ , incubated with HeLa nuclear extract and immunoprecipitated with MED15 antibody. HeLa nuclear extract alone (lane 10), an isotype antibody (lane 9) and MED25<sub>290–754</sub> construct (lane 11) were used as controls. As a positive control MED25 wild–type was used (lane 8). To monitor levels of coprecipitated Mediator the membrane was probed to an antibody which recognizes the Mediator core subunit MED7. (B) Input of the MED25 point mutants used in the immunoprecipitation assay. (C) Transcription activation analysis to test whether the mutations interfere with MED25 intrinsic transcription activation capability. MED25 point mutants were fused to a GAL4–DNA–binding domain (GAL4–DNA–BD) and transfected in Jurkat cells together with pGLRMG5 luciferase reporter. The fold activation of each mutant was calculated normalizing luciferase levels to the  $\beta$ –gal activity using the wild–type control as a reference.

### Physical interaction analysis

MED25 point mutants were expressed and radioactively labelled in reticulocytes as previously described. Figure 15B shows the input signals of the *in vitro* expressed proteins used for the immunoprecipitation assay. These constructs were loaded on an anti–MED15 associated chromatography column to test their Mediator–interaction capability and finally analyzed by autoradiography (figure 15A). As a negative control the construct 290–754 lacking the VWA domain (lane 11) and an isotype antibody (lane 9) were used. Beside E157R (lane 4), all the other constructs were coprecipitated, even though the coprecipitation of mutants T138D and Y161F seemed to be dramatically

affected (lanes 2, 5). Of interest, the replacement of T138 with an alanine was basically not affecting the binding (figure 13B, lane 19). This may underline the importance of an hydrophobic residue in this position for the binding with Mediator. The amino acid Y161 could be additionally critical for VWA domain structure. Its replacement with alanine provoked a complete loss of Mediator binding (figure 13B, lane 13) while mutation into another aromatic residue still shows binding, although very weak. Stronger bands were observed for Q137A and Y151F. However, while the effect displayed by the mutant Y151A may be due to an excessive load compared to the other coprecipitated mutants, this is not the case for the mutant Q137A (figure 15B).

### **Transcription activation analysis**

As previously described for other MED25 derivatives, the newly generated VWA–domain–MED25 point mutants were also transiently transfected in Jurkat cells together with the GAL4–luciferase reporter pGLRMG5 to test their capability to activate transcription. The transcriptional assay provided evidence for reduction of fold activation at least for some of the mutants that showed impaired binding to Mediator (lanes 2 and 5). Interestingly, E157R mutant only showed a slightly reduced transactivation capacity, despite its complete loss of binding to Mediator (lane 4). These observations, in accordance with the fact that a MED25 deletion construct missing the first 290 amino acids remains active (figure 11A, lanes 8–10), argue for a critical role for amino acids T138, Y161 and in particular E157 in Mediator complex formation. The transcriptional activation capabilities of the mutants E167A and ER175/176AA were almost not affected (lanes 6 and 7). The change of Y151A into Y151F (lane 3) reduced the activation rate to wild–type level reinforcing the hypothesis that the gain of function observed in the case of Y151A (figure 13, lane 12) was probably the consequence of a more efficient Mediator–interaction capability associated with a smaller residue. The two fold increase of transcriptional activation observed for the mutant Q137A may also be explained with the substitution of a bulky residue by a smaller one, which apparently causes also a more efficient coprecipitation of the mutant together with Mediator (lane 1).

In summary, from the data presented here we can conclude the following:

- i) Among the VWA–MED25 mutants HMVL219AMAAA, Y161A, F47A, Y66A, Y39A, RK186AA, F125A and VV18LVFL have completely lost the capability to physically interact with Mediator and the capability to activate transcription as compared to the wild type construct. However, whether this effect is specific for Mediator–interaction or only the consequence of the collapse of VWA domain structure still needs to be clarified.
- ii) In the SR2 region, mutants T138D, Y161F and E157R show impaired or no Mediator complex formation while they still have a capability to activate transcription probably associated to the 290–715 region. E167A and ER175/176AA mutants are only slightly affected in both binding and transcriptional assays as compared to the wild type. Mutant Y151A displays a stronger Mediator–interaction which associates with a significant increase of the transactivating function. A similar phenomenon was observed for the mutant Q137A. The loss of function in the case of Y151F argues for improvement of the physical interaction when the tyrosine is replaced by alanine and indicates that Y151 and probably also Q137 may negatively regulate the association with Mediator .
- iii) Concerning the ACID–MED25 mutants, all show binding to Mediator as expected. While the mutants YR487AA, FR465AA and KT440AA are comparable to the wild type in the transcriptional assay, mutants FHF473AAA, WPQK444APQA, W408A and KKIF519AAIA show impaired transactivation capacity. This observation supports the data previously presented (figure 11) where contribution of the ACID domain to the intrinsic transcription activation domain of MED25 is hypothesized.

### **3.1.3.2 Study of the transcriptional activation function of MED25 point mutants with respect to their expression levels**

To rule out the possibility that the fluctuations of activation rates observed in the transcriptional assay are due to different expression levels of the constructs, some of the VWA–domain MED25 point mutants were chosen as representative examples for normal (WT), very high (Y151A) and very low (RK186A) transcriptional activation potential. Therefore HEK293T cells were transiently transfected with titrated amounts of these constructs along with the luciferase reporter pGLRMG5. Cells were processed partially for luciferase assays (figure 16B) and partially for isolation of the nuclear

extract, in which the expression levels of the proteins were analyzed by Western blot using an antibody against MED25 (figure 16A).

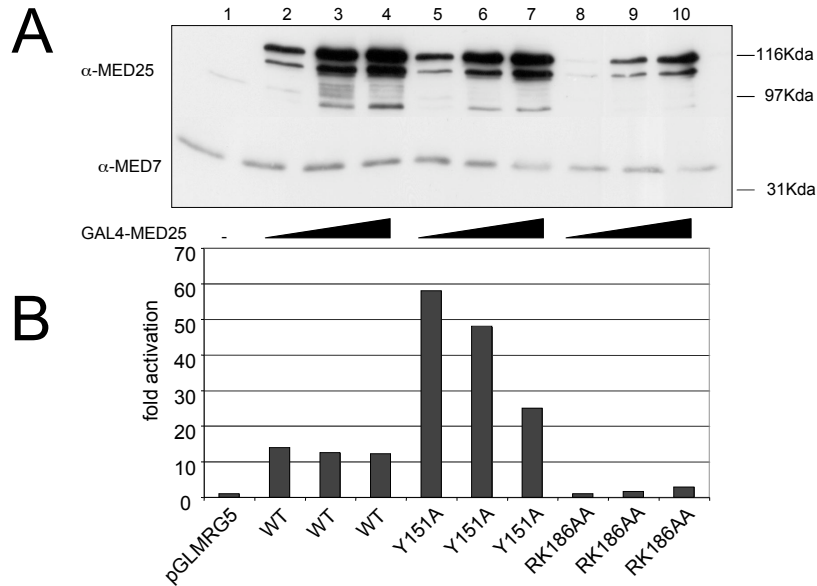


**Figure 16.** Intrinsic transcription activation capability of MED25 mutants with respect to their expression levels. Titrated amounts (60ng, 300ng and 600ng) of each GAL4-tagged MED25 point mutant and MED25 wild-type were transfected in HEK293T cells together with pGLMRG5 luciferase reporter (A) Western blot analysis of nuclear extracts using monoclonal antibodies against MED25 and against the Mediator core subunit MED7. (B) The activation rate of each MED25 construct was calculated normalizing luciferase levels to the  $\beta$ -gal activity, using the reporter alone (pGLMRG5) as a reference.

An antibody against another subunit of Mediator, MED7, was used as internal control for protein expression levels. Lanes 3, 6, and 9, which correspond to transfected amounts of GAL4-construct versus luciferase-reporter in the same ratio as used previously (figure 13C), show the activation rates of Y151A and RK186AA relative to WT are reproduced as compared to figure 13. The Western blot analysis (figure 16A) shows efficient nuclear transport for each of the constructs (the weaker signals corresponding to the lanes 8–10 seem to be rather due to a lower amount of nuclear extract that were loaded).

These data demonstrate that the different activation levels of different MED25 mutants are not related to different protein expression levels or variations in nuclear transport efficiency.



### 3.1.3.3 Dissection of the VP16–interaction domain of MED25 using ACID–domain–MED25 point mutants

To monitor the physical interaction of MED25 with VP16, MED25 full-length constructs mutated in the ACID domain were translated and labelled by [<sup>35</sup>S]–methionine in reticulocyte lysates and subjected to chromatography on a GST–VP16–H1 column. H1 represents one of the two subdomains within the VP16 activation domain. Both, the H1 and the H2 subdomains of the VP16 activation domain have been shown to bind the ACID domain of MED25 (Mittler et al., 2003). However, only H1 has been used in this study. The corresponding VP16–H1–mut derivative carrying a point mutation (F442P) within the H1 subdomain was used as negative control (figure 17A, bottom panel). As an additional control a MED25 deletion construct was used lacking the ACID domain (MED25<sub>1–290</sub>), which showed no binding to the VP16 activation domain (figure 17A, lane 10 and figure 17B, lane 11) (Mittler et al., 2003). In addition to the ACID–domain–MED25 mutants designed according to the primary sequence (table 9), another series of mutants were used to test the VP16 interaction, which were originally designed and generated in Cramer's laboratory by S. Baumli. These mutants, KKD411AAA, EKE437AAA, K478A, KKK518AAA and WT are expressing human ACID domain point mutants and wild type, respectively (lanes 12–16). Moreover, the ACID2.1 and ACID2.2 domains of the PTOV1 protein (lanes 17 and 18) were included in this study. Figure 17A shows the autoradiography of the pull down experiment carried out with the MED25 full-length point mutants. Figure 17B shows the results obtained using wild type and point mutants of the MED25 ACID domain only. The position of the targeted amino acid residues is shown in figure 17C relative to the conservation of the ACID domain throughout evolution and in different proteins (MED25 and PTOV1).

Regarding the full-length MED25 derivatives (figure 17A), the mutations YR487AA, FR465AA and KT440AA (lanes 6–8) located in the ACID domain and the LRSLL646ARSAA (lane 5) located in the C–terminus, do not seem to affect the binding to VP16. In contrast to these, the mutants FHF473AAA and WPQK444APQA (lanes 1 and 2) have lost their potential to interact with the VP16–H1 domain while the mutant W408A (lane 3) shows a dramatic reduction in binding to VP16. However, since these residues are highly conserved throughout evolution and part of predicted secondary

structures (figure 17D), an impact on the structure of ACID cannot be excluded after the conversion of aromatic/hydrophobic amino acids to alanine. The KKIF519AAIA mutation, positioned in a predicted non-structured part of the protein, characterized by positively charged and aromatic residues and also showing impaired binding to VP16 (lane 4), is more likely directly influencing the VP16–MED25 interaction. This hypothesis is supported by the fact that among the human ACID domain mutants of MED25 tested (figure 17B, lanes 12–16), the KKK518AAA mutant is the only one that fails to be precipitated by GST–VP16–H1 (figure 17B, lane 15). These results point towards a possible involvement of lysines 518, 519 and 520 in the binding to VP16 activation domain. To further investigate the contribution of these lysines in VP16 complex formation the ACID domains derived from another gene (PTOV1/ACID2) and therefore providing for natural variants in this specific region were employed (figure 17C). As shown in figure 17B, lysine 518 substituted by a negatively charged residue (glutamate) in PTOV1\_B/ACID2.2, completely prevents binding to VP16 (lane 18) in contrast to PTOV1\_A/ACID2.1 (lane 17). This observation strongly argues for a critical role for lysine 518 in the interaction of MED25 with VP16. Since K518 is not targeted in the mutant KKIF519AAIA, the low efficiency with which it is precipitated by VP16H1 indicates that the amino acid F522 very likely participates in the binding reaction, and leaves open the possibility that also K519, K520 may contribute. In conclusion these data indicate that targeting of amino acids in mutants FHF473AAA, WPQK444APQA, W408A, KKIF518AAIA and KKK518AAA eliminate or strongly affect the binding of the ACID domain to VP16H1 *in vitro*. These residues seem also to be relevant for intermolecular interactions involving the ACID domain of MED25 *in vivo*. In fact, constructs carrying the same mutations have previously displayed partial loss of transactivation capacity (figure 13, lanes 1–4).

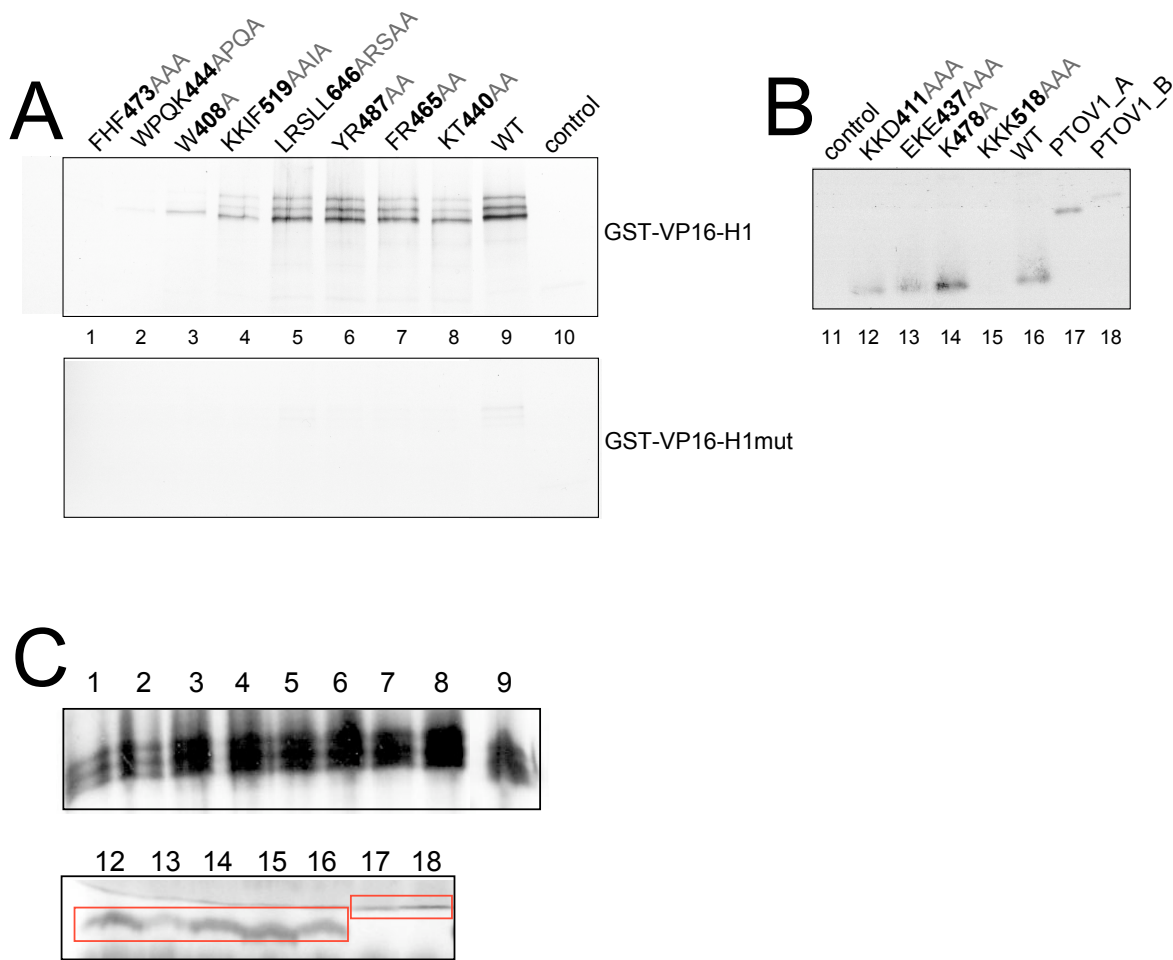


**Figure 17.** Investigation of MED25 residues critical for VP16–interaction using ACID–domain point mutants (in the context both of MED25 full–length and the ACID domain only of MED25) and single ACID domains of the PTOV1 protein. MED25 point mutants were translated in reticulocytes, radiolabelled with  $^{35}\text{S}$  and loaded into a VP16H1 or VP16H1mut columns. MED25<sub>1–290</sub> construct was used as control. (A) Upper panel, autoradiography of the VP16H1 pull–down carried out using full–length MED25 point mutants. Bottom panel, VP16H1mut pull–down was used as negative control. (B) Autoradiography of VP16H1 pull–down carried out using ACID only constructs. Point mutants of the human MED25 ACID domain (lanes 12–16) and the two ACID domains of human PTOV1 (lanes 16–17) were used. (C) Input of MED25 point mutants and ACID–domain constructs of PTOV1 used in this GST–VP16H1 pull–down assay. (D, p.96) Distribution of the ACID mutations relative to the conservation of the ACID domain throughout evolution and in different proteins. Black dots indicate the residues targeted in the full–length protein while green triangles indicate those, which have been targeted in the ACID–domain–only constructs. Predicted strand and helices are shown underneath the sequence as arrows and lines, respectively.

## D

hMED25_ACID	395	VSNKLLAWSG	VLEWQEKPK.	..PASVDANT	KIIRSLPCQV	YVNH..GE.N	438
hPTOV1_A	88	LSNKLAWSG	VLEWQEKRR.	..PYS.DSTA	KLKRTLPCQA	YVNQ..GE.N	130
hPTOV1_B	253	VNNKFLAWSG	VMEWQE.PRP	EP.....N.S	RSKRWLESHV	YVNQ..GE.I	292
mMED25_ACID	395	VSNKLLAWSG	VLEWQEKPK.	..PASVDANT	KIIRSLPCQV	YVNH..GE.N	438
mPTOV1_A	88	LSNKLAWSG	VLEWQEKRR.	..PFS.DSTA	KLKRTLPCQA	YVNQ..GE.N	130
mPTOV1_B	253	VNNKFLAWSG	VMEWQE.PRP	EP.....N.S	RSKRWLESHV	YVNQ..GE.I	292
dmMED25_ACID	519	ASLREKIWTG	VLEWSEKPK.	.....SDQQ	KIPHTLQCTV	CTNIKDGEPE	561
dmPTOV1_A	40	GDSKETIWSG	ELEWEDAQT.	.....LDQP	KTIHTVQCKI	CSMVKEGQPE	82
dmPTOV1_B	211	AIINELLWTG	SLNWSTRCAS.	.....LEEP	SIHKLECSV	YIAIKNGDPG	253
hMED25_ACID	439	LKTEQWFQKL	IMQLIEQOLL	TTLGPLFR.N	SRMVQFHFTN	KDLESKGLY	487
hPTOV1_A	131	LETDQWFQKL	IMQLIEQOLL	TTLGPLFR.N	SQLAQFHFTN	RDCDSLKGLC	179
hPTOV1_B	293	LRTEQWERKL	YMQLIEQOLL	TTLVPLFR.N	SRLVQFHFT.	KDLETLKSIC	340
mMED25_ACID	439	LKTEQWFQKL	IMQLIEQOLL	TTLGPLFR.N	SRMVQFHFTN	KDLESKGLY	487
mPTOV1_A	131	LETDQWFQKL	IMQLIEQOLL	TTLGPLFR.N	SQLAQFHFTN	RDCDSLKGLC	179
mPTOV1_B	293	LRTDQWERRL	FMQLIEQOLL	TTLVPLFR.N	SRLVQFHFT.	KDMETLKSIC	340
dmMED25_ACID	562	IKAENWPEKL	LMQLMEKHLV	GNIIGCFMKD	SKMVVFRPT.	.PGEALDSIA	609
dmPTOV1_A	83	INTENWENKL	KTQLIEKKVL	GKIGCFMKD	ARMVVRSS.	.QGEVLNLI	130
dmPTOV1_B	254	ISAEDWPTLM	FMVLMESTYL	GQFAGAFIKD	SKLIILRST.	.PGEEHDSIA	301
hMED25_ACID	488	RIMNGFAGC	VFPHTAP..	.CEVRVLMIL	YSSKKKI FMG	LIPYDQSGFV	534
hPTOV1_A	180	RIMNGFAGC	MLFPHISP..	.CEVRVLMIL	YSSKKKI FMG	LIPYDQSGFV	226
hPTOV1_B	341	RIMNGFAGC	VFFSYKAS..	.CEIRVLMIL	YSSEKKI FIG	LIPHDQGNFV	387
mMED25_ACID	488	RIMNGFAGC	VFPHTAP..	.CEVRVLMIL	YSSKKKI FMG	LIPYDQSGFV	534
mPTOV1_A	180	RIMNGFAGC	MLFPHISP..	.CEVRVLMIL	YSSKKKI FMG	LIPYDQSGFV	226
mPTOV1_B	341	RIMNGFAGC	VFFSYKAS..	.CEVRVLMIL	YSSEKKI FIG	LIPHDQSNFV	387
dmMED25_ACID	610	KMTSGYAGC	VFFSSIPNSP	ACDLKVLILL	YTPIRNAFIG	FIPNNQAMFV	659
dmPTOV1_A	131	TAMSSGFAGC	IHFPSNPN..	.CNIKALILI	YSRDHQALVG	FIPNNESEFS	177
dmPTOV1_B	302	SSMSAGSCGC	ARFSSEVV..	.CKV..IMLL	YSSFRNAFIG	FIPRDQANFV	346
hMED25_ACID	535	NGIRQVITNH	KQ	546			
hPTOV1_A	227	SAIRQVITTR	KQ	238			
hPTOV1_B	388	NGIRRVIANQ	QQ	399			
mMED25_ACID	535	NGIRQVITNH	KQ	546			
mPTOV1_A	227	NAIRQVITTR	KQ	238			
mPTOV1_B	388	NGIRRVIANQ	QQ	399			
dmMED25_ACID	660	ERLRKVIQOK	QH	671			
dmPTOV1_A	178	ERLQEILQGA	KR	189			
dmPTOV1_B	347	KRLREVLDEH	RQ	358			

### 3.2 MED25 mutation and human pathogenesis: Charcot–Marie–Tooth disease

Recently, an A335V amino acid exchange in MED25 has been linked to an autosomal recessive variant of Charcot–Marie–Tooth disease, which represents a family of genetic peripheral neuropathies. Alanine 335 is located within a proline–rich region of MED25 between the VWA domain and the ACID domain. In an unpublished study a SH3–recognition motif of the Abelson type tyrosine kinases family was predicted in the corresponding region. In humans the motif is characterized by the following sequence: PAPQLPPGPPGAPKPPPASQPS, where the mutated alanine is underlined. *In vitro* binding experiments have been carried out using peptides with or without the mutation. The conclusion from these experiments is that while the wild–type peptide displays binding specificity for the Abl kinase, the A335V mutant shows the same binding affinity for the SH3 domain of both, the Abl kinase and the Src–family kinase Lck. Because of the loss of binding specificity for SH3 domain proteins, the A335V mutation seems to be the responsible for the CMT2B2 variant of CMT disease. Here we investigate whether the presence of the A335V mutation would somehow affect major functional properties of MED25, namely transcriptional activation and Mediator–interaction capabilities, therefore providing alternative or additional mechanisms to explain the disease.

#### 3.2.1 Study of transcriptional activation potential and Mediator– binding capacity of MED25 (A335V) mutant

##### Transcriptional activation analysis.

In order to investigate whether the CMT mutation would result in impaired MED25 transcription activation function, the A335V mutation was introduced into full–length MED25 fused to the GAL4 DNA–binding domain. The transcriptional activation potential of this MED25 mutant was tested in a reporter assay in Jurkat cells using the pGLRMG5 reporter, containing five GAL4 binding sites in front of luciferase. In the reporter assay shown in figure 18B, increasing amount of wild–type and mutant MED25 were used. Luciferase values were determined and activation rates were calculated using the reporter alone as a reference. In order to monitor the expression levels of the wild–type

and mutant MED25, nuclear extracts were prepared and subjected to an immunoblot analysis using an anti-GAL4 DNA-binding domain antibody.

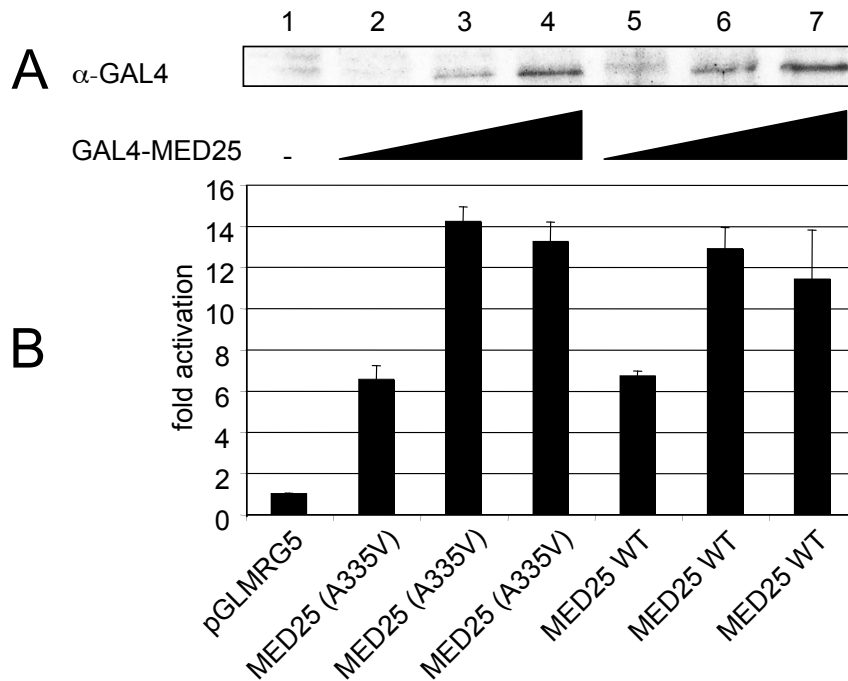


**Figure 18.** A335V mutation does not affect the intrinsic transcription activation capability of MED25. Titrated amounts (0.5  $\mu$ g, 5  $\mu$ g and 10  $\mu$ g) of GAL4-tagged MED25(A335V) point mutant and MED25 wild-type were transfected in Jurkat cells together with pGLMRG5 luciferase reporter (A) Western blot analysis of isolated nuclear extracts using an  $\alpha$ -GAL4 antibody (B). The fold activation of MED25 constructs was calculated normalizing luciferase levels to the  $\beta$ -gal activity, using the reporter alone (pGLMRG5) as a reference.

As shown in figure 18B, the fold activation values observed for the wild-type MED25 were increasing from 0.5  $\mu$ g to 10  $\mu$ g of transfected expression vector (lanes 5 and 7), reaching a plateau already at 5  $\mu$ g of transfected construct (lane 6). A direct correlation between the amount of construct transfected and the expression levels of the corresponding protein in the cells was confirmed by the increasing signals in Western blot analysis (figure 18A, lanes 5–7). For the same amounts of transfected MED25 (A335V) mutant expression vector, almost identical activation rates were obtained as compared to the wild type (figure 18B, lanes 2–4). Expression levels of the MED25 (A335V) mutant in Jurkat cells were also in accordance to the amount of construct transfected (figure 18A, lanes 2–4) and comparable to the wild-type.

### Physical interaction analysis

The MED25 (A335V) mutant does not show impaired transcriptional activation compared to the wild-type construct, and since the transcriptional activity of MED25 wild-type is also related to its capability to bind Mediator, the question was raised whether the potential of A335V mutant MED25 to interact with Mediator was unaffected as well. To address this question an immunoprecipitation assay was performed. A Flag-antibody-coupled column was loaded with nuclear extract from HEK-293T cells overexpressing a Flag tagged version of the MED25 (A335V) mutant. Non-transfected nuclear extract and naked beads were used as negative controls (lanes 3 and 5). The Western blot analysis revealed that Mediator could efficiently coprecipitate with the Flag-tagged MED25 (A335V) mutant (figure 19, lane 4).

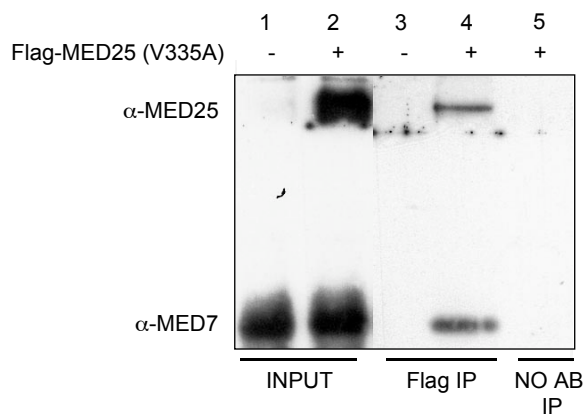


**Figure 19.** A335V mutation does not impair Mediator–interaction capability of MED25. Nuclear extracts isolated from 293T cells overexpressing Flag-tagged MED25 (A335V) mutant were immunoprecipitated with  $\alpha$ -Flag antibody. Monoclonal antibodies against MED25 to monitor MED25 (A335) mutant or against the Mediator core subunit MED7 to monitor levels of coprecipitated Mediator were employed in the Western blot analysis. Beads only were used as a control (lane 5).

### 3.3 Identification of MED25 target genes

The *in vivo* function of MED25 is still an open question. Certainly, the fact that MED25 Mediator subunit is an exclusive prerogative of higher eukaryotes can be interpreted as a hallmark of a specialized function rather than a general one. This hypothesis is in line with data recently published by Kim et al., (Kim et al., 2004), showing a specific role for MED25 in the transcriptional activation of the *Drosophila* genes *Attacin A* and *Hsp26* in contrast to other Mediator subunits. The identification of genes that are specifically regulated by MED25 in mammals would help to understand MED25 function. MED25 has been reported to interact with VP16 *in vitro* (Mittler et al., 2003). Transfection experiments revealed a dominant negative function for the Mediator–interaction domain

(MED25–NTD). Overexpression of this domain impaired dramatically transactivation by another viral factor, EBNA2 (Laux, personal communication). Together these results indicate a possible involvement of MED25 in immune response and raise the question whether MED25 regulates genes that are critical in this process.

Microarray analysis is a powerful tool to identify genes that are directly or indirectly regulated by a certain protein. In an attempt to learn more about the biological function of MED25, this approach was chosen to identify genes that were affected on a genome-wide level. Two strategies were combined:

- i) the overexpression of MED25 in a murine cell system (NIH3T3 cells)
- ii) the overexpression of a dominant negative mutant of MED25 (MED25–NTD) in a human B cell line constitutively expressing the viral activator EBNA2 (721–B–cells).

In the first approach we set out to identify the population of genes which are regulated by MED25 in a normal cellular background. In this system the regulation of MED25 target genes was expected to be enhanced by the overexpression of the ER–fusion protein. In the second approach we aimed more specifically to the identification of MED25 target genes affected in front of the background of viral infection. The use of a dominant negative mutant was supposed to interfere with genes regulated by MED25–bound Mediator and with genes exploited by the viral activator EBNA2 in order to support the viral life cycle.

In both cases the overexpressed proteins were fused to Estrogen Receptor Ligand Binding Domain (ER–LBD) in order to control the overexpression of the proteins in the nucleus (inducible system). This type of system offers the advantage of monitoring genes differentially expressed upon induction of the fusion protein at different time points compared to the non–induced situation (reference). Genes regulated at an early time point are likely to be direct target genes while genes regulated at a late time point are possibly indirect target genes.



### 3.3.1 Generation of an inducible cell line expressing MED25

A murine cell line (NIH3T3 mouse fibroblasts) was stably transfected and selected using hygromycin for stable replication of an EBV vector carrying wild-type full-length MED25 fused to the Estrogen Receptor Ligand Binding Domain (ER-LBD) at the N-terminal part of the protein. This LBD carries mutations that abolish the activation by endogenous ligands while responding activation by synthetic derivatives (Feil et al., 1997). In this system the fusion protein is constitutively expressed but kept in the cytoplasm in an inactive state due to the binding of the ER-LBD to the heat shock protein HSP90. As soon as the cells are treated with the synthetic estrogen antagonist 4-hydroxy-tamoxifen (OHT), ER-MED25 dissociates from HSP90 protein and translocates into the nucleus (figure 20A). A cell line overexpressing only ER-LBD was created as a negative control even though it has been reported that the transactivation function in the LBD is silenced by the binding to OHT (MacGregor Schafer et al., 2000). To monitor the translocation into the nucleus of ER-MED25 and of ER-LBD proteins, nuclear extracts from NIH-ER-MED25 and NIH-ER-LBD stable cell lines were collected before and three hours after induction with OHT and analyzed for MED25 expression in the nucleus via Western blot analysis using a monoclonal antibody against MED25 (figure 20B, upper panel) or against ER (figure 20B, lower panel). These data were confirmed by immunofluorescence analysis using the NIH-ER-MED25 cell line and an antibody against the ER-LBD tag (figure 20C). While the  $\alpha$ -ER antibody could visualize the translocation of ER-MED25 from the cytoplasm to the nucleus 3 hours after OHT induction in the NIH-ER-MED25 cell line, no signal could be detected in the NIH3T3 wild-type cell line, confirming the specificity of the antibody. Since the 35kDa ER-LBD fused to the N-terminus of MED25 may interfere with the potential of MED25 to interact with Mediator, the following control experiment was confirmed. ER-MED25 was transiently over-expressed in HEK-293T cells, which were harvested 48 hours later to isolate nuclear extract. In parallel, a Flag-tagged MED25 construct, known to bind Mediator, was used as a positive control. Nuclear extracts containing over-expressed either ER-MED25 or Flag-MED25 proteins were loaded on an  $\alpha$ -MED15 chromatography column and analyzed by Western blot. Two monoclonal antibodies against MED25 and MED7 were used to recognize the tagged MED25 proteins and

Mediator, respectively. As shown in figure 20D, ER–MED25 and Flag–MED25 were efficiently coimmunoprecipitated with Mediator (lanes 5 and 3) providing evidence that ER–LBD fused MED25 interacts with Mediator and is, therefore, suitable for this study.

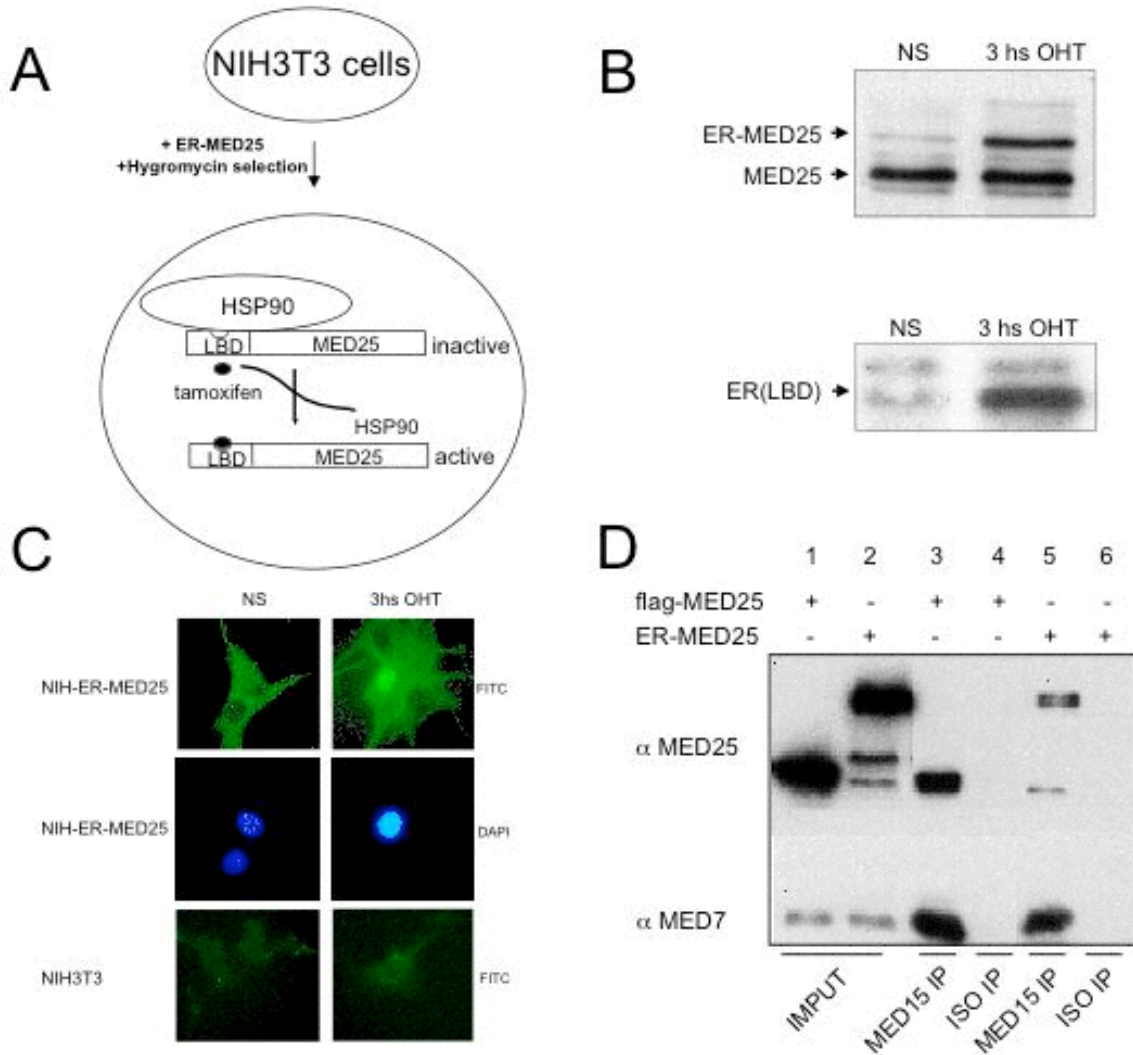


**Figure 20.** Generation of an inducible cell line expressing MED25. (A) ER–LBD tagged MED25 was stably transfected in NIH3T3 cells. HSP90 retains the protein into the cytoplasm in an inactive state. Tamoxifen binds to ER–LBD releasing the protein from the binding and allowing its translocation into the nucleus. (B) Western blot analysis of nuclear extracts collected from NIH–ER–MED25 (upper panel) and NIH–ER cells lines 0 and 3 hours after OHT induction. Antibodies against MED25 and against ER–LBD were used, respectively. (C) Immunofluorescence in NIH–ER–MED25 cell line and in wild type NIH3T3 cells performed using an antibody against ER–LBD. (D) Nuclear extracts isolated from 293T cells overexpressing ER–tagged MED25 and Flag–tagged MED25 were immunoprecipitated with MED15 antibody (lanes 3 and 5). Monoclonal antibodies against MED25 to monitor tagged and wild–type MED25 or against the Mediator core subunit MED7 to monitor the level of coprecipitated Mediator were used in the Western blot analysis. An isotype antibody was used as control (lanes 4 and 6)

### 3.3.2 RNA expression profiling of NIH–ER–MED25 cell line and RT–PCR analysis

With the previously described inducible NIH–MED25 cell line, a microarray analysis was performed in collaboration with Dr. J. Beckers and Dr. M. Horsch (IEG, GSF, Neuerberg). A glass–surface DNA–chip containing about 21000 probes was used. These probes are from the commercial Lion mouse array–TAG clone set, which is mostly derived from 3'UTRs. Translocation to the nucleus of ER–MED25 was observed as early as 3 hours after OHT induction offering the opportunity to look at genes to look at genes affected early and late. Towards this end, a time course experiment was carried out and RNA was collected from non–induced cells and from cells induced for 3 and 10 hours with Tamoxifen. RNA was used for reverse transcription and indirectly labelled with Cy3 or Cy5 fluorescent dye. Labelled cDNA from each time point was mixed with the reference cDNA solution labelled with a second dye and used to hybridise microarrays. Four chip hybridisations were performed with RNA from each time of measurement. Each chip hybridisation was performed against RNA of non–treated cells (reference RNA). For each time of measurement the chip experiments included two colour–flip experiments. After hybridisation, chips were scanned and the images analysed using an image processing software. For data analysis an in–house produced LabView based software was used. The analysis of the data revealed a very low number of genes differentially regulated upon induction. 3 hours after induction 5 genes were down–regulated (table 10); 10 hours after induction 8 genes were upregulated and 2 genes were down–regulated (table 11).

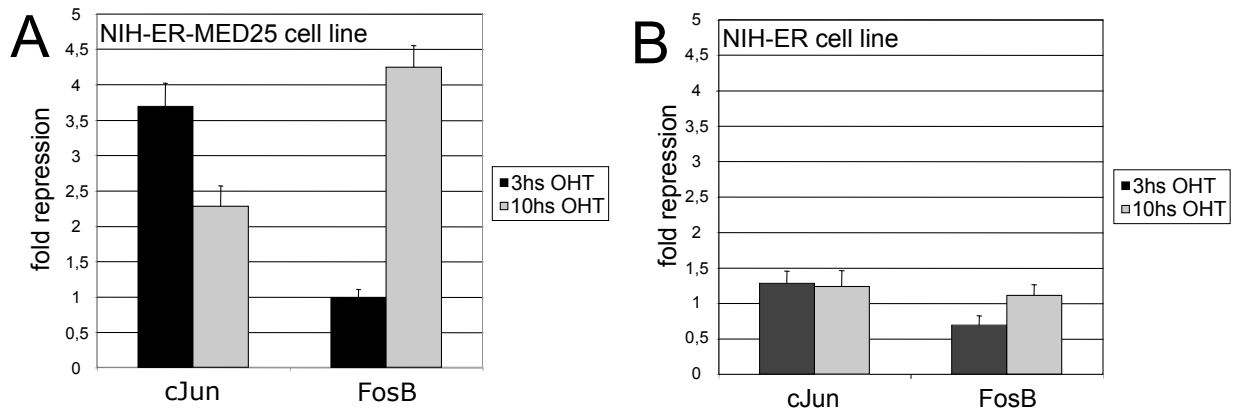
Quantitative real–time PCR was used to validate arrays for some of the listed genes (data not shown). Array data were confirmed via RT–PCR comparing RNA from the same cell line with samples from a control cell line for two down–regulated genes, cJun and FosB. While the amount of cJun and FosB transcripts detected on the NIH–ER–MED25 cell line was decreasing after OHT induction (figure 21A), it remained unchanged in the control cell line NIH–ER (figure 21B), which indicates that cJun and FosB are specifically regulated by ER–MED25.

**Table 10.** Differentially regulated genes in NIH-ER-MED25 cell line 3 hours after OHT induction.

Downregulated genes	
GENE NAME	FOLD REPRESSION
Pax5	3.8
Dio1	3.9
Ldhd	3.4
Scn1b	2.7
Angptl2	3.0

**Table 11.** Differentially regulated genes in NIH-ER-MED25 cell line 10 hours after OHT induction.

Upregulated genes	
GENE NAME	FOLD INDUCTION
Sc4mol	1.7
Cyp51	1.8
Sqle	1.7
Rps29	1.5
Dbi	1.5
Rps23	1.5
Rsp21	1.5
Rpl44	1.5
Downregulated genes	
GENE NAME	FOLD REPRESSION
FosB	1.8
cJun	1.3

**Figure 21.** Validation of array data via RT-PCR on cJun and FosB genes. RT-PCR analysis was performed using RNA isolated from NIH-ER-MED25 cell line (A) and NIH-ER cell line control (B) 0, 3 and 10 hours after OHT induction. Fold repression at 3 and 10 hours time points was calculated relatively to the 0 time point reference sample.

### 3.3.3 Generation of an inducible cell line expressing a dominant negative mutant of MED25

The N-terminal 290 amino acids (NTD), comprising the VWA domain that binds Mediator, were shown to repress transcription activation by GAL-VP16-H1 on a GAL4-luciferase reporter (Mittler et al., 2003). The aberrant MED25-NTD integrates into Mediator (figure 10, lane 5) in competition with wild type MED25 (Mittler et al., 2003). As a consequence, transcription activation by VP16 is impaired. The same phenomenon was observed when VP16 was substituted by another viral transcription activator, e.g. the Epstein-Barr virus (EBV) Nuclear Antigen 2 (EBNA2) (Gerhard Laux, personal communication). Moreover, EBNA2 and VP16 activation domains have been reported to share analogies in their function and structure (Cohen, 1992; Cohen and Kieff, 1991), which renders EBNA2 a candidate target for MED25. EBNA2 is essential for initiation and maintenance of B-cell immortalisation (Cohen et al., 1989; Hammerschmidt and Sugden, 1989; Kempkes et al., 1995). The 721-B-cell line is derived from primary B cells that were infected *in vitro* and therefore converted to an immortalized lymphoblastoid cell line constitutively expressing EBNA2. In order to analyze the effect of a dominant negative mutant of MED25 in a background of constitutive EBNA2 expression, a 721-B-cell line was generated stably expressing MED25-NTD. This approach could provide for an insight into mechanisms of gene control by EBNA2 and a useful tool to elucidate a possible role for MED25 in immunological processes. The stable 721-ER-MED25-NTD human cell line was used for the identification of differentially expressed genes upon overexpression of the MED25 dominant negative mutant at different time points. A MED25-NTD construct N-terminally fused to the ER-LBD was cloned into an episomal vector (figure 11A). Cells were stably transfected, hygromycine selected and checked for expression levels of the fusion protein translocated to the nucleus 1 hour, 10 hours and 24 hours after Tamoxifen induction. Nuclear extracts collected at different time points after induction of the cells with OHT were analysed by Western blot using antibodies against MED25 (to visualize endogenous MED25 and ER-MED25-NTD fusion protein). Additionally, an antibody against the Mediator subunit MED7 was used to visualize expression levels of a core Mediator subunit in relation to the expression levels of induced ER-MED25-NTD

protein. As shown in figure 22B, ER–MED25–NTD seems to be present in small amount in the nucleus even before induction (lane 1), which, however, might be the consequence of cytoplasmic contamination of the nuclear extract. Tamoxifen induction for 10 and 24 hours, respectively, results in translocation of the ER–MED25–NTD fusion protein into the nucleus (lanes 3 and 4) which was less evident 1 hour after induction (lane 2). At the same time, the overexpression of the dominant negative construct ER–MED25–NTD in the nucleus upon 24 hours induction results in a diminished amount of endogenous MED25 in the nucleus (lane 4). By contrast, the signals corresponding to MED7, shown as loading control, are unchanged at all times (lanes 1–4, lower bands). To demonstrate the integration of ER–MED25–NTD construct into the Mediator complex an immunoprecipitation assay was performed. For this purpose, an anti MED15 antibody column was used. The eluate obtained after immunoprecipitation was analysed by Western blot using the monoclonal antibody (VC1) against MED25 to visualize ER–MED25–NTD. Another antibody against the core Mediator subunit MED7 was employed as a control. Figure 22C shows that Mediator, represented by MED7 bands, was efficiently immunoprecipitated from nuclear extracts at all times (lanes 1–4). The coimmunoprecipitation of ER–MED25–NTD from nuclear extracts collected 1, 10 and 24 hours after Tamoxifen induction (lanes 2–4) confirmed that ER–MED25–NTD fusion protein retains Mediator–binding capacity. The amount of ER–MED25–NTD fusion protein incorporated in the complex seems to gradually increase over the time course experiment (lanes 2–4).

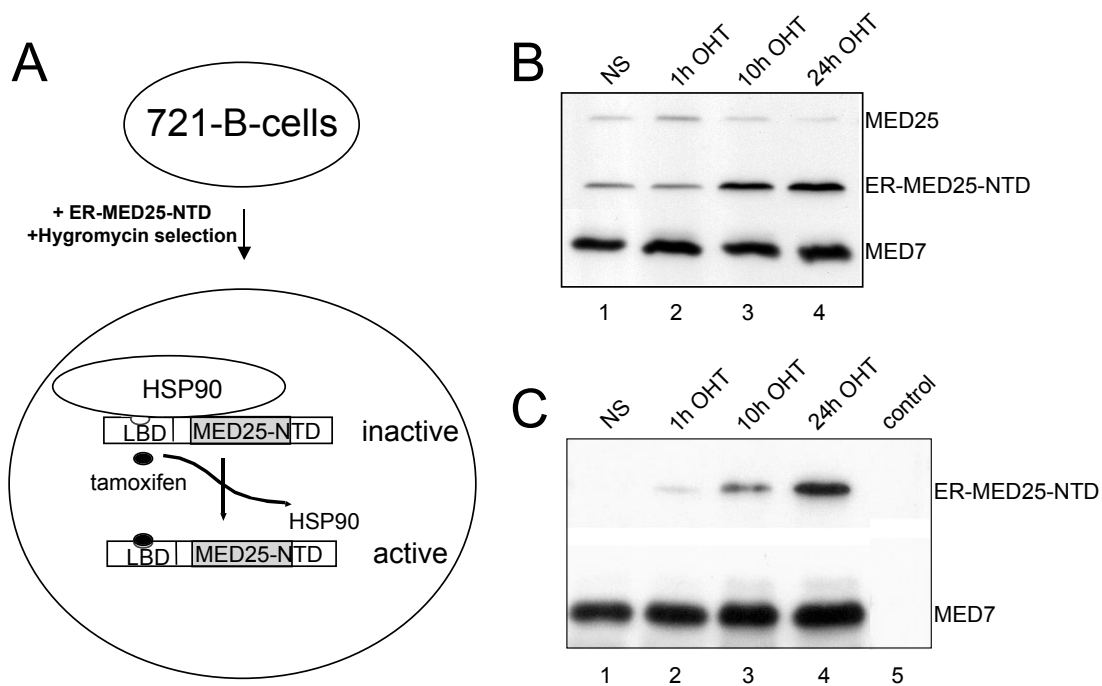


**Figure 22.** Generation of an inducible cell line expressing MED25-NTD. (A) ER-LBD tagged MED25-NTD was stably transfected in 721-B-cells. In the generated cell line HSP90 retains the protein into the cytoplasm in an inactive state. Tamoxifen binds to ER-LBD releasing the protein from the binding and allowing its translocation into the nucleus. (B) Expression levels of ER-MED25-NTD protein visualized by Western blot analysis of nuclear extracts collected from 721-ER-MED25-NTD cells line 0, 1, 10, and 24 hours after OHT induction. Antibodies against MED25 and against MED7 were used. (C) Nuclear extracts isolated from 721-ER-MED25-NTD cells 0, 1, 10, and 24 hours after OHT induction were immunoprecipitated with MED15 antibody. Monoclonal antibodies against MED25 and MED7 were used in Western blot analysis for detection of MED25 and MED7, respectively (lane 5).

### 3.3.4 Genome-wide analysis of transcriptional regulation by ER-MED25-NTD

The Tamoxifen inducible 721-ER-MED25-NTD cell line was used in a time course experiment in order to identify genes differentially regulated by MED25-NTD. RNA samples were isolated from cells 1 hour, 10 hours and 24 hours after Tamoxifen. RNA derived from non-induced cells was also collected and used as a reference. Each sample was therefore used to analyze the gene expression profiles using Affymetrix arrays. Affymetrix arrays analysis was performed by KFB, Regensburg. For this analysis an Affymetrix Human Genome U133 Plus 2.0 Array GeneChip was employed, which covers the human genome completely. The data received from the company were

analyzed according to their instructions (see 2.2.4). The total number of genes differentially regulated at the three time points are summarized in table 12.

**Table 12.** Total number of genes differentially regulated upon Tamoxifen treatment of 721–ER–MED25–NTD cell line at different time points. Genes up or down regulated less than 1.2 fold are not included.

TIME POINT	TOTAL UPREGULATED GENES	TOTAL DOWNREGULATED GENES
1 h	411	541
10 h	221	78
24 h	290	142

Because of its dominant negative effect the assumption was made that ER–MED25–NTD protein may impair the regulation of EBNA2 target genes. In order to identify EBNA2 target genes that may be downregulated by ER–MED25–NTD, genes downregulated in this microarray analysis (table 12) were compared with known EBNA2 target genes. From this analysis 13 presumptive common target genes were found.

**Table 13.** Genes downregulated by ER–MED25–NTD, which are as well reported as EBNA2–target genes. Indicated are fold repression rates.

GENES	1h down	10h down	24h down
Bcl2	2.8		
CCL4	2.8		
MAFF	2.6		
CCL3	2.5		
SNX9	2.1		
RGS1	1.9		
TRIO	1.9		
ATP1B1	1.5		
CCL5	1.3		
CD300A	1.3		1.4
CMKOR1	1.3	1.2	1.3
GADD45 $\beta$	1.3		1.3
RBBP6	1.3		

These data support the hypothesis of MED25–bound Mediator involvement in both, EBNA2 transcriptional activation mechanism and immune response.



### 3.3.5 Activation of p21 promoter by MED25

In an attempt to understand the mechanism of MED25 recruitment to its target gene promoters we looked for cellular activators containing an acidic domain resembling that of the viral activator VP16. One of them, p53, was tested on a p21 luciferase reporter containing the p21 promoter region  $-2325/+8$ . Transient overexpression of MED25 led to five-fold increase of reporter activity (data not shown). Co-transfection of MED25 together with p53, however did not lead to significantly increased activation rates. These findings indicated the activation of the p21 promoter by MED25 in a p53 independent manner. Hence the question was addressed whether MED25 might activate p21 promoter through an alternative pathway. The proximal region ( $-122$  and  $-64$ ) of the p21 promoter is GC-rich and contains six binding sites for the ubiquitous transcription factor Sp1 (Moustakas and Kardassis, 1998). One of these Sp1 sites was shown to be required for the stimulation of the p21 promoter by TGF- $\beta$  and its downstream targets, the Smad protein family. It has been reported that another Mediator subunit, MED15, is involved in this pathway via interaction with the Smad transcription activators (Kato et al., 2002). To elucidate whether the activation of the p21 promoter by MED25 functions also through this pathway, HeLa cells were transiently cotransfected with a p21 promoter variant ( $-143/+8$ , figure 23A) containing the Sp1 site mentioned above together with expression vectors for MED25, Sp1 and Smad3 (figure 23B). Luciferase measurements showed that each of the proteins contribute to activation of the p21 promoter. However, no synergistic effect could be observed when using combinations of these proteins. Hence MED25 does not seem to use the TGF- $\beta$  pathway to activate p21. These data were confirmed in HepG2 cells, a tumor-derived cell line of hepatic origin frequently used as a model to study the transcriptional regulation of the p21 gene (Moustakas and Kardassis, 1998) (data not shown).

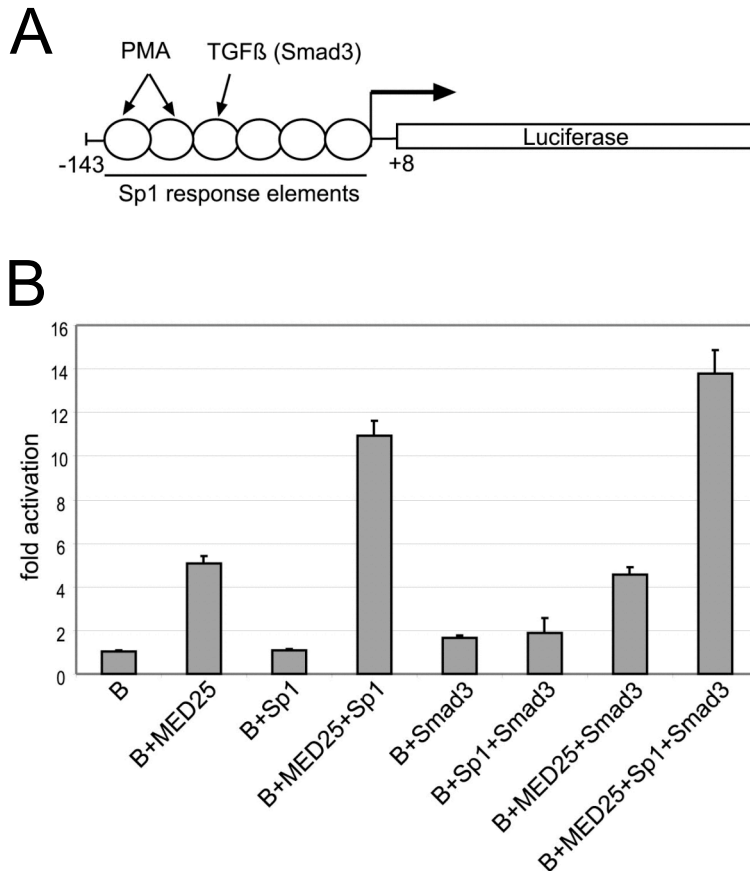


**Figure 23.** MED25 activates a p21 reporter in transiently transfected cells.

(A) Schematic view of the p21 reporter construct used in transient transfections. The six Sp1 sites are depicted. (B) Flag-tagged Med25, Sp1 and Smad3 constructs were transiently transfected in HeLa cells together with the p21 reporter.

Furthermore the activation of p21 promoter by MED25 was tested in the NIH-ER-MED25 cell line stably expressing inducible ER-MED25. Cells were transiently transfected with titrated amounts of p21 reporter (-2325/+8) 24 hours before induction. 3 hours after addition of 1mM Tamoxifen, cells were collected and luciferase levels were determined.

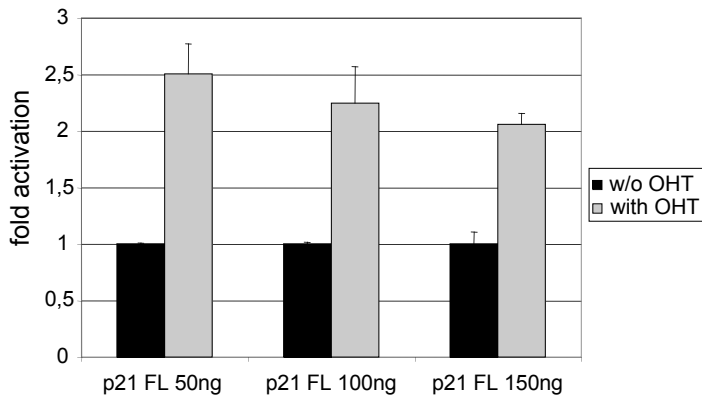


**Figure 24.** ER-MED25 induces a p21 reporter in NIH-ER-MED25 stable cell line. NIH-ER-MED25 cells were transiently transfected with titrated amounts of p21 (-2325/+8) luciferase reporter. Cells were collected 3 hours after Tamoxifen induction and luciferase activity was measured.

As shown in figure 24, the luciferase activity was increased more than two fold upon ER-MED25 translocation into the nucleus confirming the results of the transient analysis.

### 3.4 Towards the generation of a MED25 conditional knock-out mouse

In order to identify and characterize MED25 *in vivo* functions a conditional knock-out mouse approach was followed by gene targeting in mouse embryonic stem cells.

#### 3.4.1 Organization of MED25 genomic locus

In the mouse, the 13kb MED25 genomic locus (figure 25) is located on the seventh chromosome and it is characterized by 17 introns and 18 exons encoding for a 760 amino acids protein. In the MED25 locus, exons are alternated by introns of a relatively small size, except for the third intron which causes a distance of 5.5kb between the third and the fourth exon. The functional domains of MED25 with respect to the genomic organization of its locus are distributed as follows: the VWA domain is encoded by exons 1–6 while the ACID domain is encoded by exons 10–14 (figure 25). Table 14 shows the exon distribution in the MED25 cDNA murine sequence (gb BC031138.1) and the length of the corresponding introns in the MED25 genomic locus (gb NT039420).

**Table 14.** Distribution of MED25 exons in the mouse cDNA sequence and length of the corresponding introns in the mouse MED25 genome locus.

Exon	cDNA division in exons (bp)	Intron	Intron length (bp)
1	1–181	1	85
2	182–225	2	192
3	226–350	3	5511
4	351–449	4	268
5	450–568	5	281
6	569–732	6	128
7	733–864	7	155
8	865–952	8	77
9	953–1146	9	310
10	1147–1274	10	933
11	1275–1361	11	73
12	1362–1418	12	101
13	1419–1527	13	1647
14	1528–1715	14	284
15	1716–1788	15	97
16	1789–2006	16	147
17	2007–2185	17	407
18	2186–2314	–	

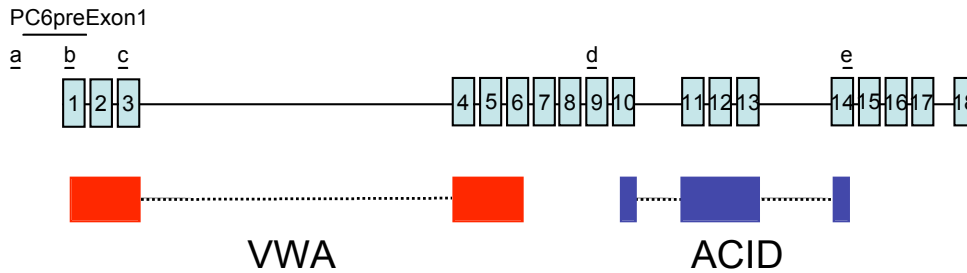


**Figure 25.** Schematic view of MED25 genomic locus. The exons are numbered from 1 to 18. VWA domain amino acids are encoded by exons 1–6 and ACID domain amino acids are encoded by exons 10–14. PC6preExon1 probe was used to screen the 129/Ola derived genomic library. Letters indicate the oligoprobes used to select the 129/Ola derived BAC clone containing the MED25 genomic locus (a=PC6prepreExon1, b=PC6Exon1up, c=PC6Exon3up, d=PC6Exon9up, e=PC6Exon14down)

### 3.4.2 Targeting strategy for the generation of a conditional null allele

At the starting point of the MED25 transgenic mouse project, the only information available about MED25 function was related to its two functional domains. Therefore the assumption was made that disruption of the Mediator–interaction domain would very likely result in a phenotype that would provide insights into MED25 *in vivo* function. Towards this end a targeting vector was designed with respect to some general rules, which are to be mentioned briefly:

1. As starting material, a genomic clone of sufficient length must be obtained from a mouse library, the strain of which should be the same as the ES cells employed.
2. The length of the homologous recombination arms is recommended to be at least 4kb of uninterrupted sequence on one side with 1–2kb on the other one.
3. For the selection of the positive ES cell clone, a neomycin (neo) cassette should be included; the additional employment of a thymidine kinase gene (TK) at the distal end of the genomic DNA construct ideally increases the number of homologous recombinants among the clones surviving selection.
4. In the case of a conditional knock–out, a site–specific DNA recombinase system is required, commonly represented by two *loxP* sites flanking the targeted portion of DNA. The use of a CRE recombinase able to selectively recognize *loxP* sequences, allows a spatially and/or temporally controlled deletion of the gene of interest. The employment of an additional recombinase system, the Flp/*FRT*, allows the removal of the neomycin cassette in an independent step.

5. A screening strategy should be designed that will provide for clear discrimination between wild type and different parental types of deletions during Southern blot analysis.

Figure 26 shows a schematic view of the MED25 targeting vector of which a detailed description is provided. A 3kb MED25 genomic region included in between exons 4–10 is followed by a neomycin cassette (positive selection marker) which is flanked by two *FRT* sites. Two *loxP* sites are located before the fourth exon (almost at the end of the third intron) and after the second *FRT* site, respectively. The 5' homologous recombination region, upstream of the first *loxP* site, is composed of the third exon and most of the third intron and includes about 5kb of the MED25 genomic locus. Upstream of the 5' homologous recombination region is located the thymidine kinase (TK) cassette encoding for the negative selection marker. Downstream of the second *loxP* site, the 3' homologous recombination includes a 1.2 kb genomic region spanning between the tenth and the thirteenth intron, which comprises the exons 11, 12 and 13. Several approaches are possible after replacement of the endogenous allele with the conditional null allele. Avoiding to use site specific recombination (with Cre or Flp) in the cells and, therefore, using the original targeting vector for the blastocyst injection, allows the generation of a mouse in which the MED25 allele is "interrupted" by a neomycin cassette. This cassette may interfere with the regulation of MED25 expression (hypomorphic allele), therefore providing a strong or mild phenotype. Mating this original line of MED25 conditional knock-out mice with Flp recombinase expressing mice allows removal of the neomycin cassette, creating a second MED25 conditional knock-out line which is comparable to a wild type mouse. Mating this second line of MED25 conditional knock-out mice with Cre recombinase expressing mice (ubiquitously or tissue-specifically) leads to the generation of a MED25 knock-out mouse where the portion of MED25 genome locus containing the exons 4–10 (encoding for amino acids 117–424) is deleted. In this MED25 knock-out mouse a chimeric MED25 protein will be translated, which contains the amino acids 1–116 fused to the amino acids 425–760. As previously shown with the structure–function analysis of MED25 protein (figure 10), an intact VWA domain (amino acids 17–226) is necessary to bind Mediator. Therefore, the designed targeting vector is suitable for the generation of a MED25 knock-out mouse, in which the Mediator–interaction capability of MED25 is impaired.

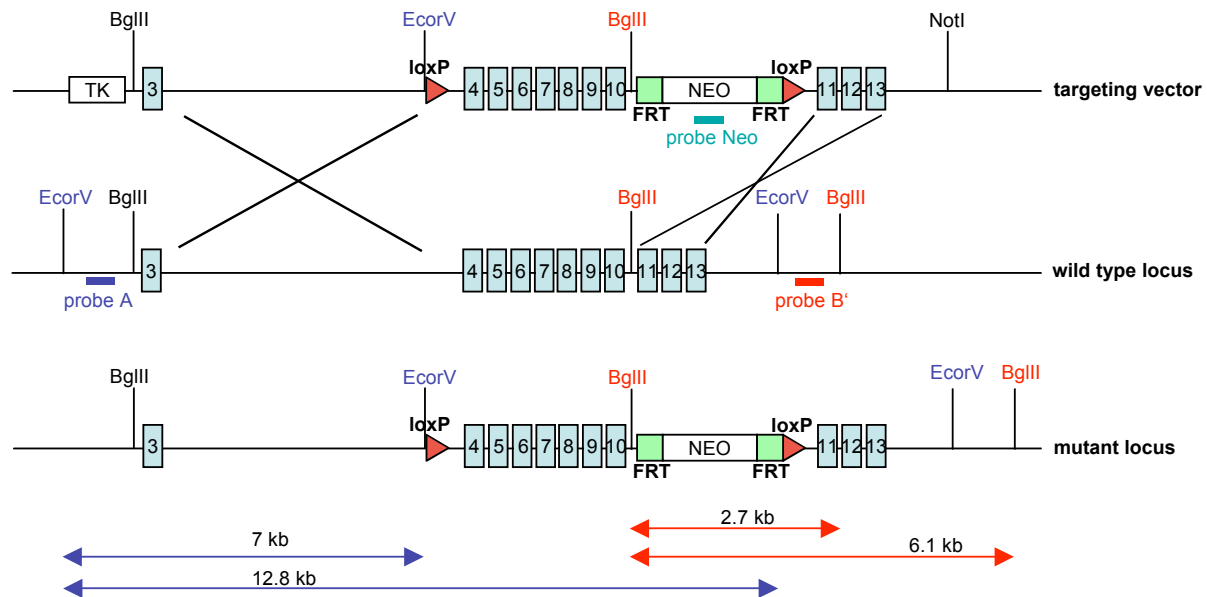


**Figure 26.** Schematic view of MED25 targeting strategy. A targeting vector was generated containing the region to be deleted (exons 4–10) floxed by two loxP sites, a neomycin cassette flanked by two FRT sites, a negative selection marker (TK) and a unique site of restriction (NotI) for linearization of the vector. For the screening by Southern blot of the ES cells clones survived after double selection, probe A (blue) and probe B (red) were used. Probe Neo (green) was used to exclude that random integration was occurring in the homologous recombinant clone.

### 3.4.3 Screening strategy by Southern blot analysis

A screening strategy was designed to distinguish wild-type from homologous recombinant ES cells and from different parental types of deletions, during southern blot analysis. Probes that recognize regions surrounding the portion of DNA replaced by the targeting vector, allow for discrimination of homologous recombinants from random integrants. Therefore, two external probes, one targeting upstream and the other one downstream of the target locus were designed. The upstream probe, probe A (represented in blue in figure 26), spans a 660bp region, which starts 420bp upstream of the transcriptional start site of MED25 genomic locus and finishes at the end of the first exon at the same locus. Digesting genomic DNA with EcoRV restriction enzyme allows to distinguish the MED25 wild-type pattern characterized by a single 12.8kb band for both alleles from the homologous recombinants, which will lead to detection of an additional 7kb band. At the 3' end, probe B' (represented in red in figure 26) is located in the thirteenth intron and spans a 540bp region which starts about 360bp downstream of

the thirteenth exon. Upon DNA restriction digestion with BglIII, wild-type-derived genomic DNA displays a single 6.1kb band in contrast to the homologous-recombinant-derived genomic DNA which is characterized by an additional 2.7kb band. To rule out the possibility that random integration was occurring in the ES cell clones positive for homologous recombination, a 380bp Neo probe (indicated in green in figure 26) recognizing the neomycin cassette was used. Upon BglIII or EcorV restriction digest of the homologous recombinant genomic DNA, a single band of 6.1kb or 11.2kb respectively should be detected.

#### **3.4.4 Selection of a genomic clone from a 129/Ola mouse library**

A 129/Ola derived ES cell line called TBV2 was provided by the Wurst laboratory (IEG, GSF, Neuherberg). In order to use isogenic DNA for the targeting construct, a 660bp probe spanning the ATG starting site and called PC6preExon1/probeA (indicated in figure 26) was obtained by PCR using pLB52 DNA BAC clone as template and sent to the rzpd screening service in Heidelberg. From a 129/Ola BAC library eight clones positive for the probe PC6preExon1/probeA were obtained. In order to identify a full-length BAC clone a dot blot analysis was performed. DNA was derived from each clone via miniprep. Five hybridisation membranes were organized in 22 squares and spotted with duplets of DNA coming from each of the eight clones (figure 27, from spot number 1 to spot number 16). The first three clones appear in 12 squares in total (1–6 and 17–22) since the membranes were spotted with DNA coming from additional maxi preps (from 17 to 22). Five oligo-probes were designed, which are spanning the entire MED25 gene locus, and are indicated by a one-letter code in figure 25 (PC6prepreExon1=a, PC6Exon1up=b, PC6Exon3up=c, PC6Exon9up=d, PC6Exon14down=e). Each membrane was hybridised with a different <sup>32</sup>P radioactively labelled oligo-probe and exposed to a film for autoradiography.

The signals at positions number 19 and 20 were stronger on every probed membrane. The clone number 2 was chosen because it contains the portion of MED25 genomic DNA necessary for the cloning of the MED25 targeting vector.



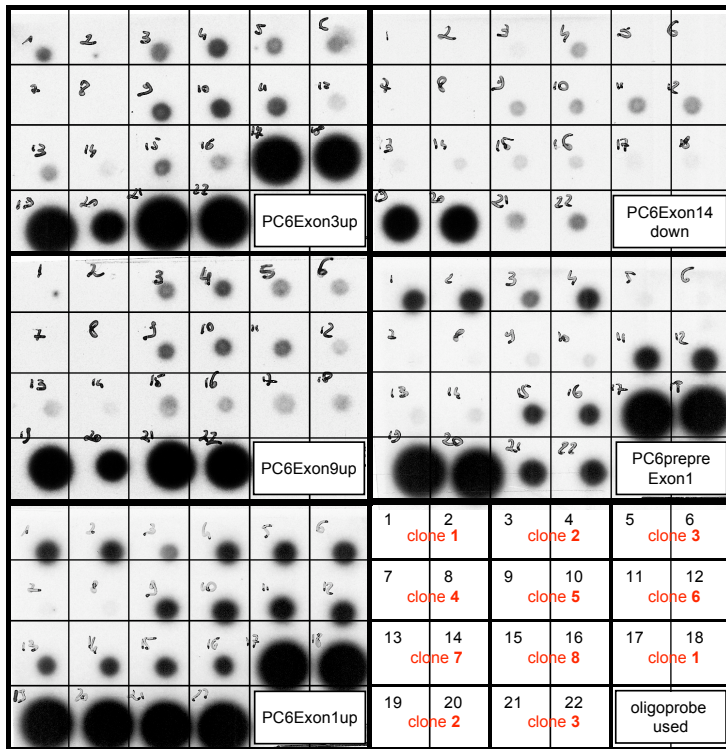


**Figure 27.** Screening of a 129/Ola genomic library to select a clone containing the entire MED25 genomic locus. Eight clones were selected from a pre-screening carried out using PC6preExon1 probe (see also figure 25). Using 5 oligo-probes spanning the entire MED25 genomic locus, a dot-blot analysis was performed to select a BAC clone suitable for the cloning of the MED25 conditional null allele.

### 3.4.5 Generation of a MED25 conditional null allele

A 8kb BgIII fragment including the DNA from the third to the tenth exon was obtained from the 129/Ola derived BAC genomic library mentioned above and inserted in between a TK cassette and a *FRT* flanked Neo cassette fused to a distal *loxP* site. A 1.2kb PCR fragment corresponding to the exons 11–13 was cloned on the 3' side to function as the 3' homologous recombinant region. The 5' homologous recombinant region was created by inserting an *EcoRV*/*loxP* site in a *SpeI* unique restriction site located in the third intron and 5kb downstream of the first BgIII site. For the electroporation of the MED25 targeting vector in ES cells, a *NotI* unique restriction site included in the multiple cloning site of the backbone plasmid and positioned immediately downstream of the thirteenth exon can be used to linearize the targeting vector.

### 3.4.6 Transfection of ES cells and determination of a homologous recombinant

Once created, the targeting vector was linearized with NotI and electroporated in TBV2 ES cells. After ES cell clone selection (see 2.3.7) genomic ES cell DNA was digested with EcoRV to test for homologous recombination at the 5' end and with BglII to test for homologous recombination at the 3' end. Restricted DNA was separated on an agarose gel, blotted and screened with probe A and probe B' respectively. Among about 500 clones picked, only one (clone 5A) turned out to have undergone homologous recombination on both sides of the allele (figure 28A). In addition to the wild-type bands, the mutant allele results in the formation of an additional band of 7kb when using EcoRV and of 6.1kb when using BglII. To rule out a random integration event in addition to the homologous recombination event on clone 5A, the membrane previously tested with probe A was stripped and subsequently hybridised to the Neo probe. The single band detected after hybridisation confirmed the presence of a unique neomycin cassette therefore excluding the additional random integration of the targeting vector in this clone (figure 28B).

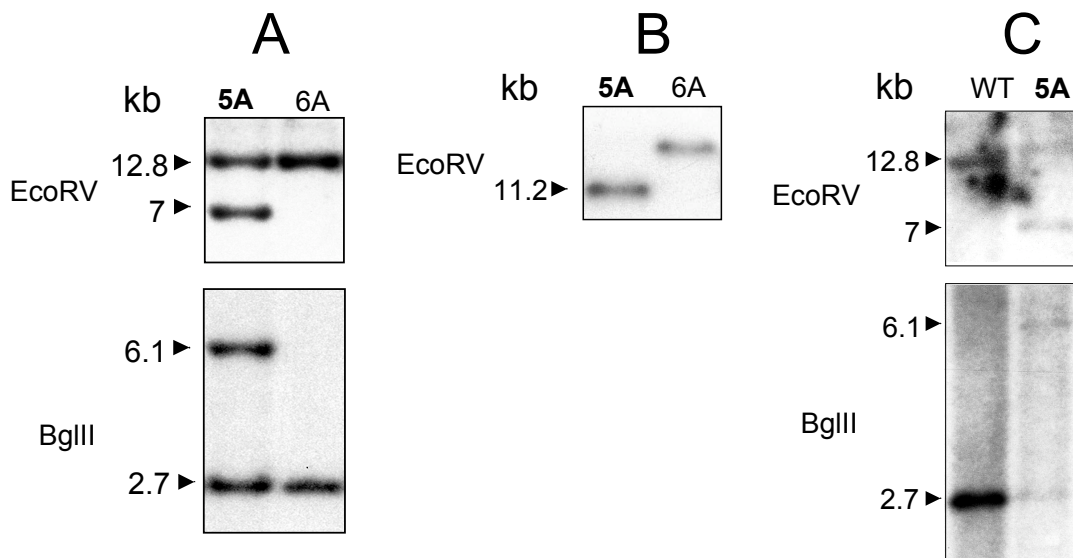


**Figure 28.** Identification of a ES cell clone carrying MED25 conditional null allele. (A) Southern blot analysis was carried out on the genomic DNA of viable clones after double selection. Genomic DNA was digested with EcoRV and probed with probe A to confirm homologous recombination on the 5' end or digested with BglII and probed with probe B' to confirm homologous recombination on the 3' end. The presence of a double band in both cases indicates that homologous recombination was occurring on clone 5A. Clone 6A shows a typical wild-type pattern. (B) The same membrane was probed with the Neo probe to exclude random integration in addition to homologous recombination. (C) Clone 5A was expanded and its genotype confirmed again via Southern blot analysis.

The positive clone 5A was thawed from one of the originally frozen 96 well plates, cultured and expanded. To guarantee a high quality of the cells a particular care was taken to keep the number of passages low and to proceed immediately after reaching the number of cells required for blastocyst injection and for a minimum of clone storage. During this period, aliquots of the cells were processed for DNA extraction in order to confirm the identity of the expanded clone via Southern blot analysis. Figure 28C shows the typical double bands of the homologous recombinant in the lane of the expanded clone 5A (right lane) compared to the single band characteristic for the wild type DNA obtained from a 129/Ola strain mouse tail (left lane).

### 3.4.7 Injection of homologous recombinant ES cells in mouse blastocysts and generation of MED25 chimeras

In order to establish a MED25 mutant mouse line, a series of steps had to be carried out, which are schematically represented in figure 29. Injections of the ES cell clone 5A into host blastocysts were carried out in the IEG department of GSF, Neuherberg. Injected viable blastocysts were subsequently re-implanted in pseudopregnant female recipient mice for the generation of coat-colour chimeras. In a first attempt, nine foster female mice recipients were implanted with injected blastocysts. In table 15 the number of wild-type versus chimeric mice obtained are given.

**Table 15.** Number of chimeras in relation to the number of clone 5A-injected blastocysts and to the number of blastocyst transfers into foster female mice.

Transfer number	Blastocysts re-implanted	Wild type pups	Male chimeras	Female chimeras
1	20	4	–	1
2	20	–	–	–
3	20	8	1	1
4	16	4	–	–
5	16	6	–	–
6	16	4	–	–
7	23	5	2	–
8	24	0	–	–
9	24	0	–	–

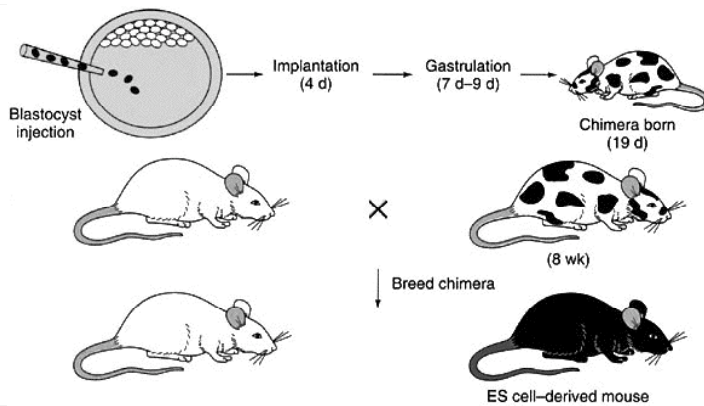


**Figure 29.** Scheme for the generation of a transgenic mouse. After blastocyst injection with the ES cell clone carrying the mutated allele, blastocysts are re-implanted into foster pseudopregnant female mice, which are going to generate coat-colour chimeras. Chimeras are mated to wild type mice to allow germ line transmission. ES-cell-derived offspring are recognized by the coat colour.

Together with the observation that these chimeras were characterized by a very low percentage of chimerism (from 10 to 20 %) they were never been able to produce offspring and therefore considered sterile. In a second round of blastocyst injection attempt a total amount of seven chimeric mice were generated and mated to wild-type female mice for F1 generation. Among them, the C57/BL6 coat-colour chimeras (figure 30, left panel) revealed to be sterile, as well as the CD1 coat-colour chimeras showing higher percentage of chimerism (figure 30, central panel). Two remaining CD1 coat-colour chimeras produced offspring (figure 30, right panel).

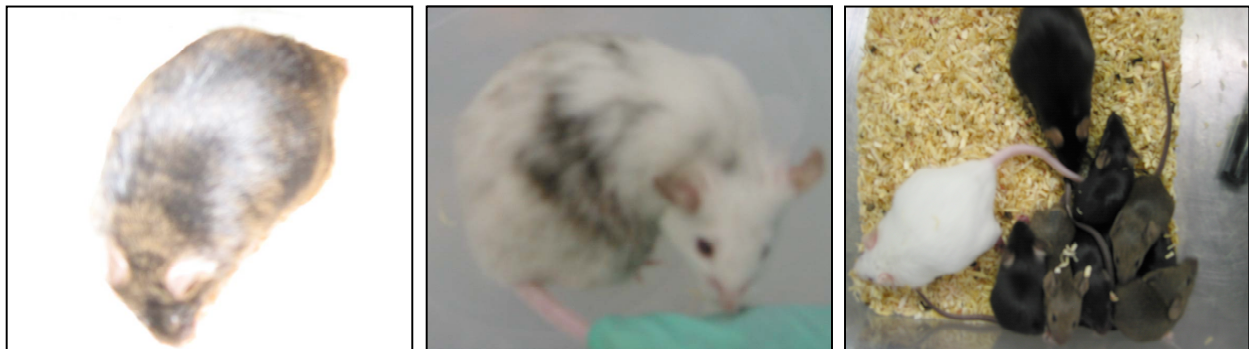


**Figure 30.** MED25 coat-colour chimeras. Right panel: C57/BL6 derived chimera. Central panel: CD1 derived chimera. Left panel: only CD1 derived chimeras were generating offspring.

Because CD1 derived blastocysts were chosen for the injection of the TBV2-derived clone 5A, it was not possible to distinguish between wild type and heterozygous litter mates by the colour of their coat. Therefore it became necessary to genotype the offspring mice using tail-derived DNA, in order to identify possible MED25 conditional

knock-out heterozygous mice. Genomic DNA derived from 36 agouti offspring mice was digested with BglII and transferred to a membrane, which was hybridised to probe B'. Figure 31 shows the result of the Southern blot analysis.

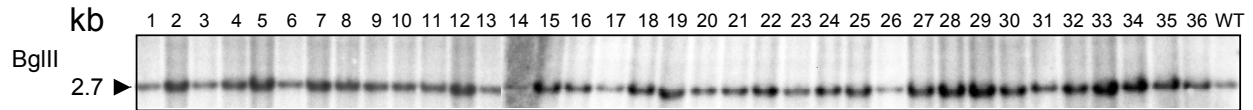


**Figure 31.** Genotype of the MED25 chimeras derived offspring. The presence of a unique band visualized by Southern blot analysis indicates that germline transmission of the MED25 conditional null allele was not occurring.

The presence of a unique band of 2.7kb in all genotyped mice revealed that the MED25 mutant allele was not germ line transmitted, and therefore that no MED25 conditional knock-out heterozygous mouse had been generated.

## 4. DISCUSSION

### 4.1 Identification and characterization of the Mediator–interacting module of MED25

The analysis of the primary sequence of MED25 in combination with a screen for homologous sequences in the data base, allowed to identify two regions, named VWA and ACID domains, which are highly conserved throughout evolution and therefore considered to be critical for the function of the protein. MED25 was isolated via VP16 affinity chromatography and shown to coprecipitate with the Mediator complex (Mittler et al., 2003). However which parts of the protein were involved in these binding reactions remained unclear and therefore a structure–function analysis of MED25 was chosen to address this question. A number of deletion mutants of MED25 were designed with respect to the domain organization as determined *in silico*. Pull down experiments using these constructs and a GST–VP16 column (Mittler et al., 2003; Yang et al., 2004) demonstrated that the region identified as ACID domain was necessary and sufficient for MED25 interaction with the viral activator. In analogy to this study a biochemical screen of MED25 deletion constructs using a Mediator specific column was carried out, which allowed the identification of the VWA domain as the minimal Mediator–interacting region (figure 10).

Even though the structure of MED25 and of its functional domains have not yet been resolved, a prediction of the secondary structure is available. Of particular interest is the high homology between the MED25 Mediator–binding module and VWA–domain containing proteins. The A region of von Willebrand factor establishes contacts with collagen while the corresponding domain the integrins CD11a/b mediates CD18 ligand interactions. VWA domains have typical features of a protein–protein interaction module. They consist of a rigid scaffold composed of helices grouped around a core that is formed by  $\beta$ –sheets. These are connected through loops that are less conserved in structure and, therefore, could be used for individual protein–protein interactions. The alignment of MED25 with other VWA domains (supplementary figure 1) revealed two specific regions, SR1 (amino acids 51–63) and SR2 (amino acids 145–167) that show

no or little conservation. In particular, SR2 shows little homology within the other VWA proteins but is highly conserved throughout evolution in MED25. Therefore the SR2 region may play a critical role for the function of the protein, namely the Mediator interaction.

To identify MED25 amino acids which are involved in Mediator–complex formation a site directed mutagenesis analysis was performed. The physical interaction and transcription activation analyses revealed the presence of critical amino acid residues in the SR2 region (figure 15). While observing the behaviour of each single mutant in the two assays, a model can be proposed concerning their contribution in complex formation. The negatively charged residue E157 shows a complete loss of physical interaction with Mediator upon replacement with a positively charged amino acid. This indicates that E157 may play a critical role in the initial electrostatic contact between MED25 and Mediator, which can be completely abolished by the change of charge. During this process, other negatively charged amino acids, which are located in proximity of the SR2 region may reinforce the ionic binding. E167 and E175 may contribute to the binding reaction. Mutations of these residues, however, did not lead to the dramatic effects observed with the E157 mutant. Once the first contact is established, MED25 and Mediator probably stabilize the interaction by the formation of hydrophobic bonds, in which amino acids T138 and Y161 are thought to be important. Finally the binding may be negatively modulated by residues like Y151 and Q137, which have displayed stronger effects in both assays when replaced by the smaller amino acid alanine. These data bring evidence for a major role played by the SR2 region in Mediator complex formation. For the future, the generation of a peptide with SR2 sequence used in binding–competition experiments would help to confirm these data.

Other amino acid residues (VVFV18, Y39, F47, Y66, F125, HMVL219) targeted in the VWA domain led to complete loss of transcriptional activation (figure 13). However, it is possible that these residues contribute to the stability of the structure and therefore that their mutation into alanine provokes collapse of the protein structure. To clarify this point, a limited proteolysis experiment should be performed to discriminate unstructured regions from correctly folded domains. Moreover, mutating these residues into amino

acids sharing similar sterical properties like the ones in the wild type should also be considered.

#### 4.2 Characterization of the VP16–interacting module of MED25

The function of VP16 activator has been extensively investigated over the last two decades, leading to the identification of several cellular targets of VP16. Among them a number of components of the transcription machinery like TFIID, TFIIB, TFIIIF, TFIIH and cofactors like PC4 and Mediator are included. Moreover VP16 has been shown to bind chromatin–related activities such as SAGA, Nu4, Swi/SNF and CBP/p300 (see 1.2.6.1). Despite all these cellular targets, MED25 is the only protein, which turned out to be necessary to drive activated transcription from VP16 *in vitro*. Its importance in VP16 transcription activation has also been demonstrated *in vivo* by the use of dominant negative mutants (Mittler et al., 2003; Yang et al., 2004).

The two transcription activation domains of VP16 are located in the carboxy–terminal region (residues 410–490) and are highly acidic. Both subdomains (VP16 H1 412–453 and VP16 H2 454–490) have been studied by mutational analysis, indicating key roles for specific hydrophobic and acidic residues (Cress and Triezenberg, 1991; Regier et al., 1993; Sullivan et al., 1998; Walker et al., 1993). The transcriptional activation domains of transcription factors often lack a folded structure under physiological conditions (Triezenberg, 1995; Wright and Dyson, 1999). These and other native highly flexible random–coil proteins are identified as intrinsically unstructured proteins (IUPs). Lack of folded structure has many advantages for the ability of the protein to bind to its targets (Dunker et al., 2002; Dunker et al., 2001; Tompa, 2002). The substantial backbone and side–chain flexibility enables the protein to overcome steric restrictions and consequently enhances binding to various targets and larger interaction surfaces. Previous structural studies of VP16 activation domain showed that there is little evidence of secondary structure for the free protein (O'Hare and Goding, 1988; Uesugi et al., 1997). However, upon binding of a VP16 peptide (469–485) to the hTAF<sub>II</sub>31 (1–181), the 472–483 region becomes  $\alpha$ –helical (Uesugi et al., 1997). In a recent study, the binding of VP16 to PC4 and TFIIB has been investigated in detail using NMR and biochemical experiments (Jonker et al., 2005; Jonker et al., 2006). The authors of this



study suggest that the two transcription activation subdomains of VP16 adopt an  $\alpha$ -helical conformation around the 429–450 and 465–488 regions upon interaction with PC4 and TFIIB. Multiple exchangeable contacts are observed between negatively charged VP16 residues and positively charged residues from the target proteins. This finding is in agreement with the previous observation that transcription was only impaired when multiple patches of negatively charged residues in VP16 H1 were mutated, suggesting that the overall acidity of the protein is important for its activity (Cress and Triezenberg, 1991). One specific residue in the VP16 H2 subdomain (E476) which significantly contributes to transcriptional activation (Sullivan et al., 1998), establishes a hydrogen bond to R85 of the structured C-terminous of PC4. The large number of charged residues increases the rate of interaction between activator and target through long-range electrostatic forces. This is demonstrated by the fact that D443 and D445 of VP16 establish hydrogen bonds to K100 and K77/K79 of PC4, residues that are important for the interaction.

It is suggested that initial binding occurs by electrostatic interactions, resulting in an unstable complex, which is slowly stabilized by specific hydrophobic bonds between the activation domain and its target (Hermann et al., 2001). Interestingly, hydrophobic residues of VP16 that have been shown to be critical for transcription (L439, F442, L444, F475, F473, and F479) have been localized in the center of the induced  $\alpha$ -helix. A model is proposed by Jonker and coworkers (Jonker et al., 2005) in which the VP16  $\alpha$ -helices are involved in many electrostatic and some hydrophobic contacts to residues in the  $\beta$ -channel regions of PC4. Obviously many contacts can be replaced by adjacent VP16 residues, since complete loss of binding is not observed upon mutation of single polar and hydrophobic residues.

In this work the binding of MED25 to activation domain of VP16 has been investigated. MED25 point mutants have been generated in which charged and hydrophobic amino acids residues of the ACID domain were targeted. A pull down assay has been performed using a GST-VP16H1 column. This subdomain has been reported to bind MED25 better than VP16H2 (Mittler et al., 2003; Yang et al., 2004). In figure 32 the region of VP16H1 containing critical residues for the binding to other factors and for transcriptional activation is depicted.



**Figure 32.** Schematic view of the 438–451 region of the VP16H1 subdomain. Hydrophobic residues are indicated in blue; negatively charged residues are framed. Some of these residues (L439, F442, L444, D443, D445) have been shown to be important for transcription and interaction of VP16 with its targets.

We observed that for the mutants FHF473AAA and WPQK444APQA the interaction with VP16H1 was completely abolished while it was strongly impaired for the mutants W408A and KKIF519AAIA (figure 17A). The cluster of lysines KKK518 seems to play a critical role in VP16 complex formation since also the ACID domain alone where these lysines are mutated to alanine loses binding (figure 17B). The MED25 ACID domain is found only in one other protein called PTOV1. PTOV1 contains two repeats of this domain (Benedit et al., 2001), the sequences of which are likely conserved with each other and with the MED25 ACID domain (figure 17). The importance of K518 was confirmed by the observation that the PTOV1\_B domain (containing a glutamate in the corresponding position) does not bind VP16H1. Interestingly, the same mutants which were showing impaired VP16 binding in the *in vitro* assay (FHF473AAA, WPQK444APQA, W408A and KKIF519AAIA) displayed a reduction of transcriptional activation capacity in the *in vivo* functional assay (figure 13, lanes 1–4). This observation may indicate the involvement of these residues in the binding to a cellular target, which obviously contributes to increase transcription rates. The viral activator may simply mimic this mechanism in order to use MED25-bound Mediator to support the viral life cycle in the eukaryotic cells.

The resolution of the structure of the ACID domain would definitely help to understand the dynamics behind the complex formation with VP16. Targeting single residues in the regions, which were found affected by double or triple mutations may also help to identify the amino acids which are essential. However, as reported previously, the binding of the ACID domain with VP16 activation domain very likely results from the contribution of many residues.

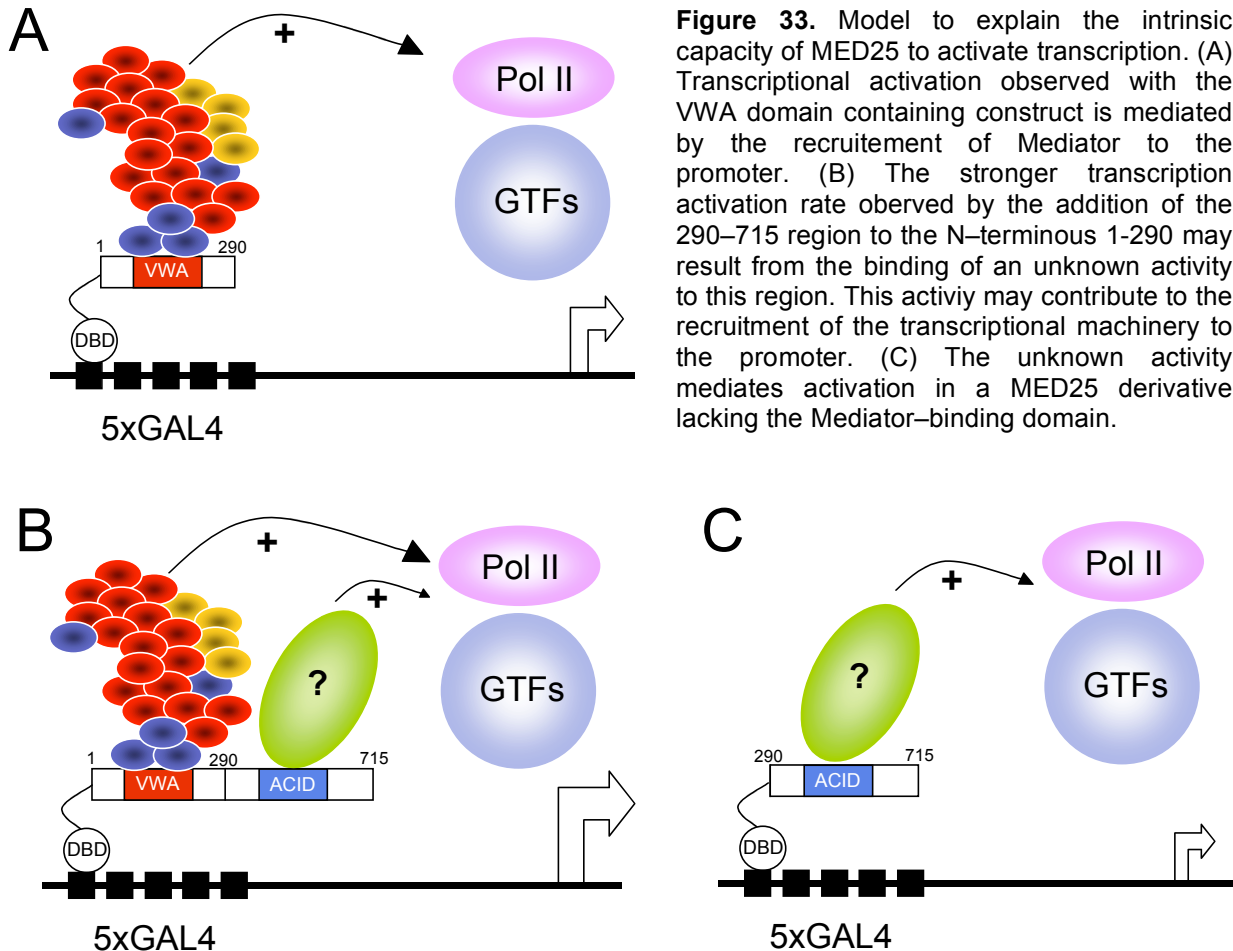
Comparing our data with other data where the binding of VP16 with other target protein has been studied a model is suggested for the formation of the ACID–VP16 complex. K518 seems to play a key role in attracting negatively charged residues (aspartates) in the VP16H1 subdomain. The other lysines in the cluster (519, 520), K447 and H474 may contribute to increase the electrostatic forces. Once in proximity to the ACID domain, VP16H1 very likely undergoes conformational change and the binding is stabilized by hydrophobic contacts, which seem to involve F473, F475, W444, W408 and F522 of MED25 ACID domain.

#### **4.3 MED25 is characterized by an intrinsic transcription activation capacity**

In contrast to the majority of Mediator subunits, MED25 is neither conserved in yeast nor in *C.elegans*. In line with the general observation, that the evolution of eukaryotes is generally accompanied by an increase in complexity of transcriptional control, this observation was supporting the hypothesis that MED25 other than representing a Mediator subunit could also have an additional function specific for higher eukaryotes.

In a recent work published by Kim et al., (2004) the role played by single subunits of *Drosophila* Mediator in transcription activation is investigated. Using small interference RNA technology (siRNA) each Mediator subunit was individually knocked down in Schneider SL2 cells. With this approach the authors could demonstrate that the depletion of each of 13 of the 23 investigated subunits caused significant defects in transcriptional activation of Attacin A and Hsp26 genes, revealing functional specificity of Mediator subunits. In addition, a screen for activator–binding Mediator subunits proved that MED23, MED17, MED25 and MED16 were physically interacting with the transcription activators of the affected genes, Dif (dmNF– $\kappa$ B) and HSF. Interestingly, the portion of *Drosophila* MED25 (amino acids 573–863) shown to bind these activators includes part of the ACID domain and part of the carboxyl–terminal region of the protein. While the mammalian homologues of MED17 and MED23 have been also identified as specific binding partners for the cellular activators p53, STAT2 and Elk–1, respectively, no cellular target has been yet identified for the mammalian homologue of MED25.

In this work the transcriptional activation assay performed with MED25 GAL–tagged deletion constructs revealed that MED25 has an intrinsic transcription activation capacity (figure 11). This is indicated by the observation that the VWA–domain lacking constructs still activate transcription, even though with reduced rates as compared to the constructs containing the Mediator–interaction domain. Based on this observation a model is proposed to explain the behaviour of MED25 derivatives in this assay (figure 33).



The capability of GAL–MED25<sub>1–290</sub> to activate transcription is probably exclusively related to the recruitment of Mediator to the promoter (figure 33A). The increased transcription rate as a consequence of C–terminal prolongation of the protein indicates that an additional activity comes into play, which synergistically contributes to the effect of Mediator (figure 33B). This activity may bind to the ACID domain, while the surrounding regions may help to stabilize this binding (290–393 and 543–715). Alternatively, more than one factor could be bound to this part of the protein (290–715),

the presence of which could sterically or functionally influence the others; however this still needs to be clarified. Finally, the GAL–MED25 derivatives lacking the VWA domain, are still able to activate transcription through the recruitment of an unknown activity, which may recruit the Pol II transcription machinery to the reporter's promoter (figure 33C).

Initial immunoprecipitation experiments using a GAL4 antibody, have demonstrated that Mediator and Pol II coprecipitate with GAL–MED25<sub>1–290</sub> as well as with GAL–MED25<sub>1–715</sub>. However, the construct GAL–MED25<sub>290–685</sub> failed to precipitate both, Mediator and Pol II. This observation may be indicative for an indirect recruitment of the transcriptional machinery by the presumptive unknown activity, an hypothesis, which is supported by the reduced effect observed in the luciferase assay. Functional data showing impaired transcription activation of ACID–domain mutants (figure 13, lanes 1–4) suggest that the unknown activity described above may specifically bind the ACID domain of MED25. Even though the identity of this factor is not yet known, the possibility of an interaction with CBP should be considered and further investigated *in vivo*. In fact, recent experiment have shown that MED25 is able to bind CBP at least *in vitro* (Uhlmann, 2006). In this view, a model can be proposed where MED25 bound to activators at promoters serves as a platform to recruit chromatin–related cofactors (i.e. CBP) and the Mediator complex. While one factor would serve to open the promoter, the other one would target the transcription machinery to it. Mass–spectrometric identification of proteins interacting with GAL–MED25<sub>290–715</sub> might be employed to reveal the mechanisms that contribute to activation through MED25.

#### **4.4 A role for MED25 in cell cycle control**

Microarray analyses were carried out in this study led to identification of cellular targets for MED25. Using different cellular systems genes were found that are important for the cell cycle regulation: cJun and FosB were repressed 10 hours after induction of ER–MED25 in NIH3T3 cells. These genes have been shown to drive entry into S–phase of the cell cycle thereby promoting cell proliferation. This is reflected by the transforming capacity of mutant versions of these cellular proto–oncogenes. The downregulation of these factors through MED25 raises the possibility that MED25 is critical for the control

of cell proliferation. Another factor involved in cell cycle regulation was identified in an independent screen in 721-B-cells, where a dominant-negative MED25 variant was employed to reveal genes whose expression is under the control of this protein. GSK3 $\beta$  was downregulated already 1 hour after induction of ER-MED25-NTD in 721-B-cells. Considering the dominant negative function of MED25-NTD, this result indicates GSK3 $\beta$  as a direct target of MED25. In line with this finding cyclin D1 protein levels have been reported to be increased following overexpression of PTOV1, a MED25 homolog lacking the Mediator interaction domain (Santamaria et al., 2003). Cyclin D1 promotes transition from G1 to S phase, increasing the cellular proliferation rate in prostate cancerogenesis. GSK3 $\beta$  phosphorylation has been also shown to be involved in cytoplasmic localization of cyclin D1 and promote its degradation (Diehl et al., 1998). Furthermore transient transfection experiments indicate that the cyclin dependent kinase inhibitor p21 is upregulated by MED25. Since p21 itself negatively regulates G1-S progression this could underline the function of MED25 in controlling cell proliferation. A schematic view of cell cycle regulation is depicted in figure 34.

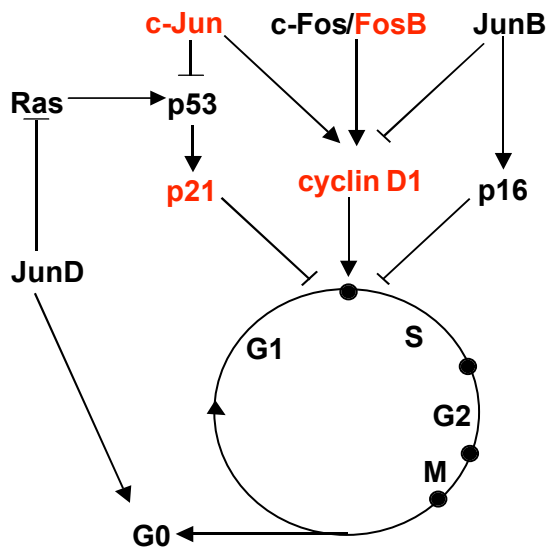


**Figure 34.** Effects of AP-1 proteins and other factors in cell cycle regulation. c-Jun stimulates G1 to S phase transition by inducing cyclin D1 and repressing p53, which in turn reduces p21 levels. c-Fos and Fos-B have redundant functions in the stimulation of S phase entry and the induction of cyclin D1 expression. JunB inhibits G1 to S phase progression by inducing p16 and repressing cyclin D1. JunD inhibits S phase entry and increases the numbers of resting cells by modulating the Ras/p53 pathway. (After (Jochum et al., 2001))

Together these findings indicate that MED25 may negatively influence cell proliferation via downregulation of c-Jun and FosB on the one hand and upregulation of GSK3 $\beta$ , a negative regulator of cyclin D1, on the other hand. The positive effect of MED25 on GSK3 $\beta$  expression might be counteracted by PTOV1, which has a positive influence on cyclin D1 levels (see above). A model can be proposed for the antagonistic regulation of

this gene by MED25 and PTOV1. Under normal conditions binding of MED25 to a transcriptional activator localized on the GSK3 $\beta$  promoter will recruit chromatin-related factors and Mediator to this site leading to expression of the gene (figure 35A). However, in transformed cells high PTOV1 expression levels might lead to binding of the chromatin-related factors in solution thereby sequestering it from promoters (figure 35B). This factor could be titrated out by PTOV1 impairing transcriptional activation of this gene.

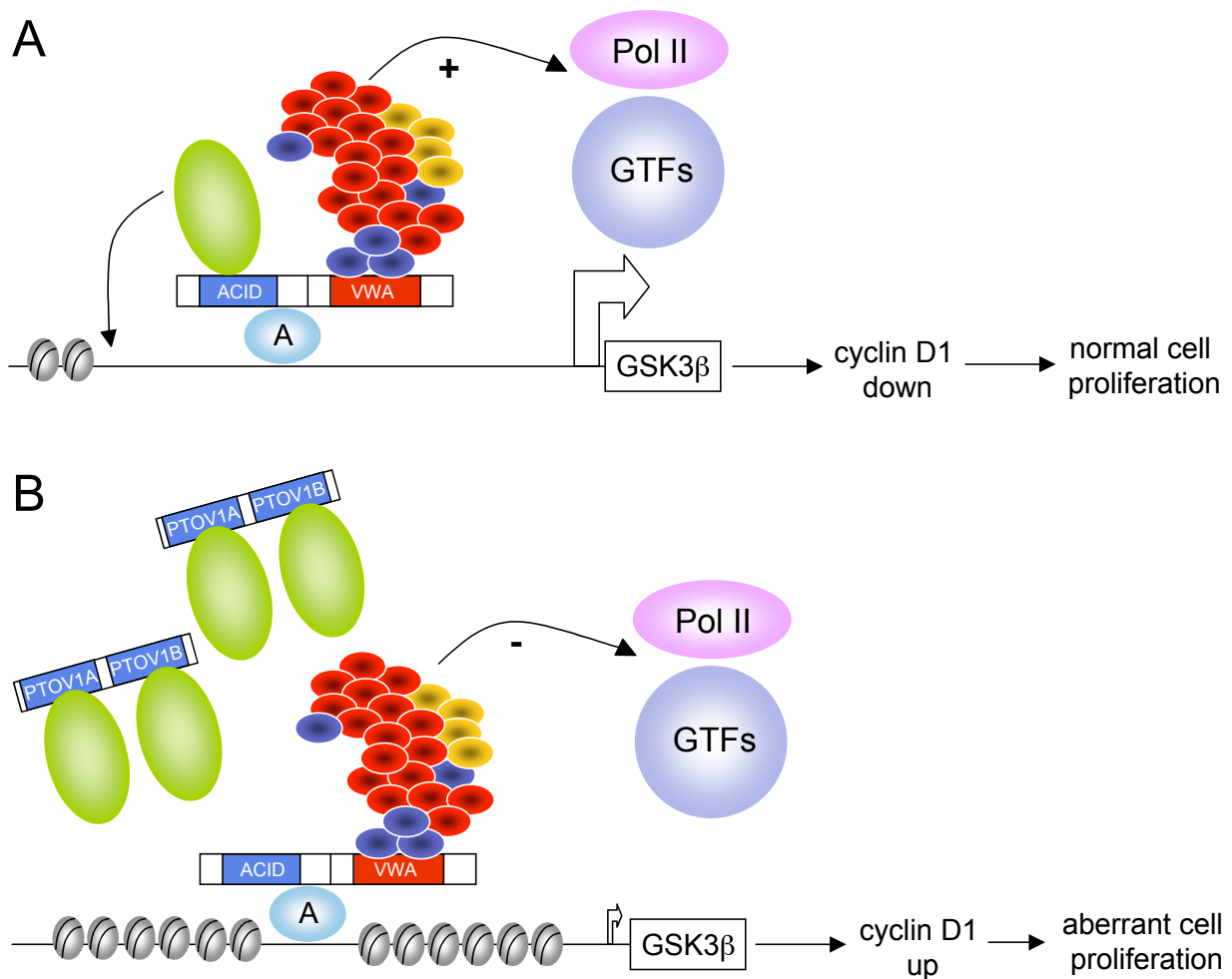


**Figure 35.** Proposed model for antagonism of PTOV1 with MED25. (A) MED25 induces GSK3 $\beta$  which in turn regulates levels of cyclin D1 promoting its degradation. (B) In tumorigenic cells, overexpressed PTOV1 sequesters important factors for transcriptional activation of the GSK3 $\beta$  therefore blocking its expression. This leads to upregulation of cyclin D1 with consequent aberrant cell proliferation.

#### 4.5 Possible implication of MED25 in EBNA2 activation

The analysis of the gene expression profile upon over-expression of ER-MED25-NTD in the nucleus was carried out in 721-B-cells, which constitutively express the Epstein-Barr Virus Nuclear Antigen 2 (EBNA2). Noteworthy, the viral activator EBNA2 is essential for regulation of virus and cell gene transcription and B lymphocyte transformation into a lymphoblastoid cell line (LCL). The possible implication of MED25 in EBNA2 function is based on experiments, which show that increasing amounts of MED25-NTD dramatically reduce the activation of a GAL4-luciferase reporter by GAL4-EBNA2 in a transient transfection assay (Laux, personal communication). In analogy with the viral activator VP16, the dominant negative effect exerted by MED25-NTD mutant could reflect the involvement of MED25 in the transactivation mechanism of EBNA2. In analogy to VP16, the recruitment to promoters of basal and activation-related transcription factors (TAF40, TFIIB, TFIID, p300/CBP, PCAF histone acetyltransferases) and the transcriptional coactivator p100 (Wang et al., 2000) by EBNA2 has been already reported. Moreover, EBNA2 contains a highly acidic 14-amino acid activation domain that directly activates transcription and is required for transformation. Although the activation domains of EBNA2 and VP16 share less than 50% amino acid identity, they have certain structural features in common. Both domains contain several negatively charged amino acids, a putative  $\alpha$ -helical structure, and hydrophobic amino acids that can be aligned in a similar pattern (figure 36).

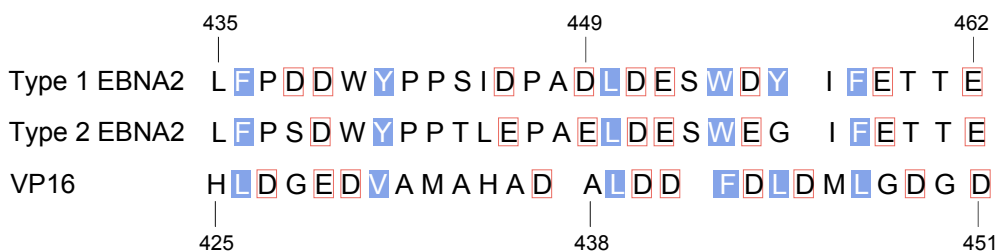


**Figure 36.** Alignment of the amino acid sequence of the transcriptional activation region of EBNA2 with a region of the VP16 H1 subdomain. Hydrophobic amino acids are in light blue while negatively charged residues are framed in red.

Chimeric EBV virus containing part of the VP16 activation domain instead of the EBNA2 activation domain was able to transform B cells and transactivate expression of EBV



and B cells (Cohen, 1992). This finding supports the hypothesis that EBNA2 and VP16 may share similar biochemical mechanisms of transcriptional activation.

The results from the microarray analysis contribute to support our theory of a relationship between MED25 and EBNA2. Experiments carried out in Kieff's laboratory (Zhao et al., 2006) have identified EBNA2-regulated genes comparing RNA levels in LCLs expressing WT EBNA2 and in LCLs expressing a Tamoxifen inducible EBNA2 (E2HTF). Based on the assumption that ER-MED25-NTD would act dominant negatively on EBNA2 we compared the genes downregulated in our array analysis with the genes upregulated by EBNA2. Table 16 lists the genes found in this work, which are also reported to be EBNA2-target genes (Zhao et al., 2006). All the genes shared by the two studies seem to respond rather early to the translocation of ER-MED25-NTD in the nucleus (1 hour after OHT induction) arguing for a direct effect. Five of these genes (RGS1, TRIO, CCL5, CD300A and GADD45 $\beta$ ) were also found to be upregulated by latency III (LTIII) infection from EBV in Burkitt lymphoma (BL41) lymphoblasts (Cahir-McFarland et al., 2004; Carter et al., 2002; Zhao et al., 2006). Although Bcl2 is not present in the EBNA2 target gene list, its contribution to B-cell immortalisation is well known. EBV-transformed LCLs are resistant to apoptosis as a consequence of LMP1-mediated NF- $\kappa$ B activation and induction of Bcl2 together with other antiapoptotic proteins like A20, Bfl1 and Mcl1 (Cahir-McFarland et al., 2004; Cahir-McFarland et al., 2000; Gregory et al., 1991; Henderson et al., 1991; Laherty et al., 1992). EBNA2 also contributes to cell survival through upregulation of GADD45 $\beta$ . (growth arrest and DNA-damage-inducible, beta) protects cells from c-Jun N-terminal kinase-mediated apoptosis (De Smaele et al., 2001). Other EBNA2-induced genes encode proteins involved in cell signalling like chemokines, cell-surface receptor molecules and intracellular mediators such as CCL5, CMKOR1, CD300A (leukocyte membrane antigen, Irp60), ATP1B1 and RGS1. CD300A belongs to the Ig protein super-family, which is characterized by an intracellular tail that has an immunoreceptor tyrosine-based inhibitory motif able to associate with SHP-1 (Cantoni et al., 1999). CMKOR1 is a G protein-coupled receptor that binds to CXCL12 and is also an HIV coreceptor (Balabanian et al., 2005). CCL5 and RGS1 are also LMP1-induced and are likely to regulate B cell chemotaxis (Cahir-McFarland et al., 2004). Other chemokines such as

CCL4 and CCL3 were also found to be EBNA2 targets (Kempkes, personal communication). In addition, a transcript named EB13 (Epstein–Barr virus induced gene 3) was down–regulated 1 hour and 24 hours after OHT induction in 721–ER–MED25–NTD cells.

**Table 16.** List of genes which were downregulated upon MED25–NTD overexpression and upregulated upon EBNA2 overexpression. In light blue are genes which were also found to be upregulated by latency III (LTIII) infection from EBV in Burkitt lymphoma (BL41) lymphoblasts.

GENES	BIOLOGICAL FUNCTION
Bcl2	antiapoptotic
CCL4	Chemotactic factor for monocytes
MAFF	v-maf musculoaponeurotic fibrosarcoma oncogene homolog F, transcription regulator
CCL3	Chemotactic factor for monocytes
SNX9	regulator of dynamin function in clathrin–mediated endocytosis
RGS1	regulaor of G protein signaling, Immediate–early response gene
TRIO	Rho guanine nucleotide exchange factor
ATP1B1	Na,K-ATPase pump
CCL5	Chemotactic factor for monocytes
CD300A	leukocyte membrane antigen
CMKOR1	G protein–coupled receptor
GADD45 $\beta$	growth arrest and DNA–damage–inducible
RBBP6	cell cycle regulation

Furthermore overexpressed MED25–NTD acts as a dominant allele also on transcription of another subset of cellular genes that are not targeted by EBNA2. Regulation of these genes might indicate another biological pathway in which MED25 is involved. Taken together the microarray results argue for a role for MED25 in transcriptional control of a certain subset of cellular genes in addition to a function for MED25 in host–virus interaction on the level of gene regulation.

#### 4.6 MED25 and Charcot–Marie–Tooth disease (CMT)

It has been recently reported that a point mutation in MED25 (A335V) directly correlates with an autosomal–recessive form of Charcot–Marie–Tooth disease found in a Costa Rican family that is characterized by an axonally pronounced myelin degenerative process (Rautenstrauss and collaborators, personal communication). In this study the proline–rich region surrounding A335 was predicted to be a potential SH3–ligand region. According to this hypothesis, both MED25 wild type and mutant represent interaction partners of the SH3 domain of the Abelson tyrosine kinase family. However, the mutation also shows an affinity to the SH3 domains of the Src–family of kinases, which results in a decreased binding specificity of the MED25 A335V mutant. Fluorescence binding experiments using peptides representing the regions involved in this predicted interactions confirmed this theory at least *in vitro*. The transcription assay carried out on a GAL4–luciferase reporter and the immunoprecipitation assay presented in this study, helped to rule out the possibility of impaired Mediator–interaction related to this mutation (figures 18 and 19). On the other hand, the mutation could affect transcription activation at the level of specific genes regulating myelin expression and/or Schwann cell differentiation, as a consequence of impaired binding of mutated MED25 to a transcription factor. In fact, autosomal types of CMT characterized by hypomyelinating neuropathy have been found to be associated with mutations in the early growth response gene 2 (*EGR2/Krox20*), a transcription factor necessary for the transition from promyelinating to myelinating stage of Schwann cell development. Moreover mutations in the genes encoding the myelin proteins PMP22 and P0 cause other forms of CMT (CMT1A and CMT1B) (Kamholz et al., 1999). Another possible explanation could be the regulation of MED25 activity by phosphorylation from tyrosine kinases. An interesting example is represented by the YT521–B protein, a nuclear protein which is located in a dynamic nuclear compartment called YT body. YT521–B is involved in splicing processes, and binds to several proteins implicated in splice site selection, which it can influence in a concentration dependent manner (Hartmann et al., 1999). YT521–B has been shown to bind to and be phosphorylated by c–Abl and c–Src kinases in the nucleus and in the cytoplasm, respectively (Rafalska et al., 2004). Phosphorylation causes insolubility of the protein which associates to nuclear structures and gets

dispersed throughout the nucleus, thereby losing association with actively transcribed genes. Due to its insolubility and spatial distribution, phosphorylated YT521-B is removed from pre-mRNA processing events and can no longer influence splice site selection (Rafalska et al., 2004). Interestingly, the phosphorylation affects mainly the localization of the protein, but not its ability to change splice sites *in vitro* (Cazalla et al., 2002). In an analogous way, MED25 participation in transcription could be regulated by c-Abl phosphorylation. However, in the case of the CMT disease one can imagine a scenario where the phosphorylation of A335V mutant is no longer controlled, and becomes aberrant therefore causing dispersion of the protein in an inactive state in the nuclear or in the cytoplasmic compartment. According to this theory, MED25 could be sequestered from transcriptionally active sites of neuronal cells. This could alter regulation of genes involved for example in myelin expression. Considering that the A335V mutation is located in a region which was contributing to the intrinsic transcription activation capacity of MED25 and which was also predicted as potential tyrosine kinase interaction domain, it is interesting to investigate whether MED25 associates with the relevant promoters and/or binds transcription factors or tyrosine kinases in order to modulate myelin expression, and whether the A335V mutant would interfere with such a mechanism.

#### **4.7 An attempt to create a MED25 conditional knock-out mouse**

The manipulation of the mouse genome represents an elegant tool to characterize the function of an unknown gene, and has facilitated the study of many biological processes. However, not all physiological processes can be assessed by constitutive gene-inactivation or transgene-expression strategies. Null mutations can result in embryonic lethality that is preventing analysis of a putative gene function later in development. For this reason conditional mutations of the target gene are employed. Moreover, conditional mutations that are confined to a particular cell lineage are extremely helpful in the analysis of gene function in a given lineage or tissue.

Hence, we decided to create a MED25 conditional knock-out mouse. Insights gained from the phenotype of these animals could have complemented the molecular biological and biochemical studies of MED25 that were carried out in parallel. First of all, the

conditional MED25 KO mouse could have been crossed with a mouse ubiquitously expressing CRE recombinase, in order to find out if and eventually at which stage of development MED25 is of vital importance. Preliminary experiments carried out in our laboratory using siRNA suggest that the knock-down of the protein to 10–20% does not affect cell growth at least for the first 36 hours after transfection. This observation together with the fact that MED25 is not present in yeast and *C.elegans* raises the possibility that it is not an essential gene. Moreover, the generation of a MED25 null cell line could have been used as a tool in biochemical assays to study the position of MED25 relative to other Mediator subunits. This approach has been exploited for other Mediator subunits (MED23 and MED24) revealing the existence of Mediator modules (Ito et al., 2002; Stevens et al., 2002).

On a second stage of our study it would have been interesting to investigate whether MED25 has a tissue-specific function. In addition to the known relationship between MED25 and VP16 we have reasons to believe that MED25 might be involved in the mechanism of other viral activators. It has been recently reported (Roupelieva, 2005) that MED25 physically interacts with the latency-associated nuclear antigen 1 (Lana-1) of the Kaposi's sarcoma associated Herpes virus (KSHV). Moreover, the observation that MED25-NTD acts dominant negatively on activated transcription driven by EBNA2 (Laux, personal communication) together with our array data, link MED25 to EBV. Together these observations lead to the hypothesis that via targeting of MED25 the viruses would not only support their viral life cycle, but also manipulate cellular functions (i.e. immune response) by titrating out MED25-associated Mediator complexes (A-Med).

Other Mediator subunits have been shown to be implicated in antiviral immunity pathways, i.e. the interferon (IFN)-activated gene regulation. Med17 binds STAT2 but does not enhance IFN-responsive transcription; Med23 facilitates IFN-driven transcription without binding the ISGF3 activation complex; Med14 shows both features (Lau et al., 2003). Since some of these subunits have been found to share other activating partners with MED25 (VP16, Dif, HSF), it is intriguing to think about a contribution of MED25 in the interferon-regulated immune response pathway. Crossing the MED25 conditional KO mouse with mice expressing CRE recombinase in the immune system would have helped to specifically address this question.

Even though homologous recombination in ES cells is a rare event compared to random integration, and the frequency with which it occurs may strongly vary depending on the investigated locus, the efficiency of gene targeting in this study was rather low (one homologous recombinant clone among 500). To improve statistics one possibility would be to include a longer 3' homologous recombination arm in the targeting vector. In fact it has been shown that there is a direct correlation between the length of homology and gene targeting frequency (Hasty et al., 1991a; Hasty et al., 1991b). The second bottleneck in the process of generating a transgenic mouse is represented by blastocyst injection. In the ideal scenario more than one ES cells clone should be injected, since, because of unknown reasons, about 50% of the positive clones consist of cells, which do not undergo germ line transmission. In our specific case the single ES cells clone 5A that was injected generated either non-proliferating chimeras or chimeras producing non-germ line transmitted offspring. Therefore we could not proceed with the phenotype analysis of MED25 conditional KO derivative mice. Despite the difficulties encountered during this first attempt, we believe that the generation of a MED25 transgenic mouse represents an important tool to investigate MED25 *in vivo* function. In the meantime the advent of gene-trap ES cells libraries has provided for alternative ways to realize this project. In fact, three MED25 ES cells clones, characterized by insertions of the gene-trap vector in different introns of MED25 genomic locus, have been found in these libraries and are currently used in the Meisterernst laboratory for the generation of different MED25 transgenic mice lines.

## 5. REFERENCES

- Ahn, S.H., M. Kim, and S. Buratowski. 2004. Phosphorylation of serine 2 within the RNA polymerase II C-terminal domain couples transcription and 3' end processing. *Mol Cell*. 13:67-76.
- Archambault, J., F. Lacroute, A. Ruet, and J.D. Friesen. 1992. Genetic interaction between transcription elongation factor TFIIS and RNA polymerase II. *Mol Cell Biol*. 12:4142-52.
- Arndt, K.T., C.A. Styles, and G.R. Fink. 1989. A suppressor of a HIS4 transcriptional defect encodes a protein with homology to the catalytic subunit of protein phosphatases. *Cell*. 56:527-37.
- Artavanis-Tsakonas, S., M.D. Rand, and R.J. Lake. 1999. Notch signaling: cell fate control and signal integration in development. *Science*. 284:770-6.
- Asturias, F.J. 2004. RNA polymerase II structure, and organization of the preinitiation complex. *Curr Opin Struct Biol*. 14:121-9.
- Asturias, F.J., Y.W. Jiang, L.C. Myers, C.M. Gustafsson, and R.D. Kornberg. 1999. Conserved structures of mediator and RNA polymerase II holoenzyme. *Science*. 283:985-7.
- Baek, H.J., Y.K. Kang, and R.G. Roeder. 2006. Human mediator enhances basal transcription by facilitating recruitment of transcription factor IIB during preinitiation complex assembly. *J Biol Chem*. 281:15172-81.
- Balabanian, K., B. Lagane, S. Infantino, K.Y. Chow, J. Harriague, B. Moepps, F. Arenzana-Seisdedos, M. Thelen, and F. Bachelier. 2005. The chemokine SDF-1/CXCL12 binds to and signals through the orphan receptor RDC1 in T lymphocytes. *J Biol Chem*. 280:35760-6.
- Bark-Jones, S.J., H.M. Webb, and M.J. West. 2006. EBV EBNA 2 stimulates CDK9-dependent transcription and RNA polymerase II phosphorylation on serine 5. *Oncogene*. 25:1775-85.
- Baumli, S., S. Hoepfner, and P. Cramer. 2005. A conserved mediator hinge revealed in the structure of the MED7.MED21 (Med7.Srb7) heterodimer. *J Biol Chem*. 280:18171-8.
- Bell, S.D., P.L. Kosa, P.B. Sigler, and S.P. Jackson. 1999. Orientation of the transcription preinitiation complex in archaea. *Proc Natl Acad Sci U S A*. 96:13662-7.
- Benedict, P., R. Paciucci, T.M. Thomson, M. Valeri, M. Nadal, C. Caceres, I. de Torres, X. Estivill, J.J. Lozano, J. Morote, and J. Reventos. 2001. PTOV1, a novel protein overexpressed in prostate cancer containing a new class of protein homology blocks. *Oncogene*. 20:1455-64.
- Bentley, D. 2002. The mRNA assembly line: transcription and processing machines in the same factory. *Curr Opin Cell Biol*. 14:336-42.

- Berghoff, C., M. Berghoff, A. Leal, B. Morera, R. Barrantes, A. Reis, B. Neundorfer, B. Rautenstrauss, G. Del Valle, and D. Heuss. 2004. Clinical and electrophysiological characteristics of autosomal recessive axonal Charcot-Marie-Tooth disease (ARCMT2B) that maps to chromosome 19q13.3. *Neuromuscul Disord.* 14:301-6.
- Berroteran, R.W., D.E. Ware, and M. Hampsey. 1994. The sua8 suppressors of *Saccharomyces cerevisiae* encode replacements of conserved residues within the largest subunit of RNA polymerase II and affect transcription start site selection similarly to sua7 (TFIIB) mutations. *Mol Cell Biol.* 14:226-37.
- Bestor, T.H. 1992. Activation of mammalian DNA methyltransferase by cleavage of a Zn binding regulatory domain. *Embo J.* 11:2611-7.
- Bhoite, L.T., Y. Yu, and D.J. Stillman. 2001. The Swi5 activator recruits the Mediator complex to the HO promoter without RNA polymerase II. *Genes Dev.* 15:2457-69.
- Blackwood, E.M., and J.T. Kadonaga. 1998. Going the distance: a current view of enhancer action. *Science.* 281:60-3.
- Blazek, E., G. Mittler, and M. Meisterernst. 2005. The mediator of RNA polymerase II. *Chromosoma.* 113:399-408.
- Bode, J., S. Goetze, H. Heng, S.A. Krawetz, and C. Benham. 2003. From DNA structure to gene expression: mediators of nuclear compartmentalization and dynamics. *Chromosome Res.* 11:435-45.
- Borggreffe, T., R. Davis, H. Erdjument-Bromage, P. Tempst, and R.D. Kornberg. 2002. A complex of the Srb8, -9, -10, and -11 transcriptional regulatory proteins from yeast. *J Biol Chem.* 277:44202-7.
- Bornkamm, G.W., and W. Hammerschmidt. 2001. Molecular virology of Epstein-Barr virus. *Philos Trans R Soc Lond B Biol Sci.* 356:437-59.
- Boube, M., C. Faucher, L. Joulia, D.L. Cribbs, and H.M. Bourbon. 2000. Drosophila homologs of transcriptional mediator complex subunits are required for adult cell and segment identity specification. *Genes Dev.* 14:2906-17.
- Bourbon, H.M., A. Aguilera, A.Z. Ansari, F.J. Asturias, A.J. Berk, S. Bjorklund, T.K. Blackwell, T. Borggreffe, M. Carey, M. Carlson, J.W. Conaway, R.C. Conaway, S.W. Emmons, J.D. Fondell, L.P. Freedman, T. Fukasawa, C.M. Gustafsson, M. Han, X. He, P.K. Herman, A.G. Hinnebusch, S. Holmberg, F.C. Holstege, J.A. Jaehning, Y.J. Kim, L. Kuras, A. Leutz, J.T. Lis, M. Meisterernst, A.M. Naar, K. Nasmyth, J.D. Parvin, M. Ptashne, D. Reinberg, H. Ronne, I. Sadowski, H. Sakurai, M. Sipiczki, P.W. Sternberg, D.J. Stillman, R. Strich, K. Struhl, J.Q. Svejstrup, S. Tuck, F. Winston, R.G. Roeder, and R.D. Kornberg. 2004. A unified nomenclature for protein subunits of mediator complexes linking transcriptional regulators to RNA polymerase II. *Mol Cell.* 14:553-7.
- Bradley, A., M. Evans, M.H. Kaufman, and E. Robertson. 1984. Formation of germ-line chimaeras from embryo-derived teratocarcinoma cell lines. *Nature.* 309:255-6.
- Branda, C.S., and S.M. Dymecki. 2004. Talking about a revolution: The impact of site-specific recombinases on genetic analyses in mice. *Dev Cell.* 6:7-28.



- Brower, C.S., S. Sato, C. Tomomori-Sato, T. Kamura, A. Pause, R. Stearman, R.D. Klausner, S. Malik, W.S. Lane, I. Sorokina, R.G. Roeder, J.W. Conaway, and R.C. Conaway. 2002. Mammalian mediator subunit mMED8 is an Elongin BC-interacting protein that can assemble with Cul2 and Rbx1 to reconstitute a ubiquitin ligase. *Proc Natl Acad Sci U S A*. 99:10353-8.
- Burgers, W.A., F. Fuks, and T. Kouzarides. 2002. DNA methyltransferases get connected to chromatin. *Trends Genet*. 18:275-7.
- Burke, T.W., and J.T. Kadonaga. 1997. The downstream core promoter element, DPE, is conserved from Drosophila to humans and is recognized by TAFII60 of Drosophila. *Genes Dev*. 11:3020-31.
- Cahir-McFarland, E.D., K. Carter, A. Rosenwald, J.M. Giltneane, S.E. Henrickson, L.M. Staudt, and E. Kieff. 2004. Role of NF-kappa B in cell survival and transcription of latent membrane protein 1-expressing or Epstein-Barr virus latency III-infected cells. *J Virol*. 78:4108-19.
- Cahir-McFarland, E.D., D.M. Davidson, S.L. Schauer, J. Duong, and E. Kieff. 2000. NF-kappa B inhibition causes spontaneous apoptosis in Epstein-Barr virus-transformed lymphoblastoid cells. *Proc Natl Acad Sci U S A*. 97:6055-60.
- Cantoni, C., C. Bottino, R. Augugliaro, L. Morelli, E. Marcenaro, R. Castriconi, M. Vitale, D. Pende, S. Sivori, R. Millo, R. Biassoni, L. Moretta, and A. Moretta. 1999. Molecular and functional characterization of IRp60, a member of the immunoglobulin superfamily that functions as an inhibitory receptor in human NK cells. *Eur J Immunol*. 29:3148-59.
- Capecchi, M.R. 1989. Altering the genome by homologous recombination. *Science*. 244:1288-92.
- Carter, K.L., E. Cahir-McFarland, and E. Kieff. 2002. Epstein-barr virus-induced changes in B-lymphocyte gene expression. *J Virol*. 76:10427-36.
- Cazalla, D., J. Zhu, L. Manche, E. Huber, A.R. Krainer, and J.F. Caceres. 2002. Nuclear export and retention signals in the RS domain of SR proteins. *Mol Cell Biol*. 22:6871-82.
- Chadick, J.Z., and F.J. Asturias. 2005. Structure of eukaryotic Mediator complexes. *Trends Biochem Sci*. 30:264-71.
- Chambers, R.S., and M.E. Dahmus. 1994. Purification and characterization of a phosphatase from HeLa cells which dephosphorylates the C-terminal domain of RNA polymerase II. *J Biol Chem*. 269:26243-8.
- Chen, W., Struhl, K. 1988. Saturation Mutagenesis of a yeast his3 "TATA element": genetic evidence for a specific TATA-binding protein. *Proc. Natl. Acad. Sci. USA*. 85:2691-2695.
- Chi, T., P. Lieberman, K. Ellwood, and M. Carey. 1995. A general mechanism for transcriptional synergy by eukaryotic activators. *Nature*. 377:254-7.
- Choy, B., and M.R. Green. 1993. Eukaryotic activators function during multiple steps of preinitiation complex assembly. *Nature*. 366:531-536.

- Coghill, E.L., A. Hugill, N. Parkinson, C. Davison, P. Glenister, S. Clements, J. Hunter, R.D. Cox, and S.D. Brown. 2002. A gene-driven approach to the identification of ENU mutants in the mouse. *Nat Genet.* 30:255-6.
- Cohen, J.I. 1992. A region of herpes simplex virus VP16 can substitute for a transforming domain of Epstein-Barr virus nuclear protein 2. *Proc Natl Acad Sci U S A.* 89:8030-4.
- Cohen, J.I., and E. Kieff. 1991. An Epstein-Barr virus nuclear protein 2 domain essential for transformation is a direct transcriptional activator. *J Virol.* 65:5880-5.
- Cohen, J.I., F. Wang, J. Mannick, and E. Kieff. 1989. Epstein-Barr virus nuclear protein 2 is a key determinant of lymphocyte transformation. *Proc Natl Acad Sci U S A.* 86:9558-62.
- Cosma, M.P., S. Panizza, and K. Nasmyth. 2001. Cdk1 triggers association of RNA polymerase to cell cycle promoters only after recruitment of the mediator by SBF. *Mol. Cell.* 7:1213-20.
- Craig, J.M. 2005. Heterochromatin--many flavours, common themes. *Bioessays.* 27:17-28.
- Cramer, P., D.A. Bushnell, J. Fu, A.L. Gnatt, B. Maier-Davis, N.E. Thompson, R.R. Burgess, A.M. Edwards, P.R. David, and R.D. Kornberg. 2000. Architecture of RNA polymerase II and implications for the transcription mechanism. *Science.* 288:640-9.
- Cramer, P., D.A. Bushnell, and R.D. Kornberg. 2001. Structural basis of transcription: RNA polymerase II at 2.8 angstrom resolution. *Science.* 292:1863-76.
- Cress, W.D., and S.J. Triezenberg. 1991. Critical structural elements of the VP16 transcriptional activation domain. *Science.* 251:87-90.
- Cuesta, A., L. Pedrola, T. Sevilla, J. Garcia-Planells, M.J. Chumillas, F. Mayordomo, E. LeGuern, I. Marin, J.J. Vilchez, and F. Palau. 2002. The gene encoding ganglioside-induced differentiation-associated protein 1 is mutated in axonal Charcot-Marie-Tooth type 4A disease. *Nat Genet.* 30:22-5.
- Davis, J.A., Y. Takagi, R.D. Kornberg, and F.A. Asturias. 2002. Structure of the yeast RNA polymerase II holoenzyme: Mediator conformation and polymerase interaction. *Mol Cell.* 10:409-15.
- De Sandre-Giovannoli, A., M. Chaouch, S. Kozlov, J.M. Vallat, M. Tazir, N. Kassouri, P. Szepetowski, T. Hammadouche, A. Vandenberghe, C.L. Stewart, D. Grid, and N. Levy. 2002. Homozygous defects in LMNA, encoding lamin A/C nuclear-envelope proteins, cause autosomal recessive axonal neuropathy in human (Charcot-Marie-Tooth disorder type 2) and mouse. *Am J Hum Genet.* 70:726-36.
- De Smaele, E., F. Zazzeroni, S. Papa, D.U. Nguyen, R. Jin, J. Jones, R. Cong, and G. Franzoso. 2001. Induction of gadd45beta by NF-kappaB downregulates pro-apoptotic JNK signalling. *Nature.* 414:308-13.
- Diehl, J.A., M. Cheng, M.F. Roussel, and C.J. Sherr. 1998. Glycogen synthase kinase-3beta regulates cyclin D1 proteolysis and subcellular localization. *Genes Dev.* 12:3499-511.

- Doerks, T., R. Copley, and P. Bork. 2001. DDT -- a novel domain in different transcription and chromosome remodeling factors. *Trends Biochem Sci.* 26:145-6.
- Dotson, M.R., C.X. Yuan, R.G. Roeder, L.C. Myers, C.M. Gustafsson, Y.W. Jiang, Y. Li, R.D. Kornberg, and F.J. Asturias. 2000. Structural organization of yeast and mammalian mediator complexes. *Proc. Natl. Acad. Sci. U.S.A.* 97:14307-10.
- Dunker, A.K., C.J. Brown, J.D. Lawson, L.M. Iakoucheva, and Z. Obradovic. 2002. Intrinsic disorder and protein function. *Biochemistry.* 41:6573-82.
- Dunker, A.K., J.D. Lawson, C.J. Brown, R.M. Williams, P. Romero, J.S. Oh, C.J. Oldfield, A.M. Campen, C.M. Ratliff, K.W. Hipps, J. Ausio, M.S. Nissen, R. Reeves, C. Kang, C.R. Kissinger, R.W. Bailey, M.D. Griswold, W. Chiu, E.C. Garner, and Z. Obradovic. 2001. Intrinsically disordered protein. *J Mol Graph Model.* 19:26-59.
- Dymecki, S.M. 1996. A modular set of Flp, FRT and lacZ fusion vectors for manipulating genes by site-specific recombination. *Gene.* 171:197-201.
- Edwards, A.M., C.M. Kane, R.A. Young, and R.D. Kornberg. 1991. Two dissociable subunits of yeast RNA polymerase II stimulate the initiation of transcription at a promoter in vitro. *J Biol Chem.* 266:71-5.
- Elgin, S.C., and S.I. Grewal. 2003. Heterochromatin: silence is golden. *Curr Biol.* 13:R895-8.
- Evans, M.J., and M.H. Kaufman. 1981. Establishment in culture of pluripotential cells from mouse embryos. *Nature.* 292:154-6.
- Feil, R., J. Wagner, D. Metzger, and P. Chambon. 1997. Regulation of Cre recombinase activity by mutated estrogen receptor ligand-binding domains. *Biochem Biophys Res Commun.* 237:752-7.
- Feng, Q., and Y. Zhang. 2001. The MeCP1 complex represses transcription through preferential binding, remodeling, and deacetylating methylated nucleosomes. *Genes Dev.* 15:827-32.
- Fischle, W., Y. Wang, and C.D. Allis. 2003. Histone and chromatin cross-talk. *Curr Opin Cell Biol.* 15:172-83.
- Flanagan, P.M., R.J. Kelleher, 3rd, M.H. Sayre, H. Tschochner, and R.D. Kornberg. 1991. A mediator required for activation of RNA polymerase II transcription in vitro. *Nature.* 350:436-8.
- Fondell, J.D., F. Brunel, K. Hisatake, and R.G. Roeder. 1996. Unliganded thyroid hormone receptor alpha can target TATA-binding protein for transcriptional repression. *Mol. Cell. Biol.* 16:281-7.
- Fondell, J.D., M. Guermah, S. Malik, and R.G. Roeder. 1999. Thyroid hormone receptor-associated proteins and general positive cofactors mediate thyroid hormone receptor function in the absence of the TATA box-binding protein-associated factors of TFIID. *Proc. Natl. Acad. Sci. U S A.* 96:1959-64.

- Ge, H., and R.G. Roeder. 1994. Purification, cloning, and characterization of a human coactivator, PC4, that mediates transcriptional activation of class II genes. *Cell*. 78:513-523.
- Ge, K., M. Guermah, C.X. Yuan, M. Ito, A.E. Wallberg, B.M. Spiegelman, and R.G. Roeder. 2002. Transcription coactivator TRAP220 is required for PPAR gamma 2-stimulated adipogenesis. *Nature*. 417:563-7.
- Gerster, T., and R.G. Roeder. 1988. A herpesvirus trans-activating protein interacts with transcription factor OTF-1 and other cellular proteins. *Proc Natl Acad Sci U S A*. 85:6347-51.
- Ghosh, S., C. Toth, M. Peterlin, and E. Seto. 1996. Synergistic activation of transcription by the mutant and wild-type minimal transcriptional activation domain of VP16. *J. Biol. Chem*. 271:9911-9918.
- Gilbert, N., S. Boyle, H. Fiegler, K. Woodfine, N.P. Carter, and W.A. Bickmore. 2004. Chromatin architecture of the human genome: gene-rich domains are enriched in open chromatin fibers. *Cell*. 118:555-66.
- Gim, B.S., J.M. Park, J.H. Yoon, C. Kang, and Y.J. Kim. 2001. Drosophila Med6 is required for elevated expression of a large but distinct set of developmentally regulated genes. *Mol. Cell. Biol*. 21:5242-55.
- Gnatt, A.L., P. Cramer, J. Fu, D.A. Bushnell, and R.D. Kornberg. 2001. Structural basis of transcription: an RNA polymerase II elongation complex at 3.3 A resolution. *Science*. 292:1876-82.
- Gossler, A., A.L. Joyner, J. Rossant, and W.C. Skarnes. 1989. Mouse embryonic stem cells and reporter constructs to detect developmentally regulated genes. *Science*. 244:463-5.
- Greaves, R., and P. O'Hare. 1989. Separation of requirements for protein-DNA complex assembly from those for functional activity in the herpes simplex virus regulatory protein Vmw65. *J Virol*. 63:1641-50.
- Gregory, C.D., C. Dive, S. Henderson, C.A. Smith, G.T. Williams, J. Gordon, and A.B. Rickinson. 1991. Activation of Epstein-Barr virus latent genes protects human B cells from death by apoptosis. *Nature*. 349:612-4.
- Grewal, S.I., and D. Moazed. 2003. Heterochromatin and epigenetic control of gene expression. *Science*. 301:798-802.
- Grossman, S.R., E. Johannsen, X. Tong, R. Yalamanchili, and E. Kieff. 1994. The Epstein-Barr virus nuclear antigen 2 transactivator is directed to response elements by the J kappa recombination signal binding protein. *Proc Natl Acad Sci U S A*. 91:7568-72.
- Gu, H., Y.R. Zou, and K. Rajewsky. 1993. Independent control of immunoglobulin switch recombination at individual switch regions evidenced through Cre-loxP-mediated gene targeting. *Cell*. 73:1155-64.
- Gu, W., S. Malik, M. Ito, C.X. Yuan, J.D. Fondell, X. Zhang, E. Martinez, J. Qin, and R.G. Roeder. 1999. A novel human SRB/MED-containing cofactor complex, SMCC, involved in transcription regulation. *Mol. Cell*. 3:97-108.

- Guarente, L., and E. Hoar. 1984. Upstream activation sites of the *CYC1* gene of *Saccharomyces cerevisiae* are active when inverted but not when placed downstream of the "TATA box". *Proc Natl Acad Sci U S A.* 81:7860-4.
- Guglielmi, B., N.L. van Berkum, B. Klapholz, T. Bijma, M. Boube, C. Boschiero, H.M. Bourbon, F.C. Holstege, and M. Werner. 2004. A high resolution protein interaction map of the yeast Mediator complex. *Nucleic Acids Res.* 32:5379-91.
- Hahn, S. 2004. Structure and mechanism of the RNA polymerase II transcription machinery. *Nat Struct Mol Biol.* 11:394-403.
- Hammerschmidt, W., and B. Sugden. 1989. Genetic analysis of immortalizing functions of Epstein-Barr virus in human B lymphocytes. *Nature.* 340:393-7.
- Hampsey, M. 1998. Molecular genetics of the RNA polymerase II general transcriptional machinery. *Microbiol. Mol. Biol. Rev.* 62:465-503.
- Hansen, J., T. Floss, P. Van Sloun, E.M. Fuchtbauer, F. Vauti, H.H. Arnold, F. Schnutgen, W. Wurst, H. von Melchner, and P. Ruiz. 2003. A large-scale, gene-driven mutagenesis approach for the functional analysis of the mouse genome. *Proc Natl Acad Sci U S A.* 100:9918-22.
- Hartmann, A.M., O. Nayler, F.W. Schwaiger, A. Obermeier, and S. Stamm. 1999. The interaction and colocalization of Sam68 with the splicing-associated factor YT521-B in nuclear dots is regulated by the Src family kinase p59(fyn). *Mol Biol Cell.* 10:3909-26.
- Hasty, P., J. Rivera-Perez, and A. Bradley. 1991a. The length of homology required for gene targeting in embryonic stem cells. *Mol Cell Biol.* 11:5586-91.
- Hasty, P., J. Rivera-Perez, C. Chang, and A. Bradley. 1991b. Target frequency and integration pattern for insertion and replacement vectors in embryonic stem cells. *Mol Cell Biol.* 11:4509-17.
- Hekmatpanah, D.S., and R.A. Young. 1991. Mutations in a conserved region of RNA polymerase II influence the accuracy of mRNA start site selection. *Mol Cell Biol.* 11:5781-91.
- Henderson, S., M. Rowe, C. Gregory, D. Croom-Carter, F. Wang, R. Longnecker, E. Kieff, and A. Rickinson. 1991. Induction of *bcl-2* expression by Epstein-Barr virus latent membrane protein 1 protects infected B cells from programmed cell death. *Cell.* 65:1107-15.
- Heng, H.H., S. Goetze, C.J. Ye, G. Liu, J.B. Stevens, S.W. Bremer, S.M. Wykes, J. Bode, and S.A. Krawetz. 2004. Chromatin loops are selectively anchored using scaffold/matrix-attachment regions. *J Cell Sci.* 117:999-1008.
- Hengartner, C.J., C.M. Thompson, J. Zhang, D.M. Chao, S.M. Liao, A.J. Koleske, S. Okamura, and R.A. Young. 1995. Association of an activator with an RNA polymerase II holoenzyme. *Genes Dev.* 9:897-910.
- Henkel, T., P.D. Ling, S.D. Hayward, and M.G. Peterson. 1994. Mediation of Epstein-Barr virus EBNA2 transactivation by recombination signal-binding protein J kappa. *Science.* 265:92-5.

- Hermann, S., K.D. Berndt, and A.P. Wright. 2001. How transcriptional activators bind target proteins. *J Biol Chem.* 276:40127-32.
- Hernandez, N. 1993. TBP, a universal eukaryotic transcription factor? *Genes Dev.* 7:1291-308.
- Herrera, F.J., and S.J. Triezenberg. 2004. VP16-dependent association of chromatin-modifying coactivators and underrepresentation of histones at immediate-early gene promoters during herpes simplex virus infection. *J Virol.* 78:9689-96.
- Herron, B.J., W. Lu, C. Rao, S. Liu, H. Peters, R.T. Bronson, M.J. Justice, J.D. McDonald, and D.R. Beier. 2002. Efficient generation and mapping of recessive developmental mutations using ENU mutagenesis. *Nat Genet.* 30:185-9.
- Hilton, D.J. 1992. LIF: lots of interesting functions. *Trends Biochem Sci.* 17:72-6.
- Hirose, Y., and J.L. Manley. 2000. RNA polymerase II and the integration of nuclear events. *Genes Dev.* 14:1415-29.
- Hooper, M., K. Hardy, A. Handyside, S. Hunter, and M. Monk. 1987. HPRT-deficient (Lesch-Nyhan) mouse embryos derived from germline colonization by cultured cells. *Nature.* 326:292-5.
- Hrabe de Angelis, M.H., H. Flaswinkel, H. Fuchs, B. Rathkolb, D. Soewarto, S. Marschall, S. Heffner, W. Pargent, K. Wuensch, M. Jung, A. Reis, T. Richter, F. Alessandrini, T. Jakob, E. Fuchs, H. Kolb, E. Kremmer, K. Schaeble, B. Rollinski, A. Roscher, C. Peters, T. Meitinger, T. Strom, T. Steckler, F. Holsboer, T. Klopstock, F. Gekeler, C. Schindewolf, T. Jung, K. Avraham, H. Behrendt, J. Ring, A. Zimmer, K. Schughart, K. Pfeffer, E. Wolf, and R. Balling. 2000. Genome-wide, large-scale production of mutant mice by ENU mutagenesis. *Nat Genet.* 25:444-7.
- Hsieh, J.J., and S.D. Hayward. 1995. Masking of the CBF1/RBPJ kappa transcriptional repression domain by Epstein-Barr virus EBNA2. *Science.* 268:560-3.
- Hsieh, J.J., S. Zhou, L. Chen, D.B. Young, and S.D. Hayward. 1999. CIR, a corepressor linking the DNA binding factor CBF1 to the histone deacetylase complex. *Proc Natl Acad Sci U S A.* 96:23-8.
- Ikeda, K., D.J. Steger, A. Eberharter, and J.L. Workman. 1999. Activation domain-specific and general transcription stimulation by native histone acetyltransferase complexes. *Mol. Cell. Biol.* 19:855-63.
- Ikeda, K., T. Stuehler, and M. Meisterernst. 2002. The H1 and H2 regions of the activation domain of herpes simplex virion protein 16 stimulate transcription through distinct molecular mechanisms. *Genes Cells.* 7:49-58.
- Ingles, C.J., M. Shales, W.D. Cress, S.J. Triezenberg, and J. Greenblatt. 1991. Reduced binding of TFIID to transcriptionally compromised mutants of VP16. *Nature.* 351:588-90.
- Ito, M., H.J. Okano, R.B. Darnell, and R.G. Roeder. 2002. The TRAP100 component of the TRAP/Mediator complex is essential in broad transcriptional events and development. *Embo J.* 21:3464-75.

- Ito, M., C.X. Yuan, S. Malik, W. Gu, J.D. Fondell, S. Yamamura, Z.Y. Fu, X. Zhang, J. Qin, and R.G. Roeder. 1999. Identity between TRAP and SMCC complexes indicates novel pathways for the function of nuclear receptors and diverse mammalian activators. *Mol. Cell.* 3:361-70.
- Ito, M., C.X. Yuan, H.J. Okano, R.B. Darnell, and R.G. Roeder. 2000. Involvement of the TRAP220 component of the TRAP/SMCC coactivator complex in embryonic development and thyroid hormone action. *Mol Cell.* 5:683-93.
- Janody, F., Z. Martirosyan, A. Benlali, and J.E. Treisman. 2003. Two subunits of the Drosophila mediator complex act together to control cell affinity. *Development.* 130:3691-701.
- Jeanmougin, F., J.M. Wurtz, B. Le Douarin, P. Chambon, and R. Losson. 1997. The bromodomain revisited. *Trends Biochem Sci.* 22:151-3.
- Jenuwein, T., and C.D. Allis. 2001. Translating the histone code. *Science.* 293:1074-80.
- Jiang, Y., S. Triezenberg, and J.D. Gralla. 1994. Defective transcriptional activation by diverse VP16 mutants associated with a common inability to form open promoter complexes. *J. Biol. Chem.* 269:5505-5508.
- Jiang, Y.W., P. Veschambre, H. Erdjument-Bromage, P. Tempst, J.W. Conaway, R.C. Conaway, and R.D. Kornberg. 1998. Mammalian mediator of transcriptional regulation and its possible role as an end-point of signal transduction pathways. *Proc. Natl. Acad. Sci. U.S.A.* 95:8538-43.
- Jochum, W., E. Passegue, and E.F. Wagner. 2001. AP-1 in mouse development and tumorigenesis. *Oncogene.* 20:2401-12.
- Johannsen, E., E. Koh, G. Mosialos, X. Tong, E. Kieff, and S.R. Grossman. 1995. Epstein-Barr virus nuclear protein 2 transactivation of the latent membrane protein 1 promoter is mediated by J kappa and PU.1. *J Virol.* 69:253-62.
- Johnson, A.D. 1995. The price of repression. *Cell.* 81:655-8.
- Jones, P.L., G.J. Veenstra, P.A. Wade, D. Vermaak, S.U. Kass, N. Landsberger, J. Strouboulis, and A.P. Wolffe. 1998. Methylated DNA and MeCP2 recruit histone deacetylase to repress transcription. *Nat Genet.* 19:187-91.
- Jonker, H.R., R.W. Wechselberger, R. Boelens, G.E. Folkers, and R. Kaptein. 2005. Structural properties of the promiscuous VP16 activation domain. *Biochemistry.* 44:827-39.
- Jonker, H.R., R.W. Wechselberger, R. Boelens, R. Kaptein, and G.E. Folkers. 2006. The intrinsically unstructured domain of PC4 modulates the activity of the structured core through inter- and intramolecular interactions. *Biochemistry.* 45:5067-81.
- Kaartinen, V., and A. Nagy. 2001. Removal of the floxed neo gene from a conditional knockout allele by the adenoviral Cre recombinase in vivo. *Genesis.* 31:126-9.
- Kamholz, J., R. Awatramani, D. Menichella, H. Jiang, W. Xu, and M. Shy. 1999. Regulation of myelin-specific gene expression. Relevance to CMT1. *Ann N Y Acad Sci.* 883:91-108.

- Kao, H.Y., P. Ordentlich, N. Koyano-Nakagawa, Z. Tang, M. Downes, C.R. Kintner, R.M. Evans, and T. Kadesch. 1998. A histone deacetylase corepressor complex regulates the Notch signal transduction pathway. *Genes Dev.* 12:2269-77.
- Katan, M., A. Haigh, C.P. Verrijzer, P.C. van der Vliet, and P. O'Hare. 1990. Characterization of a cellular factor which interacts functionally with Oct-1 in the assembly of a multicomponent transcription complex. *Nucleic Acids Res.* 18:6871-80.
- Kato, Y., R. Habas, Y. Katsuyama, A.M. Naar, and X. He. 2002. A component of the ARC/Mediator complex required for TGF beta/Nodal signalling. *Nature.* 418:641-6.
- Kempkes, B., D. Pich, R. Zeidler, B. Sugden, and W. Hammerschmidt. 1995. Immortalization of human B lymphocytes by a plasmid containing 71 kilobase pairs of Epstein-Barr virus DNA. *J Virol.* 69:231-8.
- Kim, T.W., Y.J. Kwon, J.M. Kim, Y.H. Song, S.N. Kim, and Y.J. Kim. 2004. MED16 and MED23 of Mediator are coactivators of lipopolysaccharide- and heat-shock-induced transcriptional activators. *Proc Natl Acad Sci U S A.* 101:12153-8.
- Kim, Y.-J., S. Bjorklund, Y. Li, M.H. Sayer, and R.D. Kornberg. 1994a. A Multiprotein Mediator of Transcriptional Activation and its Interaction with the C-Terminal Repeat Domain of RNA Polymerase II. *Cell.* 77:599-608.
- Kim, Y.J., S. Bjorklund, Y. Li, M.H. Sayre, and R.D. Kornberg. 1994b. A multiprotein mediator of transcriptional activation and its interaction with the C-terminal repeat domain of RNA polymerase II. *Cell.* 77:599-608.
- Koh, S.S., A.Z. Ansari, M. Ptashne, and R.A. Young. 1998. An activator target in the RNA polymerase II holoenzyme. *Mol. Cell.* 1:895-904.
- Koleske, A.J., and R.A. Young. 1994. An RNA polymerase II holoenzyme responsive to activators. *Nature.* 368:466-469.
- Komarnitsky, P., E.J. Cho, and S. Buratowski. 2000. Different phosphorylated forms of RNA polymerase II and associated mRNA processing factors during transcription. *Genes Dev.* 14:2452-60.
- Kraus, W.L., E.T. Manning, and J.T. Kadonaga. 1999. Biochemical Analysis of Distinct Activation Functions in p300 That Enhance Transcription Initiation with Chromatin Templates. *Mol Cell Biol.* 19:8123-8135.
- Kretschmar, M., K. Kaiser, F. Lottspeich, and M. Meisterernst. 1994. A novel mediator of class II gene transcription with homology to viral immediate-early transcriptional regulators. *Cell.* 78:525-34.
- Kristie, T.M., J.H. LeBowitz, and P.A. Sharp. 1989. The octamer-binding proteins form multi-protein--DNA complexes with the HSV alpha TIF regulatory protein. *Embo J.* 8:4229-38.
- Kwon, J.Y., J.M. Park, B.S. Gim, S.J. Han, J. Lee, and Y.J. Kim. 1999. Caenorhabditis elegans mediator complexes are required for developmental-specific transcriptional activation. *Proc. Natl. Acad. Sci. U.S.A.* 96:14990-5.



- Lagrange, T., A.N. Kapanidis, H. Tang, D. Reinberg, and R.H. Ebricht. 1998. New core promoter element in RNA polymerase II-dependent transcription: sequence-specific DNA binding by transcription factor IIB. *Genes Dev.* 12:34-44.
- Laherty, C.D., H.M. Hu, A.W. Opipari, F. Wang, and V.M. Dixit. 1992. The Epstein-Barr virus LMP1 gene product induces A20 zinc finger protein expression by activating nuclear factor kappa B. *J Biol Chem.* 267:24157-60.
- Lau, J.F., I. Nusinzon, D. Burakov, L.P. Freedman, and C.M. Horvath. 2003. Role of metazoan mediator proteins in interferon-responsive transcription. *Mol Cell Biol.* 23:620-8.
- Laux, G., B. Adam, L.J. Strobl, and F. Moreau-Gachelin. 1994. The Spi-1/PU.1 and Spi-B ets family transcription factors and the recombination signal binding protein RBP-J kappa interact with an Epstein-Barr virus nuclear antigen 2 responsive cis-element. *Embo J.* 13:5624-32.
- Leal, A., B. Morera, G. Del Valle, D. Heuss, C. Kayser, M. Berghoff, R. Villegas, E. Hernandez, M. Mendez, H.C. Hennies, B. Neundorfer, R. Barrantes, A. Reis, and B. Rautenstrauss. 2001. A second locus for an axonal form of autosomal recessive Charcot-Marie-Tooth disease maps to chromosome 19q13.3. *Am J Hum Genet.* 68:269-74.
- Lee, T.I., H.C. Causton, F.C. Holstege, W.C. Shen, N. Hannett, E.G. Jennings, F. Winston, M.R. Green, and R.A. Young. 2000. Redundant roles for the TFIID and SAGA complexes in global transcription. *Nature.* 405:701-4.
- Lee, T.I., and R.A. Young. 2000. Transcription of eukaryotic protein-coding genes. *Annu. Rev. Genet.* 34:77-137.
- Lee, Y.C., J.M. Park, S. Min, S.J. Han, and Y.J. Kim. 1999. An activator binding module of yeast RNA polymerase II holoenzyme. *Mol. Cell. Biol.* 19:2967-76.
- Lefstin, J.A., and K.R. Yamamoto. 1998. Allosteric effects of DNA on transcriptional regulators. *Nature.* 392:885-8.
- Leneuve, P., S. Colnot, G. Hamard, F. Francis, M. Niwa-Kawakita, M. Giovannini, and M. Holzenberger. 2003. Cre-mediated germline mosaicism: a new transgenic mouse for the selective removal of residual markers from tri-lox conditional alleles. *Nucleic Acids Res.* 31:e21.
- Lerner, A., L. D'Adamio, A.C. Diener, L.K. Clayton, and E.L. Reinherz. 1993. CD3 zeta/eta/theta locus is colinear with and transcribed antisense to the gene encoding the transcription factor Oct-1. *J Immunol.* 151:3152-62.
- Lewandoski, M. 2001. Conditional control of gene expression in the mouse. *Nat Rev Genet.* 2:743-55.
- Lin, Y.-S., and M.R. Green. 1991. Mechanism of action of an acidic transcriptional activator in vitro. *Cell.* 64:971-981.
- Littlefield, O., Y. Korkhin, and P.B. Sigler. 1999. The structural basis for the oriented assembly of a TBP/TFB/promoter complex. *Proc Natl Acad Sci U S A.* 96:13668-73.

- Liu, Y., C. Kung, J. Fishburn, A.Z. Ansari, K.M. Shokat, and S. Hahn. 2004. Two cyclin-dependent kinases promote RNA polymerase II transcription and formation of the scaffold complex. *Mol Cell Biol.* 24:1721-35.
- Luger, K., and T.J. Richmond. 1998. DNA binding within the nucleosome core. *Curr Opin Struct Biol.* 8:33-40.
- MacGregor Schafer, J., H. Liu, D.J. Bentrem, J.W. Zapf, and V.C. Jordan. 2000. Allosteric silencing of activating function 1 in the 4-hydroxytamoxifen estrogen receptor complex is induced by substituting glycine for aspartate at amino acid 351. *Cancer Res.* 60:5097-105.
- Malik, S., H.J. Baek, W. Wu, and R.G. Roeder. 2005. Structural and functional characterization of PC2 and RNA polymerase II-associated subpopulations of metazoan Mediator. *Mol Cell Biol.* 25:2117-29.
- Malik, S., W. Gu, W. Wu, J. Qin, and R.G. Roeder. 2000. The USA-derived transcriptional coactivator PC2 is a submodule of TRAP/SMCC and acts synergistically with other PCs. *Mol. Cell.* 5:753-60.
- Malik, S., and R.G. Roeder. 2000. Transcriptional regulation through Mediator-like coactivators in yeast and metazoan cells. *Trends Biochem. Sci.* 25:277-83.
- Martin, G.R. 1981. Isolation of a pluripotent cell line from early mouse embryos cultured in medium conditioned by teratocarcinoma stem cells. *Proc Natl Acad Sci U S A.* 78:7634-8.
- McKenna, N.J., and B.W. O'Malley. 2002. Combinatorial control of gene expression by nuclear receptors and coregulators. *Cell.* 108:465-74.
- McKune, K., P.A. Moore, M.W. Hull, and N.A. Woychik. 1995. Six human RNA polymerase subunits functionally substitute for their yeast counterparts. *Mol Cell Biol.* 15:6895-900.
- Meisterernst, M., A.L. Roy, H.M. Lieu, and R.G. Roeder. 1991. Activation of class II gene transcription by regulatory factors is potentiated by a novel activity. *Cell.* 66:981-93.
- Memedula, S., and A.S. Belmont. 2003. Sequential recruitment of HAT and SWI/SNF components to condensed chromatin by VP16. *Curr Biol.* 13:241-6.
- Mittler, G., T. Stuhler, L. Santolin, T. Uhlmann, E. Kremmer, F. Lottspeich, L. Berti, and M. Meisterernst. 2003. A novel docking site on Mediator is critical for activation by VP16 in mammalian cells. *Embo J.* 22:6494-504.
- Moghal, N., and P.W. Sternberg. 2003. A component of the transcriptional mediator complex inhibits RAS-dependent vulval fate specification in *C. elegans*. *Development.* 130:57-69.
- Moon, A.M., and M.R. Capecchi. 2000. Fgf8 is required for outgrowth and patterning of the limbs. *Nat Genet.* 26:455-9.
- Mostacciolo, M.L., G. Micaglio, P. Fardin, and G.A. Danieli. 1991. Genetic epidemiology of hereditary motor sensory neuropathies (type I). *Am J Med Genet.* 39:479-81.

- Moustakas, A., and D. Kardassis. 1998. Regulation of the human p21/WAF1/Cip1 promoter in hepatic cells by functional interactions between Sp1 and Smad family members. *Proc Natl Acad Sci U S A*. 95:6733-8.
- Myers, L.C., and R.D. Kornberg. 2000. Mediator of transcriptional regulation. *Annu. Rev. Biochem.* 69:729-49.
- Naar, A.M., P.A. Beurang, S. Zhou, S. Abraham, W. Solomon, and R. Tjian. 1999. Composite co-activator ARC mediates chromatin-directed transcriptional activation. *Nature*. 398:828-32.
- Naar, A.M., D.J. Taatjes, W. Zhai, E. Nogales, and R. Tjian. 2002. Human CRSP interacts with RNA polymerase II CTD and adopts a specific CTD-bound conformation. *Genes Dev.* 16:1339-44.
- Nan, X., H.H. Ng, C.A. Johnson, C.D. Laherty, B.M. Turner, R.N. Eisenman, and A. Bird. 1998. Transcriptional repression by the methyl-CpG-binding protein MeCP2 involves a histone deacetylase complex. *Nature*. 393:386-9.
- Narlikar, G.J., H.Y. Fan, and R.E. Kingston. 2002. Cooperation between complexes that regulate chromatin structure and transcription. *Cell*. 108:475-87.
- Neely, K.E., A.H. Hassan, A.E. Wallberg, D.J. Steger, B.R. Cairns, A.P. Wright, and J.L. Workman. 1999. Activation domain-mediated targeting of the SWI/SNF complex to promoters stimulates transcription from nucleosome arrays. *Mol. Cell*. 4:649-55.
- Ng, H.H., Y. Zhang, B. Hendrich, C.A. Johnson, B.M. Turner, H. Erdjument-Bromage, P. Tempst, D. Reinberg, and A. Bird. 1999. MBD2 is a transcriptional repressor belonging to the MeCP1 histone deacetylase complex. *Nat Genet*. 23:58-61.
- Nikolov, D.B., and S.K. Burley. 1994. 2.1 Å resolution refined structure of a TATA box-binding protein (TBP). *Nat Struct Biol*. 1:621-37.
- Nishioka, K., S. Chuikov, K. Sarma, H. Erdjument-Bromage, C.D. Allis, P. Tempst, and D. Reinberg. 2002. Set9, a novel histone H3 methyltransferase that facilitates transcription by precluding histone tail modifications required for heterochromatin formation. *Genes Dev.* 16:479-89.
- Nolan, P.M., J. Peters, L. Vitor, M. Strivens, R. Washbourne, T. Hough, C. Wells, P. Glenister, C. Thornton, J. Martin, E. Fisher, D. Rogers, J. Hagan, C. Reavill, I. Gray, J. Wood, N. Spurr, M. Browne, S. Rastan, J. Hunter, and S.D. Brown. 2000. Implementation of a large-scale ENU mutagenesis program: towards increasing the mouse mutant resource. *Mamm Genome*. 11:500-6.
- O'Hare, P., and C.R. Goding. 1988. Herpes simplex virus regulatory elements and the immunoglobulin octamer domain bind a common factor and are both targets for virion transactivation. *Cell*. 52:435-45.
- Oelgeschlager, T., C.M. Chiang, and R.G. Roeder. 1996. Topology and reorganization of a human TFIIID-promoter complex. *Nature*. 382:735-8.
- Ohler, U., G.C. Liao, H. Niemann, and G.M. Rubin. 2002. Computational analysis of core promoters in the Drosophila genome. *Genome Biol*. 3:RESEARCH0087.

- Ohno, H., S. Goto, S. Taki, T. Shirasawa, H. Nakano, S. Miyatake, T. Aoe, Y. Ishida, H. Maeda, T. Shirai, and et al. 1994. Targeted disruption of the CD3 eta locus causes high lethality in mice: modulation of Oct-1 transcription on the opposite strand. *Embo J.* 13:1157-65.
- Okano, M., and E. Li. 2002. Genetic analyses of DNA methyltransferase genes in mouse model system. *J Nutr.* 132:2462S-2465S.
- Olave, I., D. Reinberg, and L.D. Vales. 1998. The mammalian transcriptional repressor RBP (CBF1) targets TFIID and TFIIA to prevent activated transcription. *Genes Dev.* 12:1621-37.
- Orphanides, G., T. Lagrange, and D. Reinberg. 1996. The general transcriptional factors of RNA polymerase II. *Genes & Dev.* 10:2657-2683.
- Orphanides, G., and D. Reinberg. 2002. A unified theory of gene expression. *Cell.* 108:439-51.
- Park, J.M., B.S. Gim, J.M. Kim, J.H. Yoon, H.S. Kim, J.G. Kang, and Y.J. Kim. 2001a. Drosophila Mediator complex is broadly utilized by diverse gene-specific transcription factors at different types of core promoters. *Mol. Cell. Biol.* 21:2312-23.
- Park, J.M., J.M. Kim, L.K. Kim, S.N. Kim, J. Kim-Ha, J.H. Kim, and Y.J. Kim. 2003. Signal-induced transcriptional activation by Dif requires the dTRAP80 mediator module. *Mol Cell Biol.* 23:1358-67.
- Park, J.M., J. Werner, J.M. Kim, J.T. Lis, and Y.J. Kim. 2001b. Mediator, not holoenzyme, is directly recruited to the heat shock promoter by HSF upon heat shock. *Mol. Cell.* 8:9-19.
- Peterson, C.L. 2002. Chromatin remodeling: nucleosomes bulging at the seams. *Curr Biol.* 12:R245-7.
- Powell, W., and D. Reines. 1996. Mutations in the second largest subunit of RNA polymerase II cause 6-azauracil sensitivity in yeast and increased transcriptional arrest in vitro. *J Biol Chem.* 271:6866-73.
- Prokhortchouk, A., B. Hendrich, H. Jorgensen, A. Ruzov, M. Wilm, G. Georgiev, A. Bird, and E. Prokhortchouk. 2001. The p120 catenin partner Kaiso is a DNA methylation-dependent transcriptional repressor. *Genes Dev.* 15:1613-8.
- Proudfoot, N.J., A. Furger, and M.J. Dye. 2002. Integrating mRNA processing with transcription. *Cell.* 108:501-12.
- Qureshi, S.A., and S.P. Jackson. 1998. Sequence-specific DNA binding by the *S. shibatae* TFIIB homolog, TFB, and its effect on promoter strength. *Mol Cell.* 1:389-400.
- Rachez, C., B.D. Lemon, Z. Suldan, V. Bromleigh, M. Gamble, A.M. Naar, H. Erdjument-Bromage, P. Tempst, and L.P. Freedman. 1999. Ligand-dependent transcription activation by nuclear receptors requires the DRIP complex. *Nature.* 398:824-8.
- Rafalska, I., Z. Zhang, N. Benderska, H. Wolff, A.M. Hartmann, R. Brack-Werner, and S. Stamm. 2004. The intranuclear localization and function of YT521-B is regulated by tyrosine phosphorylation. *Hum Mol Genet.* 13:1535-49.

- Ranish, J.A., N. Yudkovsky, and S. Hahn. 1999. Intermediates in formation and activity of the RNA polymerase II preinitiation complex: holoenzyme recruitment and a postrecruitment role for the TATA box and TFIIB. *Genes Dev.* 13:49-63.
- Regier, J.L., F. Shen, and S.J. Triezengerg. 1993. Pattern of aromatic and hydrophobic amino acids critical for one of two subdomains of the VP16 transcriptional activator. *Proc. Natl. Acad. Sci. U.S.A.* 90:883-887.
- Richards, E.J., and S.C. Elgin. 2002. Epigenetic codes for heterochromatin formation and silencing: rounding up the usual suspects. *Cell.* 108:489-500.
- Roeder, R.G. 1996. The role of general initiation factors in transcription by RNA polymerase II. *Trends Biochem. Sci.* 21:327-35.
- Roguev, A., D. Schaft, A. Shevchenko, W.W. Pijnappel, M. Wilm, R. Aasland, and A.F. Stewart. 2001. The *Saccharomyces cerevisiae* Set1 complex includes an Ash2 homologue and methylates histone 3 lysine 4. *Embo J.* 20:7137-48.
- Roth, S.Y., J.M. Denu, and C.D. Allis. 2001. Histone acetyltransferases. *Annu. Rev. Biochem.* 70:81-120.
- Roupelieva, M. 2005. ORFeome-based arrays in eukaryotic expression vectors - a new approach to screen for the function of viral proteins: LANA-1 meets the mediator. *PhD thesis.*
- Ryu, S., S. Zhou, A.G. Ladurner, and R. Tjian. 1999. The transcriptional cofactor complex CRSP is required for activity of the enhancer-binding protein Sp1. *Nature.* 397:446-50.
- Sadowski, P.D. 1995. The Flp recombinase of the 2-microns plasmid of *Saccharomyces cerevisiae*. *Prog Nucleic Acid Res Mol Biol.* 51:53-91.
- Salghetti, S.E., A.A. Caudy, J.G. Chenoweth, and W.P. Tansey. 2001. Regulation of transcriptional activation domain function by ubiquitin. *Science.* 293:1651-3.
- Sambrook, J., Fritsch E. F., and Maniatis, T. 1989. Molecular cloning, a laboratory manual. Cold Spring Harbor Laboratory Press, New York.
- Santamaria, A., E. Castellanos, V. Gomez, P. Bénédit, J. Renau-Piqueras, J. Morote, J. Reventos, T.M. Thomson, and R. Paciucci. 2005. PTOV1 enables the nuclear translocation and mitogenic activity of flotillin-1, a major protein of lipid rafts. *Mol Cell Biol.* 25:1900-11.
- Santamaria, A., P.L. Fernandez, X. Farre, P. Bénédit, J. Reventos, J. Morote, R. Paciucci, and T.M. Thomson. 2003. PTOV-1, a novel protein overexpressed in prostate cancer, shuttles between the cytoplasm and the nucleus and promotes entry into the S phase of the cell division cycle. *Am J Pathol.* 162:897-905.
- Sato, S., C. Tomomori-Sato, C.A. Banks, T.J. Parmely, I. Sorokina, C.S. Brower, R.C. Conaway, and J.W. Conaway. 2003a. A mammalian homolog of *Drosophila melanogaster* transcriptional coactivator intersex is a subunit of the mammalian Mediator complex. *J Biol Chem.* 278:49671-4.
- Sato, S., C. Tomomori-Sato, C.A. Banks, I. Sorokina, T.J. Parmely, S.E. Kong, J. Jin, Y. Cai, W.S. Lane, C.S. Brower, R.C. Conaway, and J.W. Conaway. 2003b.

- Identification of mammalian Mediator subunits with similarities to yeast Mediator subunits Srb5, Srb6, Med11, and Rox3. *J Biol Chem.* 278:15123-7.
- Sato, S., C. Tomomori-Sato, T.J. Parmely, L. Florens, B. Zybaylov, S.K. Swanson, C.A. Banks, J. Jin, Y. Cai, M.P. Washburn, J.W. Conaway, and R.C. Conaway. 2004. A set of consensus mammalian mediator subunits identified by multidimensional protein identification technology. *Mol Cell.* 14:685-91.
- Shang, Y., X. Hu, J. DiRenzo, M.A. Lazar, and M. Brown. 2000. Cofactor dynamics and sufficiency in estrogen receptor-regulated transcription. *Cell.* 103:843-52.
- Sharma, D., and J.D. Fondell. 2002. Ordered recruitment of histone acetyltransferases and the TRAP/Mediator complex to thyroid hormone-responsive promoters in vivo. *Proc Natl Acad Sci U S A.* 99:7934-9.
- Shatkin, A.J., and J.L. Manley. 2000. The ends of the affair: capping and polyadenylation. *Nat Struct Biol.* 7:838-42.
- Shy, M.E., J. Blake, K. Krajewski, D.R. Fuerst, M. Laura, A.F. Hahn, J. Li, R.A. Lewis, and M. Reilly. 2005. Reliability and validity of the CMT neuropathy score as a measure of disability. *Neurology.* 64:1209-14.
- Simon, I., T. Tenzen, R. Mostoslavsky, E. Fibach, L. Lande, E. Milot, J. Gribnau, F. Grosveld, P. Fraser, and H. Cedar. 2001. Developmental regulation of DNA replication timing at the human beta globin locus. *Embo J.* 20:6150-7.
- Singer, V.L., C.R. Wobbe, and K. Struhl. 1990. A wide variety of DNA sequences can functionally replace a yeast TATA element for transcriptional activation. *Genes & Dev.* 4:636-645.
- Singh, N., and M. Han. 1995. sur-2, a novel gene, functions late in the let-60 ras-mediated signaling pathway during *Caenorhabditis elegans* vulval induction. *Genes Dev.* 9:2251-65.
- Sjoblom, A., A. Jansson, W. Yang, S. Lain, T. Nilsson, and L. Rymo. 1995. PU box-binding transcription factors and a POU domain protein cooperate in the Epstein-Barr virus (EBV) nuclear antigen 2-induced transactivation of the EBV latent membrane protein 1 promoter. *J Gen Virol.* 76 ( Pt 11):2679-92.
- Skre, H. 1974. Genetic and clinical aspects of Charcot-Marie-Tooth's disease. *Clin Genet.* 6:98-118.
- Smale, S.T., and J.T. Kadonaga. 2003. The RNA polymerase II core promoter. *Annu Rev Biochem.* 72:449-79.
- Smithies, O., R.G. Gregg, S.S. Boggs, M.A. Koralewski, and R.S. Kucherlapati. 1985. Insertion of DNA sequences into the human chromosomal beta-globin locus by homologous recombination. *Nature.* 317:230-4.
- Stanford, W.L., J.B. Cohn, and S.P. Cordes. 2001. Gene-trap mutagenesis: past, present and beyond. *Nat Rev Genet.* 2:756-68.
- Stark, W.M., M.R. Boocock, and D.J. Sherratt. 1992. Catalysis by site-specific recombinases. *Trends Genet.* 8:432-9.

- Stevens, J.L., G.T. Cantin, G. Wang, A. Shevchenko, and A.J. Berk. 2002. Transcription control by E1A and MAP kinase pathway via Sur2 mediator subunit. *Science*. 296:755-8.
- Strahl, B.D., and C.D. Allis. 2000. The language of covalent histone modifications. *Nature*. 403:41-5.
- Stringer, K.F., C.J. Ingles, and J. Greenblatt. 1990. Direct and selective binding of an acidic transcriptional activation domain to the TATA-box factor TFIID. *Nature*. 345:783-786.
- Struhl, K. 1984. Genetic properties and chromatin structure of the yeast gal regulatory element: an enhancer-like sequence. *Proc Natl Acad Sci U S A*. 81:7865-9.
- Struhl, K. 1998. Histone acetylation and transcriptional regulatory mechanisms. *Genes Dev*. 12:599-606.
- Stryke, D., M. Kawamoto, C.C. Huang, S.J. Johns, L.A. King, C.A. Harper, E.C. Meng, R.E. Lee, A. Yee, L. L'Italien, P.T. Chuang, S.G. Young, W.C. Skarnes, P.C. Babbitt, and T.E. Ferrin. 2003. BayGenomics: a resource of insertional mutations in mouse embryonic stem cells. *Nucleic Acids Res*. 31:278-81.
- Sullivan, S.M., P.J. Horn, V.A. Olson, A.H. Koop, W. Niu, R.H. Ebright, and S.J. Triezenberg. 1998. Mutational analysis of a transcriptional activation region of the VP16 protein of herpes simplex virus. *Nucleic Acids Res*. 26:4487-96.
- Sun, X., Y. Zhang, H. Cho, P. Rickert, E. Lees, W. Lane, and D. Reinberg. 1998. NAT, a human complex containing Srb polypeptides that functions as a negative regulator of activated transcription. *Mol. Cell*. 2:213-22.
- Sun, Z.W., A. Tessmer, and M. Hampsey. 1996. Functional interaction between TFIIB and the Rpb9 (Ssu73) subunit of RNA polymerase II in *Saccharomyces cerevisiae*. *Nucleic Acids Res*. 24:2560-6.
- Szutorisz, H., N. Dillon, and L. Tora. 2005. The role of enhancers as centres for general transcription factor recruitment. *Trends Biochem Sci*. 30:593-9.
- Taatjes, D.J., A.M. Naar, F. Andel, 3rd, E. Nogales, and R. Tjian. 2002. Structure, function, and activator-induced conformations of the CRSP coactivator. *Science*. 295:1058-62.
- Taatjes, D.J., T. Schneider-Poetsch, and R. Tjian. 2004. Distinct conformational states of nuclear receptor-bound CRSP-Med complexes. *Nat Struct Mol Biol*. 11:664-71.
- Tal-Singer, R., R. Pichyangkura, E. Chung, T.M. Lasner, B.P. Randazzo, J.Q. Trojanowski, N.W. Fraser, and S.J. Triezenberg. 1999. The transcriptional activation domain of VP16 is required for efficient infection and establishment of latency by HSV-1 in the murine peripheral and central nervous systems. *Virology*. 259:20-33.
- Tomomori-Sato, C., S. Sato, T.J. Parmely, C.A. Banks, I. Sorokina, L. Florens, B. Zybaylov, M.P. Washburn, C.S. Brower, R.C. Conaway, and J.W. Conaway. 2004. A mammalian mediator subunit that shares properties with *Saccharomyces cerevisiae* mediator subunit Cse2. *J Biol Chem*. 279:5846-51.
- Tompa, P. 2002. Intrinsically unstructured proteins. *Trends Biochem Sci*. 27:527-33.

- Tong, X., R. Drapkin, R. Yalamanchili, G. Mosialos, and E. Kieff. 1995a. The Epstein-Barr virus nuclear protein 2 acidic domain forms a complex with a novel cellular coactivator that can interact with TFIIE. *Mol Cell Biol.* 15:4735-44.
- Tong, X., F. Wang, C.J. Thut, and E. Kieff. 1995b. The Epstein-Barr virus nuclear protein 2 acidic domain can interact with TFIIB, TAF40, and RPA70 but not with TATA-binding protein. *J Virol.* 69:585-8.
- Treisman, J. 2001. Drosophila homologues of the transcriptional coactivation complex subunits TRAP240 and TRAP230 are required for identical processes in eye-antennal disc development. *Development.* 128:603-15.
- Triezenberg, S.J. 1995. Structure and function of transcriptional activation domains. *Curr Opin Genet Dev.* 5:190-6.
- Triezenberg, S.J., R.C. Kingsbury, and S.L. McKnight. 1988a. Functional dissection of VP16, the trans-activator of herpes simplex virus immediate early gene expression. *Genes Dev.* 2:718-729.
- Triezenberg, S.J., K.L. LaMarco, and S.L. McKnight. 1988b. Evidence of DNA: protein interactions that mediate HSV-1 immediate early gene activation by VP16. *Genes & Development.* 2:730-742.
- Turner, B.M. 2000. Histone acetylation and an epigenetic code. *Bioessays.* 22:836-45.
- Uesugi, M., O. Nyanguile, H. Lu, A.J. Levine, and G.L. Verdine. 1997. Induced alpha helix in the VP16 activation domain upon binding to a human TAF. *Science.* 277:1310-3.
- Uhlmann, T. 2006. Regulation of transcription by the viral activator VP16. *PhD thesis.*
- Utey, R.T., K. Ikeda, P.A. Grant, J. Cote, D.J. Steger, A. Eberharter, S. John, and J.L. Workman. 1998. Transcriptional activators direct histone acetyltransferase complexes to nucleosomes. *Nature.* 394:498-502.
- van Driel, R., P.F. Fransz, and P.J. Verschure. 2003. The eukaryotic genome: a system regulated at different hierarchical levels. *J Cell Sci.* 116:4067-75.
- Vance, J.M. 2000. The many faces of Charcot-Marie-Tooth disease. *Arch Neurol.* 57:638-40.
- Wade, P.A., A. Geronne, P.L. Jones, E. Ballestar, F. Aubry, and A.P. Wolffe. 1999. Mi-2 complex couples DNA methylation to chromatin remodelling and histone deacetylation. *Nat Genet.* 23:62-6.
- Walker, S., R. Greaves, and P. O'Hare. 1993. Transcriptional activation by the acidic domain of Vmw65 requires the integrity of the domain and involves additional determinants distinct from those necessary for TFIIB binding. *Mol. Cell. Biol.* 13:5233-5244.
- Waltzer, L., F. Logeat, C. Brou, A. Israel, A. Sergeant, and E. Manet. 1994. The human J kappa recombination signal sequence binding protein (RBP-J kappa) targets the Epstein-Barr virus EBNA2 protein to its DNA responsive elements. *Embo J.* 13:5633-8.

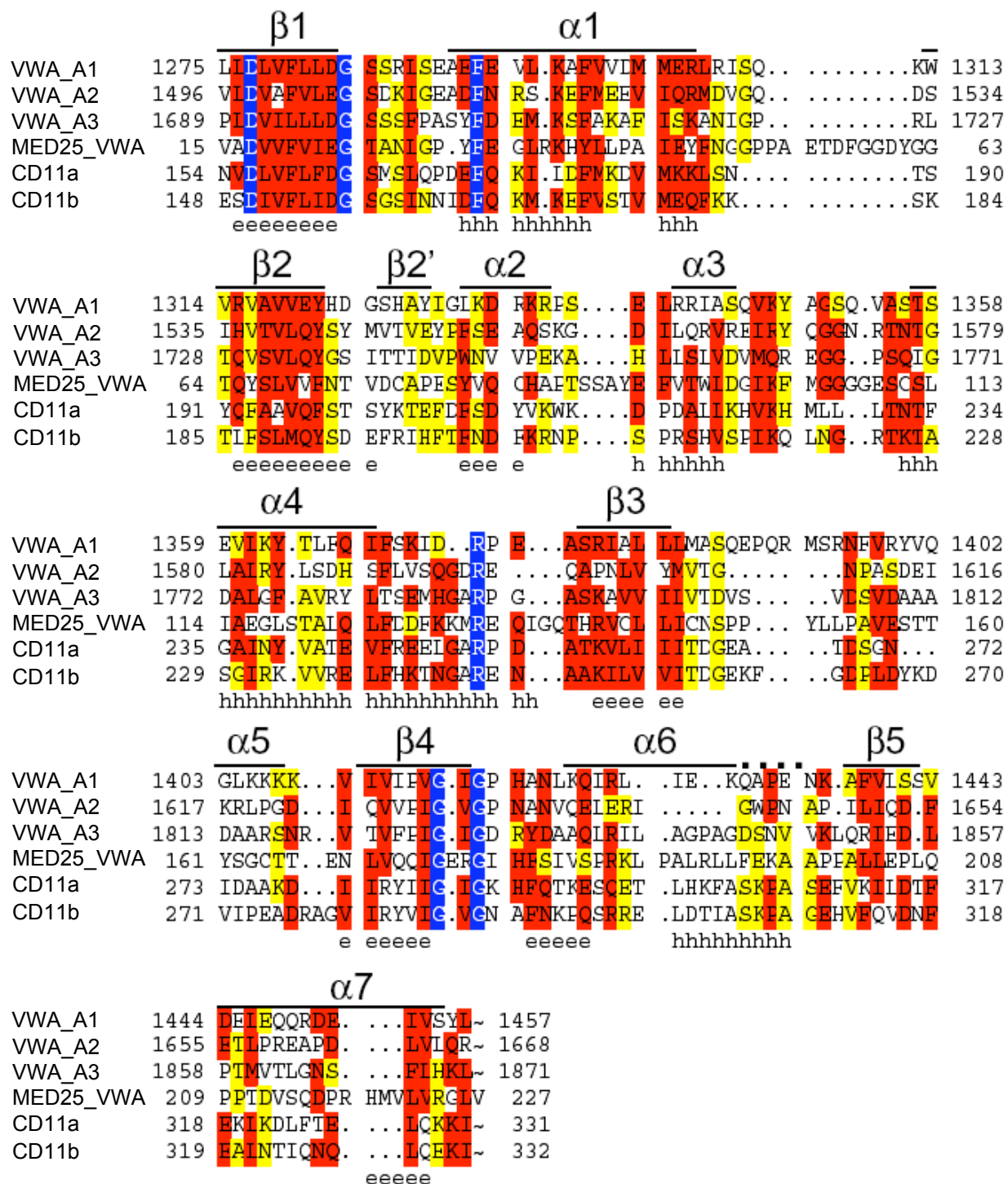


- Wang, G., and A.J. Berk. 2002. In vivo association of adenovirus large E1A protein with the human mediator complex in adenovirus-infected and -transformed cells. *J Virol.* 76:9186-93.
- Wang, L., S.R. Grossman, and E. Kieff. 2000. Epstein-Barr virus nuclear protein 2 interacts with p300, CBP, and PCAF histone acetyltransferases in activation of the LMP1 promoter. *Proc Natl Acad Sci U S A.* 97:430-5.
- Wang, S., K. Ge, R.G. Roeder, and O. Hankinson. 2004. Role of mediator in transcriptional activation by the aryl hydrocarbon receptor. *J Biol Chem.* 279:13593-600.
- Wang, W., M. Carey, and J.D. Gralla. 1992. Polymerase II promoter activation: closed complex formation and ATP-driven start site opening. *Science.* 255:450-3.
- Weis, L., and D. Reinberg. 1992. Transcription by RNA polymerase II: initiator-directed formation of transcription-competent complexes. *Faseb J.* 6:3300-9.
- Werstuck, G., and J.P. Capone. 1989. Mutational analysis of the herpes simplex virus trans-inducing factor Vmw65. *Gene.* 75:213-24.
- Wobbe, C.R., and K. Struhl. 1990. Yeast and human TATA-binding proteins have nearly identical DNA sequence requirements for transcription in vitro. *Mol Cell Biol.* 10:3859-67.
- Wright, P.E., and H.J. Dyson. 1999. Intrinsically unstructured proteins: re-assessing the protein structure-function paradigm. *J Mol Biol.* 293:321-31.
- Wu, D.Y., G.V. Kalpana, S.P. Goff, and W.H. Schubach. 1996. Epstein-Barr virus nuclear protein 2 (EBNA2) binds to a component of the human SNF-SWI complex, hSNF5/Ini1. *J Virol.* 70:6020-8.
- Wu, R., A.V. Terry, P.B. Singh, and D.M. Gilbert. 2005. Differential subnuclear localization and replication timing of histone H3 lysine 9 methylation states. *Mol Biol Cell.* 16:2872-81.
- Xiao, P., and J.P. Capone. 1990. A cellular factor binds to the herpes simplex virus type 1 transactivator Vmw65 and is required for Vmw65-dependent protein-DNA complex assembly with Oct-1. *Mol Cell Biol.* 10:4974-7.
- Yang, F., R. DeBeaumont, S. Zhou, and A.M. Naar. 2004. The activator-recruited cofactor/Mediator coactivator subunit ARC92 is a functionally important target of the VP16 transcriptional activator. *Proc Natl Acad Sci U S A.* 101:2339-44.
- Yankulov, K., J. Blau, T. Purton, S. Roberts, and D.L. Bentley. 1994. Transcriptional elongation by RNA polymerase II is stimulated by transactivators. *Cell.* 77:749-59.
- Zhang, G., E.A. Campbell, L. Minakhin, C. Richter, K. Severinov, and S.A. Darst. 1999a. Crystal structure of *Thermus aquaticus* core RNA polymerase at 3.3 Å resolution. *Cell.* 98:811-24.
- Zhang, H., and S.W. Emmons. 2000. A *C. elegans* mediator protein confers regulatory selectivity on lineage-specific expression of a transcription factor gene. *Genes Dev.* 14:2161-72.

- Zhang, Y., H.H. Ng, H. Erdjument-Bromage, P. Tempst, A. Bird, and D. Reinberg. 1999b. Analysis of the NuRD subunits reveals a histone deacetylase core complex and a connection with DNA methylation. *Genes Dev.* 13:1924-35.
- Zhang, Y., and D. Reinberg. 2001. Transcription regulation by histone methylation: interplay between different covalent modifications of the core histone tails. *Genes Dev.* 15:2343-60.
- Zhao, B., S. Maruo, A. Cooper, R.C. M, E. Johannsen, E. Kieff, and E. Cahir-McFarland. 2006. RNAs induced by Epstein-Barr virus nuclear antigen 2 in lymphoblastoid cell lines. *Proc Natl Acad Sci U S A.* 103:1900-5.
- Zhu, H., V. Joliot, and R. Prywes. 1994. Role of transcription factor TFIIIF in serum response factor-activated transcription. *J. Biol. Chem.* 269:3489-97.
- Zimber-Strobl, U., and L.J. Strobl. 2001. EBNA2 and Notch signalling in Epstein-Barr virus mediated immortalization of B lymphocytes. *Semin Cancer Biol.* 11:423-34.
- Zimber-Strobl, U., L.J. Strobl, C. Meitinger, R. Hinrichs, T. Sakai, T. Furukawa, T. Honjo, and G.W. Bornkamm. 1994. Epstein-Barr virus nuclear antigen 2 exerts its transactivating function through interaction with recombination signal binding protein RBP-J kappa, the homologue of Drosophila Suppressor of Hairless. *Embo J.* 13:4973-82.
- Zou, Y.R., W. Muller, H. Gu, and K. Rajewsky. 1994. Cre-loxP-mediated gene replacement: a mouse strain producing humanized antibodies. *Curr Biol.* 4:1099-103.

## 6. APPENDIX

## 6.1 Supplementary figures



Supplementary figure1. Sequence alignment of VWA domains from different species.

## 6.2 Microarray analysis

**Table 17.** Genes downregulated 1 hour after induction of ER–MED25–NTD in 721–B–cells

FLJ90036	hypothetical protein FLJ90036	84,4
WDR49	WD repeat domain 49	14,9
FLJ11016	hypothetical protein FLJ11016	13,0
ZNF395 /// FBXO16	zinc finger protein 395 /// F-box protein 16	10,6
LIN7B	lin-7 homolog B (C. elegans)	8,0
PFKFB4	6-phosphofructo-2-kinase/fructose-2,6-biphosphatase 4	4,0
BNIP3	BCL2/adenovirus E1B 19kDa interacting protein 3	3,7
SLC2A11	solute carrier family 2 (facilitated glucose transporter), member 11	3,7
BCL2	B-cell CLL/lymphoma 2	2,8
CCL4	chemokine (C-C motif) ligand 4	2,8
MFN1	Mitofusin 1	2,8
APOL1	apolipoprotein L, 1	2,6
JMJD2B	jumonji domain containing 2B	2,6
MAFF	v-maf musculoaponeurotic fibrosarcoma oncogene homolog F (avian)	2,6
SRRM2	serine/arginine repetitive matrix 2	2,6
SSH2	Slingshot homolog 2 (Drosophila)	2,6
TRIP12	Thyroid hormone receptor interactor 12	2,6
CCL3 /// CCL3L1 /// MGC12815	chemokine (C-C motif) ligand 3 /// chemokine (C-C motif) ligand 3-like 1 /// chemokine (C-C motif) ligand 3-like, centromeric	2,5
FLJ14503	hypothetical protein FLJ14503	2,5
PIK3C2A	Phosphoinositide-3-kinase, class 2, alpha polypeptide	2,5
SGOL2	shugoshin-like 2 (S. pombe)	2,5
TULP4	Tubby like protein 4	2,5
BBP	Beta-amyloid binding protein precursor	2,3
BNIP3L	BCL2/adenovirus E1B 19kDa interacting protein 3-like /// BCL2/adenovirus E1B 19kDa interacting protein 3-like	2,3
EGR2	early growth response 2 (Krox-20 homolog, Drosophila)	2,3
EGR3	early growth response 3	2,3
FLJ13855	hypothetical protein FLJ13855	2,3
FLJ20054	hypothetical protein FLJ20054	2,3
HSD17B12	Hydroxysteroid (17-beta) dehydrogenase 12	2,3
KIF3A	kinesin family member 3A	2,3
Lrp2bp	low density lipoprotein receptor-related protein binding protein	2,3
MGC19764	hypothetical protein MGC19764	2,3
PRRG4	proline rich Gla (G-carboxylglutamic acid) 4 (transmembrane)	2,3
SENP6	SUMO1/sentrin specific protease 6	2,3
CCNG2	cyclin G2	2,1
DUSP4	dual specificity phosphatase 4	2,1
FLJ90709	hypothetical protein FLJ90709	2,1
HIG2	hypoxia-inducible protein 2	2,1
LOC153222	adult retina protein	2,1
MGC20460	hypothetical protein MGC20460	2,1
PCTK2	PCTAIRE protein kinase 2	2,1
PDK1	pyruvate dehydrogenase kinase, isoenzyme 1	2,1
PICALM	Phosphatidylinositol binding clathrin assembly protein	2,1
PSCD1	Pleckstrin homology, Sec7 and coiled-coil domains 1(cytohesin 1)	2,1

RNPC2	RNA-binding region (RNP1, RRM) containing 2	2,1
RPL23	Ribosomal protein L23	2,1
SAT	spermidine/spermine N1-acetyltransferase	2,1
SNX9	sorting nexin 9	2,1
TAOK1	TAO kinase 1	2,1
YEATS2	YEATS domain containing 2	2,1
ZCCHC6	Zinc finger, CCHC domain containing 6	2,1
ZNF395	zinc finger protein 395	2,1
AFTIPHILIN	Aftiphilin protein	2,0
DDX17	DEAD (Asp-Glu-Ala-Asp) box polypeptide 17	2,0
DUSP5	dual specificity phosphatase 5	2,0
GAS7	growth arrest-specific 7	2,0
GSK3B	glycogen synthase kinase 3 beta	2,0
JMJD1A	jumonji domain containing 1A	2,0
LOC284757	hypothetical protein LOC284757	2,0
MBTD1	mbt domain containing 1	2,0
MLL3	myeloid/lymphoid or mixed-lineage leukemia 3	2,0
NEK1	NIMA (never in mitosis gene a)-related kinase 1	2,0
SGPP2	sphingosine-1-phosphate phosphatase 2	2,0
SOX9	SRY (sex determining region Y)-box 9 (campomelic dysplasia, autosomal sex-reversal)	2,0
TRA2A	Transformer-2 alpha	2,0
UHMK1	U2AF homology motif (UHM) kinase 1	2,0
ZA20D3	Zinc finger, A20 domain containing 3	2,0

**Table 18.** Genes upregulated 1 hour after induction of ER-MED25-NTD in 721-B-cells

SIPA1L2	signal-induced proliferation-associated 1 like 2	19,7
CXCL11	chemokine (C-X-C motif) ligand 11	13,9
NRAP	nebulin-related anchoring protein	13,0
SCHIP1	Schwannomin interacting protein 1	13,0
CFH /// CFHL3	complement factor H /// complement factor H-related 3	11,3
GNG2	Guanine nucleotide binding protein (G protein), gamma 2	11,3
MGC3234	Hypothetical protein MGC3234	9,8
CELSR1	cadherin, EGF LAG seven-pass G-type receptor 1 (flamingo homolog, Drosophila)	9,2
BCL10	B-cell CLL/lymphoma 10	8,6
MBD2	methyl-CpG binding domain protein 2	8,6
MYH10	myosin, heavy polypeptide 10, non-muscle	8,6
FAT3	FAT tumor suppressor homolog 3 (Drosophila)	8,0
LOC203510	similar to High mobility group protein 4 (HMG-4) (High mobility group protein 2a) (HMG-2a)	8,0
KELCHL	kelch-like	7,5
C10orf51	chromosome 10 open reading frame 51	7,0
SRC	V-src sarcoma (Schmidt-Ruppin A-2) viral oncogene homolog (avian)	7,0
SLC8A1	solute carrier family 8 (sodium/calcium exchanger), member 1	6,5
ZNF638	Zinc finger protein 638	6,5
MAP2K6	mitogen-activated protein kinase kinase 6	6,1
ADAMTS6	A disintegrin-like and metalloprotease (reprolysin type) with thrombospondin type 1 motif, 6	5,3
HTR2A	5-hydroxytryptamine (serotonin) receptor 2A /// 5-hydroxytryptamine (serotonin) receptor 2A	5,3
RPA4	replication protein A4, 34kDa	5,3
IL7R	Interleukin 7 receptor	4,9

ARMC8	Armadillo repeat containing 8	4,6
CEBPD	CCAAT/enhancer binding protein (C/EBP), delta	4,6
LOC283140	hypothetical protein LOC283140	4,6
BLCAP	Bladder cancer associated protein	4,3
MGC10765	Hypothetical protein MGC10765	4,0
WDR6	WD repeat domain 6	4,0
DNAJC13	DnaJ (Hsp40) homolog, subfamily C, member 13	3,7
GAL3ST2	Galactose-3-O-sulfotransferase 2	3,5
ATF7	activating transcription factor 7	3,2
LOC163131	hypothetical BC331191_1	3,2
IL1RAPL1	Interleukin 1 receptor accessory protein-like 1	3,0
KRTAP4-9	keratin associated protein 4-9	3,0
POLR3A	polymerase (RNA) III (DNA directed) polypeptide A, 155kDa	3,0
TNRC6A	trinucleotide repeat containing 6A	3,0
ARHGDI1A	Rho GDP dissociation inhibitor (GDI) alpha	2,8
DAPK1	death-associated protein kinase 1	2,8
DGUOK	deoxyguanosine kinase	2,8
SUHW4	suppressor of hairy wing homolog 4 (Drosophila)	2,8
BCAP29	B-cell receptor-associated protein 29	2,6
C14orf114	chromosome 14 open reading frame 114	2,6
CNOT3	CCR4-NOT transcription complex, subunit 3	2,6
CPSF6	Cleavage and polyadenylation specific factor 6, 68kDa	2,6
EPHA10	EPH receptor A10	2,6
MRGX1	G protein-coupled receptor MRGX1	2,6
QDPR	Quinoid dihydropteridine reductase	2,6
SVH	SVH protein	2,6
PSPH	phosphoserine phosphatase	2,5
TFRC	transferrin receptor (p90, CD71)	2,5
TP73L	tumor protein p73-like	2,5
CALR	calreticulin	2,3
DKFZp434H1419	hypothetical protein DKFZp434H1419	2,3
FGD6	FYVE, RhoGEF and PH domain containing 6	2,3
ITGAL	integrin, alpha L (antigen CD11A (p180), lymphocyte function-associated antigen 1; alpha polypeptide)	2,3
LMAN1	lectin, mannose-binding, 1	2,3
SFN	stratifin	2,3
STK4	serine/threonine kinase 4	2,3
ZNF17	zinc finger protein 17 (HPF3, KOX 10)	2,3
AMOTL2	angiomin like 2	2,1
ANKRD7	ankyrin repeat domain 7	2,1
C10orf18	chromosome 10 open reading frame 18	2,1
CCNE2	cyclin E2	2,1
CHS1	Chediak-Higashi syndrome 1	2,1
DDX3X	DEAD (Asp-Glu-Ala-Asp) box polypeptide 3, X-linked	2,1
FREB	Fc receptor homolog expressed in B cells	2,1
FRS2	fibroblast growth factor receptor substrate 2	2,1
FUS	fusion (involved in t(12;16) in malignant liposarcoma)	2,1
TTY5	Testis-specific transcript, Y-linked 5	2,1
UGCG1	UDP-glucose ceramide glucosyltransferase-like 1	2,1
C21orf86	Chromosome 21 open reading frame 86	2,0

C9orf71	chromosome 9 open reading frame 71	2,0
CASQ1	Calsequestrin 1 (fast-twitch, skeletal muscle)	2,0
DDX11	DEAD/H (Asp-Glu-Ala-Asp/His) box polypeptide 11 (CHL1-like helicase homolog, <i>S. cerevisiae</i> )	2,0
FABP7	fatty acid binding protein 7, brain	2,0
GNB1	Guanine nucleotide binding protein (G protein), beta polypeptide 1	2,0
KIAA0674	KIAA0674	2,0
KIAA1102	KIAA1102 protein	2,0
KRT25A	keratin 25A	2,0
NEDL1	NEDD4-like ubiquitin-protein ligase 1	2,0
NUTF2	Nuclear transport factor 2	2,0
RKHD1	ring finger and KH domain containing 1	2,0
SRPR	signal recognition particle receptor ('docking protein')	2,0
TAF1L	TAF1-like RNA polymerase II, TATA box binding protein (TBP)-associated factor, 210kDa	2,0
THAP5	THAP domain containing 5	2,0

**Table 19.** Genes downregulated 10 hours after induction of ER-MED25-NTD in 721-B-cells

FLJ90036	hypothetical protein FLJ90036	52,0
FAM12A	family with sequence similarity 12, member A	19,7
SLC10A2	solute carrier family 10 (sodium/bile acid cotransporter family), member 2	13,9
WDR49	WD repeat domain 49	12,1
BCL11B	B-cell CLL/lymphoma 11B (zinc finger protein)	9,8
RGS5	regulator of G-protein signalling 5	4,6
MCF2L2	MCF.2 cell line derived transforming sequence-like 2	2,5
PAWR	PRKC, apoptosis, WT1, regulator	2,0

**Table 20.** Genes upregulated 10 hours after induction of ER-MED25-NTD in 721-B-cells

MGC35130	hypothetical protein MGC35130	17,1
CALD1	caldesmon 1	13,0
AREG	Amphiregulin (schwannoma-derived growth factor)	9,8
SPAG16	sperm associated antigen 16	9,8
CEBPD	CCAAT/enhancer binding protein (C/EBP), delta	7,5
C20orf26	chromosome 20 open reading frame 26	5,7
MRE11A	MRE11 meiotic recombination 11 homolog A ( <i>S. cerevisiae</i> )	5,7
AQP3	aquaporin 3	5,3
ELMO2	Engulfment and cell motility 2 (ced-12 homolog, <i>C. elegans</i> )	4,3
KIR3DL2	killer cell immunoglobulin-like receptor, three domains, long cytoplasmic tail, 2	4,3
ABLIM2	actin binding LIM protein family, member 2	3,2
C20orf22	chromosome 20 open reading frame 22	3,2
RICS	Rho GTPase-activating protein	3,0
STK38	Serine/threonine kinase 38	3,0
PFTK1	PFTAIRE protein kinase 1	2,8
ADAM6	a disintegrin and metalloproteinase domain 6	2,6
ZNF230	Zinc finger protein 230	2,5
LOC340351	Hypothetical protein LOC340351	2,3
PCAF	P300/CBP-associated factor	2,1
SEC61B	Sec61 beta subunit	2,1
DNAJC3	DnaJ (Hsp40) homolog, subfamily C, member 3	2,0

SLC38A6	solute carrier family 38, member 6	2,0
ZNF20	zinc finger protein 20 (KOX 13)	2,0

**Table 21.** Genes downregulated 24 hours after induction of ER–MED25–NTD in 721–B–cells

LOC400581	GRB2-related adaptor protein-like	21,1
ALS2CR14	amyotrophic lateral sclerosis 2 (juvenile) chromosome region, candidate 14	16,0
PCGEM1	prostate-specific non-coding gene	14,9
FLJ38564	Hypothetical protein FLJ38564	8,6
ITIH2	inter-alpha (globulin) inhibitor H2	8,0
CASR	Calcium-sensing receptor (hypocalciuric hypercalcemia 1, severe neonatal hyperparathyroidism)	4,9
PRG1	Proteoglycan 1, secretory granule	4,6
FLJ21103	hypothetical protein FLJ21103	3,7
DKFZP566D1346	hypothetical protein DKFZp566D1346	3,0
HABP2	hyaluronan binding protein 2	2,8
CLDN1	claudin 1	2,5
LEPR	leptin receptor	2,5
DACT1	dapper homolog 1, antagonist of beta-catenin (xenopus)	2,3
DNMT3B	DNA (cytosine-5-)-methyltransferase 3 beta	2,3
KARS	Lysyl-tRNA synthetase	2,1
FCHSD2	FCH and double SH3 domains 2	2,0
SLC39A3	Solute carrier family 39 (zinc transporter), member 3	2,0

**Table 22.** Genes upregulated 24 hours after induction of ER–MED25–NTD in 721–B–cells

KLF12	Kruppel-like factor 12	26,0
LOC399947	similar to expressed sequence AI593442	19,7
RNF152	ring finger protein 152	13,9
C10orf84	chromosome 10 open reading frame 84	13,0
CFH /// CFHL3	complement factor H /// complement factor H-related 3	10,6
CHRNA1	cholinergic receptor, nicotinic, alpha polypeptide 1 (muscle) /// cholinergic receptor, nicotinic, alpha polypeptide 1 (muscle)	8,6
FLJ21963	FLJ21963 protein	7,5
DYX1C1	dyslexia susceptibility 1 candidate 1	4,9
SLC24A6	solute carrier family 24 (sodium/potassium/calcium exchanger), member 6	4,9
LOC440320	similar to hypothetical protein FLJ36144	4,0
EPHA5	EPH receptor A5	3,7
IPO9	importin 9	3,7
LOC158830	similar to Ab2-183	3,5
MAML2	Mastermind-like 2 (Drosophila)	3,5
RICS	Rho GTPase-activating protein	3,5
AHI1	Abelson helper integration site	3,2
ABAT	4-aminobutyrate aminotransferase	3,0
RFX3	Regulatory factor X, 3 (influences HLA class II expression)	3,0
SFRS12	Splicing factor, arginine/serine-rich 12	3,0
SLC23A3	solute carrier family 23 (nucleobase transporters), member 3	3,0
GOSR1	golgi SNAP receptor complex member 1	2,6
ZHX2	Zinc fingers and homeoboxes 2	2,6
LOC137392	Similar to CG6405 gene product	2,5
LOC221810	hypothetical protein LOC221810	2,5



TMEFF1	transmembrane protein with EGF-like and two follistatin-like domains 1	2,5
DKFZP434N1817	Hypothetical protein DKFZp434N1817	2,3
DKFZP586A0522	DKFZP586A0522 protein	2,3
ERBB2IP	ErbB2 interacting protein	2,3
NUDT4	nudix (nucleoside diphosphate linked moiety X)-type motif 4	2,3
EVI2A	ecotropic viral integration site 2A	2,1
KCNH5	potassium voltage-gated channel, subfamily H (eag-related), member 5	2,1
SGPP2	sphingosine-1-phosphate phosphatase 2	2,1
TAF1B	TATA box binding protein (TBP)-associated factor, RNA polymerase I, B, 63kDa	2,1
UBTD1	ubiquitin domain containing 1	2,1
C15orf28	chromosome 15 open reading frame 28	2,0
FLJ38281	hypothetical protein FLJ38281	2,0
HERC3	hect domain and RLD 3	2,0
TTBK2	tau tubulin kinase 2	2,0
ZNF596	zinc finger protein 596	2,0

## ACKNOWLEDGEMENTS

I would like to thank my supervisor Michael Meisterernst for giving me the opportunity to realize this work in his lab and for his constant intellectual and economical support.

I am very grateful to Gerhard who was introducing me into the field of biochemistry, to Lucia who helped me with the ES cell culture and to Gema who has been of great help, not only scientifically but also personally.

Special thanks go to Wera for being always available for scientific discussions, helpful suggestions, and for critical comments on this manuscript.

Tom, Michi and Markus were excellent box-mates providing for a very pleasant atmosphere in the lab and for interesting scientific discussions. Elisa became my Italian family in Munich and now one of my best friends.

I especially thank Dr. Nathalie Uyttersprot and Dr. Ursula Zimmer-Strobl for precious advice regarding the mouse project.

I am grateful to the people who contributed to this work through collaborations: Dr. Ralf Kühn, Susanne Bourier, Dr. Marion Horsch, Dr. Sonja Baumli and Dr. Bernd Rautenstrauss.

Many thanks to Roswitha and Angela who were always incredibly efficient in solving any bureaucratic issue.

Finally, I thank my parents for their constant support.

## CURRICULUM VITAE

### Personal data

First name: Lisa  
Surname: Santolin  
Date of birth: 10-04-1973  
Place of birth: San Bonifacio (VR), Italy.  
Nationality: Italian  
Marital status: single  
Address: Johannes Scharrerstr. 7  
80686 München

### Education

1987-1992: High school Graduation  
Liceo Scientifico Statale "A.M. Roveggio"  
Cologna Veneta (VR), Italy  
1992-1999: First degree in Pharmaceutical Chemistry  
(score 107/110)  
University of Padua, Italy  
2000-2001: Research assistant in the department of  
Neuroscience, Baylor College of Medicine, Houston,  
Texas.  
since 2002: PhD student in the Michael Meisterernst group,  
department of Genexpression,  
GSF-Forschungszentrum für Umwelt und Gesundheit,  
Munich

Munich, 31.07.06